Aus dem Institut für Virologie
Leiter: Prof. Dr. Stephan Becker

Des Fachbereichs Medizin der Universität Marburg

Measles Virus as Vaccine Platform against Highly Pathogenic Emerging Viruses

Inaugural-Dissertation zur Erlangung des Doktorgrades
der gesamten Naturwissenschaften (Dr. rer. nat.)

dem Fachbereich Medizin der Philipps-Universität Marburg
vorgelegt von

Anna Helena Fiedler, geb. Malczyk
Geboren in Schwientochlowitz

Marburg, 2017

Angenommen vom Fachbereich Medizin der Philipps-Universität Marburg
am: 24.05.2017

Gedruckt mit Genehmigung des Fachbereichs

Dekan: Prof. Dr. Helmut Schäfer
Referent: Prof. Dr. Stephan Becker
1. Korreferent: PD. Dr. Alexander Visekruna

Für meine Eltern, meine Schwester

und meinen Ehemann Björn

“There exists a passion for comprehension, just as there exists a passion for music. That passion is rather common in children, but gets lost in most people later on. Without this passion there would be neither mathematics nor natural science “

—Albert Einstein –

CONTENT

PRELIMINARY NOTE

This PhD thesis is written as cumulative dissertation in accordance to the study and examination regulations of the Philipps University of Marburg (15.07.2009 §9). It summarizes three thematically linked publications as well as unpublished data. The unpublished data have been included in the thesis to underlie the broad application of measles virus-based vaccines against emerging viral infections. The incorporated publications are listed below. Descriptions pointing to published figures will cite the author and year of publication and the figure number in the publication (for example Scheuplein *et al*., 2015, Fig. 1B). Descriptions pointing to unpublished figures include an ongoing numbering (for example Fig. 1).

1) **High secretion of interferons by human plasmacytoid dendritic cells upon recognition of Middle East respiratory syndrome coronavirus**. Scheuplein VA, Seifried J*, **Malczyk AH***, Miller L, Höcker L, Vergara-Alert J, Dolnik O, Zielecki F, Becker B, Spreitzer I, König R, Becker S, Waibler Z, Mühlebach MD. J Virol. 2015 Apr;89(7):3859-69. doi: 10.1128/JVI.03607-14. Epub 2015 Jan 21.

2) **Lentiviral Protein Transfer Vectors Are an Efficient Vaccine Platform and Induce a Strong Antigen-Specific Cytotoxic T Cell Response**. Uhlig KM, Schülke S, Scheuplein VA, **Malczyk AH**, Reusch J, Kugelmann S, Muth A, Koch V, Hutzler S, Bodmer BS, Schambach A, Buchholz CJ, Waibler Z, Scheurer S, Mühlebach MD. J Virol. 2015 Sep;89(17):9044-60. doi: 10.1128/JVI.00844-15. Epub 2015 Jun 17.

3) **A Highly Immunogenic and Protective Middle East Respiratory Syndrome Coronavirus Vaccine Based on a Recombinant Measles Virus Vaccine Platform**. **Malczyk AH**, Kupke A*, Prüfer S*, Scheuplein VA, Hutzler S, Kreuz D, Beissert T, Bauer S, Hubich-Rau S, Tondera C, Eldin HS, Schmidt J, Vergara-Alert J, Süzer Y, Seifried J, Hanschmann KM, Kalinke U, Herold S, Sahin U, Cichutek K, Waibler Z, Eickmann M, Becker S, Mühlebach MD. J Virol. 2015 Nov;89(22):11654-67. doi: 10.1128/JVI.01815-15. Epub 2015 Sep 9.

*equally contributed

ZUSAMMENFASSUNG

Hochpathogene Viren stellen eine globale Gefahr dar, da sie im Zuge des internationalen Personen- und Warentransportes fast ungehindert verbreitet werden können. Eine besondere Bedrohung geht dabei von neuartigen viralen Erregern aus, für die keine adäquaten Behandlungsmethoden implementiert sind. Um auf lokale oder sogar globale Ausbrüche dieser Viren angemessen reagieren zu können, besteht eine Maßnahme in der frühzeitigen Entwicklung schützender Impfstoffe. Vektorbasierende Impfstoffplattformen, wie z. B. replikationskompetente rekombinante Masernviren (rMV), sind für diese Zwecke besonders interessant, da diese nach Standardisierung einen einfachen Austausch der für Antigene kodierender Genabschnitte ermöglichen und somit eine schnelle Produktion erlauben können.

Um ihre Eignung als protektive Impfstoffplattform gegen hochpathogene virale Erreger zu untersuchen, wurden innerhalb der vorliegenden Arbeit rMV hergestellt, welche jeweils für Antigene der neuartigen Erreger *Middle East respiratory syndrom coronavirus* (MERS-CoV), Influenza-Virus H7N9 oder des Erregers des hämorrhagischen Krim-Kongo-Fiebers (engl. *Crimean-Congo haemorrhagic fever virus,* CCHFV) kodierende Gene enthalten. Dieser Einbau ermöglichte eine hier nachgewiesene Expression des MERS-CoV Spike Oberflächenproteins in membrangebundener (MERS-S) oder löslicher Form (MERS-solS), des MERS-CoV Nukleokapsidproteins (MERS-N), des Hämagglutinins bzw. der Neuraminidase von H7N9 (H7 bzw. N9), des CCHFV Glycoproteins Gc (CCHFV-Gc) oder des CCHFV-Nukleokapsidproteins (CCHFV-N) in mit dem jeweiligen Impfstoff infizierten Zellen. Die Immunisierung MV-suszeptibler Mäuse mit MERS-S-, H7- oder N9-exprimierenden rMVs zeigte, dass humorale Immunantworten ausgelöst werden, bei denen nach Vakzinierung mit MV-MERS-S, MV-MERS-solS oder MV-H7 Virus-neutralisierende Antikörper (nAKs) nachgewiesen werden konnten. Die Herstellung von für die jeweiligen Antigene transgenen, zum Mausmodell syngenen Dendritische Zellen (*Dendritic cells*, DC)-Zelllinien ermöglichte zudem eine effiziente Re-stimulation von Antigen-spezifischen T-Zellen unabhängig der Kenntnis jeweils immunogener Epitope oder der Verfügbarkeit des Antigens in Proteinform. Mit Hilfe dieser Antigen-spezifischen DC-Zelllinien konnten durch MV-MERS-S, MV-MERS-solS, MV-MERS-N sowie MV-H7 induzierte zelluläre Immunantworten über IFN-γ-ELISpot nachgewiesen werden. MERS-S spezifische $CD8^+$ T-Zellen aus immunisierten Tieren reagierten zudem mit einer MERS-S-abhängigen Proliferation und MERS-S spezifischen Zytotoxizität auf entsprechende Re-stimulation. Mit MV-MERS-S oder MV-MERS-solS vakzinierte Mäuse zeigten im Belastungsversuch mit MERS-CoV eine Reduktion der Viruslast sowie Virus-induzierter Entzündungsreaktionen

im Lungengewebe. Dies demonstrierte eindrucksvoll die Schutzwirkung eines MV-basierenden Impfstoffkandidaten gegen MERS-CoV.

In einem zweiten Teil dieser Arbeit wurden zudem durch MERS-CoV ausgelöste angeborene Immunreaktionen in humanen und murinen Antigen-präsentierenden Zellen untersucht. Dabei wurden humane plasmazytoide DCs (pDCs) als Quelle erheblicher Mengen antiviraler Typ I (IFN-α, IFN-β) oder Typ III (IFN-λ) Interferone identifiziert, die in Folge einer Infektion dieser Zellen mit MERS-CoV ausgeschüttet wurden. pDCs könnten als bisher einzig nachgewiesene Quelle antiviraler Typ I Interferone eine wichtige Rolle innerhalb der Pathogenese von MERS-CoV im Menschen einnehmen.

Diese Arbeit zeigte folglich beispielhaft Interaktionen eines neuartigen Erregers, MERS-CoV, mit genau definierten Immunzellen, was die Entwicklung zukünftiger Therapien maßgeblich unterstützen könnte. Als potentieller Impfstoffkandidat wurde innerhalb dieser Arbeit eine MV-basierende Impfstoffplattform erzeugt und deren Schutzwirkung gezeigt. Die schnell umsetzbare Erzeugung solcher MV-basierenden Impfstoffkandidaten gerichtet gegen drei unterschiedliche virale Erreger, die effiziente Induktion humoraler und zellulärer Immunantworten sowie die Schutzwirkung im Belastungsversuch verdeutlichen das Potential von rMV als effiziente Impfstoffplattform gegen neuartige Erreger.

SUMMARY

Highly pathogenic viruses are a significant global danger since they can be spread by worldwide travel and trade almost without restriction. One particular threat comes from emerging infections, for which no adequate treatment options currently exist. To guard against local or global outbreaks of these viruses, the development of protective vaccines at an early stage is therefore a desirable form of intervention. Vector-based vaccine platforms, such as that of replication-competent recombinant measles virus (rMV), constitute good prospective vaccine candidates, since they have the potential to allow for an easy exchange of antigen-encoding genes, thereby enabling rapid vaccine production after standardisation. To assess their suitability as a potential vaccine platform against highly infectious viral pathogens, rMVs were generated as part of the practical element of this thesis. These encoded for antigens of the following emerging pathogens: Middle East respiratory syndrome coronavirus (MERS-CoV), influenza virus H7N9 or Crimean-Congo haemorrhagic fever virus (CCHFV). Insertions of antigen-encoding genes resulted in the detectable expression of the MERS-CoV spike glycoprotein in both membrane-bound (MERS-S) and soluble form (MERS-solS), the MERS-CoV nucleocapsidprotein (MERS-N), haemagluttinin or neuraminidase of H7N9 (H7 or N9), the CCHFV glycoprotein Gc (CCHFV-Gc); and the CCHFV-nucleocapsid protein (CCHFV-N), in cells infected with respective vaccines.

Immunisation of MV susceptible mice with MERS-S-, MERS-solS-, H7-, or N9-encoding vaccines also resulted in the induction of humoral immune responses. These included virus-neutralising antibodies (nAbs), if mice were vaccinated with MV-MERS-S, MV-MERS-solS or MV-H7. Generation of syngeneic for the respective antigens' transgenic dendritic cell (DC) cell lines, moreover, enabled an efficient re-stimulation of antigen-specific T cells without knowledge of immunogenic epitopes or the availability of antigens as proteins. When using these transgenic DC cell lines, MV-MERS-S-, MV-MERS-solS-, MV-MERS-N-, and MV-H7-induced cellular immune responses were demonstrated in an IFN-γ-ELISpot. Moreover, MERS-S specific $CD8^+$T cells of immunised mice responded to respective re-stimulation by MERS-S-dependent proliferation and MERS-S-specific cytotoxicity. A reduction of viral loads, as well as virus-induced inflammation of lung tissue, was observed in MV-MERS-S- or MV-MERS-solS-vaccinated mice within a MERS-CoV challenge model. This impressively demonstrated the protective efficacy of an MV-based vaccine against MERS-CoV.

In the second part of this thesis, MERS-CoV-induced innate immune responses in human and murine antigen-presenting cells (APCs) were analysed. As a result, human plasmoid DCs (pDCs) were identified as a source of significant amounts of antiviral type I (IFN-α, IFN-β) and Typ III (IFN-λ) interferons (IFNs), which were secreted upon infection with MERS-

CoV. As a so far exclusively-identified source of type I and III IFNs pDC might hence play a significant role in MERS-CoV-induced pathogenesis in humans.

Thus, by using MERS-CoV as an example, this thesis identified several key interactions between an emerging pathogen and defined immune cells, which might prove to be of clinical significance, particularly in the future development of antiviral drugs. As potential vaccine candidate, an MV-based vaccine platform was generated as part of this thesis; and its protection efficacy was demonstrated. A rapidly conducted production of MV-based vaccine platforms against three different viral pathogens, an efficient induction of humoral and cellular immunity as well as protection efficacy in a challenge model indicated the potential of recombinant MV to be used as an effective vaccine platform to protect against emerging viral pathogens.

1. INTRODUCTION

1.1. Emerging infections

Over the last few decades, several new infectious diseases, caused by bacteria, viruses or parasitic pathogens, have suddenly emerged or re-emerged (220, 257). Of these pathogens, viruses most commonly enter the human population through so-called zoonoses, a transmission from an animal reservoir to human patients. In fact, 50-60% of all viruses (271) and 70% of emerging or re-emerging viruses (64, 132) are of zoonotic origin. Among these are the human immunodeficiency virus (HIV)-1, which emerged in the early 20th century (328), the Ebola virus in 1976 (117), and severe acute respiratory syndrome coronavirus (SARS-CoV) in 2002 (227). More recently, the coronavirus Middle East respiratory syndrome coronavirus (MERS-CoV) (320), and the avian influenza virus (H7N9) (135) entered the human population in 2012 and 2013, respectively, and still cause severe disease.

Zoonotic viruses can be transmitted to human patients directly through wildlife or more commonly, through livestock such as Arabian dromedary camels in the case of MERS-CoV (108); or poultry, which transmits H7N9 (162). Such transmission events most frequently occur in developing countries, where close contact between animals and people favours contagion (317). However, the emergent viruses can then be spread by worldwide travel and trade (257) making the development of vaccines during a pre-pandemic phase sensible, so as to be prepared for the possible onset of a global pandemic.

Thus, the next subsections will describe pathogenicity and assess the pandemic risk of selected highly pathogenic viruses in order to emphasise the need for pre-pandemic vaccines. Due to their phylogenetical distance and recent emergence, the biosafety-level (BSL) 3 viruses MERS-CoV and H7N9, or the frequently re-emerging BSL-4 pathogen Crimean-Congo haemorrhagic fever virus (CCHFV) were chosen as targets for this thesis.

1.1.1. Middle East respiratory syndrome coronavirus (MERS-CoV)

In November 2012, a virus isolated from a Saudi Arabian patient was identified as a new member of the coronavirus family (*Coronaviridae*), initially termed hCoV-EMC (320), but later renamed as Middle East respiratory syndrome coronavirus (MERS-CoV). Comparable to the related severe acute respiratory syndrome coronavirus (SARS-CoV), an infection with MERS-CoV induces severe pneumonia in human patients, which is often accompanied by leukopenia and lymphopenia (320). In severe cases, MERS-CoV additionally induces septic

shock, renal or multi-organ failure (79). To date, the virus has infected 1,905 patients in 27 countries, of whom 677 have succumbed to disease, yielding a mortality rate of approximately 36%. Eighty percent of confirmed cases were reported from Saudi-Arabia (297) (Fig. 1).

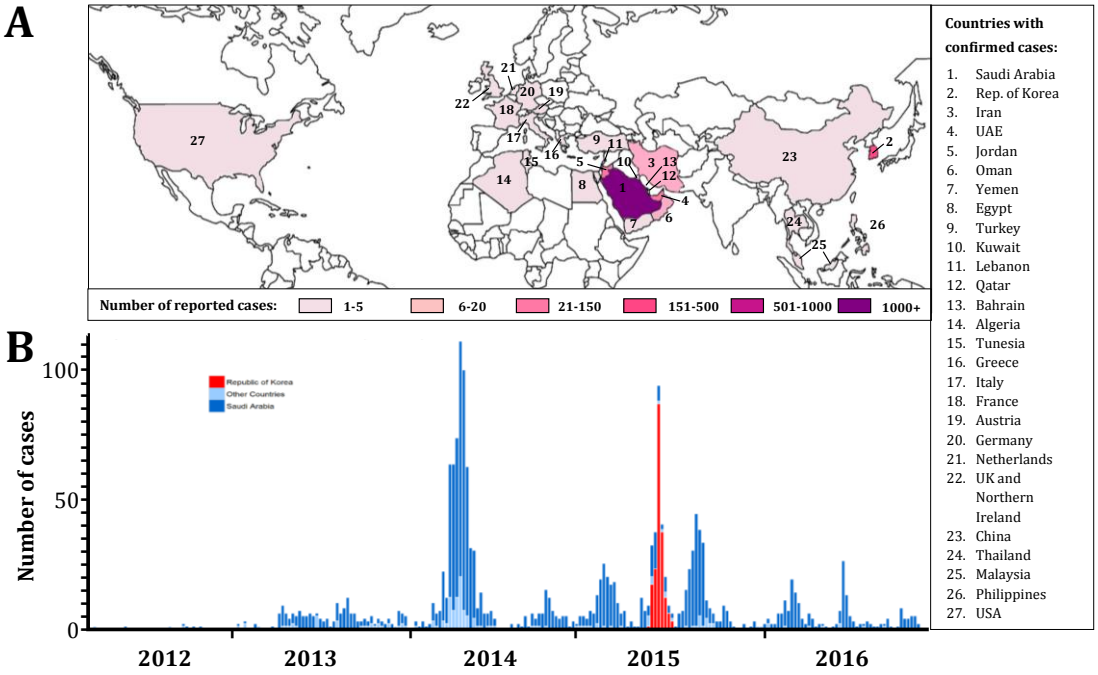

Fig. 1 Distribution of MERS-CoV and epicurve of confirmed cases. **(A)** Global distribution of human cases with confirmed MERS-CoV infection. Countries of confirmed cases are marked purple. **(B)** Epicurve of confirmed human cases from 2012 to 2016. Dark blue, Saudi-Arabia; red, Korea; light blue, other countries. Modified after (297).

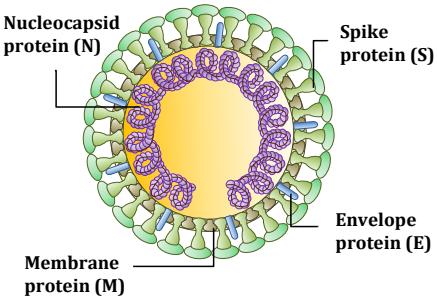

Fig. 2 Structure of MERS-CoV. Schematic depiction of a Middle east respiratory syndrom coronavirus (MERS-CoV) particle. The viral envelope proteins Spike (S), membrane (M) and envelope protein (E) are embedded into the membrane, which surrounds the RNA complexed with nucloecapsid proteins (N).

As with all coronaviruses, MERS-CoV is a spherical, enveloped virus with a single-stranded, positive-sensed (ss(+)) RNA-genome (25, 300). Its genome encodes for four structural proteins, the nucleocapsid protein (N) wrapping the viral RNA, and three proteins anchored in the viral membrane: envelope protein (E), membrane protein (M) and spike glycoprotein (S) (199) (Fig. 2). The spike glycoprotein binds the cellular receptor Dipeptidylpeptidase-4 (DPP-4) and mediates viral entry into the cell (167) via fusion with the plasma or endosomal membrane (217).

MERS-CoV is of zoonotic origin, capable of infecting dromedary camels (54, 93, 191). Since virus isolates originating from this host are genetically similar to human viruses (108, 179), it is proposed that most human cases arise from contagion from camels. So far, the virus is

poorly transmitted from person to person. However, 106 confirmed third-generation and 11 fourth-generation cases during an outbreak in Korea in 2015 (58, 210) indicate substantial transmission amongst the human population. By way of comparison SARS-CoV caused a significant outbreak in 2002, in which approximately 1,000 of more than 8,000 patients succumbed to disease (293). The analogy of symptoms between SARS- and MERS-CoV (320) and MERS-CoVs higher case fatality rate of 35% (297) arouses the fear that MERS-CoV could induce a comparable or even worse global outbreak than SARS-CoV. Although the human-to-human transmission of MERS-CoV is generally limited, the ongoing level of infections since 2012 make the generation of an efficient vaccine advisable so as to be prepared for the potential onset of a global pandemic. In any event, a MERS-CoV-vaccine would be helpful in fighting the local epidemic in Saudi-Arabia and the Middle East.

1.1.2. Influenza virus H7N9

Since 2013, 918 laboratory-confirmed infections with another recently-emerged virus, the avian influenza A virus H7N9, have been reported to the World Health Organisation (WHO) (296)(Fig. 3A). The virus was originally isolated from three Chinese patients in February and March 2013 (100), who fatally suffered from severe respiratory tract infections and pneumonia (129). The contagion of people is presumably mediated through contact with infected poultry, mostly in poultry markets (162, 317). Although the virus occasionally infects humans with limited human-to-human transmission, and exhibits a restricted distribution in China (312), the high case fatality rate of about 36% is alarming (129, 262) (Fig. 3B). By comparison, the pandemic induced by Influenza H1N1 resulted in a mortality rate of about 0.03% (43, 74).

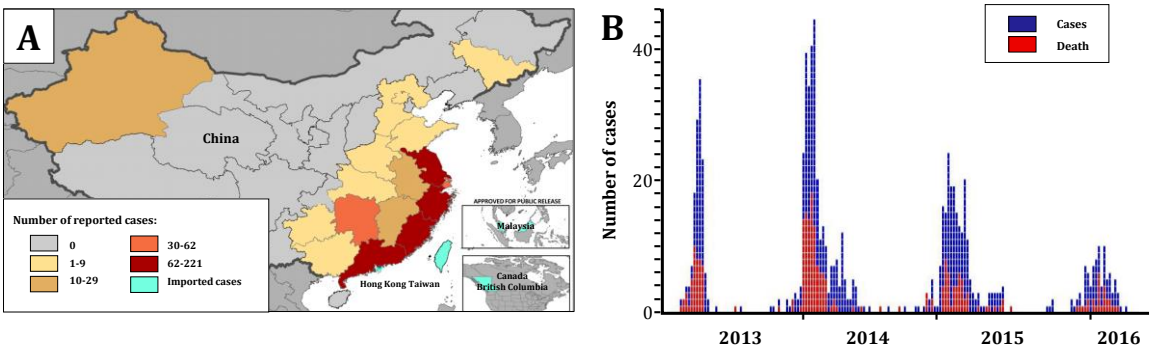

Fig. 3 Distribution of H7N9 and epicurve of confirmed cases. **(A)** Global distribution of human cases with confirmed H7N9 infection. Countries of confirmed cases are colored. Beige, brown, orange and red; cases in China; light-blue, imported cases. modified after (90). **(B)** Epicurve of confirmed human cases from 2013 to 2016. Dark blue, number of Cases; red, number of Deaths. Modified after (296).

As with other influenza A viruses in the family *Orthomyxoviridae,* H7N9 is a segmented, single-stranded negative-sense (ss(-)) RNA virus. The eight RNA segments encode for the structural proteins, which are the polymerase subunits (PB1, PB2, PA, PB1-F2), nucleocapsid protein (N), hemagglutinin (HA), neuraminidase (NA), and matrix proteins (M1, M2) as well as two non-structural proteins (NS1, NS2) (Fig. 4) (273, 304).

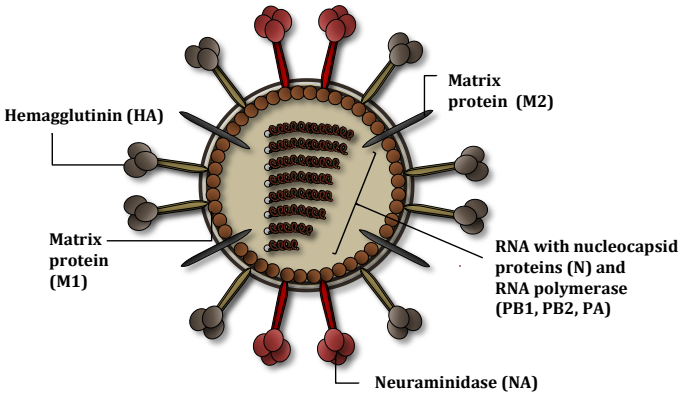

Fig. 4 Structure of H7N9. Schematic depiction of an Influenza virus particle (as H7N9). The RNA is organized in eight segments, which are complexed with nucleocapsid proteins (N) and RNA polymerase proteins (PB1, PB2, PA) and surrounded by the Matrix proteins (M1). The viral envelop proteins hemagglutinin (HA), neuraminidase (NA), the matrix proteins (M2) are embedded into the membrane.

The HA, which is like NA, embedded in the viral envelope, mediates binding to the entry receptor sialic acid and subsequent uptake via the endocytic route. NA on the surface of productively infected host cells catalyses the cleavage of the receptor to release the virus particles (273, 304). Since human cells are covered with α2,6-linked sialic acids (56), they are normally not infected by avian influenza viruses, which predominantly utilize α2,3-linked sialic acids for entry (20). However, the influenza virus subtype H7N9 bears genetic changes associated with an adaptation to mammalian cells (100), resulting in an efficient replication in human airway epithelial cells (22). Moreover, the virus is efficiently transmitted between infected ferrets via direct contact (22, 327) and at least for the Anhui/1 strain also through airborne transmission (323). Although human-to-human transmission of H7N9 is still limited to few family clusters (296), the adaptations to mammalian cells, especially the principle capacity of airborne transmission (323), are alarming. Moreover, the shedding of the infectious virus by ferrets before the onset of influenza symptoms (323) makes a rapid transmission of H7N9 likely, especially if the virus adapts more efficiently to the human host. The potential spread of the virus could be prevented; and people at risk, protected if efficient vaccines were available.

1.1.3. Crimean-Congo haemorrhagic fever virus (CCHFV)

During World War II, an until then unidentified virus was isolated from 200 soldiers in the Crimea who had suffered from severe haemorrhagic fever (120, 185). The isolated virus was later shown to be antigenically indistinguishable from the Congo virus isolated in the Belgian Congo in 1956 (305) and consequently termed Crimean-Congo haemorrhagic fever

virus (CCHFV) (120). Crimean-Congo haemorrhagic fever (CCHF) is a tick-borne viral disease, which is endemic in the Balkans, the Middle East, Asia and parts of Africa (120) (Fig. 5). There, the virus frequently infects patients, and is, thus, responsible for 140 outbreaks and 5,000 cases since its discovery (10). Infected patients suffer from haemorrhage, myalgia and fever, and succumb to disease in 3 to 30% of cases (86, 185). The virus is transmitted to humans or other mammals by arthropod tick vectors of the *Hyolomma* genus (120, 185). However, people may also become infected via contact with body fluids of patients in the acute phase of infection, or by contact with blood or tissue of viraemic livestock (292).

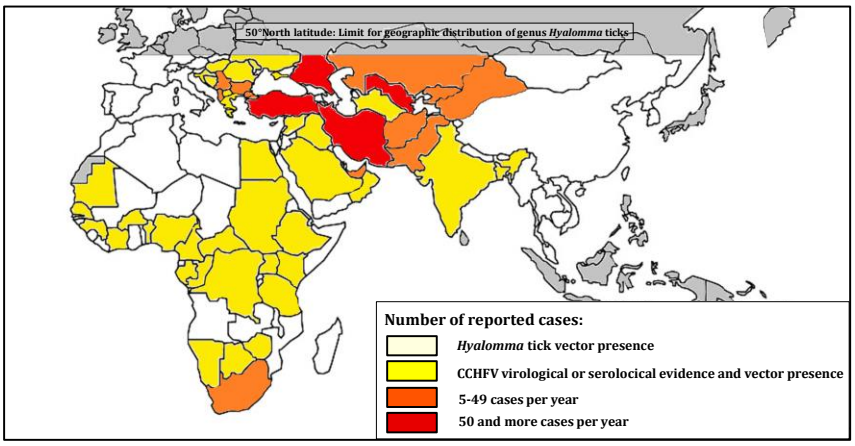

Fig. 5 Distribution of CCHFV. Global distribution of human cases with confirmed CCHFV infections. Countries of confirmed cases are colored in yellow or red depending on case numbers. White, presence of the genus *Hyalomma* ticks. Modified after (299).

CCHFV is an enveloped single-stranded negative-sense (ss(-)) RNA virus and belongs to the family of *Bunyaviridae* and the genus *Nairovirus* (83). The segmented genome consists of three RNA segments, the S (small), M (medium), and L (Large) segment, which encode for the nucleoprotein, the glycoproteins Gn and Gc (previously G1 and G2), and the RNA-dependent polymerase, respectively (110) (Fig. 6). The glycoproteins, probably Gc, are responsible for viral attachment to the receptor, which so far remains unidentified, but is presumably nucleolin in humans (308).

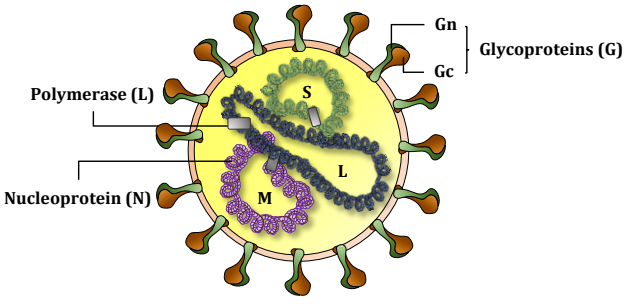

Fig. 6 Structure of CCHFV. Schematic depiction of a Crimean-Congo haemorrhagic fever virus (CCHFV) particle. The RNA is organized in three segments, the small (S), middle (M) and large segment (L). The S segment encodes for the nucleocapsid proteins (N), the L segment for RNA polymerase proteins (L) and the M Segment for the glycoproteins (G) Gc and Gn.

Although the M segment encoding for Gn and Gc reveal 31% nucleotide or 27% amino acid (aa) variability among seven different strains (71), Gn and Gc are usual targets of experimental vaccines. So far developed vaccines include a DNA vaccine (256), transgenic plants (101), or modified vaccinia virus Ankara (MVA) (40, 77). Indeed, in contrast to the more conserved N protein (20 and 8% nucleotide or aa variability, respectively) (76), expression of the glycoproteins by MVA was shown to induce protective immune responses

in mice (40, 77). However, the only vaccine used in humans so far, which was introduced in 1974, is based on inactivated material of infected mouse brains (207). Although the vaccine induced antibody (Ab) responses in 96 % of immunized patients (185), it is not well characterised and the method of preparation makes a broad applicability unachievable. Moreover, antiviral treatment of infected patients with ribavirin is beneficial, but not approved in many countries (87). Consequently, the wide distribution of the BSL-4 virus; the severity of the disease; high-case fatality, as well as a fear of bio-terrorism, makes development of appropriate vaccines prudent (87). Moreover, factors like climate change favour the distribution of ticks as vectors and may thus lead to infection cases in more temperate climate zones (88, 104).

What the emerging viruses MERS-CoV and H7N9, as well as the frequently re-emerging CCHFV, have in common is that they reveal a high pathogenicity and an alarming case fatality rate in human patients. Pathogenicity of a virus is mostly determined by the capability of the human innate and adaptive immune system to control the virus. Viruses which evade or suppress the immune responses will usually persist in the patient's body for a longer period of time. This, consequently, may not only increase the frequency of virus-induced damages to the organism, but may also extent the period of virus transmissibility among patients. Thus, the role of the innate and adaptive immune system in viral clearance, as well as potential evasion strategies will be described in the following sections.

1.2. Viral clearance by type I INFs

Usually, pathogen associated molecular patterns (PAMPs) such as conserved molecular motifs of viral RNA or DNA, are immediately recognised by pattern recognition receptors (PRR) after pathogen entry (193). This recognition then initiates signalling cascades, resulting in innate immune responses which are mediated by, for example, the secretion of various proinflammatory cytokines. These cytokines may act antivirally by, for example, the recruitment of other immune cells (chemokines) or binding to specific receptors in an autocrine or paracrine manner. The binding then results in the expression of antiviral factors through the activation of signal cascades (106). A potent group of antiviral proinflammatory cytokines exists in the family of interferons (IFNs), the type I, II, and III IFNs (127). Among these, the type I IFNs, including the well-characterized IFN-α family and IFN-β, are the most immediate and most effective innate immune response against many viruses (106, 173, 240). Therefore, this section will focus on mechanisms inducing type I IFNs and their downstream effects.

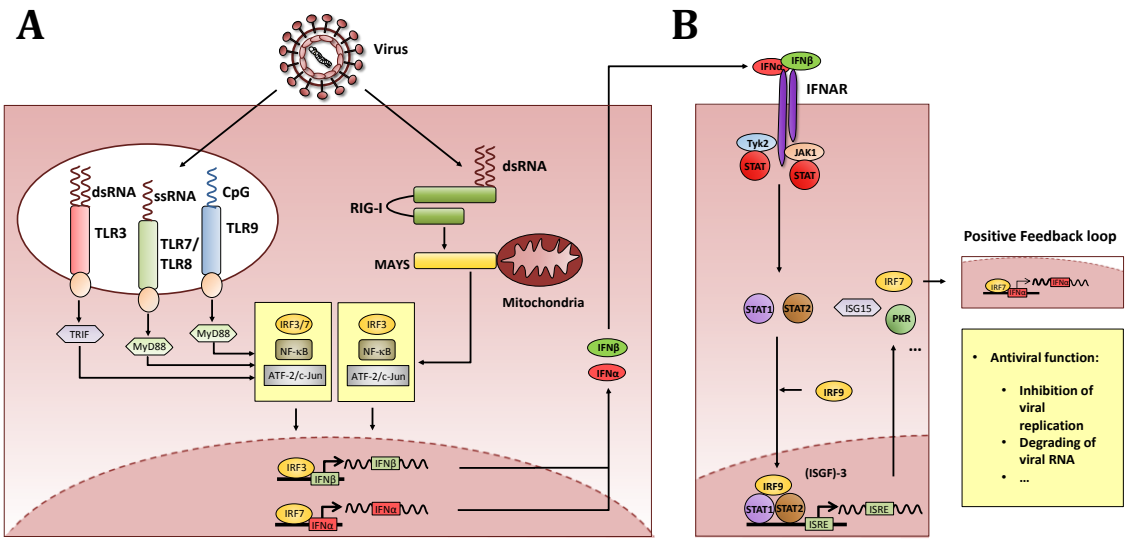

Fig. 7 Expression and effects of type I IFNs. **(A)** Schematic depiction of signal cascades triggering type I IFN expression. Viral nucleotides are sensed by TLR3 (dsRNA), 7, 8 (ssRNA) and 9 (CpG motives of DNA) in the endosome or RIG-I (dsRNA) in the cytosol after viral entry. TLR activation results in a TRIF or MyD88 dependent activation of transcription factors (TF) IRF3/7, NFκB and activating transcription factor-2/c-Jun (ATF-2/c-Jun). RIG-I sensing causes an MAYS dependent activation of IRF3, NFκB and ATF-2/c-Jun. The binding of TFs to the IFN-α/β promotors results in the expression of IFN-α/β. **(B)** Schematic depiction of signal cascades downstream of IFNAR binding. IFN-α/β bind in an autocrine or paracrine manner to the IFN-α/β receptor (IFNAR), which induces an Tyk2/JAK1 dependent activation of STAT. IRF9 forms a complex with activated STAT molecules resulting in the transcription of ISRE including IRF7 and other antiviral molecules. IRF7 induces further expression of IFN-α/β. Modified after (240, 115).

Almost every cell type is capable of secreting type I IFNs upon viral infection (193). However, while non-immune cells like epithelial cells or fibroblasts predominantly secrete IFN-β, haematopoietic cells, especially plasmacytoid dendritic cells (pDCs), are the major producer of IFN-α in addition to IFN-β (127). The expression and secretion of both type I INFs upon viral infection is induced after sensing viral nucleotides within the cells (29) or for some viruses like cytomegalovirus (CMV) (28, 52) or respiratory syncytial virus (RSV) (113, 156) by the recognition of viral proteins via Toll-like receptors (TLR) 2 or 4 at the cell surface (29, 306). Viral nucleotides, including DNA and RNA, are sensed by TLR3, 7, 8, or 9 within endosomes (4), or by retinoic acid inducible gene (RIG-I)-like receptors (RLRs), including RIG-I (315), MDA5 (melanoma differentiation factor 5) (9), or LPG2 (laboratory of genetics and physiology 2) (316) in the cytosol (315). After binding their cognate PAMP, both PRR families, TLRs and RLRs, induce signal cascades resulting in the phosphorylation of the transcription factors IRF-3, IRF-7, NF-κB, or activating transcription factor-2/c-Jun (ATF-2/c-Jun) (193)(Fig. 7A). These factors initiate the expression of IFN-α/β and, simultaneously, genes encoding for another group of IFNs, the type III IFNs IFN- λ1, IFN- λ2 and IFN- λ3, which have the same antiviral functions (204).

Subsequently, IFN-α/β bind in an autocrine or paracrine manner to the IFN-α/β receptor (IFNAR) resulting in the expression of IFN stimulated genes (ISGs). These genes encode for various antiviral and immune-modulatory factors, which mediate further IFN-α/β secretion through a positive feedback loop (IRF-7) (119, 127, 240); or trigger mechanisms like the

degrading of viral RNA, or an inhibition of viral translation (193) (Fig. 7B). Several reports demonstrated that IFNAR knockout mice (IFNAR$^{-/-}$) reveal significantly higher lethality upon infection with various viruses; among others CCHFV (24), chikungunya virus (CHIKV) (234) or the measles virus (189). These data clearly emphasise the significant role of type I IFN-induced immune responses for viral defence.

Many viruses therefore, usually develop mechanisms to evade these innate immune responses. Influenza A viruses, for instance, are known to hide their dsRNA from recognition by RIG-I through encapsidation (111). Moreover, influenza viruses inhibit the activation of IRF-3 (268), NF-κB (286) or ATF-2/c-Jun (166) by the viral non-structural protein NS1. Coronaviruses likewise encapsidate IFN-inducing-RNA PAMPs (152, 168) and hide cytosolic dsRNA in double-membrane vesicles during replication (151, 277, 278). These strategies make viral RNA less visible for cytosolic PRR recognition. Moreover, proteins encoded by SARS-CoV-like nsp-16, prevent RNA recognition by MDA-5 (180, 334) or interfere with upstream (for example, IRF3-activation (70, 98)) or downstream IFN signalling (for example, STAT1 phosphorylation (289)). Interestingly, MERS-CoV has also failed to induce type I IFN responses in human epithelial cells (46, 147, 330) or macrophages (325), thus indicating that the virus does also counteract the IFN system. In fact, MERS-CoV encodes for IFN suppressive proteins like ORF4a, that interact with dsRNA (200, 249), suppresses the PACT mediated activation of RIG-I and MDA-5 (250) and inhibits ISG transcription (311).

Evasion strategies from innate immune responses like those described for SARS- or MERS-CoV might result in inefficient viral clearance and thus, increased pathogenicity or prolonged persistence of the virus (149). On the other hand, a dysregulation of cytokine secretion by cells of the innate immune system, might even cause immuno-pathogenicity, as is already assumed for SARS-CoV (41, 63). Both immune evasion and exaggerated immune responses, demonstrate that pathogenicity of a virus might be associated with an aberrant innate immune response. However, in addition to viral clearance mediated by cells of the innate immune system, viral infections are also counteracted by adaptive immune responses. Thus, the important role of the adaptive immune system in viral defence, which is utilised by vaccination, will be described in the subsequent section.

1.3. Viral clearance by immunological memory

As a reaction to a primary infection by a given pathogen, a T and B cell-mediated adaptive immune response develops, which is based on specific recognition of individual pathogens. The necessity of adaptive immunity for efficient viral clearance has been demonstrated for various viruses, amongst others, rotavirus (222), coronavirus JMH (122), influenza virus (206) or hepatitis B virus (310).

The high specificity of adaptive immune responses is due to the fact that each maturing T and B lymphocyte expresses an individual B (BCR) or T cell receptor (TCR) which specifically binds to a distinct antigen (193). When TCRs of naïve T cells recognise their specific peptide, presented by professional antigen presenting cells (APCs) on major histocompatibility complexes (MHCs), they will differentiate into effector T cells (17, 178, 214). Among these are cluster of differentiation (CD)8^+ cytotoxic T cells (CTLs), which recognise intracellularly-produced peptides presented on MHC class I (258). CTLs induce apoptosis in infected cells by a binding of upregulated Fas ligands (FasL) to Fas (CD95 or APO-1), that is expressed on the target cell (68, 228), or by the release of cytotoxic granules containing perforin and granzymes (193, 211). In addition to direct cell killing, and thus cellular immunity, CTLs induce antiviral immune responses through the secretion of the antiviral or immunomodulatory cytokines IFN-γ, Tumor necrosis factor-α (TNF-a), and IL-2 (68). CTLs are normally detected 5-7 days after onset of infection (68, 106) (Fig. 8).

Another effector T cell population, so-called T helper cells (T_H), are activated if extracellular antigens are internalised, processed and presented on MHC class II to naïve antigen-specific $CD4^+$ T cells by APCs (106). Their role in viral clearance consists in the secretion of antiviral, but also immunomodulatory cytokines, which regulate adaptive and innate immune responses (186, 263, 275). Moreover, $CD4^+$ T cells interact with CTLs and B cells by direct cell contact and the secretion of immunomodulatory cytokines. Thereby T_H cells support those to fulfil their respective effector function or to differentiate into memory cells (263).

Humoral immune responses are characterised by the secretion of immunoglobulin(Ig)s, the antibodies (Abs), by plasma cells. Naïve B cells will differentiate into plasma cells, if those recognize an a specific antigen (extracellular or presented by follicular DC (FDC)-presented antigen) (243) and, consequently become activated in a T_H cells dependent or independent manner (2). Abs secreted by plasma cells can attach to proteins on the viral surface and thereby induce aggregation, or prevent surface proteins from binding to the respective receptor and thus viral entry (neutralising Abs; nAbs) (53, 106). Moreover, Ab-covered pathogens are recognised by the complement system or Fc-receptor-expressing phagocytes resulting in viral clearance by phagocytosis (39, 53). In addition to the pathogen, Abs also bind to infected cells covered by viral proteins on their surface. Subsequently, such

opsonized cells are lysed through complement-dependent cytotoxicity (CDC) or antibody-dependent cellular cytotoxicity (ADCC), mediated by, for example, NK cells or macrophages (112, 272, 284).

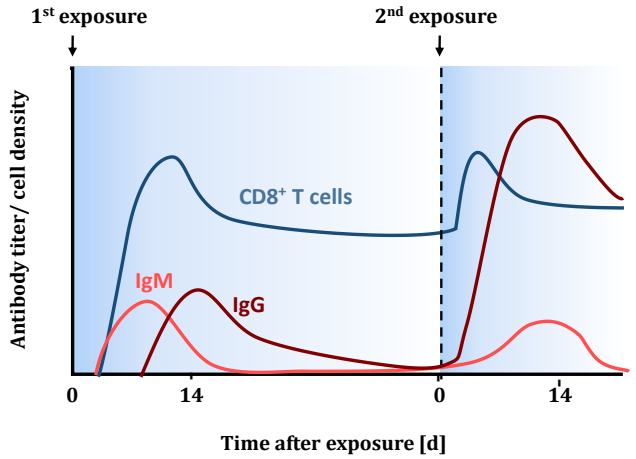

Fig. 8 CD8⁺ T cell and Ab responses after an initial and secondary pathogen exposure. Immune responses after a secondary exposure are more rapidly activated. Abs secreted by B cells consists of more highly-affine IgGs and less low-affine IgMs. Modified after (10, 65)

A few days after pathogen exposure, secreted antibodies are mostly composed of IgMs usually revealing a relatively low affinity to the antigen (2). Highly affine IgGs, which underwent affinity maturation and isotype switching, are, by contrast, detectable approximately one week after onset of infection at the earliest (14) (Fig. 8). Thus, highly affine antibody and efficient CTL responses take at least one week to develop during a primary infection. In contrast, these are immediately triggered in subsequent infections, which is based on the development of immunological memory (2). B cells contribute to this immunological memory by affinity-maturation into long-lasting plasma cells (155) or memory B cells expressing class-switched highly-affine BCRs (150, 270). Long-lived plasma cells in the bone-marrow are capable of secreting Abs for more than 8 months after clearance of infection (60, 159, 252). These Abs, which are mostly composed of highly-affine IgGs, can than immediately coat and neutralise newly intruding viruses (251). The pool of Ab-producing long-lived plasma cells is replenished by immediately activated highly-affine memory B cells upon pathogen exposure, resulting in a protection persisting for decades (59). T cells will also differentiate into memory T cells if effector cells, which are normally removed after viral clearance to re-balance the immune system, evade activation-induced cell death (AICD) (2). $CCR7^+$ effector memory T cells are immediately activated in subsequent infections to take over effector function and are continuously replenished by re-activated $CCR7^-$ central-memory T cells under these conditions (158).

During a second exposure to a pathogen then, an immediate, highly-affine, and effective protection is mediated by pre-formed Abs, as well as memory B and T cells. Such an immunological memory is not only induced by natural infections, but also by the use of vaccines. Effectiveness of vaccines is thus optimally characterised by an induction of long-lasting Abs and memory T and B cells.

1.4. Induction of adaptive immunity by vaccination

The efficacy of classic anti-viral vaccines is mostly ascribed to induction of humoral immune responses, since protection often correlates with the presence of specific Abs, particularly nAbs (331, 332). Such correlation between humoral immunity and protection has been shown for several viruses like SARS-CoV (261, 313), HBV (8) or CHIKV (3, 33). However, highly variable viruses like influenza (75) or HIV (246) often evade humoral immune responses since broadly reactive Abs are rarely induced and viral escape mutants arise quickly (19). CTL responses, on the contrary, are known to target more conserved motifs, particularly of inner proteins. Thus, induction of cellular immunity often correlates with protection against more variable viruses as, for example, has been determined for Influenza viruses (95, 176, 177). Consequently, modern vaccine approaches aim to activate both or rather, an appropriate arm of immunity dependent on the individual biology of the respective virus. Since immune responses, which might protect against emerging viruses, are mostly not known, an induction of both humoral as well as cellular immune responses will maximize the chance of being prophylactic.

1.4.1. Classic vaccine strategies: Live-attenuated pathogen, inactivated pathogen, or subunit vaccines

To evoke protection, similar or even superior to that induced by infections, but without pathogenicity, less virulent (live-attenuated) strains of the respective pathogen have been developed for a range of pathogens like polio virus (7), measles virus (102) or tuberculosis (290). In the late 18th century, Edward Jenner observed that cowpox, a bovine, less virulent relative of smallpox, prevented smallpox infection (128). This observation was later transferred to specifically attenuate virulent microorganisms by passaging them in another species or on different cells *in vitro* (193). However, the use of life-attenuated vaccines may also carry risks of reversion to a pathogenic form, as observed in poliovirus (114) or yellow fever virus vaccines (160). Furthermore, life-attenuated vaccines can become virulent in immunodeficient patients (193). To avoid the risks of reversion, vaccines have also been generated by inactivating the pathogen using, for example, formaldehyde (229), gamma irradiation (6), or UV treatment (37). The inactivation process may, however, alter epitopes or induce atypical immune responses, which might even worsen pathogen-induced disease in vaccinated patients after exposure (231). Such adverse effects have actually stopped any further application of formaldehyde-inactivated respiratory syncytial virus (RSV) (136) or formaldehyde-inactivated measles vaccines (103). Moreover, vaccines based on whole

pathogens like killed *Bordetella pertussis* vaccine (225) might include components which display toxic effects or alter immune responses in general (61).

With the purification or recombinant production of single pathogen subunits, such toxic or immunogenic components are removed and their respective side-effects reduced. However, the choice of appropriate immunogenic and non-toxic antigens depends on extensive knowledge of the pathogen's interaction with its host, such as immune evasion strategies (61). Although subunit vaccines offer a more preferable safety profile than inactivated or life-attenuated vaccines and face fewer regulatory licensure hurdles than life-attenuated pathogens (321), they include the critical disadvantage of low intrinsic immunogenicity (Tab. 1). Therefore, application of multiple doses or the addition of immune-stimulatory adjuvants becomes necessary (61, 209), which raises the costs of production or administration (231). Live-attenuated vaccines, on the contrary, have the advantage of a strong inherent immunogenicity. Moreover, they efficiently initiate CTL effector responses due to the intracellular production of antigens (30, 163) (Tab. 1). Even though live-attenuated vaccines bear a potential risk of residual pathogenicity (61) effectively used vaccines against diseases like measles, mumps and rubella (Tab. 1) have never reverted to a pathogenic form (102). This indicates an excellent safety profile in these examples.

Tab. 1 Comparison of life-attenuated, inactivated and Subunit vaccines. ++, very beneficial; +, beneficial; -, unfavourable.

	Life-attenuated vaccines	Inactivated vaccines	Subunit vaccines
Immunogenicity			
Safety			
Costs	+	++	-
Induced immune responses	humoral and cellular	humoral	humoral

1.4.2. Modern vaccine strategies: Enhancement of immunogenicity and antigen delivery into cells

Modern molecular biological techniques enable the development of new vaccine strategies which combine the safety of subunits with the immunogenicity of life-attenuated vaccines. Recombinant proteins become more immunogenic if they are, for example, fused to immune-stimulatory components like flagellin (274) or assembled into virus-like particles (VLPs) (201). Indeed, VLPs presenting viral antigens are already successfully used as commercial vaccines against HBV (259), human papillomavirus (HPV) (97, 244), or hepatitis E (326). Such modernised subunit vaccines nevertheless still have a disadvantage in that they normally fail to induce CTL responses (30). Consequently, new vaccine

approaches not only aim to enhance the immunogenicity, but also to deliver the antigen into the cell. Then, processed antigen peptide becomes presented on MHC-I to trigger CTL responses. Intracellular expression can be gained, for example, by transfection of DNA plasmids encoding the antigen (140, 163) or by a gene transfer through viral vectors. Focusing on the latter, suitable vectors are, for example, replication-competent or -incompetent adenoviruses (Ads), replication-competent vesicular stomatitis virus (VSV), or replication-incompetent modified vaccinia virus Ankara (MVA) (198, 226). Several preclinical studies using viral vectors targeting viral diseases like AIDS (137) or Ebola (133) have shown that respective vectors elicit both humoral as well as cellular immune responses and may protect animals from lethal challenge.

One important advantage of vector-based vaccines is that they provide an opportunity for genetic manipulation to, for example, specifically alter vector tropism to target cells like APCs (62, 309). Such alteration of tropism can be mediated by expression of foreign glycoproteins (62, 99, 181, 309) or a fusion of, for example, single chain fragments directed against a specific receptor to already expressed glycoproteins (254, 99, 196). Furthermore, immunomodulatory molecules can be co-expressed with inserted antigens to further enhance immunogenicity (1). Depending on the organism that the vectors are derived from, they also vary in the way the antigen is transferred (198). Retroviral vectors, for instance, stably integrate reversely transcribed vector genome into the host's genome. Thus, respective genes of interest, for example, the antigen-encoding genes, become stably expressed and peptides continuously presented (36). Other viral vectors like those derived from Ad, VSV or MV, are characterized by a lack of integration into the host genome. Here, antigens are temporary expressed by infected cells and peptides thus presented for a limited period of time (224). A temporal presentation of peptides can also be achieved by fusion of proteins fused to structural vector proteins, which are then transferred into respective target (276, 279). These different methods of manipulation then enable specific targeting of individual cell populations, a regulation of immunogenicity, or antigen persistence and thereby, adaption to individual characteristics of pathogens.

Indeed, several viral vectors are already licensed as veterinary vaccines like a vaccinia virus vector against rabies (35) or canarypox vector against canine distemper virus (CDV) (213). Moreover, the protective efficacy of the VSV vector-based Ebola-vaccine in a phase III trial during the recent Ebola outbreak in West Africa (153) demonstrates the future potential of vector-based vaccines for application also in human medicine. Indeed, a recombinant chimeric yellow-fever based vaccine (YFV 17D) expressing the structural prM and E proteins of Japanese-encephalitis Virus (JAV) strain JEV SA_{14} -14-2 is already available for

human vaccination against JAV in Australia and Thailand (ChimeriVax-Je, IMOJEV, JE-CV, or THAIJEV) (226, 319).

Thus, potential vaccine strategies against MERS-CoV, H7N9 or CCHFV may consist in life-attenuated or inactivated whole viral particles. While these approaches would include risk of reversion to wild type form or of altered immune responses by inactivation, administration of purified antigens would reveal poor immunogenicity. To combine the immunogenicity of life-attenuated vaccines with the safety of recombinant proteins, antigens of these pathogens might be co-expressed by already characterised (and hence, safe) vaccine platforms. Among life-attenuated virus vaccines, the measles virus (MV) vaccine combines efficacy, characterized by long-lasting immunity, with remarkable safety (102) and may thus be used as a suitable vaccine platform.

1.5. MV as vaccine platform

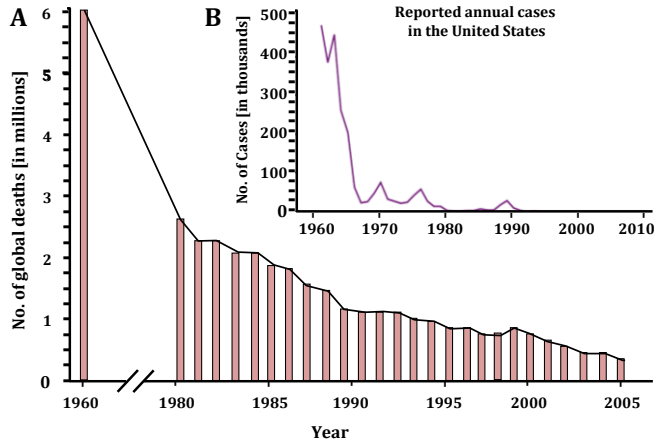

Fig. 9 Trends in worldwide measles mortality. (**A**) Schematic depiction of estimated global measles death cases in millions. Modified after (307). (**B**) Schematic depiction of estimated annual case numbers in the U.S.. Modified after

The approval of the life-attenuated measles virus (MV) vaccine in the 1960s (102, 238) resulted in a significant reduction of MV-associated worldwide death cases, from more than 6,000,000 yearly in 1963 to approximately 345,000 in 2005 (302) (Fig. 9). This illustrated efficacy is, moreover, accompanied by an excellent safety profile, which is depicted by a low rate of adverse effects during its application as vaccine in billions of doses over more than 60 years (102, 238).

Attenuation of the original Edmonston wild type (wt) MV isolate from 1959 to vaccine strains was conducted by passages in chicken embryo fibroblasts (84). This *in vitro* passaging resulted in mutations which, amongst other effects, shifted the virus tropism (267). MV, in its virulent form, targets the signalling lymphocyte activation molecule (SLAM or CD150) expressed on immune cells (269) as well as Nectin-4 on epithelial cells (190, 202). The SLAM-mediated specificity for immune cells is expected to be a cause for MV-induced immunosuppression (12, 187, 203) and thus causative for serious secondary infections (96, 124). MV vaccine strains, on the contrary, use CD46 as an additional receptor,

which is expressed on all nucleated cells. Thus, additional binding to CD46 results in a reduction of the virus specificity for immune cells (197).

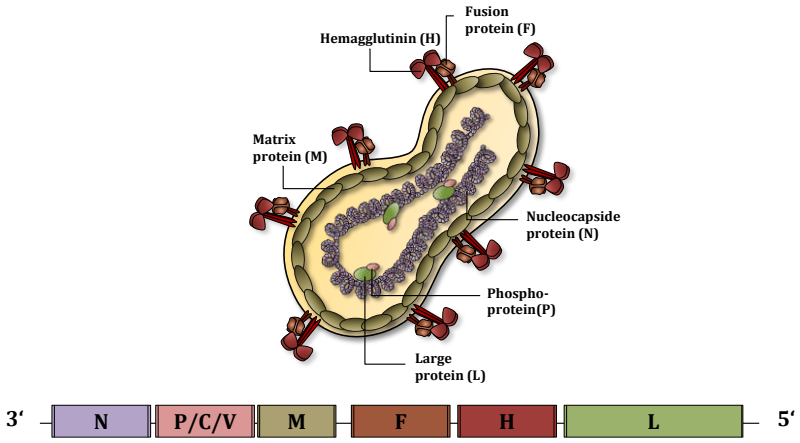

Fig. 10 Measles viruses structure. Schematic depiction of a measles virus particle. The genome encodes for the structural proteins nucleocapsid protein (N), phosphoprotein (P), matrix protein (M), fusion protein (F), hemagglutinin (H) and the large (L) proteins as well as the accessory proteins C and V. The genes are organized in transcriptions units.

Due to availability of a recombinant rescue system (175, 218) recombinant MV vaccines (rMVs) can be rapidly produced from DNA plasmids. This allows genetic manipulations like the insertion of additional gene segments. In general, MVs non-segmented viral ss(-)RNA genome is organised in gene cassettes separated by intergenic regions, which contain sequences regulating viral gene transcription. Since each transcription unit is flanked by individual start and stop sequences, the viral polymerase complex individually transcribes each genome cassette. This organisation allows easy insertion of additional transcription units (ATUs) up to 6 kb between different genome cassettes into the genome (27). These ATUs are then co-expressed with the viral proteins, the nucleocapsid protein (N), phosphoprotein (P), matrix protein (M), fusion protein (F), hemagglutinin (H) and the large proteins (L) (78) (Fig. 10). Re-initiation of transcription is not 100% successful at each start-stop signal, and thus leads to a transcription gradient of the MV genome from 3’ to 5’ with the highest expression of the N- gene (42). This property can be utilised to regulate the expression of the inserted genes by the choice of genomic position the genes are inserted into (67).

Recombinant rescue technology enables not only the production of MV expressing marker genes (81) or immunomodulatory proteins like IL-12 (247), but also foreign bacterial (125) or viral antigens, as summarised in Tab. 2. These experimental MV-based vaccines were shown to induce both antigen-specific humoral as well as cellular immunity against viruses like HIV (164), SARS-CoV (161), or chikungunya virus (CHIKV) (33). Moreover, induced immune responses protected mice (HIV, WNV, CHIKV) (33, 69, 164) and non-human primates (HIV, WNV) (32, 164) against lethal challenge with HIV, WNV or CHIKV and thus demonstrated MVs efficiency as a vaccine platform. Interestingly, pre-formed immunity against MV was shown to have no effect on the induction of pathogen-specific antibodies in MV-CHIKV vaccinated mice (33, 164), MV-HIV vaccinated non-human primates (164) or

even in MV-CHIKV vaccinated human patients (219). Moreover, vaccinated mice were protected against CHIKV exposure (33) irrespective of pre-existing immunity. These results indicate that MV-based vaccine platforms are applicable in both naïve and pre-immune patients.

Tab. 2 Experimental MV-derived vaccines. n.t not tested

Pathogen	Antigen	Position	Response	Protection	Reference
HBV	sHBsAg	P, H, L	α-HBsAg-Abs, nAbs	n.t. (**MV**)	(248, 67)
Mumps	HN or F	P	n.t.	n.t.	(287)
SIVmac	Env (+ Gag)	P	α-SIV-env-Abs	n.t.	(287, 333)
WNV	E	P	nAbs	**Yes**	(69)
HIV-1	Env	P	α-HIV-1-env-Abs, nAbs, IFN-γ-ICS	n.t.	(164, 165)
Dengue	EDIII, ectoM	P	α-EDIII/M-Abs, nAbs, Cytokines	n.t.	(31)
SARS-CoV	S, N	P	α-SARS-S-Abs, α-SARS-N-Abs nAbs, IFN-γ-ELISpot	n.t.	(161)
CHIKV	C-E3-E2-6K-E1 (VLPs)	P	α-CHIKV-E2-Abs, nAbs, IFN-γ-ELISpot, **nAbs in humans**	**Yes**	(33, 219)

Taken together, rMVs can be rapidly and easily produced and allow the insertion and co-expression of antigens encoded by heterologous gene fragments up to at least 6 kb. Moreover, they induce both humoral and cellular immunity, which have been shown to be protective in challenge experiments. These characteristics, as well as MV's efficacy and safety, illustrated by a 50-year application without severe adverse effects, make it a promising pre-pandemic vaccine platform.

1.6. The aim of this thesis

The aim of this PhD thesis was to generate and characterise potential pre-pandemic vaccine candidates derived from the well-known replication-competent MV vaccine platform. To test MV's applicability against phylogenetically distinct viruses, the highly-pathogenic emergent viruses MERS-CoV and H7N9, as well as the frequently re-emergent CCHFV have been chosen as examples. However, the development of most efficient antiviral drugs and vaccines is based on detailed knowledge of how viral mechanisms mediate pathogenicity. Since knowledge is limited for emerging viruses, this thesis also aimed to gain insights into MERS-CoV's pathomechanisms, thereby focusing on induced innate immune responses.

Interaction of MERS-CoV with innate immune cells: Previous studies demonstrated that MERS-CoV failed to induce a secretion of antiviral type I IFNs in human epithelial cells (330, 46, 147) or macrophages (325). These observations indicate that MERS-CoV developed a mechanism to inhibit type I IFN responses, which might be crucial for the progress of disease. Consequently, this thesis aims to identify potential alternative sources of type I and II IFN production via the inoculation of different human and murine APCs (Macrophages, B cells, pDCs, or mDCs) with MERS-CoV. The insights gained into the interaction of MERS-CoV with cells of the innate immune system might uncover new opportunities to develop antiviral drugs and vaccines in the future.

Setting up a system to re-stimulate T cells ex vivo and to analyse T cell responses: In conjunction with the generation of vaccine candidates, appropriate immune assays such as the neutralisation test, ELISpot- or T-cell killing assays, had to be established in advance to analyse immune responses in vaccinated animals. For this purpose, antigen-transgene DC cell lines were generated and tested to re-stimulate *in vivo* primed T cells, independent of knowledge about immunodominance and commercial availability of respective immunogenic peptides. Respective DC cell clones should not only be used to test material from mice vaccinated with recombinant MVs, but also with a distinct platform: LV protein transfer vectors (LV-PTVs).

Generation and characterisation of vaccine-derived MV as pre-pandemic vaccine platform: The main part of this thesis aims to test the applicability of MV as a vaccine platform against emerging infections. For that purpose, recombinant MVs expressing full-length and truncated forms of envelope or nucleoproteins of MERS-CoV, H7N9 and CCHFV should be generated to identify the most immunogenic vaccine candidates. Subsequent *in vitro* characterisation of these vaccines should than include a validation of their stable integration into rMV's genome, as well as antigen expression and their impact on the vaccine's replication. After vaccination of MV-susceptible IFNAR$^{-/-}$CD46Ge mice, induced humoral and cellular immunity should be tested using the established methods. Finally, a set of appropriate challenge experiments had to be established to demonstrate whether the induced immune responses are effective in protecting against viral infection.

Consequently, the results gained from this thesis will uncover whether MV constitutes a sufficiently robust and efficient platform to protect against emerging infections. It is hoped that recombinant vaccine-derived MVs can be used in the future to immediately react to increased pandemic threats involving key viruses, as well as offering a way to act against any new emerging pathogens.

2. OWN CONTRIBUTION

Three publications form part of this cumulative PhD thesis. My own contribution to these publications in detail is as follows:

a) **High secretion of interferons by human plasmacytoid dendritic cells upon recognition of Middle East respiratory syndrome coronavirus**. Scheuplein VA, Seifried J*, **Malczyk AH***, Miller L, Höcker L, Vergara-Alert J, Dolnik O, Zielecki F, Becker B, Spreitzer I, König R, Becker S, Waibler Z, Mühlebach MD. J Virol. 2015 Apr;89(7):3859-69. doi: 10.1128/JVI.03607-14. Epub 2015 Jan 21.
*equally contributed

As a contributing author to the publication "High secretion of interferons by human plasmacytoid dendritic cells upon recognition of Middle East respiratory syndrome coronavirus", I provided detailed, hands-on support during the planning and execution phases of the experiments. In detail, I supported Dr Scheuplein in isolating murine bone-marrow derived cells in two independent experiments. Moreover, I participated in several infection experiments of murine and human immune cells with MERS-CoV, as well as the execution of ELISAs (Fig. 1A, Fig. 2A, Fig. 3A-L, Fig. 4C), the determination of MERS-CoV's replication kinetics on different APCs (Fig. 1B, Fig. 2A) and the isolation of viral RNA (Fig. 2B). Additionally, I was responsible for western blot analysis (Fig. 5 B-D) and for the design of Fig. 6. Furthermore, I participated in the data analysis of all respective experiments and in the proofreading of the final manuscript.

b) **Lentiviral Protein Transfer Vectors Are an Efficient Vaccine Platform and Induce a Strong Antigen-Specific Cytotoxic T Cell Response**. Uhlig KM, Schülke S, Scheuplein VA, **Malczyk AH**, Reusch J, Kugelmann S, Muth A, Koch V, Hutzler S, Bodmer BS, Schambach A, Buchholz CJ, Waibler Z, Scheurer S, Mühlebach MD. J Virol. 2015 Sep;89(17):9044-60. doi: 10.1128/JVI.00844-15. Epub 2015 Jun 17.

Regarding the publication "Lentiviral Protein Transfer Vectors Are an Efficient Vaccine Platform and Induce a Strong Antigen-Specific Cytotoxic T Cell Response", I was responsible for the set-up and implementation of assays for determining T cell-mediated cellular immunity. For that purpose, I conducted preliminary experiments to establish appropriate cell numbers and peptide concentrations in order to re-stimulate T cells which were isolated from vaccinated mice. I supported the diploma student Bianca Bodmer by performing preliminary experiments aimed at revealing the applicability of the Ova-transgenic DC cell line JAWSII$_{Green}$-Ova (generated by Bianca Bodmer) to stimulate Ova-specific T cells using OT-1 or OT-2 T cells from respective transgenic mice. I also assisted

during the isolation of splenocytes from vaccinated mice, magnetic bead sorting and the re-stimulation of T cells (Fig. 7, Fig. 8). Moreover, I evaluated the ELISpot analysis (Fig. 7, Fig. 8) and operated the western blot analysis detecting VSV-G, MV-H, or MV-F (Fig. 2D-F, 3G-I). In addition, I participated in data analysis of the respective experiments and proofreading the manuscript.

c) **A Highly Immunogenic and Protective Middle East Respiratory Syndrome Coronavirus Vaccine Based on a Recombinant Measles Virus Vaccine Platform**. **Malczyk AH**, Kupke A*, Prüfer S*, Scheuplein VA, Hutzler S, Kreuz D, Beissert T, Bauer S, Hubich-Rau S, Tondera C, Eldin HS, Schmidt J, Vergara-Alert J, Süzer Y, Seifried J, Hanschmann KM, Kalinke U, Herold S, Sahin U, Cichutek K, Waibler Z, Eickmann M, Becker S, Mühlebach MD. J Virol. 2015 Nov;89(22):11654-67. doi: 10.1128/JVI.01815-15. Epub 2015 Sep 9.
*equally contributed

In connection with the publication, "A Highly Immunogenic and Protective Middle East Respiratory Syndrome Coronavirus Vaccine Based on a Recombinant Measles Virus Vaccine Platform", I was responsible for the set-up of the main experiments. I obtained the recombinant MV-MERS vaccines in passage 3 by Steffen Prüfer and subsequently characterised the vaccines *in vitro.* Here, I was responsible for the isolation and sequencing of viral RNA, as well as validation of antigen expression, analysis of replication kinetics, and long-term passaging of viral vaccines until passage 10, with subsequent re-characterisation for conserved vaccine properties. I also generated respective lentiviral gene transfer vectors (cloning, transfection, purification) to produce MERS-S- or MV-N-transgenic DC cell lines and selected the most appropriate cell clones after validation of stable antigen expression. Furthermore, I established the assays for analysis of cellular (ELISpot, proliferation, killing assay) and humoral (α-MERS-S ELISA and α-MERS neutralisation assay) immune responses. Supported by Steffen Prüfer and Dr Scheuplein, I immunised MV-susceptible IFNAR$^{-/-}$ CD46Ge mice, which had been bred with the assistance of Dorothea Kreuz, using C57BL/6 background IFNAR$^{-/-}$ mice provided by Prof Kalinke. Supported by Steffen Prüfer, Dr Scheuplein, and Dr Hutzler, I collected mouse tissue, and with support of Dr Scheuplein, I analysed the induced humoral and cellular immune responses. Additionally, I was responsible for vaccinating mice for the challenge experiments. These were shipped to our collaborating partners in Marburg, where a challenge model had been set up (in cooperation with colleagues from the University of Gießen). In Marburg, the transduction as well as challenge of mice were conducted. I was responsible for generating respective figures based on all experimental data. Together with Dr Mühlebach, I also wrote the text for the manuscript.

OWN CONTRIBUTION

The results published in these manuscripts, as well as some as yet unpublished data, are all described in Section 3 as continuous text, irrespective of my own contribution. Nonetheless, those experiments where I did not participate are clearly indicated and the respective persons who did in fact conduct the experiments, are all named in footnotes.

With my signature, I confirm the correctness of the declaration in section 2.

Marburg, 28-02-17

Anna Fiedler	Prof. Dr Stephan Becker
(author)	(supervisor)

3. RESULTS

3.1. Analysis of interactions of MERS-CoV with the innate immune system

Among antiviral innate immune responses, the secretion and action of type I IFNs has a significant role in virus clearance (193). However, initial studies have demonstrated that MERS-CoV fails to induce the production of type IFNα/β in human epithelial cells (330, 46, 147) and macrophages (325), thereby indicating that the virus somehow inhibits the production of IFNs. Interestingly, the coronavirus relative SARS-CoV, does provoke a type I IFN response by pDCs (44) even though the virus failed to induce a secretion of IFN-α or IFN-β by epithelial cells (46) or macrophages (47, 329). Since MERS-CoV is even more sensitive to type I IFN treatment than SARS-CoV (330), a comparable IFN-α/β production by pDCs or other APCs may prove to be crucial for the outcome of disease. Thus, the first part of this PhD thesis aimed to identify possible sources of type I or III IFNs upon MERS-CoV infection by the inoculation of different APCs of murine and human origin with MERS-CoV.

3.1.1. Analysis of type I IFNs and viral replication in murine and human APCs

To first test the capability of murine APCs to secrete type I or III IFNs upon MERS-CoV infection, mDCs, pDCs and macrophages were derived from bone marrow cells and peritoneal exudate cells (PECs) isolated from the peritoneal cavity of wildtype (wt) C57BL/6 (BL/6) mice[1]. After inoculation with MERS-CoV, the secretion of IFN-α, -β, and -λ into supernatants were analyzed by enzyme-linked immunosorbent assay (ELISA). However, none of the analyzed murine APCs secreted type I or III IFNs upon MERS-CoV infection, although they were in general responsive to treatment with appropriate positive controls (Scheuplein *et al.*, 2015, Fig. 1A). Moreover, the virus did not replicate in murine cells (Scheuplein *et al.*, 2015, Fig. 1B), which is consistent with absent capacity of MERS-CoV to infect murine cells, as later published (51).

To analyse the IFN response by human APCs, B cells, pDCs, and monocytes were isolated from the blood of healthy human donors and monocytes were differentiated into monocyte-derived DCs (MDDCs), M1, or M2 macrophages[2]. APCs were then inoculated with MERS-CoV. Subsequent analysis of type I and III IFN secretion showed that neither M1

[1] For most experiments, cells were isolated by Dr Miller and Dr Höcker, Paul-Ehrlich-Institut, Langen
[2] Cells isolated by Dr Scheuplein, Dr Miller, or Dr Seilfried, Paul-Ehrlich-Institut, Langen

macrophages, M2 macrophages, B cells, nor MDDCs secreted IFN-α, -β, or -λ upon MERS-CoV infection (Scheuplein *et al*., 2015, Fig. 2A). Furthermore, the virus did not replicate in those cells (Scheuplein *et al*., 2015, Fig. 2C). On the other hand, pDCs, secreted both IFN-β and -λ, as well as high amounts of IFN-α. The secretion of IFN-α and IFN-β was significantly enhanced in comparison with SARS-CoV (Scheuplein *et al*., 2015, Fig. 2A). Moreover, pDCs became initially infected by MERS-CoV, since viral RNA copy numbers of MERS-E protein (Scheuplein *et al*., 2015, Fig. 2B) and expression of MERS-CoV nucleocapsid protein (MERS-N) (Scheuplein *et al*., 2015, Fig. 5) was demonstrated in infected cells. However, as observed in other APCs, the virus failed to fully replicate in pDCs (Scheuplein *et al*., 2015, Fig. 2C).

3.1.2. Role of receptor binding and endosomal transport for MERS-CoV infection and IFN secretion

While MERS-CoV did not trigger a type I or III IFN response in most human APCs, pDCs secreted high amounts of, particularly, IFN-α. Interestingly, human, but not murine pDCs, were responsive to MERS-CoV inoculation. Since MERS-CoV has in the meantime been shown to utilise human DPP-4, but not murine DPP-4 for cell entry (49), it was hypothesised that the observed IFN secretion depends on receptor binding. To test this hypothesis, pDCs were pre-treated with the receptor binding domain (RBD) of MERS-CoV Spike protein (MERS-S), which binds to huDPP-4 and thus hinders MERS-CoV from receptor binding (188). It was discovered that, pre-incubation with RBD, but not control protein, is in fact responsible for the inhibited production of IFN-α, -β, and -λ (Scheuplein *et al*., 2015, Fig. 3D-F). However, in the case of unspecific CpG treatment, used as general stimulus for the IFN induction, IFN secretion of RBD-co-treated pDCs also became abolished (Scheuplein *et al*., 2015, Fig. 4C). This indicates that MERS-S RBD may possess general immune-suppressive properties. Nevertheless, both the RBD and, in particular, polyclonal sera binding DPP-4, inhibited the expression of MERS-N in pre-incubated cells. This demonstrates that the infection of pDCs depends on the binding of MERS-CoV to DPP-4 (Scheuplein *et al*., 2015, Fig. 5C).

When the acidification of endosomes was blocked by chloroquine treatment, the numbers of MERS-CoV-N and MERS-CoV-E RNA copies appeared to be significantly reduced (Scheuplein *et al*., 2015, Fig. 5A). The secretion of IFN-α, -β, or -λ was likewise significantly inhibited, indicating that the infection and IFN secretion depends on endosomal uptake (Scheuplein *et al*., 2015, Fig. 3G-I). Moreover, pre-treatment with the TLR7 inhibitor IRS661, reduced the secretion of IFN-α, -β, or -λ (Scheuplein *et al*., 2015, Fig. 3J-L). These results imply that secretion of these IFNs is most likely, at least in part, mediated through

recognition of viral RNA via TLR7. Interestingly, UV-inactivated MERS-CoV[3] induced similar amounts of IFN-α and IFN-λ, but significantly less IFN-β (Scheuplein *et al.*, 2015, Fig. 3A-C). These results further indicate that secretion of IFN-β depends on recognition of intact viral RNA.

Thus, this data, published in Scheuplein *et al.*, demonstrated that MERS-CoV predominantly triggers secretion of type I and III IFN by human pDCs. These antiviral innate immune responses were shown to depend on endosomal, probably DPP-4-mediated, uptake and at least in part, on the sensing of viral RNA via TLR-7 in the endosome. The relevance of the exclusively pDC-attributed type I and III IFN production for MERS-CoV pathogenicity is so far not understood. However, to protect against pathogenicity of MERS-CoV, the generation of vaccines against MERS-CoV is considered to be beneficial to efficiently clear virus infection.

3.2. Generation and *in vitro* characterisation of MV-MERS-CoV, MV-H7N9 and MV-CCHFV vaccines

During the ongoing epidemic in the Middle East, MERS-CoV was identified as a priority pathogen for vaccine development in the WHO research and development (R&D) blueprint plan, in addition to, CCHFV and other highly pathogenic viruses (295). Consequently, the aim of this thesis was to produce broadly immunogenic MV based-vaccines, not only against MERS-CoV and CCHFV, but also against influenza A virus subtype H7N9 - another highly pathogenic emergent virus.

For this purpose, certain envelope glycoproteins that mediate receptor binding were chosen to act as suitable antigens to induce particulary neutralising antibodies (nAbs). The glycoproteins chosen were spike protein (MERS-S) of MERS-CoV, the haemagglutinin of subtype 7 (H7) of H7N9, and Gc and Gn of CCHFV. However, in contrast to membrane-bound proteins like viral envelope glycoproteins, soluble antigens are normally more efficiently taken up by B cells (16, 21, 208) and are thus more efficient in inducing humoral immune responses (85). Since protection against SARS-CoV correlates with humoral immunity (261, 313), a truncated soluble version of MERS-S (MERS-solS) was consequently cloned to further enhance humoral immunity. This approach was also applied to the prospective CCHFV-vaccine. Soluble and membrane-bound variants of CCHFV-Gc and CCHFV-Gn were inserted into the MV genome (Fig. 11). Since influenza viruses are known to evade nAbs directed against HA, the more conserved envelope glycoprotein neuraminidase (NA) N9

[3] Inactivation performed by Dr Scheuplein, Paul-Ehrlich-Institut, Langen

was chosen as another suitable antigen for an MV-based vaccine against H7N9. The nucleocapsid proteins of MERS-CoV (MERS-N) and CCHFV (CCHFV-N) were additionally selected to induce cellular immune responses directed against the more conserved inner proteins of MERS-CoV and CCHFV.

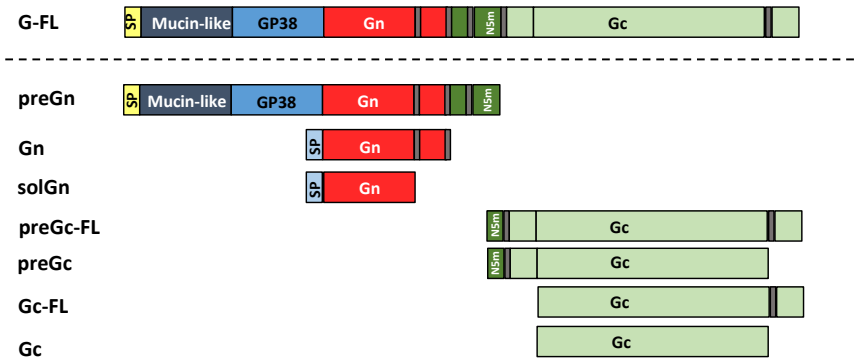

Fig. 11 Schematic illustration of cloned CCHFV variants. Different polyprotein domains after cleavage are depicted in different colors. Grey, transmembrane domain; SP, signal peptide.

These antigens were inserted into additional transcription units (ATUs) after the gene cassettes encoding for the P (post-P) or the H protein (post-H) (Malczyk *et al.*, 2015, Fig. 1A) of the Moraten vaccine strain clone MV_{vac2}, respectively. The insertion into two different positions enabled a different expression of the antigens, which is normally higher in the post-P, as opposed to the post-H, position. All viruses were successfully rescued and MV_{vac2}-MERS[4] and MV_{vac2}-H7N9[5] viruses passaged until passage 10 (P10).

No mutations in the extra expression cassettes in the viral genome were identified, even after ten passages, indicating the genetic stability of these vaccines. Moreover, the viruses efficiently expressed MERS-S, MERS-solS (Malczyk *et al.*, 2015, Fig. 1B), MERS-N (Fig. 12A), H7 (Fig. 12B), N9 (Fig. 12E), CCHFV-Gc, CCHFV-Gc-FL, CCHFV-preGc, CCHFV-preGc-FL, CCHFV-G-FL (Fig. 12D) or CCHFV-N (Fig. 12C). As expected, all viruses, except for MERS-S and MERS-solS, revealed stronger antigen expression when the antigens were encoded by the post-P ATU. However, the Ab utilised for the detection of CCHFV-Gn failed to display expression of Gn variants encoded by the respective recombinant vaccines, or in an appropriate positive control, inactivated CCHFV-particles (data not shown).

[4] Plasmids cloned by Christiane Tondera, viruses rescued by Steffen Prüfer, Paul-Ehrlich-Institut, Langen
[5] Plasmids and viruses generated by Bianca Bodmer during her internship under supervision of Dr Hutzler, Paul-Ehrlich-Institut, Langen

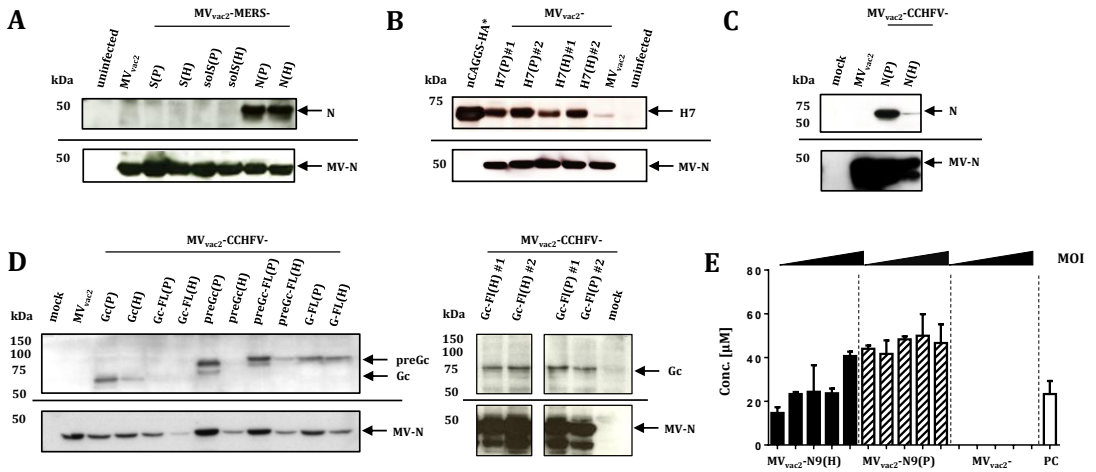

Fig. 12 Antigen expression triggered by prospective MV derived vaccines against MERS-CoV, H7N9, or CCHFV. (A-E) Immunoblot analysis of Vero cells infected at an MOI of 0.03 with indicated viruses. Uninfected cells served as mock controls. Arrows indicate specific bands. Lower blots were probed using a mAb reactive against MV-N. Upper blots were probed using **(A)** α-MERS-CoV rabbit serum, **(B)** rabbit serum reactive against H7N1, **(C)** a mouse α-CCHFV-N # 9D5 mAb, or **(D)** a mouse α-CCHFV-preGc # 11E5 mAb. **(E)** Neuraminidase activity assay for analysis of N9 expression. Uninfected or MV_{vac2}-GFP(N) infected cells served as negative and pGAGGS-NA transfected 293T cells as positive controls (PC);*transfected 293 T cells; n=3.

Despite the insertion of gene fragments up to 5 kb, 22 out of 24 viruses showed no significant changes in their replication pattern when compared to control viruses expressing GFP (Malczyk *et al.*, 2015, Fig. 1C-D) (Fig. 13A-E). However, MV_{vac2}-CCHFV-solGn(P) and MV_{vac2}- CCHFV-G-FL(P) reached 34-fold ($7.6x10^4$ $TCID_{50}$/ml versus $2.6x10^6$ $TCID_{50}$/ml MV_{vac2}- GFP(P)) and 45-fold ($5.8x10^4$ $TCID_{50}$/ml versus $2.6x10^6$ $TCID_{50}$/ml MV_{vac2}- GFP(P)) reduced maximum cell-associated titres compared to control viruses, respectively, indicating that the expression of these antigens somehow impairs viral replication (Fig. 13C, E; red curves).

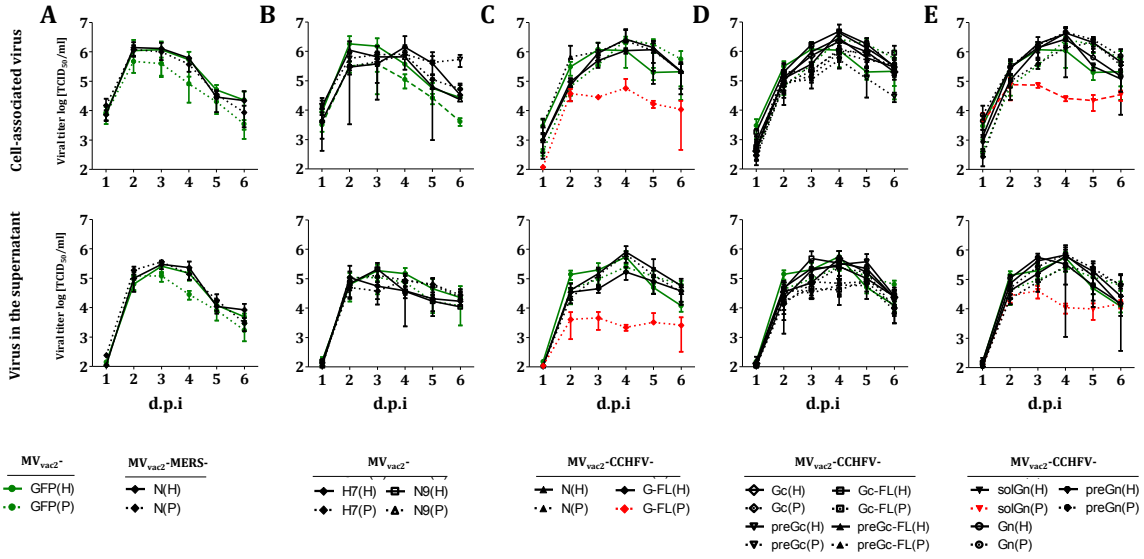

Fig. 13 Growth kinetics of prospective MV-derived vaccines against MERS-CoV, H7N9, or CCHFV. Growth kinetics of recombinant MV on Vero cells infected at an MOI of 0.03 with indicated MV_{vac2} encoding for **(A)** MERS-CoV-N, **(B)** H7, N9, or **(C)** CCHFV-G-FL, CCHFV-N, **(D)**CCHFV-preGc-FL, CCHFV-preGc, CCHFV-Gc-FL, CCHFV-Gc, **(E)** CCHFV-preGn, CCHFV-Gn, or CCHFV-solGn. MV_{vac2}-GFP viruses served as control vaccines (green). Means ± SD; n=3.

Taken together, recombinant MVs encoding for antigens of three distinct viruses, MERS-CoV, H7N9, or CCHFV, were produced, which expressed the inserted antigens, mostly without significant effects on viral replication. Moreover, long-term passaging did not result in mutations, thus demonstrating the genetic stability of these viruses. After successful *in vitro* characterisation, vaccines against MERS-CoV and H7N9 were tested for their ability to induce immune responses *in vivo*.

3.3. Characterisation of induced humoral immune responses

Based on their high levels of antigen expression, the prospective vaccines MV_{vac2}-MERS-S(H), MV_{vac2}-MERS-solS(H), MV_{vac2}-H7(P), and MV_{vac2}-N9(P) were chosen for subsequent *in vivo* characterisation. Although the expression of MERS-N was higher after insertion into the post-P ATU of MV_{vac2}, MV_{vac2}-MERS-N(H) was selected to enable an appropriate comparison to MV_{vac2}-MERS-S(H) and MV_{vac2}-MERS-solS(H). For this purpose, IFNAR$^{-/-}$ CD46Ge mice, which transgenically express the human CD46 and lack the type I IFN receptor[6], were vaccinated with $1x10^5$ $TCID_{50}$ of the respective vaccines, as well as a medium (OptiMEM) or control vaccine virus (MV_{vac2}-ATU(P)) in a prime-boost setting (Fig. 14). Sera collected on days 0, 28 and 72 were then analysed for the presence of total (α-CoV-S, α-H7N9) and neutralising antibodies (nAbs) (α-MERS-CoV, α-H7N9, and α-MV).

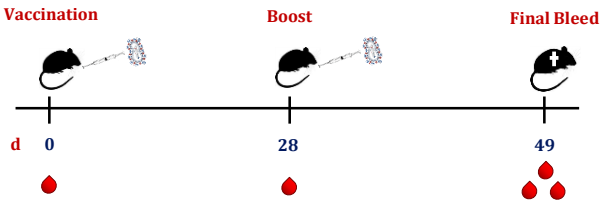

Fig. 14 Vaccination set-up to analyse humoral immunity. IFNAR$^{-/-}$CD46Ge mice were intraperitonally vaccinated with $1x10^5$ $TCID_{50}$ of respective vaccines on days 0 and 28 and blood was sampled on day 0, 28, and 49.

3.3.1. Induction of humoral immune responses by prospective MV-MERS vaccines

The analysis of humoral immune responses directed against MERS-CoV demonstrated that a vaccination with MV_{vac2}-MERS-S(H) and MV_{vac2}-MERS-solS(H), but not with OptiMEM or MV_{vac2}-ATU(P), resulted in the production of α-MERS-S Abs, determined in an α-MERS-S ELISA[7] (Malczyk *et al.*, 2015, Fig. 2). To test whether these Abs were functional and neutralised forms of MERS-CoV, nAbs in mouse sera were titrated to determine respective virus-neutralising titres (VNTs). As expected, MV_{vac2}-MERS-S(H) and MV_{vac2}-MERS-solS(H)

[6] Breeding performed by Dorothea Kreuz, Paul-Ehrlich Institut, using BL-6 background IFNAR$^{-/-}$ mice provided by Prof. Kalinke, TWINCORE and Center for Infection Research, Hannover

[7] Recombinant MERS-S protein for ELISA plate coating was produced and kindly provided by Dr Beissert, Prof. Sahin, TRON GmbH, Mainz, and Dr Hubich-Rau and Prof. Sahin, University of Mainz

(Malczyk *et al*., 2015, Fig. 3B), but not MV_{vac2}-MERS-N(H) (Fig. 15) provoked an induction of MERS-CoV VNTs above detection limit. MV_{vac2}-MERS-S(H), or MV_{vac2}-MERS-solS(H) induced VNTs were five- to seven-fold boosted by the second immunisation (167±137 to 847±1012, or 96±86 to 640±710 VNT, respectively) (Malczyk *et al*., 2015, Fig. 3C). In parallel, the induction of α-MV nAbs was also tested and revealed anti-MV immunogenicity of MV_{vac2}-MERS-S(H), MV_{vac2}-MERS-solS(H), MV_{vac2}-CoV-N(H) and MV_{vac2}-ATU(P) (Malczyk *et al*., 2015, Fig. 3D-F) (Fig. 15). The vaccines therefore, did not vary in infectivity.

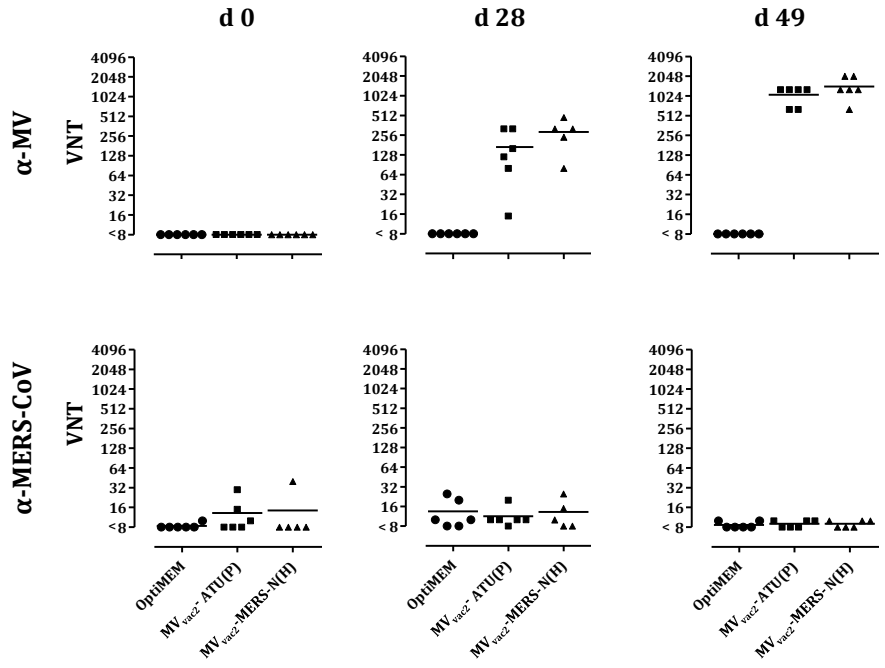

Fig. 15 Analysis of neutralising antibodies. Virus neutralising titers (VNTs) for animals vaccinated on days 0 and 28 with indicated viruses. Sera were sampled on day 0, 28, and 49. Medium (OptiMEM) or MV backbone inoculated (MVvac2-ATU(P)) mice served as controls. VNT were calculated as reciprocal of the highest dilution abolishing infectivity of 200 TCID50 of MERS-CoV or 50 pfu of MV. Dots represent single animals (n = 6). Horizontal line represents mean per group. Y axis starts at detection limit. All mice at detection limit had no detectable VNT.

To analyse whether the induction of nAbs depends on the replication of the vaccine viruses, mice were vaccinated with the same amounts of live or UV-inactivated MV_{vac2}-MERS-S(H). In contrast to the replication-competent MV_{vac2}-MERS-S(H), the UV-inactivated vaccine neither induced α-MERS-CoV nAbs, nor α-MV nAbs. This indicates that the induction of humoral immune responses required active replication of MV-derived vaccines (Fig. 16).

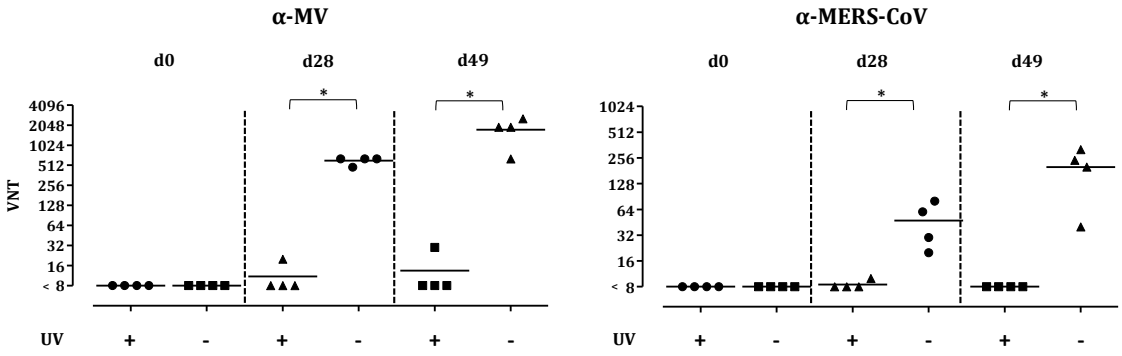

Fig. 16 VNTs induced by UV-inactivated or replicating MV-MERS-S. Virus neutralising titers (VNTs) for animals vaccinated on days 0 and 28 with indicated viruses. Sera were sampled on day 0, 28, and 49. Medium (OptiMEM) or MV backbone inoculated (MV_{vac2}-ATU(P)) mice served as controls. VNTs were calculated as reciprocal of the highest dilution abolishing infectivity of 200 $TCID_{50}$ of MERS-CoV or 50 pfu of MV. Dots represent single animals (n = 4). Horizontal line represents mean per group. Y axis starts at detection limit. All mice at detection limit had no detectable VNT. Mann-Whitney-test (unpaired values); *,P<0,05.

To further investigate whether MV-derived vaccines against H7N9 are also capable of inducing humoral immune responses *in vivo*, sera of vaccinated mice were tested for the presence of H7N9-specific, or H7N9 nAbs.

3.3.2. Induction of humoral immune responses by MV-H7 or MV-N9

Here, vaccination with either MV_{vac2}-H7(P) or MV_{vac2}-N9(P), but not with MV_{vac2}-ATU(P), tended to induce α-H7N9 binding Abs, determined by an immune peroxidase monolayer assay (IPMA) (Fig. 17). Abs triggered by MV_{vac2}-H7(P), but not by MV_{vac2}-N9(P) or MV_{vac2}-ATU(P), moreover inhibited the haemagglutination of A/Puerto Rico/8/1934 H7N9, as determined in haemagglutination inhibition assay (HAI) (Fig. 17). Contrary to expectation, antibodies induced by either MV_{vac2}-N9(P) or MV_{vac2}-H7(P) inhibited the neuraminidase activity of A/Puerto Rico/8/1934 H7N9, as determined by enzyme-Linked Lectin Assay (ELLA). This indicates that α-HA Abs affect the NA cleavage of sialic-acids when binding H7 complexed with N9 on the surface of virus particles (Fig. 17). Both IPMA and HAI titres of MV_{vac2}-H7(P) were boosted 1.5-fold (4667±1633 to 7555±4352 IPMA titers, or 167±82 to 240±88 HI titers); the IPMA titre of MV_{vac2}-N9(P), 3.3-fold (2535±1631 to 8001±5631 IPMA titers) by the second vaccination. However, the 50% NA inhibitory concentration (IC_{50}) for most mice, proved to be beyond the upper limit of detection (>640) after the first immunisation, so boosting could, consequently, not be observed. Interestingly, H7N9-specific Abs (on d28 and d49) were abortive in one MV_{vac2}-N9(P) vaccinated mouse (mouse 599) and IPMA titres (on d49; d28 not tested) were 32-fold lower, compared to other mice. Thus mouse 599 was likely not responsive to vaccination.

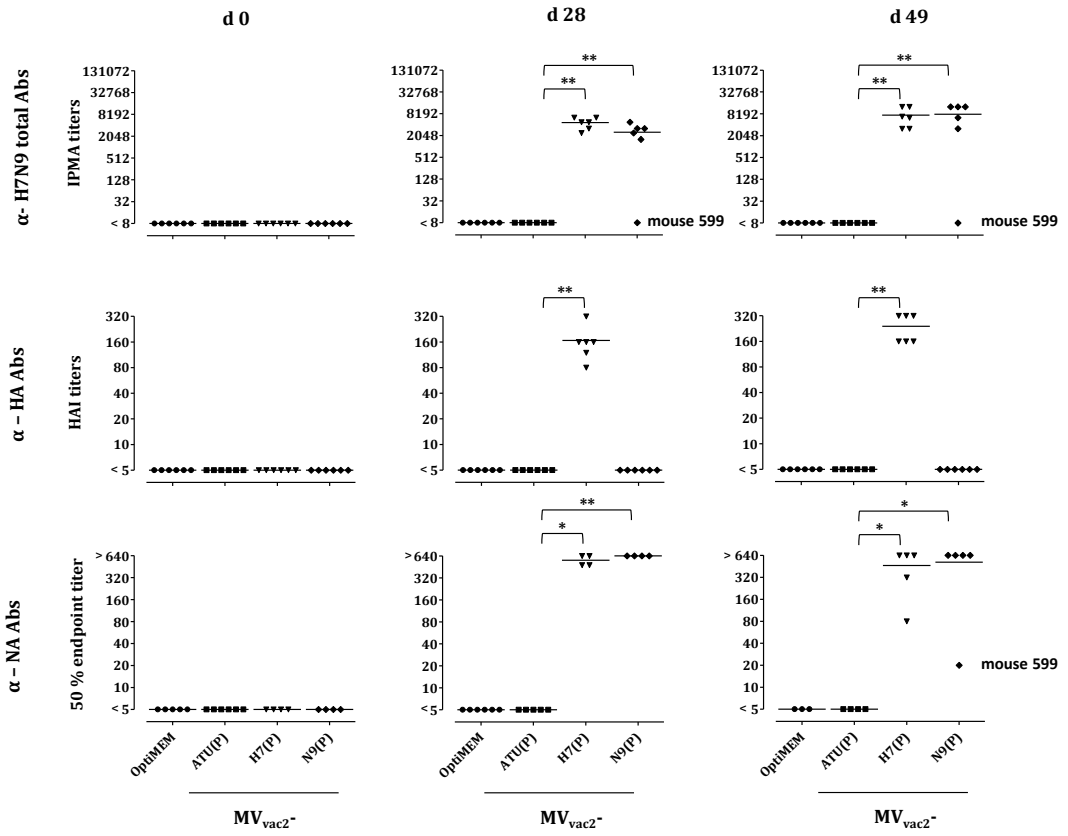

Fig. 17 Induction of H7N9-specific antibodies. Blood of mice vaccinated on days 0 and 28 with indicated viruses was sampled on day 0, 28 and 49. Sera were analyzed for total H7N9-binding Abs, hemagglutination inhibiting titers (HAI-Titers) and neuraminidase inhibiting titers (NAI). Medium (OptiMEM) or MV backbone inoculated (MV_{vac2}-ATU(P)) mice served as controls. Total α-H7N9 Abs were determined as the reciprocal of the highest serum dilution staining A/Puerto Rico/8/1934 H7N9 infected cells in IPMA. HAI-Titers were calculated as the highest serum dilution abolishing the hemagglutination properties of H7. Neuraminidase Inhibition was calculated as the 50% NA inhibitory concentration (IC_{50}) after incubation of A/Puerto Rico/8/1934 H7N9 with mice sera in ELLA. Dots represent single animals (n = 6). Horizontal line represents mean per group. Y-axis starts at detection limit. All mice at detection limit had no detectable titers. Mann-Whitney-test (unpaired values); *, P<0.05; **, P<0.01.

The capacity of MV_{vac2}-H7(P), or MV_{vac2}-N9(P) Abs to prevent infection by A/Puerto Rico/8/1934 H7N9 was tested in a neutralisation assay. As expected, MV_{vac2}-H7(P), but not MV_{vac2}-N9(P), or MV_{vac2}-ATU(P), induced high amounts of nAbs, which were 1.5-fold boosted by a second immunisation (573±270 to 933±310 VNT) (Fig. 18). Consistent with the data obtained for the putative MERS-CoV vaccines, MV_{vac2}-H7(P), MV_{vac2}-N9(P) and MV_{vac2}-ATU(P), did not differ in the induction of α-MV nAbs (Fig. 18). However, as for H7N9 specific Abs, α-MV nAbs were abortive in mouse 599, indicating that this individual mouse was generally non-responsive to MV vaccination.

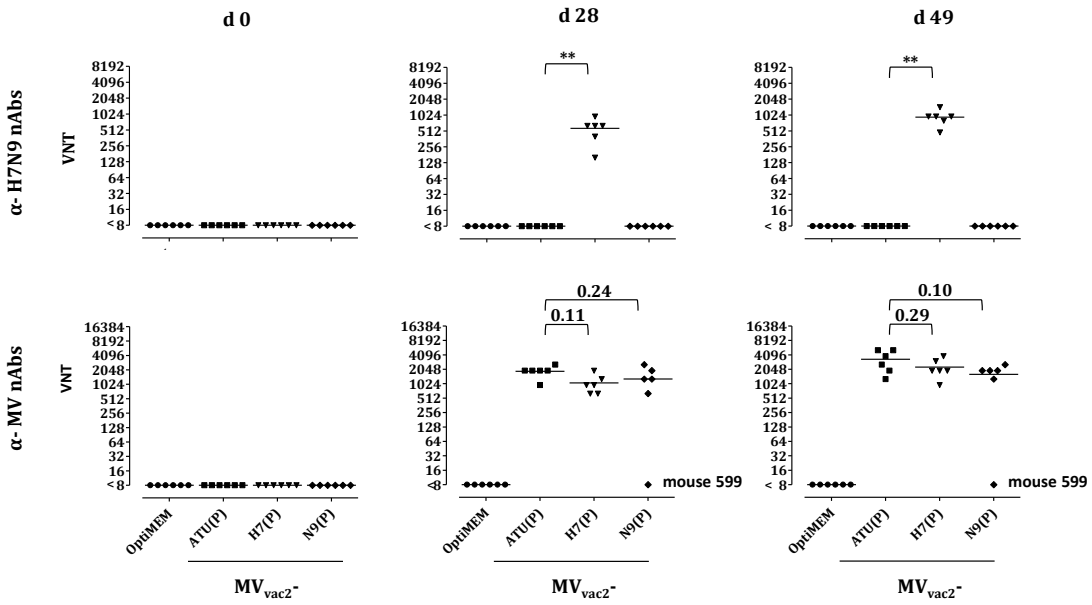

Fig. 18 Induction of H7N9 neutralising antibodies. Blood of mice vaccinated on days 0 and 28 with indicated viruses was sampled on day 0, 28 and 49. Sera were analyzed for H7N9 neutralising antibodies (nAbs) and MV nAbs. Medium (OptiMEM) or MV backbone inoculated (MV_{vac2}-ATU(P)) mice served as mock. Virus neutralising titers (VNTs) were calculated as the reciprocal of the highest serum dilution totally neutralising infectivity of 100 $TCID_{50}$ A/Puerto Rico/8/1934 H7N9 or 50 pfu of MV. Dots represent single animals (n = 6). Horizontal line represents mean per group. Y-axis starts at detection limit. All mice at detection limit had no detectable VNT. Mann-Whitney-test (unpaired values); *, P<0.05; **, P<0.01

To summarise, recombinant MVs encoding antigens of MERS-CoV and H7N9 were shown to induce humoral immune responses directed against the inserted antigens. Moreover, MVs expressing receptor binding antigens appeared to induce Abs that were capable of neutralising the corresponding virus.

3.4. Analysis of cellular immunity

3.4.1. Generation and characterisation of transgenic cell lines

The requirement for most effective pre-pandemic vaccines against some viruses, like influenza viruses (75), often includes the induction of cellular immunity, in addition to humoral immune responses. However, no commercial assays to analyse induced T cell responses are usually available for emerging pathogens making the establishment of appropriate assays mandatory.

To this end, this PhD thesis aimed to produce transgenic DC cell lines which stably expressed the antigens encoded by the vaccines, in order to re-stimulate respective antigen-specific T cells *ex vivo*. An antigen-expressing suspension cell line, EL-4, needed to be generated to serve as target cells in a CTL killing assay. For that purpose, lentiviral vectors (LVs) transferring genes encoding for the marker gene GFP and the antigens MV-N, MERS-S, MERS-N, H7 or N9, linked by an IRES sequence, were generated during this thesis. These vectors were then used to transduce the DC cell lines JAWSII, DC2.4, or DC3.2, so that these

cells expressed the respective antigen and, simultaneously, GFP for visual confirmation of successful transduction.

To produce LVs, 293T cells were transfected with cloned transfer vector plasmids pCSCW2-MERS-S-IRES-GFP, pCSCW2-MERS-N-IRES-GFP, pCSCW2-H7-IRES-GFP, pCSCW2-N9-IRES-GFP, or pCSCW2-MV-N-IRES-GFP, in addition to a packaging construct pCMVΔR8.9 and envelope (VSV-G) expression plasmid pMDG.2. The transfection resulted in an expression of GFP and the inserted antigens (Fig. 19A, Fig. 20B-E), indicating that both were simultaneously translated. After transduction of DC cell lines and EL-4 cells using LVs purified from supernatants of triple-transfected 293T cells, bulk populations of transduced cells (bulk) were enriched to GFP expression using a cell sorter. Moreover, individual cell clones were separated by limiting dilution, and single cell clones showing the highest GFP expression were chosen for further characterisation (Fig. 19).

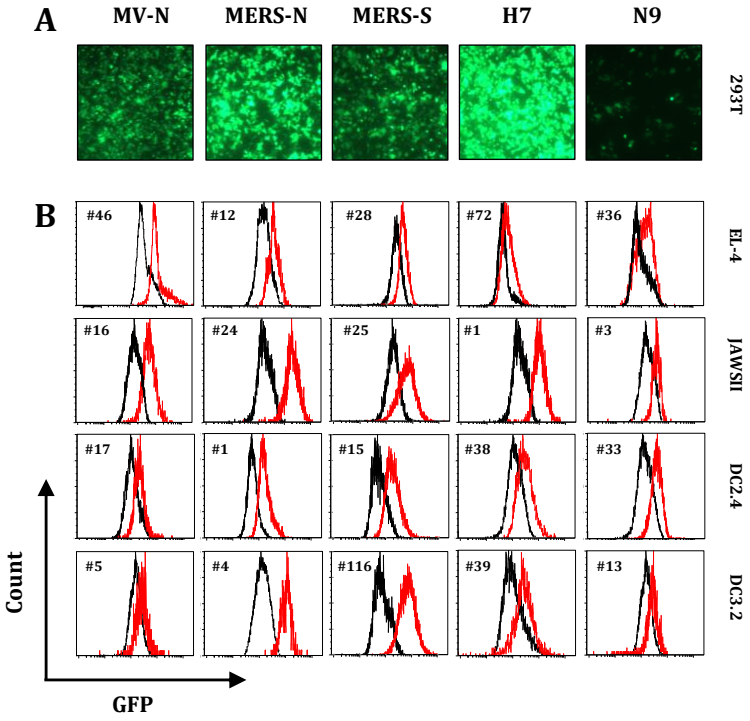

Fig. 19 GFP expression of transfected cells and selected cell clones. **(A)** Fluorescence microscopy pictures of $1x10^7$ 293 T cells transfected with 17.5 µg of respective pCSCW2-Antigen-IRES-GFP transfer vector, 6.23 µg pMD2.G, and 11.27 µg pCMVΔR8.9 to produce LVs [$HIV_{MV\text{-}N\text{-}IRES\text{-}GFP}$(VSV-G)] (MV-N), [$HIV_{MERS\text{-}N\text{-}IRES\text{-}GFP}$(VSV-G)] (MERS-N), [$HIV_{MERS\text{-}S\text{-}IRES\text{-}GFP}$(VSV-G)] (MERS-S), [$HIV_{H7\text{-}IRES\text{-}GFP}$(VSV-G)] (H7), or [$HIV_{N9\text{-}IRES\text{-}GFP}$(VSV-G)] (N9). **(B)** EL-4, JAWSII, DC2.4, and DC3.2 cells were transduced with purified respective LVs. Single cell clones were obtained by limiting dilution. The expression of GFP was validated by flow cytometry. Red, Antigen specific cell clones revealing the highest GFP expression; black untransduced cells.

Even though the stable integration of all antigens into the genome of transduced cells was confirmed by PCR (Fig. 20A), neither MERS-S (Fig. 20C), H7 (Fig. 20D) nor N9 (Fig. 20E) were detectable by western blot using a polyclonal rabbit serum, or neuraminidase activation assay for detection of N9. The expression of MERS-N was detectable in JAWSII and DC3.2, but not in EL-4 or DC2.4 cells (Fig. 20B).

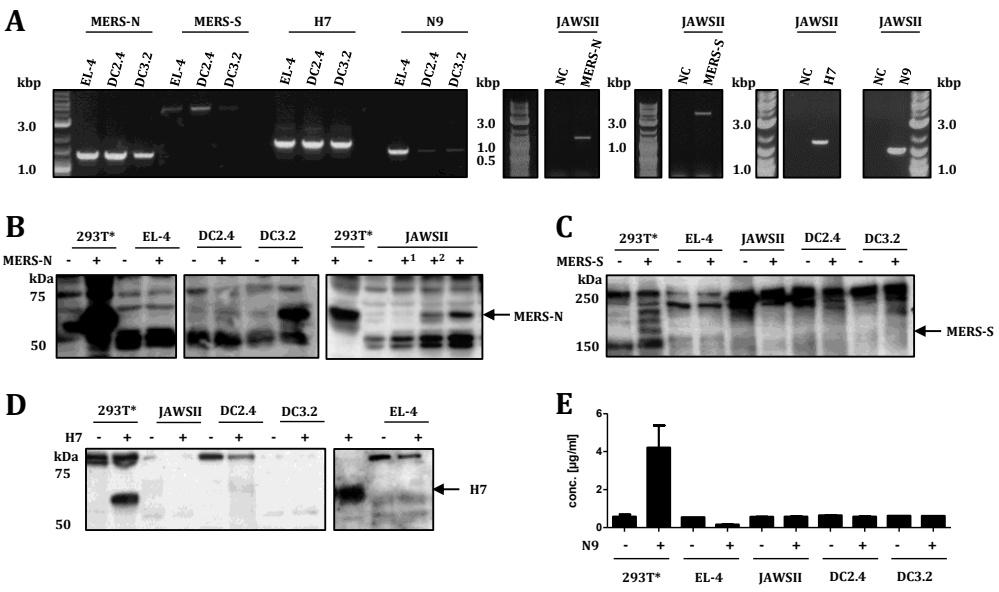

Fig. 20 Integration of antigen-encoding genes and determination of antigen expression by transduced DC cell lines or EL-4 cell line. **(A)** Integration of respective antigen-encoding genes into the genome of transduced single cell clones of EL-4, JAWSII, DC2.4 or DC3.2 was determined by PCR amplification. PCR amplification of isolated DNA was performed using antigen-specific forward and revers primers. DNA fragments were separated by gel electrophoresis. Expected bands: MERS-N: 1.24 kbp; MERS-S: 4.06 kpb; H7: 1.68 kpb, N9: 1.43 kbp. Expression of **(B)** MERS-N, **(C)** MERS-S and **(D)** H7 was determined by immunoblot using **(B,C)** α-MERS-CoV or **(D)** α-H7N1 rabbit serum. Expression of **(E)** N9 was tested by neuraminidase assay. Depicted are single cell clones with highest GFP expression except of [1] Bulk culture, or [2]MERS-N#5. Untransduced cells served as negative controls (NC). Arrows indicate specific bands. * 293T cells were transfected with respective pCSCW2-Antigen-IRES-GFP transfer vectors as positive control.

However, MV-N in JAWSII$_{Green}$-MV-N was detected by western blot analysis; and, as expected, expression shown to correlate with GFP fluorescence intensity (Fig. 21A). A correlation between antigen and GFP expression was, moreover, confirmed by western blot analysis of transgenic JAWSII, which expressed the model antigen ovalbumin (Ova)[8] (Fig. 21B).

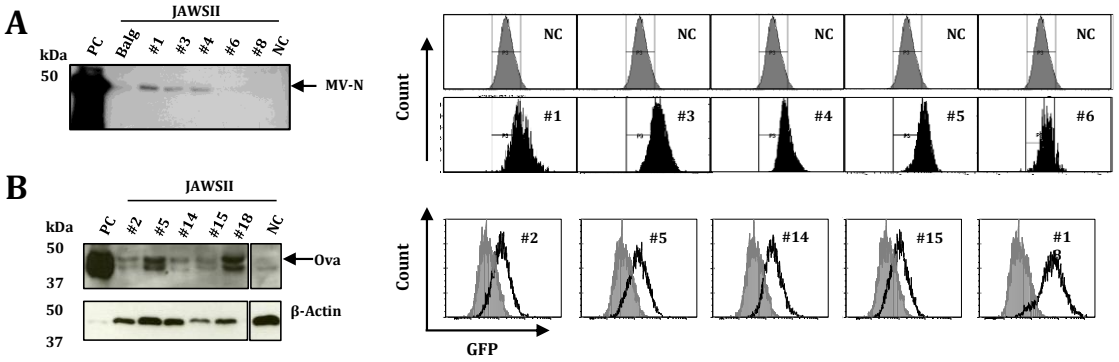

Fig. 21 Correlation between antigen and GFP expression. (**A**)α-Ova or, (**B**) α-MV-N immunoblot of JAWSII single cell clones transgenic for (**A**) Ova or (**B**) MV-N. Cells were previously transduced with respective LVs and single cell clones obtained by limiting dilution. Untransduced cells served as mock. 293T cells transfected with respective pCSCW2-Antigen-IRES-GFP transfer vectors as positive control (PC). Arrows indicate specific bands. Expression of GFP was determined by flow cytometry.

[8] Generated and characterized by Bianca Bodmer during her diploma thesis, Paul-Ehrlich-Institut, Langen

Consequently, GFP fluorescence intensity was taken as correlate of antigen expression and cell clones exhibiting the highest GFP expression used for re-stimulation of T cells in subsequent experiments. Since the respective antigens were integrated into the genome of transduced cell clones, the respective abortive proof of antigen expression was attributed to expression below detection limit of western blot or neuraminidase activation assay.

3.4.2. Induction of cellular immune responses by prospective MV-MERS vaccines

Subsequently, this thesis aimed to investigate whether these antigen-transgenic DC cell lines were suitable to re-stimulate antigen-specific T cells that were induced by vaccination. For that purpose, 21 days after booster vaccination, splenocytes were isolated from mice vaccinated with MV_{vac2}-ATU(P), MV_{vac2}-MERS-S(H), MV_{vac2}-MERS-solS(H), or MV_{vac2}-MERS-N(H).

Splenocytes labelled with CFSE were first re-stimulated with respective transgenic bulk $JAWSII_{green}$ cells to test whether T cells among splenocytes proliferated upon antigen stimulation. This would be indicated by a decreasing CFSE signal (Fig. 22 A). In fact, $CD3^+CD8^+$ T cells (Malczyk *et al.*, 2015, Fig. 5A), but not $CD3^+CD4^+$ T (Fig. 22 B) cells of mice vaccinated with MV_{vac2}-MERS-solS(H) (29±20% of $CD3^+CD8^+$ T cells; 3.8±1.9% of $CD3^+CD4^+$ T cells) or MV_{vac2}-MERS-S(H) (41±12% of $CD3^+CD8^+$ T cells; 3.4±1.4% of $CD3^+CD4^+$ T cells) specifically, proliferated upon re-stimulation with $JAWSII_{Green}$MERS-S. By contrast, $JAWSII_{Green}$-MERS-N (Fig. 22 B) cells neither triggered proliferation of $CD3^+CD8^+$ (0.9±0.34%) nor of $CD3^+CD4^+$ T cells (1.4±0.4%) isolated from mice vaccinated with MV_{vac2}-MERS-N(H). MERS-S or MERS-N specific proliferation was not detectable in control mice, as expected.

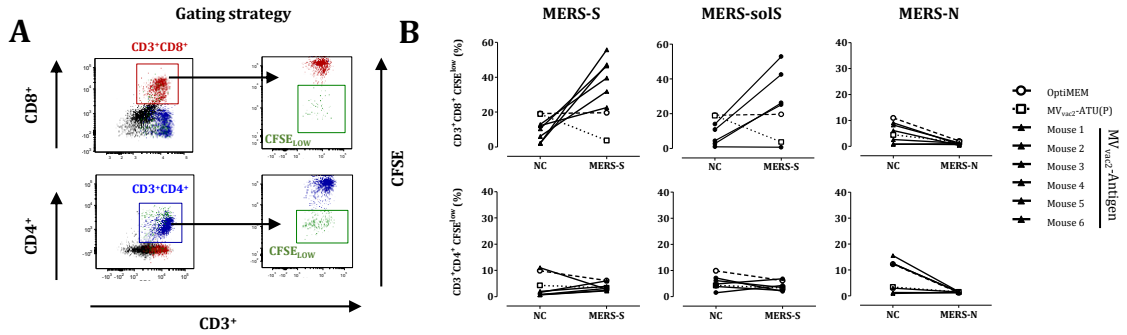

Fig. 22 Induction of MERS-S-specific T memory cells. Proliferation of splenocytes from mice vaccinated on days 0 and 28 with indicated viruses and isolated 21 d after booster immunization. Medium (OptiMEM) or MV backbone inoculated (MV_{vac2}-ATU(P)) mice served as controls. CFSE-labeled splenocytes were co-cultured with bulk cultures of transduced JAWSII DC lines transgenic for respective antigen or untransduced controls (NC) for 6 days. **(A)** Percentages of $CD8^+$ or $CD4^+$ T cells with low CFSE were determined by flow cytometry. Low CFSE signals indicates proliferation in the samples. **(B)** Results for splenocytes of vaccinated mice are displayed individually and trend between paired unstimulated and re-stimulated samples is outlined. Splenocytes of control mice were pooled.

$CD3^+CD8^+$ T cells were, in general, responsive to re-stimulation with Concanavalin A (ConA) (Fig. 23 A) and $CD3^+CD4^+$ T cells of all MV vaccinated to re-stimulation with MV bulk antigens. These results demonstrated that abortive MERS-N specific proliferation of T cells was neither attributable to non-responsiveness of T cells nor to a general failure of vaccination (Fig. 23 B).

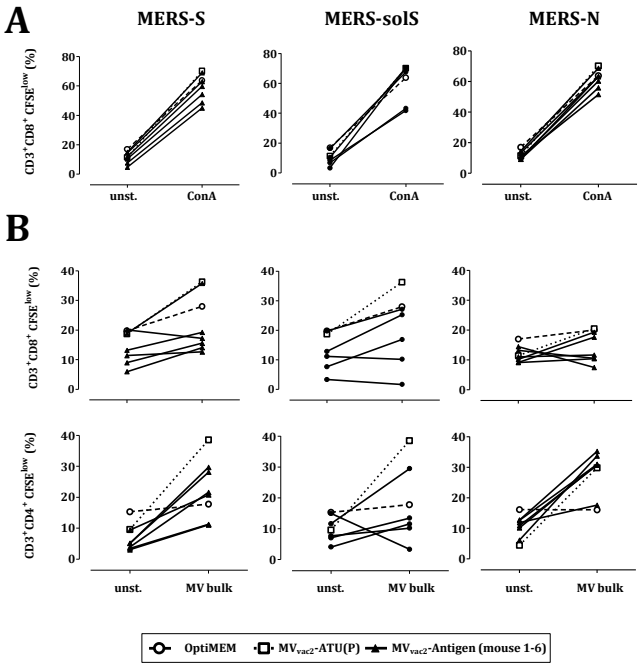

Fig. 23 Proliferation of T cells upon re-stimulation with positive controls. Proliferation of splenocytes from mice vaccinated on days 0 and 28 with indicated viruses and isolated 21 d after booster immunization. Medium (OptiMEM) or MV backbone inoculated (MV_{vac2}-ATU(P)) mice served as controls. CFSE labeled splenocytes were re-stimulated with 10 µg/ml ConA or MV bulk antigens for 6 days. Medium served as mock. Percentages of $CD8^+$ or $CD4^+$ T cells with low CFSE were determined by flow cytometry. Low CFSE signals indicates proliferation in the samples. Results for splenocytes of vaccinated mice are displayed individually and trend between paired unstimulated and re-stimulated samples is outlined. Splenocytes of control mice were pooled.

Consequently, the ability of MERS-S or MERS-N-specific T cells to secrete antiviral IFN-γ or to exert effector T cell responses as alternative correlates of T cell activation were tested in the next steps. Since most effector T cells are normally detectable a few days after pathogen exposure (Fig. 14), splenocytes of vaccinated mice were isolated four days after booster vaccination for subsequent experiments (Fig. 24). In addition, transgenic single cell clones, rather than bulk populations of transgenic JAWSII, DC2.4 and DC3.2 clones, were selected as defined antigen-specific DC cell-populations for re-stimulation.

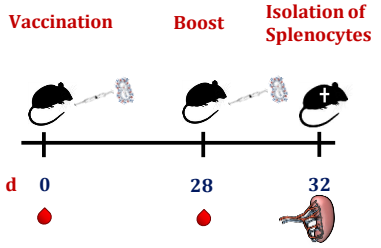

Fig. 24 Vaccination set-up for analysis of cellular immunity. IFNAR$^{-/-}$CD46Ge mice were intraperitonally vaccinated with $1x10^5$ $TCID_{50}$ of respective vaccines on days 0 and 28 and splenocytes isolated 4 d after boost immunization.

Consistent with T cell proliferation, a MERS-S-specific re-stimulation of splenocytes from mice vaccinated with MV_{vac2}-MERS-S(H) or MV_{vac2}-MERS-solS(H) by MERS-S-transgenic JAWSII, DC2.4, or DC3.2 resulted in a significantly enhanced IFN-γ secretion compared to control mice ($JAWSII_{Green}$-MERS-S: approx. 2,400 versus 200 spot forming cells (SFC) / 10^6 splenocytes) (Malczyk *et al.*, 2015, Fig. 4). Moreover, MERS-N-transgenic JAWSII and DC2.4 cells provoked an IFN-γ secretion by splenocytes isolated from mice vaccinated with MV_{vac2}-

MERS-N(H) (298±213, or 237±244 SFC/ 10^6 splenocytes, respectively), but not in control mice (vector control 54±29, or 21±25 SFC/ 10^6 splenocytes, respectively). This demonstrates the ability of the vaccine to induce MERS-N-specific T cell responses (Fig. 25A). Nevertheless, the numbers of IFN-γ secreting cells induced by re-stimulation with MERS-N-transgenic DCs were at least five-fold lower compared to those induced by MERS-S in T cells of respectively vaccinated groups (Malczyk *et al.*, 2015, Fig. 4). This reduced activity of splenocytes of MV_{vac2}-MERS-N(H) vaccinated mice were not attributed to general activity of splenocytes since responsiveness to ConA or MV bulk antigen stimulation was comparable to other groups (Fig. 25B). Differences did also not become evident after re-stimulation with $JAWSII_{green}$MV-N cells (Fig. 25B).

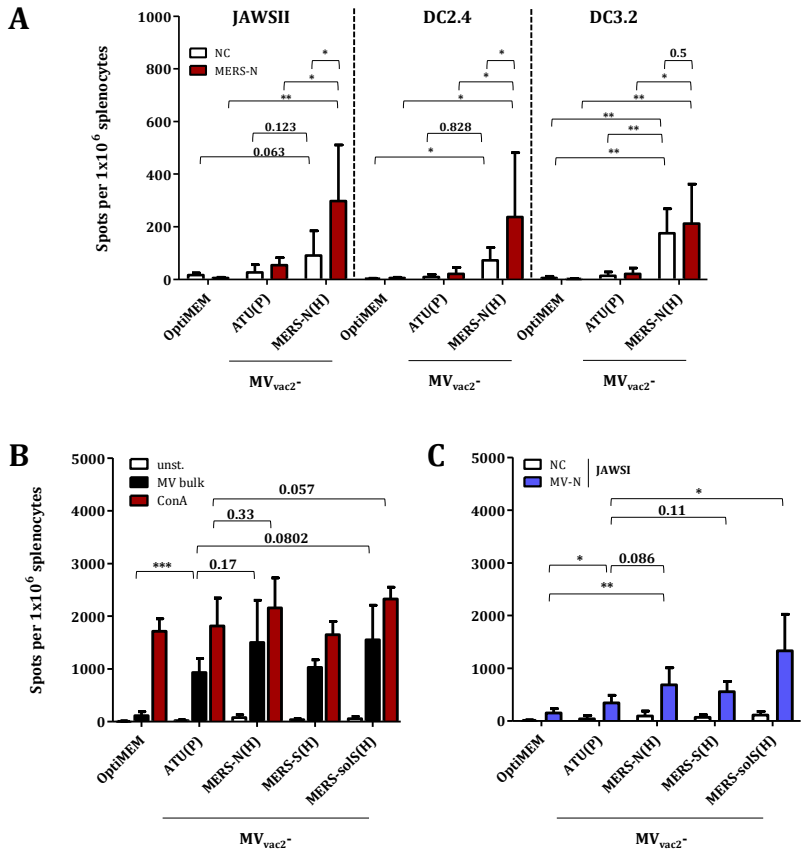

Fig. 25 α-MERS-N cellular immune responses. Splenocytes were isolated 4 d after boost immunization and analyzed for IFN-γ secretion by ELISpot. For antigen-specific recall, splenocytes were co-cultured with single cell clones of **(A)** JAWSII-MERS-N, DC2.4 MERS-N, or DC3.2-MERS-N (red colums) at a ratio 1:10 for 36h. Re-stimulation with **(B)** 10 mg/ml, MV bulk antigen (black columns), 10 mg/ml ConA (red columns) or **(C)** JAWSII-MV-N (blue columns) were used as control stimuli. Medium (unst.) or untransduced cells (NC) served as negative controls (white columns). Depicted are means ± SD (n = 6). Students T test (unpaired between different mouse groups; paired between values of one group); *, P<0.05; **, P<0.01.

As already demonstrated for humoral immunity (Fig. 16), no IFN-γ was secreted by splenocytes from mice vaccinated with UV-inactivated MV_{vac2}-MERS-S(H) and subsequently stimulated by $JAWSII_{Green}$-MERS-S cells (Fig. 26). This data reveals that induction of considerable cellular immune response by MV_{vac2}-MERS-S(H) depends on replication of MV-derived vaccines.

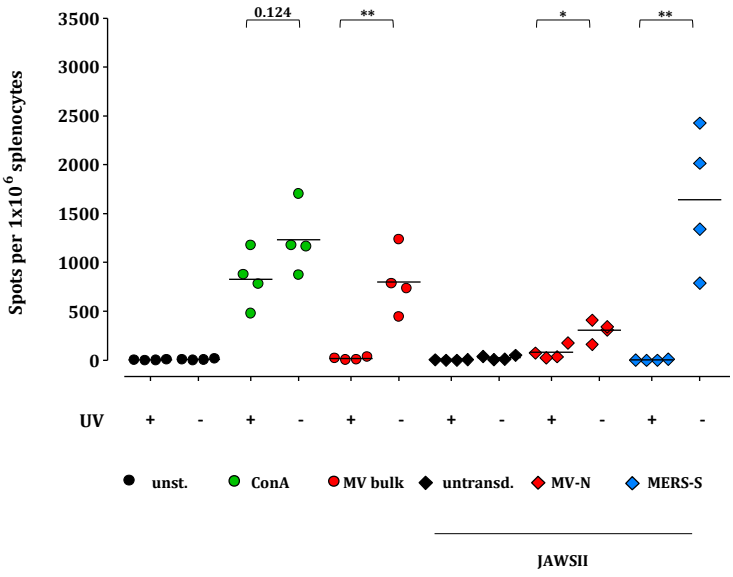

Fig. 26 Cellular immunity induced by UV-inactivated or replicating MV-MERS-S. Splenocytes of mice vaccinated on days 0 and 28 with indicated viruses were isolated 21 d after boost immunization and analysed for IFN-γ secretion by ELISpot. For recall of T cells, splenocytes were stimulated with 10 mg/ml $Ova_{257-264}$peptide (NC)(black circles), MV bulk antigens (green circles), ConA (red circles), or co-cultured with single cell clones of JAWSII-MERS-S (blue diamonds), JAWSII-MV-N (red diamonds) or untransduced cells (black diamonds) for 36h. Dots represent single animals (n = 4). Horizontal line represents mean per group. Students T test (unpaired between different mouse groups; paired between values of one group); *, P<0.05; **, P<0.01.

Finally, to monitor CTL effector responses of reactive T cells after vaccination with MV_{vac2}-MERS-S(H), MV_{vac2}-MERS-solS(H), or MV_{vac2}-MERS-N(H), the killing of respective antigen-expressing EL-4 cells was tested in the next step.

In contrast to the T cells of control mice, those induced by MV_{vac2}-MERS-S(H), or MV_{vac2}-MERS-solS(H)- vaccination specifically, killed MERS-S-expressing target EL-4 cells (Malczyk *et al.*, 2015, Fig. 5C). However, T cells of MV_{vac2}-MERS-N(H) vaccinated animals did not exhibit CTL effector responses against MERS-N-expressing cells (Fig. 27). This absence of MERS-N but also MV-N-specific killing in the presence of respectively reactive T cells (Fig. 25) indicated that those antigen-specific T cells did not exhibit detectible CTL responses in the killing assay that had been performed.

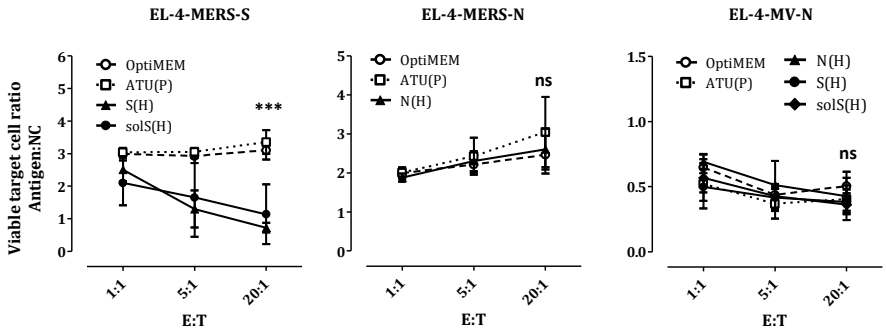

Fig. 27 CTL effector responses. Splenocytes, isolated 4 d after boost vaccination, were cocultured with untransduced JAWSII or with single cell clones of JAWSII-MERS-S, JAWSII-MERS-N or JAWSII-MV-N for 6 days. Activated CTLs were co-cultured with respective EL-4-Antigen target cells (Antigen) and $EL\text{-}4_{red}$ control cells (NC) at indicated E:T ratios for 4 h. Number of living cells was determined by flow cytometry and ratio of living target to non-target cells (Antigen:NC) calculated. Depicted are means ± SD (n = 6). Statistics: a linear curve was fitted for antigen, versus the log-transformed effector-target ratio (E:T). The P values for differences in slopes were calculated. ns, not significant; *** P<0.001.

This chapter demonstrates the suitability of transgenic DC cell lines, like JAWSII, DC2.4, or DC3.2 to re-stimulate antigen-specific T cell responses, as shown for three distinct antigens: MV-N, MERS-S, and MERS-N. Using these transgenic DC cell lines, the capacity of MV-derived

recombinant vaccines encoding either MERS-N or MERS-S as extra transgene cargo, to induce T cell responses was demonstrated. MERS-S was shown to be more immunogenic than MERS-N, in that it induced four- to five-fold higher numbers of IFN-γ secreting antigen-specific T cells. Also, antigen-specific T cell proliferation and CTL effector responses were detectable for MERS-S, but not for MERS-N.

3.4.3. Comparison of re-stimulation capacity of transgenic JAWSII to peptides

To further strengthen the evidence that transgenic DC cell lines are suitable for antigen-specific re-stimulation of vaccine-induced T cells, we aimed to compare the capacity of transgenic JAWSII$_{Green}$Ova cells[9] (3.4.1) for recall of Ovalbumin (Ova)-specific T cells to that of immunodominant peptides specific for $CD8^+$ or $CD4^+$ T-cell responses (SIINFEKL $OVA_{257-264}$ or $OVA_{323-339}$, respectively). For this purpose, we utilized Ova-specific purified pan T cells, which were separated from frozen splenocytes. These splenocytes originated from mice, which were previously vaccinated with a lentiviral protein-transfer vector transferring the model antigen Ova to APCs (Ova-PTVs). Four days after booster vaccination these splenocytes were initially isolated, and directly after isolation examined for numbers of Ova-specific IFN-γ secreting cells in an ELISpot-assay using $OVA_{257-264}$, $OVA_{323-339}$ or recombinant Ova proteins for Ova-specific recall. Upon initial examination, it was found that splenocytes of $IFNAR^{-/-}$ mice vaccinated with VSV-G-pseudotyped Ova-PTV HIV-$Ova_{Katushka}$(VSV) [10] contained significant numbers of IFN-γ secreting cells (>600/10^6 splenocytes), which, however, became evident irrespective of the stimuli used for antigen-specific recall (Uhlig *et al*., 2015, Fig. 7B). To identify the reason for unspecific activity of T cells, pan T cells were consequently separated from other splenocytes by magnetic bead sorting and co-cultured with untreated bone-marrow-derived mDCs or mDCs pulsed with $OVA_{257-264}$, $OVA_{323-339}$, or recombinant Ova. Interestingly, the baseline level of T cells from HIV-$Ova_{Katushka}$(VSV) vaccinated mice was five-fold reduced when pooled untouched pan T cells were examined for IFN-γ producing cells in an ELISpot assay (Uhlig *et al*., 2015, Fig. 8A). When the APC-containing retentate of these mice was co-cultured with splenocytes of OT-I (transgenic TCR specific for MHCI restricted epitope $OVA_{257-264}$), OT-II (transgenic TCR specific for MHCII restricted epitope $OVA_{323-339}$) or BL/6 wt mice, 15-fold more IFN-γ secreting cells were detected among splenocytes of OT-I mice compared to BL/6 wt mice (Uhlig *et al*., 2015, Fig. 8C). This results indicated that the APCs of vaccinated mice were still

[9] Generated by Bianca Bodmer during her diploma thesis, Paul-Ehrlich-Institut, Langen
[10] Vaccination performed by Dr Uhlig, Paul-Ehrlich-Institut, Langen

presenting Ova peptides and thereby activating Ova-specific, (here $CD8^+$) T cells, four days after vaccination by lentiviral PTVs.

Anyway, during examination of pan T cells, numbers IFN-γ secreting cells activated by $JAWSII_{Green}Ova$ were similar to those induced by 5 µg/ml $OVA_{257-264}$ (Uhlig *et al.*, 2015, Fig. 8A) indicating that antigen-specific re-stimulation of T cells by transgenic DC cell lines can be as effective as re-stimulation by immunodominant, antigen-peptides loaded onto primary DCs. In this setting, re-stimulation by JAWSII cells was, moreover, comparable to a stimulus specific for $CD8^+$ T but not $CD4^+$ T cells. These results were later confirmed as the meanwhile characterized MERS-CoV peptide S1165, which represent an immunodominant MHCI restricted MERS-CoV epitope, was compared to $JAWSII_{Green}$-MERS-S cells. Here, numbers of re-stimulated IFNγ-secreting T cells among splenocytes did not significantly differ from those induced by $JAWSII_{Green}$-MERS-S, irrespective if 1 µM or 10 µM of S1165 were used for re-stimulation (Fig. 28).

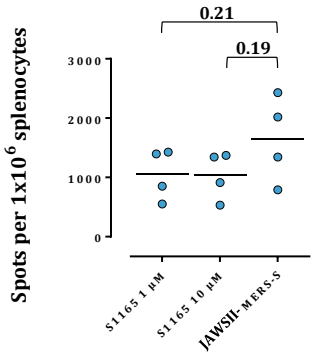

Fig. 28 Comparison of $JAWSII_{Green}$-MERS-S cells to peptide S1165. Splenocytes of mice vaccinated on days 0 and 28 with indicated viruses were isolated 21 d after boost immunization and analysed for IFN-γ secretion by ELISpot. For recall of T cells, splenocytes were stimulated with 1 µMor 10 µM S1165 peptide or co-cultured with single cell clones of JAWSII-MERS-S (blue diamonds),for 36h. Dots represent single animals (n = 4). Horizontal line represents mean per group. Students T test (paired between values of one group).

Thus, these results, demonstrated that the re-stimulating properties of transgenic DC cell lines can be comparable to re-stimulation by immunodominant peptides. The powerful cellular immune responses induced by particularly MV_{vac2}-MERS-S(H) and MV_{vac2}-MERS-solS(H) and are hence most likely not attributed to stimulation properties of transgenic DC cell lines. As a consequence, those can be used especially when these peptides are not available; and production of recombinant antigens, hardly possible. Therefore, transgenic DC cell lines were also utilized to test the properties of MV_{vac2}-H7(P), and MV_{vac2}-N9(P) to induce cellular immune responses, as already demonstrated for MV-based vaccines against MERS-CoV.

3.4.4. Induction of cellular immune responses by MV-H7 or MV-N9

For that purpose, splenocytes of respectively vaccinated mice were isolated four days after boost vaccination (Fig. 24) and antigen-specific T cells re-stimulated by antigen-encoding

Here, an H7-specific recall of splenocytes from MV_{vac2}-H7(P) vaccinated mice resulted in a significant number of IFN-γ secreting T cells (358±141 SFC/ 10^6 after re-stimulation with $JAWSII_{Green}$-H7), whereas hardly any IFN-γ secreting splenocytes were obtained from mice

injected with OptiMEM (JAWSII$_{Green}$-H7: 23±26 SFC / 10^6 splenocytes) or vector control groups (JAWSII$_{Green}$-H7: 63±44 SFC/ 10^6 splenocytes). Statistically significant differences between MV$_{vac2}$-H7(P) vaccinated mice and vector control mice became evident for JAWSII$_{Green}$H7, DC2.4$_{Green}$H7 and DC3.2$_{Green}$H7 respectively, indicating that H7-specific immunity was not attributable to a specific cell line (Fig. 29A).

IFN-γ secreting T cells were also abundant among splenocytes of mice vaccinated with MV$_{vac2}$-N9(P) (JAWSII$_{Green}$-N9: 518±304 SFC/ 10^6 splenocytes), while lower numbers of IFN-γ secreting T cells were found among splenocytes of medium (JAWSII$_{Green}$-N9: 147±123 SFC/ 10^6 splenocytes) or vector control (JAWSII$_{Green}$-N9: 246±157 SFC/ 10^6 splenocytes) treated mice. However, these differences in T cell activation also became evident if untransduced DCs were used for recall, indicating that activity of splenocytes from MV$_{vac2}$-N9(P) vaccinated mice was attributable rather to DC co-culture than to N9-specific re-call (Fig. 29B). Nevertheless, comparable reactivity of these splenocytes in general, and comparable responsiveness of mice to MV vaccination were confirmed by unspecific recall with ConA (Fig. 29C) or MV-specific recall with MV bulk antigens (Fig. 29 C) or JAWSII$_{Green}$-MV-N cells (Fig. 29D), respectively.

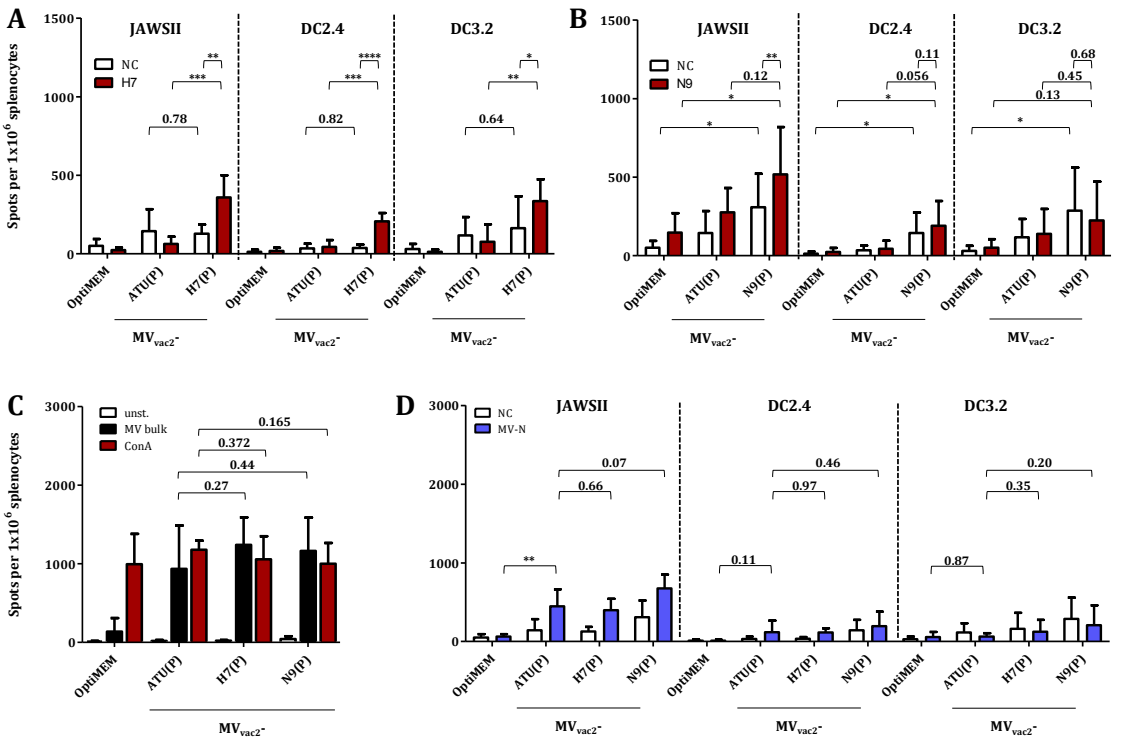

Fig. 29 Secretion of IFN-γ after H7- or N9-specific re-stimulation of splenocytes. IFN-γ ELISpot analysis of murine splenocytes isolated 4 d after boost immunization. **(A)** H7 or **(B)** N9 specific T cells were detected after co-culture with with single cell clones of JAWSII, DC2.4 or DC3.2 dendritic cell lines transgenic for H7 or N9 (red colums). Restimulation with **(C)** 10 mg/ml MV bulk antigen (black columns), 10 mg/ml ConA (red columns) or **(D)** JAWSII-MV-N (blue columns) were used as control stimuli. Medium (unst.) or untransduced cells (NC) served as negative controls (white columns). Depicted are means ± SD (n = 6). Students T Test (unpaired values between different groups, paired values of one animal group); *, p<0.05; **, p<0.01; ***, p<0.001; ****, p<0.0001.

However, although MV_{vac2}-H7(P) was potent to induce H7-specific T-cell responses in an IFN-γ ELISpot assay, cytotoxic activity against H7-, or MV-N-encoding target cells could not be demonstrated (Fig. 30).

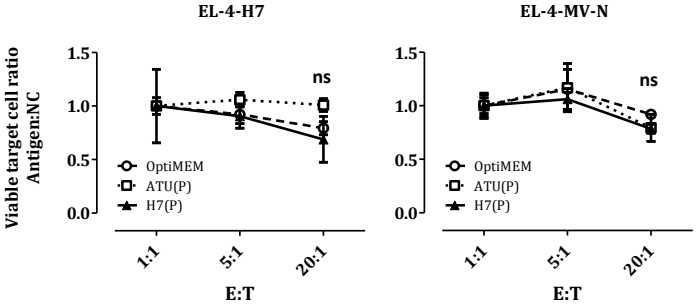

Fig. 30 α-H7 CTL effector responses. Splenocytes, isolated 4 d after boost vaccination, were cocultured with untransduced JAWSII or with single cell clones of JAWSII-H7, or JAWSII-MV-N for 6 days. Activated CTLs were co-cultured with respective EL-4-Antigen target cells (Antigen) and $EL\text{-}4_{red}$ control cells (NC) at indicated E:T ratios for 4 h. Number of living cells was determined by flow cytometry and ratio of living target to non-target cells (Antigen:NC) calculated. Depicted are means ± SD (n = 6). Statistics: a linear curve was fitted for antigen, versus the log-transformed effector-target ratio (E:T). The P values for differences in slopes were calculated. ns, not significant.

Thus, this part of the work demonstrated that MV_{vac2}-H7(P) induced H7-specific cellular immune responses which are characterised by a secretion of antiviral IFN-γ. By contrast, NA-specific cellular immune responses were not detectable in mice vaccinated with MV_{vac2}-N9(P) vaccine.

3.5. Analysis of protection capacity of MV-MERS-S

MV-derived vaccines against two distinct viruses, MERS-CoV and H7N9, were potent in inducing humoral (see 3.3.2) and cellular immunity (see 3.4.2, and 3.4.4) *in vivo*. To finally characterise whether those immune responses were protective against the respective pathogen, MV-derived vaccines against MERS-CoV were tested in an appropriate challenge model. Since MV_{vac2}-MERS-S(H) and MV_{vac2}-MERS-solS(H) induced MERS-CoV nAbs as well as strong MERS-S-specific cellular immune responses, these constructs were used as preceding vaccines to be tested.

Thus, in two independent experiments, 5 mice per group (n=10) were vaccinated with medium (mock control), MV_{vac2}-ATU(P) (vector control), MV_{vac2}-MERS-S(H), or MV_{vac2}-MERS-solS(H) in a prime-boost-set-up (Fig. 14). Since mice are naturally not susceptible to MERS-CoV infection (51), the respiratory tracts of mice were transduced with mCherry marked adenoviral vectors encoding the human DPP4 gene (AdV-hDPP4) on day 6[11]. Due to the expression of huDPP4, the entry receptor of MERS-CoV, mice become susceptible and

[11] Performed by Dr Kupke with support of Dr Jörg Schmidt, Dr Vergara-Alert and Dr Eickmann of Prof. Becker's group, University of Marburg, in collaboration with Dr Herold, University of Gießen

were subsequently infected on day 68. Lungs of infected mice were isolated on day 72[12] and analysed for MERS-N RNA copy numbers, titres of infectious virus and signs of inflammation, as determined by histological examination after haematoxylin and eosin (H&E) staining (Fig. 31).

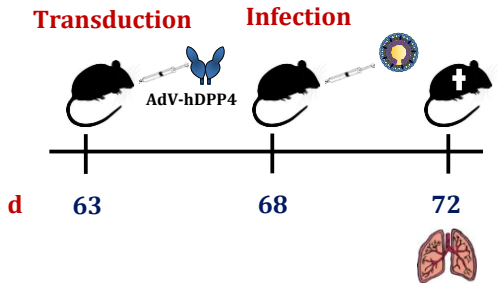

Fig. 31 Set-up for MERS-CoV challenge. IFNAR$^{-/-}$CD46Ge mice were vaccinated on days 0 and 28. Mice were intranasally transduced with 2.5x10^{8} pfu AdV-DPP4 on day 63 and challenged with 7x10^{4} $TCID_{50}$ MERS-CoV on day 68. Lungs of vaccinated mice were isolated on day 72.

Indeed, the vaccination with MV_{vac2}-MERS-solS(H) or MV_{vac2}-MERS-S(H) resulted in a reduction of viral copy numbers compared to medium inoculated mice (9,649±3,045 to 51±32, or 74±60 MERS-CoV genome copies/ng RNA, respectively) which was significant for MV_{vac2}-MERS-solS(H) (p=0.0329), and close to significance (p=0.057) for MV_{vac2}-MERS-S(H) (Malczyk *et al.*, 2015, Fig. 6A). Although titres of infectious MERS-CoV were generally low, the results corresponded to qRT-PCR data. Here, a vaccination with MV_{vac2}-MERS-solS(H) resulted in a three-fold (868±692 to 318±198 $TCID_{50}$), reduction of viral titres compared to the medium control (Malczyk *et al.*, 2015, Fig. 6B). For MV_{vac2}-MERS-S(H), the reduction was seven-fold (868±692 to 122±136 $TCID_{50}$). However, completely negative PCR results and undetectable viral titres were observed for 40% of challenged mice, indicating that they were not infected by MERS-CoV. Lack of infectivity was attributable to failed transduction by AdV-hDPP4 in 37% of affected mice, while the reason for lack of infectivity in the remaining mice remains so far unclear. However, the groups did not generally vary in mCherry loads, indicating that the reduction of MERS-CoV RNA copy numbers and titres after vaccination with MV_{vac2}-MERS-solS(H) or MV_{vac2}-MERS-S(H) was not due to low transduction efficiency (Malczyk *et al.*, 2015, Fig. 6C). Histopathological examination of infected lungs revealed that the lung tissues of control animals (OptiMEM and MV_{vac2}-CoV-ATU(P)) showed areas of inflammation which were accompanied by a positive MERS-CoV-S immunostaining[13], indicating pathology that correlates with infection. By contrast, inflammation and MERS-S expression were clearly reduced in animals vaccinated with MV_{vac2}-MERS-S(H) or MV_{vac2}-MERS-solS(H) (Malczyk *et al.*, 2015, Fig. 7). Expression of mCherry, as a control for successful transduction, generally did not vary between the groups, (Malczyk *et al.*, 2015, Fig. 7), but correlated with a lack of MERS-CoV infectivity in some mice, as already indicated by mRNA expression levels.

[12] Conducted by Dr Kupke and colleagues
[13] Conducted by Dr Kupke and colleagues

Taken together, these results demonstrate that the powerful humoral and cellular immune responses induced by vaccination with MV_{vac2}-MERS-S(H) and MV_{vac2}-MERS-solS(H) do indeed protect vaccinated mice from MERS-CoV challenge. This protection was not only demonstrated by a reduction of viral loads in the lung tissues of MERS-CoV infected mice, but also by a reduction of relevant clinical signs of disease.

3.6. Analysis of the impact of pre-existing anti-measles immunity on the efficacy of MV-MERS-S

Since most human beings are vaccinated against measles as infants, pre-existing nAbs have long been suspected to counteract the efficacy of MV-derived vaccine vectors. Consequently, the final aim of this thesis was to analyse the impact of pre-immunity on the induction of humoral and cellular immune responses directed against MERS-CoV by generated MV-MERS vaccines.

For this purpose, $IFNAR^{-/-}$CD46Ge mice were pre-immunised once (1xATU(P)) or twice (2xATU(P)) with MV_{vac2}-ATU(P) to induce MV immunity, or else inoculated with medium as a control. Three months after pre-vaccination, the animals were vaccinated with MV_{vac2}-MERS-S(H) in a prime-boost set-up as used for naïve mice. Sera were collected on days 0, 28, 49, 147, 168 and 189, and analysed for the presence of α-MV and α-MERS-CoV nAbs at each time point. Splenocytes isolated on day 189 were examined for IFN-γ secretion upon MERS-S specific re-stimulation by peptide S1165 or by $JAWSII_{green}$MERS-S cells.

As expected, α-MV nAbs were boosted by each immunisation and were thus significantly higher in twice pre-immunised mice compared to once pre-immunised mice at the time point of vaccination with MV_{vac2}-MERS-S(H) (1,072±649 versus 420±244 VNTs). Consistent with previously published data (164, 33), a single pre-immunisation had no effect on α-MERS-CoV nAbs titres compared to naïve mice (18.3±14.7 versus 15±14.1 VNTs) (Malczyk *et al.*, 2015, Fig. 3). By contrast, twice pre-vaccinated animals revealed no detectable α-MERS-CoV nAbs when vaccinated afterwards with MV_{vac2}-MERS-S(H) (Fig. 32). However, titres even in naïve animals were unexpectedly low, when compared to previous experiments.

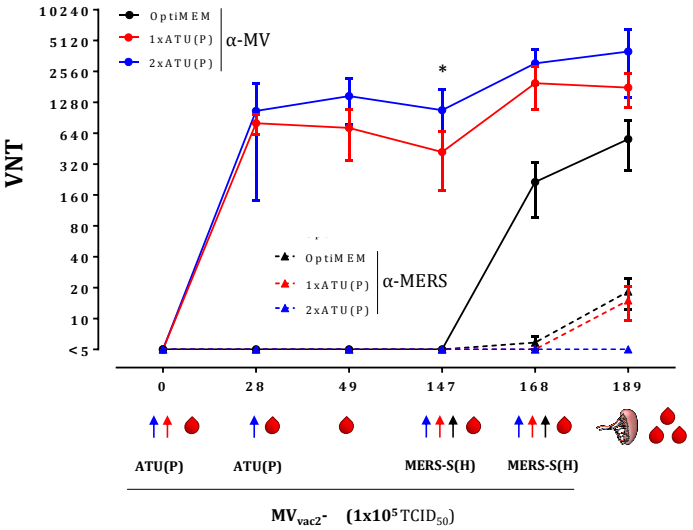

Fig. 32 Humoral immune responses in the presence of pre-existing immunity. Mice were once or twice pre-vaccinated with $1x10^5$ $TCID_{50}$ MV_{vac2}-ATU(P). Control mice were treated with OptiMEM. 147 and 168 days after the initial vaccination all mice were vaccinated with $1x10^5$ $TCID_{50}$ MV_{vac2}-MERS-S(H) in a prime-boost set-up. Mouse sera sampled on day 0, 28, 49, 147, 168 and 169 were analysed for virus neutralising titers (VNT). VNTs were calculated as reciprocal of the highest dilution abolishing infectivity of 200 $TCID_{50}$ of MERS-CoV or 50 pfu of MV. Y axis starts at limit of detection. Depicted are Means ± SD (n = 4-7); Students T Test (unpaired values between different groups); *, $p<0.05$.

Next, the impact of pre-existing α-MV immunity on MV_{vac2}-MERS-S(H)-induced antigen-specific cellular immune responses was considered. Here, splenocytes of all mice were responsive to MV-specific re-stimulation (MV bulk antigens and $JAWSII_{Green}$-MV-N) as expected. However, no significant differences in MV-specific cellular immunity became evident between the groups, even though those differed in the quantity of MV immunisations. Considering MERS-S specific immunity in naïve mice, the numbers of IFN-γ secreting cells after re-stimulation of splenocytes with $JAWSII_{Green}$-MERS-S cells or 10 µM S1165 were high and comparable to previous experiments (Fig. 28) ($JAWSII_{Green}$-MERS-S: 1,509±467 versus 1,644±625 SFC/10^6 splenocytes). This indicates that general responsiveness of mice to vaccination with MV_{vac2}-MERS-S(H) was as usual. However, MERS-S specific immune responses were approximately 20-fold reduced if mice were once or twice pre-vaccinated ($JAWSII_{Green}$-MERS-S: 1,509±467 versus 93.6±83.5 or 83.8±41.6 SFC /10^6 splenocytes, respectively). These results imply that pre-immunity directed against MV significantly affects the induction of MERS-S specific cellular immunity by MV_{vac2}-MERS-S(H). However, although this impact is quite considerable, numbers of MERS-S specific IFN-γ secreting cells (S1165 or $JAWSII_{Green}$-MERS-S) were still significantly higher compared to respective control stimuli, even in twice pre-immunised mice (untransduced JAWSII: 19.4±15.8 or 27±17.6 SFC /10^6 splenocytes in once or twice pre-vaccinated mice, respectively) (Fig. 33). This indicates preservation of basal immunogenicity also in animals with significant pre-formed MV immunity.

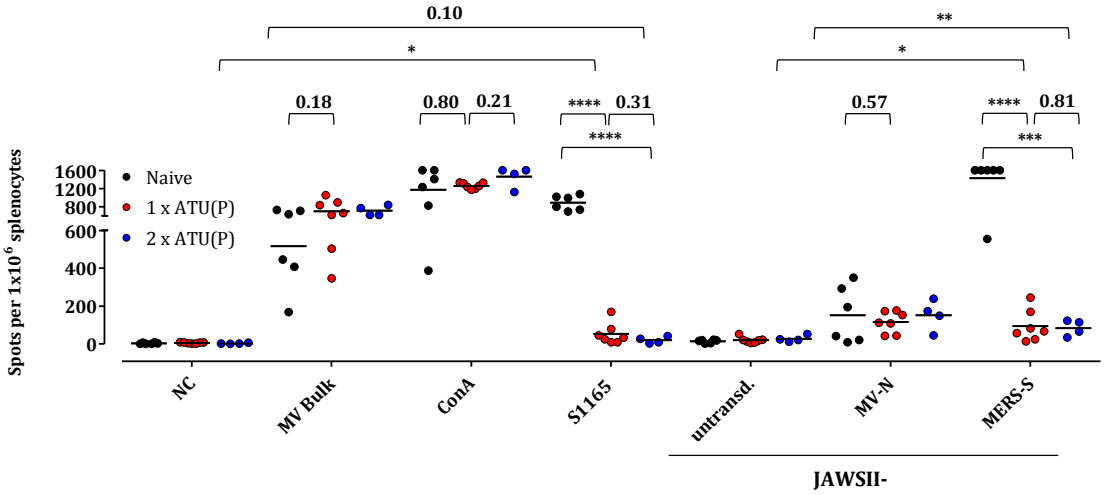

Fig. 33 Cellular immune responses in the presence of pre-existing MV immunity. Mice were once or twice pre-vaccinated with $1x10^5$ $TCID_{50}$ of MV_{vac2}-ATU(P). Control mice were treated with OptiMEM. 147 and 168 days after the initial vaccination all mice were vaccinated with $1x10^5$ $TCID_{50}$ MV_{vac2}-MERS-S(H) in a prime-boost set-up. Splenocytes of mice were isolated on day 189 and analyzed for IFN-γ secretion by ELISpot assay. For antigen-specific recall, splenocytes were co-cultured with single cell clones of JAWSII-MERS-S, JAWSII-MV-N (red circles) or stimulated with 10 µM S1165, 10 µg/ml MV bulk antigens or 10 µg/ml ConA for 36h. Medium or untransduced cells (untransd.) served as negative control (NC). Dots represent single animals (n = 4-7). Horizontal line represents mean per group. Students T Test (unpaired values between different groups, paired values of one animal group);*, $p<0.05$ **, $p<0.01$; ***, $p<0.001$; ****, $p<0.0001$.

Thus, even though pre-formed MV immunity was shown to considerably affect antigen-specific cellular immune responses induced by a MV-derived vaccine, effects on induced humoral immune responses, at least in once-pre-vaccinated mice, seem to be marginal. Therefore, the contribution and thresholds of both processes on the protection efficacy of the vaccine have to be elucidated in further experiments. These experiments will allow an appropriate evaluation of the effects of pre-existing immunity of the vaccines efficacy.

4. DISCUSSION

Our limited experience with new pathogens allows for the undetected spread of newly-emerged, highly pathogenic viruses by worldwide travel and trade. Prevention of larger outbreaks therefore relies on further investigation into viral pathomechanisms that would provide a basis for the development of pre-pandemic anti-viral drugs and vaccines. Success of the latter is emphasised by the eradication of smallpox by 1980 (92), but also by the high levels of protection efficacies (up to 99%) (123) of vaccines against, for example, measles, hepatitis A, and polio.

Infections with the 2012 newly-discovered MERS-CoV resulted in an alarming case fatality rate of about 35% (297). This pathogen is thus an appropriate example of an emerging highly pathogenic virus. Extensive research on interactions of SARS-CoV with the human immune system (180, 334, 249, 48) provides us with some insight into pathogenicity and immune evasion strategies of human coronaviruses. However, immune responses induced by MERS-CoV, as well as the mechanisms mediating protection, were unknown directly after its emergence. Therefore, an efficient protection from MERS-CoV-induced epidemics requires the production of pre-pandemic vaccines, but also, in parallel, an investigation of MERS-CoV's interaction with the immune system. This acquired knowledge might consequently be applied to further improve antiviral drugs and vaccine strategies.

4.1. pDCs as potent source of type I and III IFNs upon infection with MERS-CoV

The observation that some patients who failed to promote type I IFN production upon MERS-CoV infection (91) suffered from a more severe disease, indicates a correlation of innate immune responses with progress of the disease. However, human epithelial cells (46, 147, 330), macrophages (325) and bronchial and lung tissue samples from healthy donors cultured *ex vivo* (46) failed to secrete type I IFNs upon MERS-CoV infection. Consistent with these publications, we could demonstrate that MERS-CoV was not capable of triggering type I and III IFNs in most human immune cells, including macrophages, B cells, and human monocyte-derived DCs (MDDCs). By contrast, the secretion of IFN-β, IFN-λ, and particularly IFN-α by plasmacytoid dendritic cells (pDCs), helped identify pDCs as a potent source of type I IFNs in response to MERS-CoV by the human immune system. The identified mechanisms involved in infection of pDCs and induction of type I IFN responses are summarised in Fig. 34:

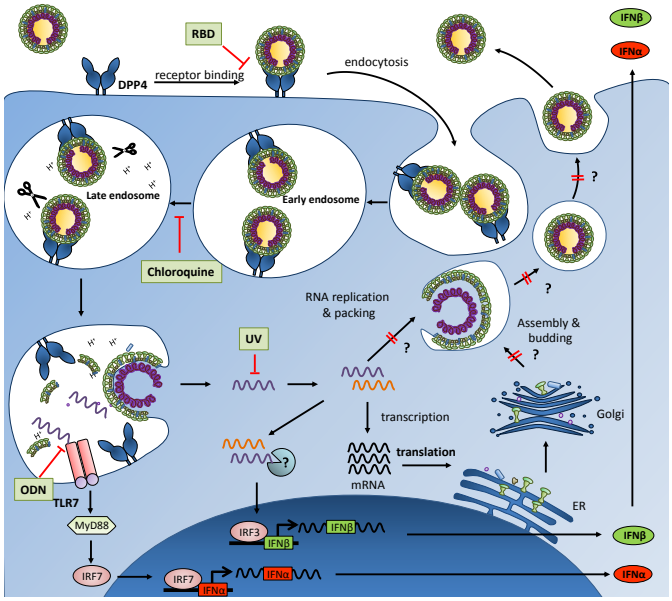

Fig. 34 Model for MERS-CoV-induced infection and type I IFN secretion in human pDCs. The figure schematically depicts the life cycle of MERS-CoV in human pDCs. MERS-CoV most likely enters pDCs after binding to DPP-4 and subsequent endocytosis. Amplification of viral RNA and expression of viral protein takes place after release of the replication machinery into the cytosol. Further steps of assembly, budding or release of viral particles are inhibited. Viral ssRNA is sensed via TLR7 in the endosome resulting in the expression of particularly IFN-α. Replication intermediates like dsRNA are sensed by unknown mechanisms, which results in the production of IFN-β. Written in bold letters and greenly edged are treatments which were experimentally conducted by Scheuplein *et al.*, 2015. Questions marks indicate supposed mechanisms, which remain to be investigated (239)

MERS-CoV was shown to initially infect pDCs via binding to DPP-4 and subsequent endosomal uptake. Amplification and transcription of viral RNA likely takes place after release of the viral replication machinery into the cytosol. The sensing of MERS-CoVs RNA by PRRs in the endosomes thereby induces secretion of type I and III IFNs, particularly IFN-α. Secretion of IFN-β is likely to be mediated by sensing of amplified MERS-CoV dsRNA after release of the viral replication machinery into the cytosol in addition. However, MERS-CoV failed to fully replicate in pDCs, which indicates that further steps during viral assembly, budding, or release are blocked after transcription and amplification of viral RNA.

Besides giving insights into viral replication, our results appear important in unravelling potential factors of MERS-CoV-induced severe pathogenicity. Several reports demonstrated that type I IFNs play a significant role in the clearance of various viruses like CCHFV (24), chikungunya virus (CHIKV) (234) or measles virus (MV) (189). Our findings, combined with previously published results (46, 147, 325, 330), question the role that the considerable, but exclusively pDC-mediated type I IFN production might have in humans. In fact, MERS-CoV replication *in vitro* has been shown to be highly sensitive to treatment with IFN-α in ng/ml concentrations (89, 298) indicating that the amounts secreted by pDCs might be relevant. However, while the production of type I and III IFNs may be a cause of suppressed MERS-CoV replication in pDC cell culture, its relevance *in vivo* remains to be investigated in animal models or clinical studies.

Regarding other viruses, IFN production by pDCs has been demonstrated to be responsible for clearance of respiratory syncytial virus (RSV) (253, 282), vesicular stomatitis virus (VSV) (264) or murine cytomegalovirus (MCMV) (264) in mice (264). However, at high viral doses, the role of pDCs in MCMV clearance, for example, has been negligible. This may have been due to the low numbers of pDCs at the sites of viral replication (264). Interestingly,

MERS-CoV infections and especially those with severe outcome, are mostly found in the elderly (6), who are known to have fewer and less functional pDCs (131, 245). Consequently, decline of type I IFN production by pDCs in elderly patients might be a correlate of severe disease and would suggest that pDCs play a significant role in MERS-CoV clearance.

On the other hand, severe pathogenicity of some viruses like influenza subtype H5N1 (134) or human enterovirus (EV71) (285), is characterised by immunopathogenicity based on overshooting cytokine responses (148). The latter is also considered to be a cause of SARS-CoV-induced severe inflammation of lung tissue (45). Accordingly, SARS-CoV infected patients, who suffered from a more severe outcome and were more likely to succumb to disease (41), exhibited elevated levels of pro-inflammatory cytokines in the serum (303).
A potential cause of this postulated immunopathogenicity is assumed to exist in delayed type I IFN responses accompanied by rapid replication of the virus (149). In infected mice, both factors — secretion of type I IFNs and considerable replication of SARS-CoV — synergistically resulted in a vast secretion of immunopathogenic pro-inflammatory cytokines by recruited inflammatory monocyte-macrophages (IMMs) (45). Delayed type I IFNs responses are assumed to be mediated, particularly if the immediate secretion of type I IFN by infected cells is inhibited. This has been observed for coronaviruses that evade cytosolic RLR sensing, like SARS-CoV or mouse hepatitis virus (MHV) (149).
While SARS-CoV, like MERS-CoV, tends to suppress type I IFNs in human epithelial cells, macrophages (329) and cDCs (44, 329); human pDCs have also been identified as potent producers of IFN-α/β upon SARS-CoV infection (45). The exclusive capability of pDCs to secrete type I IFNs was assumed to result in potent, but delayed IFN-I secretion in mice infected with SARS-CoV and thus likely in immunopathogenicity (149).
Type I IFN production by pDCs upon infection with ssRNA viruses is mostly mediated through the sensing of viral ssRNA via TRL7 (13, 205). In contrast, non-haematopoetic cells are known to secrete IFN-β exclusively and macrophages and cDCs mostly (in addition to TLR-3 in the endosomes) (13) after sensing of viral dsRNA by cytosolic MDA-5 (long dsRNA) (265) or RIG-I (phosphorylated ssRNA, short dsRNA) (265). Consistent with the findings of previous publications, we demonstrated that the secretion of IFN-α (138, 174), IFN-β (232), and IFN-λ (205) by pDCs depends on recognition of viral RNA by TLR-7 in the endosomes. Interestingly, immune evasion strategies proposed for MERS-CoV mostly assume interference with the sensing of dsRNA by cytolic RLR (298) or RLR-induced signalling pathways (15, 249). By implication then, it would be probable to suppose that type I IFN by pDCs might be unimpaired as a consequence of ssRNA sensing via TLR-7. By contrast, RLR-mediated sensing of RNA is known to play a subordinate role in pDCs (240). It has so far

only been shown for some negative-sense RNA viruses like human respiratory syncytial virus (hRSV) (121) or VSV (18), which enter the cell via the plasma membrane. For other viruses, like influenza viruses (73), type I IFN secretion tends to be independent of viral replication. In our study, secretion of IFN-β, but not IFN-α or IFN-λ by pDCs was shown to depend on live virus and hence, the presence of replication intermediates like dsRNA, in the cytosol. Whether expression of IFN-β upon MERS-CoV infection is mediated via RLR sensing remains to be investigated.

Nevertheless, the fact that type I IFN responses are restricted to pDCs (44) taken together with the similarity of symptoms in both SARS-CoV and MERS-CoV (320), indicates that immunopathogenicity may also play a role for MERS-CoV. In line with this argument, Zhou *et al*. previously observed that MERS-CoV induces the secretion of large amounts of pro-inflammatory cytokines like IL-12 and IFN-γ and chemokines like IP-10, CXCL-10 or RANTES in human macrophages (325). Moreover, infiltration of macrophages and neutrophils into infected lung tissue was observed in MERS-CoV-infected patients (105, 320), rhesus macaques (192), and also in MERS-CoV susceptible mice (172, 280). Whether this infiltration of immune cells and pathogenicity is associated with potentially delayed type I IFN secretion by pDCs, as proposed for SARS-CoV, remains to be investigated. However, then, regulation of type I IFN production by pDCs could be considered as potential target of antiviral therapy.

In any event, an effective vaccine, inducing protective adaptive immune responses, would be beneficial, especially in at-risk patients. Consequently, this thesis aimed to produce and characterise such a potential pre-pandemic vaccine to protect against the highly-pathogenic MERS-CoV.

4.2. MV-MERS-S is an efficient vaccine to protect against MERS-CoV

A putative vaccine against MERS-CoV or similar emerging infections should be safe, immunogenic, rapidly available and its production should be cost efficient. For this purpose, replication-competent measles virus (MV) constitutes a promising tool, since it is based on an efficient vaccine with a remarkable safety profile (102, 238). Moreover, an established rescue system (218) not only enables the fast generation of recombinant MV clones from DNA plasmids; but also, the insertion of open reading frames (ORFs) encoding for foreign antigens into MV's genome. For this reason MV has already been utilised as a vaccine platform protecting against MV and a wide variety of other foreign pathogens (69, 164, 248) as described in 1.5 (Tab. 2).

To characterise whether MV also constitutes an appropriate vaccine platform against MERS-CoV, we generated recombinant viruses which expressed the full-length surface protein spike (MERS-S) of MERS-CoV and a truncated version of MERS-S lacking the transmembrane domain (MERS-solS). Comparable to other so-far developed vaccines (Tab. 3), replication-competent MV-MERS-S and MV-MERS-solS[14] induced potent antibody responses capable of neutralising infectivity of MERS-CoV. However, although we aimed to induce stronger humoral immune responses by generation of MV-MERS-solS, VNTs provoked by this vaccine were similar; and MERS-S-specific Abs, just slightly higher than those induced by MV-MERS-S. Interestingly, a DNA vaccine encoding MERS-S lacking the transmembrane (TM) domain (MERS-SΔTM) did even induce significantly lower titres of nAbs than MERS-S (283). For SARS-S, where a similar phenomenon has been observed (313), conformational alteration of the soluble spike protein and thereby induction of Abs which do not efficiently bind to native SARS-S was supposed to be the putative cause (313). Such alterations might also apply for MERS-solS and affect the conformation of the MERS-RBD, thereby resulting in less functional MERS-CoV- neutralising Abs.

Although most experimental vaccines rely on full-length MERS-S and are thus comparable to our vaccine approach, methodological differences in Ab titre determination makes direct comparison a challenge. However, VNTs induced by MVA-MERS-S (255) and Ad5.MERS-S (144) were calculated as the reciprocal of the highest dilution absolutely neutralising MERS-CoV infectivity and are hence, at least based on methodology, comparable to our vaccines. Considering that 10^3-fold fewer viral particles than MVA and 10^6-fold fewer than Ad5 were applied in our study, MV-MERS-S still induced robust VNTs (Tab. 3). That aside, it should be noted that MVA and Ad5-induced immune responses were tested in Balb/c wt mice, whereas IFNAR$^{-/-}$CD46Ge mice on a C57BL/6(BL/6) background were used for examination of MV-MERS-S. While Balb/c mice are predominantly characterised by a Th2-mediated (and thus humoral) immune response, Th1- and hence, cellular immunity prevails in BL/6 mice after vaccination (34, 182, 237). Furthermore, vaccine-induced Ab production by B cells (94, 55) may also be influenced by the abortive effects of IFNAR signalling (see 1.2) (119, 127, 240) in IFNAR$^{-/-}$CD46Ge.

Focusing on cellular immunity, T cell responses have so far been demonstrated for DNA (195) and VLPs (281) in non-human primates; and recombinant RBD (157), DNA (195), MVA (280), Ad5/Ad45 (107) and MV (172), in mice (Tab. 3).

[14] MV_{vac2}-MERS-S(H) and MV_{vac2}-MERS-S(H) for simplification termed MV-MERS-S and MV-MERS-solS

Tab. 3 Experimental MERS-CoV vaccines. *clinical trial started; underlined, assays comparable to MV-MERS-S or MV-MERS-solS; grey, not tested.

Vaccine platform	Construct	Pre-clinical development		Reference
		Immunogenicity	**Protection**	
Life-attenuated	recMERS-CoV			(5)
Subunit	Full lenght S trimers	**Mice (Balb/c)**: • Humoral (VNTs)		(50)
	RBD fused with human FC	**Mice (Balb/c)**: • Humoral (VNTs) • Cellular (IFNγ ICS) **Rabbits** • Humoral (VNTs)	**Mice (Balb/c)**: • reduced viral titers (below detection limit after vaccination)	(170, 171, 322)
	Truncated RBD	**Mice (Balb/c)**: • Humoral (MERS-S1 Abs, VNTs) • Cellular (IFNγ -ELISpot: approx. ca. 200 SFC/10^6 splenocytes, cytokines)		(80, 157, 188)
	MERS-CoV VLPs	**Rhesus macaques**: • Humoral (MERS-S-RBD Abs, VNTs) • Cellular (IFNγ / IL-4 ELISpot)		(281)
DNA*	Full length MERS-S	**Mice (C57BL/6)**: • Humoral (MERS-S Abs, VNTs) • Cellular (IFNγ -ELISpot: approx. 3,000 SFC/10^6 splenocytes; IFNγ-, TNF-α and IL-2 ICS) **Rhesus macaques**: • Humoral (MERS-S- Abs, VNTs) • Cellular (IFNγ ELISpot/ICS, TNF-α and IL-2 ICS) **Dromedary camels:** • Humoral (MERS-S Abs, VNTs)	**Rhesus macaques:** • reduced viral loads • reduced clinical signs	(195)
		Mice (Balb/c): • Humoral (MERS-S1 Abs, VNTs) **Rhesus macaques**: • Humoral (MERS-S-RBD Abs, VNTs) • Cellular (IFNγ / IL-4 ELISpot)	**Rhesus macaques:** • reduced clinical signs	(283)
	MERS-S1, MERS-SΔTM	**Mice (Balb/c)**: • Humoral (MERS-S1 Abs, VNTs)		(283)
Rec. vectors	Ad5.MERS-S or S1	**Mice (Balb/c)**: • Humoral (MERS-S RBD Abs, VNTs: MERS-S: approx. 1,500, MERS-S1 approx. 2,048)		(144)
	Ad5/ Ad45 S	**Mice (Balb/c)**: • Humoral (MERS-S RBD Abs, VNTs) • Cellular (IFNγ -ELISpot: approx. ca. 400 SFC/10^6 splenocytes, cytokines)		(107)
	MV-S/ MV-solS	**Mice (IFNAR$^{-/-}$CD46Ge BL/6)**: • Humoral (MERS-S Abs, VNTs: approx. 840) • Cellular (IFNγ ELISpot: approx. 2,000 SFC/10^6 splenocytes, Proliferation, CTL response)	**Mice**: • reduced viral loads (130- -190-fold) • reduced viral titers (5- -13-fold reduction) • reduced clinical signs	(172)
	MVA-MERS-S	**Mice (Balb/c):** • Humoral (VNTs: approx. 1,500) • Cellular (IFNγ -ELISpot: approx. 1,500 SFC/10^6 splenocytes) **Dromedary camels:** • Humoral (mucosal, VNTs)	**Mice (Balb/c):** • reduced viral loads (50- -700-fold reduction) • reduced clinical signs **dromedary camels:** • reduced excreted infectious virus • reduced excreted viral RNA transcripts	(108, 255, 280)
	RABV-MERS-S1	**Mice (Balb/c):** • Humoral (MERS-S1 Abs, VNTs)	**Mice (Balb/c):** • reduced viral loads (390-fold reduction) • reduced viral titers (below detection limit after vaccination)	(299)
	VRP-MERS-S	**Mice (Balb/c)**: • Humoral (protective sera, titers not shown)	**Mice**: • reduced viral titers (below detection limit after vaccination)	(324)

Taking into consideration the numbers of IFN-γ secreting T cells among splenocytes, the expression of MERS-S by DNA (195), MVA (280), and MV (172) induced the most potent cellular immune responses (Tab. 3). However, in contrast to other studies, T cell responses induced by MV-MERS-S and MV -MERS-solS, were detected after co-cultivation of splenocytes with MERS-S expressing DC cell lines for antigen-specific recall. Nevertheless, T cell responses re-stimulated by these cell lines were comparable to those reactivated by the immunodominant MERS-CoV peptide S1165 (324) as also demonstrated for Ova expressing cells. Thus, transgenic DC cell lines were shown to be a suitable alternative for antigen-specific recall without intensive knowledge of immunodominant peptides and the time-consuming production of recombinant proteins. By application of these cell lines, T cells of MV-MERS-S and MV-MERS-solS vaccinated mice – as only vaccines so far –were additionally shown to respond to MERS-S specific recall by antigen- specific proliferation of $CD8^+$ T cells and CTL effector responses. CTL effector responses may be critical for protection as demonstrated for a number of viruses like influenza (223) or CMV (38).

With regards to studies of protection efficacy, the lack of susceptibility of mice to MERS-CoV infection (49) was overcome by i. n. transduction with AdV-hDDP-4. Mice treated this way became susceptible to infection by expression of the MERS-CoV entry receptor (324) and could then be used to test the efficacy of different experimental vaccines against MERS-CoV (280). Using this method, protection efficacy in Balb/c mice has been demonstrated for recombinant MERS-S RBD fused with human FC (322), as well as the vector-based vaccines Venezuelan equine encephalitis virus replicon particles encoding MERS-S (VRP-MERS-S) (324), MVA- MERS-S (280) and RABV- MERS-S1 (299) (Tab. 3).
However, in contrast to Balb/c mice, 40% of $IFNAR^{-/-}$CD46Ge mice used in our study were not susceptible to MERS-CoV infection, even though AdV-hDDP-4 transduction in 60% of these mice was efficient. The reasons for lack of MERS-CoV susceptibility in the remaining mice is so far not understood, but indicates that AdV-hDDP-4-transduced $IFNAR^{-/-}$CD46Ge mice do not appear to be an optimal model for characterisation of protection efficacy by MV-based vaccines against MERS-CoV. Nevertheless, despite the drop-out rate, significant differences in viral loads, reduced infectious titres and, most importantly, reduction of clinical signs between control and MERS-S-vaccinated became evident. Thus far, MV-based MERS-CoV vaccines are one of only six different experimental vaccines that have showed robust protection efficacy in appropriate animal models

Remarkably, experimental MVA-MERS-S (109) and DNA vaccine encoding full-length MERS-S induced humoral immune responses in dromedary camels (195), the suspected natural reservoir of MERS-CoV (108, 179). A reduced shedding of MERS-CoV as demonstrated for MVA-MERS-S vaccinated camels (109) might then prevent transmission of MERS-CoV to

humans if dromedary camels are vaccinated. Such veterinary use of MV-based vaccines seems quite unlikely, certainly initially, since efficacy of protection depends on active replication of rMV in the vaccinated host, as demonstrated (Fig. 16, Fig. 26). However, dromedary camels can be infected with Peste des petits ruminants (PPR) (139) or Rinderpest virus (RPV) (72), two close relatives of MV. Interestingly, camel kidney cells have also been shown to be susceptible *in vitro,* at least under certain circumstances, to MV infection (183). Moreover, the MV vaccine is, in principle, able to induce immune responses in non-human species such as dogs (11) or cattle, where it is has been shown to protect calves against RPV challenge (215). Thus, it might be considered to test the immunogenicity of MV-MERS vaccines in camels.

As a first step, though, clinical trials have been started, or are in the planning stages, in order to analyse the efficacy of experimental vaccines in man (184). Among potential vector-based vaccines, inactivated RABV or replication-competent MV as platform, have the advantage of being based on vaccines historically known to be efficient and safe for use in humans (102, 238, 294). On the other hand, already-implemented vaccination in patients carries with it the potential risk that pre-existing immunity might reduce the efficacy of these vaccine platforms.

Considering the effects of pre-formed MV immunity in mice, we observed that single-pre-vaccination with pure MV vaccine did not impair MV-MERS-S-induced nAb titres in a preliminary experiment. This observation is consistent with previously published results, where the induction of respective pathogen-specific Abs by MV-HIV (164) or MV-CHIKV vaccines (33) was also not affected by single-pre-vaccination of mice with an empty MV vaccine strain. However, neither the effects on induced cellular immune responses, nor the effects of double-pre-vaccination, have yet been tested so far. Here, we observed that MERS-S-specific cellular immune responses were significantly reduced if mice were pre-vaccinated once or twice with pure MV vaccine. Whether these reduced, yet still detectible T cell responses, and still induced MERS-CoV nAbs are protective against MERS-CoV, remains to be analysed. Interestingly, residual MV-CHIKV-induced CHIKV-specific immune responses in mice pre-vaccinated once prior, did prove protective against CHIKV challenge (33). Thus, if nAbs are a correlate of protection, as they are for CHIKV (33), then humoral immune responses, at least in once-pre-vaccinated mice, might be sufficient for protection, even if T cell responses are significantly reduced. Indeed, there are indications for a correlation between humoral immunity and protection since passively transferred sera from VRP-MERS-S immunized mice were shown to be protective (324).

Keeping in mind that VNTs in this single experiment were unusually low, a reduction of MERS-CoV nAbs to titre levels below detection after double-pre-vaccination might, on the

contrary, be of relevance. However, it has to be noted that mice were vaccinated with MV-MERS only two months after boost pre-vaccination and hence, at time points of high MV nAb titres. In the light of biological relevance, humans would be vaccinated years after initial MV vaccination and consequently, at time points of lower nAb titres, which are known to decrease over time (65, 66). In line with this argument, a recant phase-I clinical trial has impressively demonstrated that MV-CHIKV was potent in inducing α- CHIKV Abs in measles pre-immune patients (219). Here, immunogenicity of a MV-based vaccine was not only transferred from mice to men, but also shown to be indeed unaffected by pre-existing immunity. Thus, whether the used pre-vaccination set-up is an appropriate model to display the physiological situation in man, remains to be tested in a clinical trial.

Taken together, we could demonstrate that MV-MERS-S and MV-MERS-solS are efficient experimental vaccines that are capable of triggering protective MERS-CoV specific humoral and cellular immunity *in vivo*. Besides the five other experimental vaccines that have so far demonstrated protection efficacy, these, consequently, merit testing as vaccines against-MERS-CoV in clinical trials.

Vaccination targeting MERS-S is likely to be successful, since circulating MERS-CoV stains represent one single serotype (194), indicating that MERS-S has so far not undergone significant amino acid changes. Nevertheless, already-described mutations in MERS-CoVs glycoproteins (143, 146, 169) do indicate the potential for antigenic variations in future. A positive selection of escape mutants would therefore make a supportive vaccination prudent. These mutants would have to be of unaffected or even enhanced virulence; and the vaccination would need to be based on usually more conserved nucleocapsid proteins. Given these possibilities, this thesis also aimed to characterise an alternative MV-derived vaccine encoding MERS-N.

4.3. MV-MERS-N as alternative vaccine against MERS-CoV

Although the glycoprotein spike is the primary target of prophylactic vaccines against coronaviruses, targeting the coronavirus nucleocapsid protein (N) of, for example, SARS-CoV (145, 161), mouse hepatitis virus (MHV) (260), or avian infectious bronchitis virus (IBV) (239) has also been shown to induce potent cellular immune responses *in vivo*. For IBV, N-specific immune responses induced by Semliki Forest virus (SFV) vector (239) or recombinant fowl poxvirus (rFPV) (318) encoding IBV-N have proved to be even protective against IBV challenge in chickens.

By generating MV-MERS-N[15], we demonstrated that a potential vaccine candidate against MERS-CoV targeting MERS-N was also potent to induce antigen-specific cellular immunity. Here, the immune response was comparable to that of MV-N or H7-specific cellular immunity, although still significantly lower than those triggered by MV-MERS-S or MV-MERS-solS. Notably, besides considerable MERS-S-specific IFN-γ secretion by T-cells, MERS-S was additionally the only antigen which triggered proliferation and CTL effector responses when testing splenocytes of immunised mice. This indicates a remarkably strong immunogenicity of MERS-S, particularly to induce $CD8^+$ T cell responses. Interestingly, most immunodominant $H2^b$-restricted T epitopes that were recognised by MERS-CoV-induced $CD8^+$ T cells of BL/6 mice, were located in the S; but not N, protein (324). This observation might explain the considerable MERS-S specific CTL-responses in $IFNAR^{-/-}$ CD46Ge mice (BL/6 background). By contrast, at least one epitope of MERS-N, N214, was shown to be immunodominant in Balb/c mice (324). Therefore, results might look different in these mice, that have another peptide-presenting haplotype. Nevertheless, detection of MERS-N specific IFN-γ secreting T cells among splenocytes of MV-MERS-N immunized mice indicates that MERS-N indeed includes immunodominant $H2^b$-restricted epitopes. Whether these are recognized by $CD8^+$ or $CD4^+$ T cells and whether the observed immunogenicity or potential immunogenicity in other models is relevant for protection though, should be tested as a next step.

In conclusion, then, this weaker immunogenicity in comparison to MERS-S might be a bias resulting from the animal model, but might still be due to peptide presentation by the transgenic DC cell lines, and so warrants further investigation. Nevertheless, MV-MERS-N could serve as an alternative or supportive vaccine approach against MERS-CoV. Both MERS-N and MERS-S could even be co-expressed by recombinant MV to induce neutralising Abs, as well as cellular immunity by targeting a conserved nucleoprotein.

4.4. MV as vaccine platform against other highly pathogenic viruses like H7N9 or CCHFV

To further utilise MV and analyse its properties as a vaccine platform against highly pathogenic viruses other than MERS-CoV, this thesis also aimed to generate MV-derived vaccines against the avian influenza virus H7N9 and Crimean-Congo haemorrhagic fever virus (CCHFV).

[15] MV_{vac2}-MERS-N(H) for simplification termed MV-MERS-N

Insofar as MVs targeting MERS-CoV are concerned, recombinant vaccines encoding antigens of those viruses have the potential to be rapidly rescued; and the expression of most antigens in cells infected with respective vaccines confirmed. However, the so far unsuccessful detection of the glycoprotein Gn of CCHFV demonstrates that *in vitro* examination of vaccines against pathogens that are not yet well characterized can be challenging. The failure to detect preGn, even in an inactivated CCHFV lysate used as a positive control, was, in this instance, most likely due to the unsuitability of the two antibodies used to bind preGn under denaturing conditions in western blot analysis, as has already been described (26).

With regards to replication of MV-H7N9 and MV-CCHFV vaccines, the insertion of respective antigen encoding genes had no effect on propagation of MV-H7, MV-N9 and 16 of 18 MV-CCHFV constructs. However, two vaccines, MV_{vac2}-CCHFV-solGn(P) and particularly MV_{vac2}-CCHFV-G-FL(P), revealed instances of impaired replication. The considerable size of the inserted CCHFV-M segment (5.4 kb) might be a factor here. It may somehow interfere with the growth of MV_{vac2}-CCHFV-G-FL(P), even though insertions of approximately 4 kb appeared to have no impact, as shown for full-length spike proteins of SARS-CoV (161) or MERS-CoV (172). Interestingly, interference in both cases was only observed when additional gene cassettes were inserted into a position proximal to the promotor (post P) and not in post H position. However, while insertions upstream of the N gene are known to affect growth of recombinant MV in some cases (221), insertion into positions distal to the N gene should normally not be problematic. Nevertheless, expression of antigens by the post P position of MV is higher compared to positions distal to the promotor and potential interference of expressed antigens, consequently stronger (27). Such interference might be exerted by toxicity of the antigens on infected cells, as described for MVs expressing ecto domains of dengue (31), thereby affecting replication of the vaccine. However, toxicity of CCHFV glycoproteins has not been described thus far (26, 307). Another possibility might entail interference of membrane-bound proteins, like those encoded by MV_{vac2}-CCHFV-G-FL(P), with, for example, viral assembly by competition with MV glycoproteins, as described for an MV encoded fusion protein (F) of mumps virus (MuV) (287). Moreover, the complex processing machinery of CCHFV glycoproteins (230) could also somehow interfere with the replication cycle of MV. However, this needs to be investigated further.

In the case of CCHFV-solGn, interference might be due to a misfolded protein with altered characteristics caused by truncation. Indeed, abortive localisation to the Golgi-apparatus and hence, expression of a misfolded protein has been described for Gn constructs lacking the mucin-like and P35 region of preGn (26). Although abortive localisation to the Golgi-apparatus hence predicts altered folding for both MV-CCHFV-Gn and MV-CCHFV-solGn, the

additional truncation of the transmembrane might also result in altered characteristics such as, for example, toxicity. However, the exact effects of such constructs remain open to question and warrant further investigation.

Thus, although most MV-CCHFV constructs expressed the inserted antigens without causing any effects on the vaccines replication, further *in vitro* analysis is required to select the most promising CCHFV vaccine candidates for testing *in vivo*. Since an experimental MVA vaccine encoding both glycoproteins (encoded by full-length CCHFV-M segment) has been shown to induce protective humoral and cellular immunity (40, 77) *in vivo*, MV_{vac2}-CCHFV-G-FL, might also prove to be a promising vaccine candidate. Immune responses against the more conserved nucleocapsid protein of CCHFV (116), which were not protective in the case of MVA (77), could, moreover, support the efficacy of MV_{vac2}-CCHFV-G-FL for example. This could result in increased cross-protection against the seven different CCHFV strains (71).

In contrast to MV-CCHFV, the immunogenicity of MV-H7 and MV-N9[16] has already been demonstrated *in vivo* during this thesis. Here, both vaccines induced considerable titres of H7N9 binding Abs, while Abs that completely neutralised H7N9 A/Shanghai/2/2013-A/PR/8/34 infectivity were detectible after vaccination with MV-H7, but not with MV-N9. Induction of nAbs by MV-H7 was expected, since α-HA Abs induced by vaccination may hinder HA – the receptor binding protein of influenza viruses – from binding to sialic acids and consequently prevent viral entry (242). Influenza NA, by contrast, is responsible for virus particle release by removal of bound sialic acids from the cell and virus surface (141, 241, 266, 301). Hence, induced Abs binding NA prevent removal of sialic acids by NA, which results in increased aggregation of viruses on the cell surface (266, 301). Even though these Abs are not completely neutralising in terms of their effect, the aggregation of particles may result in reduced shedding of viral particles and thereby help to mediate protection *in vivo* (235). Indeed, α-N9 Abs induced by N9 expressing vaccinia virus (rVac-N9 NA) were shown to reduce the replication of H7N9 *in vitro* (130).

Although the effects of MV-N9-induced Abs on replication of H7N9 have so far not been tested, they did show evidence of being able to inhibit the enzymatic functionality of N9 to cleave sialic acid. This demonstrated inhibition of enzymatic functionality will most likely result in aggregation of viral particles (266, 301) and consequently, reduced replication (130). Surprisingly, Abs induced by MV-H7 also inhibited the NA-specific activity of H7N9 A/Shanghai/2/2013-A/PR/8/34. This NA inhibition by α-HA Abs is likely attributable to the steric hindrance of H7N9 A/Shanghai/2/2013-A/PR/8/34 NA by Abs bound to the HA, a mechanisms already described elsewhere (57, 142).

[16] MV_{vac2}-H/(P) and MV_{vac2}-N9(P) for simplification termed MV-H7 and MV-N9

Although protection against many viruses such as SARS-CoV (261, 313) is mediated by antibodies, influenza viruses are known to continuously evade neutralising Abs by antigenic shift (point mutations in the glycoproteins) and drift (exchange of genomic segments against other subtypes) (75). Thus, Abs induced by vaccines often do not protect against escape mutants. By contrast, cellular immunity mediates higher cross-protection against other influenza subtypes (95, 177, 291) and was generally shown to be important for recovery from influenza viruses like H3N2 or H1N1 - at least in animal experiments (23). In line with this observation, the induction of cytotoxic T cell responses also appears to correlate with reduced H7N9 pathogenicity in human patients (288).

In addition to Abs neutralising H7N9, MV-H7 was shown to induce H7-specific cellular immune responses, which were characterised by a H7-specific IFN-γ secretion from isolated spleen cells. These detected T cell responses might hence increase the likelihood of the vaccine to be protective (288). However, although splenocytes from MV-N9-vaccinated mice contained more IFN-γ secreting cells than those of control mice, these responses were not restricted to re-stimulation by N9-expressing DCs but also provoked by untransduced DC cell lines. Even though DC cell lines also provoked a slight unspecific IFN-γ response by, for example, MERS-N or H7-specific T cells, background responses were approximately three-fold higher for T cells of MV-N9-vaccinated mice. This observation indicated that unspecific re-stimulation correlated with immune responses induced by this specific vaccine. Interestingly, MV_{vac2}-N9(P) exhibited a slightly more stable replication than other viral vaccines generated during the course of this thesis. Thus, it might be possible that viral proteins may still be present among splenocytes due to the longer persistence of MV_{vac2}-N9(P) in the spleen. In Uhlig *et al.* we demonstrated that APCs isolated four days after vaccination with Ova-transferring PTVs are still capable of activating Ova-specific T cells. These results indicated that presentation of Ova-peptides was still ongoing at this time-point of splenocyte isolation (286). This being the case, further expressed viral proteins might be taken up by DCs, thereby resulting in an unspecific re-call of virus-specific T cells. This could also be an explanation for the generally high background stimulation of DC3.2 cells, which are known to be potent in their expression of exogenous antigen (253). Further investigation concerning this long presentation of antigens but also regarding possible influences of DC cell-lines in this example seems therefore to be worthwhile.

Even though both MV-H7 and MV-N9 induced humoral responses, with at least MV-H7 showing evidence of cellular immune responses, as yet, protection by these vaccines has not been tested. Already though, several published experimental vaccines, including VLPs (216, 236), DNA (314) and MVA (154) have shown efficacy in protecting ferrets (216, 154) and mice (216, 236, 314) from challenge with H7N9 by induction of H7-specific immune

responses. Considering humoral immune responses, HAI titres of about 18-40 are normally associated with 50% infection risk in human patients (82, 118, 212). Titres of 160 were even shown to reduce the likelihood of infection with influenza H3N2 by 95 % (212). Experimental DNA or VLP vaccines, targeting H7 as antigen, induced HI titres of approx. 60 (216), 50 (236) and 150 (314), respectively, and were protective in mice. Hence, HI titres of about 200 induced by MV-H7 are also likely to be protective against H7N9 challenge. Moreover, cellular immunity induced by MV-H7 is comparable to T cell responses provoked by a protective DNA vaccine ($400/10^6$ splenocytes vs. $500/10^6$ splenocytes) and might be a further indicator for protection.

Thus, this PhD thesis has demonstrated that MV-derived vaccines have the potential to be used as vaccines against highly pathogenic viruses like H7N9 of the *Orthomyxoviridae* or CCHFV of the *Bunyaviridae* family. Taken together, the data suggests that vaccine-derived MV has the potential to become a promising vaccine platform that may be applied as a first line of defence against different emerging, highly pathogenic viruses.

4.5. Conclusion

This thesis contribution towards the development of potential vaccines against emerging infections by providing insights into the pathomechanisms of a highly pathogenic emerging virus, as well as establishing the appropriate assays needed to test the immunogenicity of vaccines *in vivo*, and by outlining a potential vaccine platform derived from recombinant measles viruses. To summarise:

Interaction of MERS-CoV with innate immune cells: We identified pDCs as a remarkably potent but exclusive source of antiviral type I and type III IFNs (233). Here, we uncovered the mechanisms of viral entry, as well as the replication and sensing of viral RNA essential in the production of type I and III IFNs by infected pDCs. These results may serve as a basis from which to analyse the protective properties of pDCs as well as their role as a potential pathomechanism of MERS-CoV. Such knowledge might prove essential for future antiviral drug development or vaccine design focusing on pDCs as potential targets.

Setting up a system to re-stimulate T cells *ex vivo* and to analyse T cell responses: We established set-ups for vaccination and immunological assays in order to analyse cellular immune responses (172, 276). The application of transgenic DC cell lines, which stably express full-length ORFs of antigens, was found to be suitable for the re-stimulation of antigen-specific T cells for five different antigens induced by two different vaccine platforms. Hence, it was established from this work that transgenic DC cell-lines allow for

the re-stimulation of T-cells without any need for deeper knowledge of immunodominant peptides or the availability of recombinant proteins.

Generation and characterisation of vaccine-derived MV as pre-pandemic vaccine platform: We generated MV-derived vaccines against emerging infections, which were characterised as follows:

1. Rapid production of vaccines against three viruses belonging to three distinct families *Coronaviridae*, *Orthomyxoviridae* and *Bunyaviridae*
2. Insertion of antigen-encoding ORFs up to 5 kb and expression of full-length antigens in infected cells
3. Induction of humoral immune responses by MV_{vac2}-H7(P), MV_{vac2}-N9(P), MV_{vac2}-MERS-S(H) and MV_{vac2}-solS(H)
4. Induction of cellular immune response by MV_{vac2}-H7(P), MV_{vac2}-MERS-N(H), MV_{vac2}-MERS-S(H) and MV_{vac2}-solS(H)
5. Protection efficacy as demonstrated against MERS-CoV challenge in mice.

These findings, when combined with already published data, serve to demonstrate that MV is a promising vaccine platform that may be used against various viruses. These include DNA viruses like HBV (*Hepadnaviridae*) (248), but also RNA viruses like HIV (*Retroviridae*) (164), WNV (*Flaviviridae*) (32) or the demonstrated MERS-CoV (*Coronaviridae*) (172) and H7N9 (*Orthomyxoviridae*). All these vaccines have the advantage of being expressed in the backbone of a long-term applied, efficient, and safe vaccine.

5. REFERENCES

1. **Abaitua F, Rodriguez,** JR, **Garzon A, Rodriguez D, Esteban M.** 2006. Improving recombinant MVA immune responses: potentiation of the immune responses to HIV-1 with MVA and DNA vectors expressing Env and the cytokines IL-12 and IFN-gamma. Virus Res. 116:11–20.
2. **Ahmed R, Gray D.** 1996. Immunological Memory and Protective Immunity: Understanding Their Relation. Science 272:54–60.
3. **Akahata W, Yang Z-Y, Andersen H, Sun S, Holdaway HA, Kong W-P, Lewis MG, Higgs S, Rossmann MG, Rao S, Nabel GJ.** 2010. A virus-like particle vaccine for epidemic Chikungunya virus protects nonhuman primates against infection. Nat Med 16:334–338.
4. **Akira S, Takeda K.** 2004. Toll-like receptor signalling. Nature Reviews Immunology 4:499–511.
5. **Almazán F, DeDiego ML, Sola I, Zuñiga S, Nieto-Torres JL, Marquez-Jurado S, Andrés G, Enjuanes L.** 2013. Engineering a Replication-Competent, Propagation-Defective Middle East Respiratory Syndrome Coronavirus as a Vaccine Candidate. MBio 4.
6. **Alsharifi M, Mullbacher A.** 2010. The gamma-irradiated influenza vaccine and the prospect of producing safe vaccines in general. Immunol Cell Biol 88:103–104.
7. **Am McBean, Thoms ML, Albrecht P, Cuthie JC, Bernier R.** 1988. Serologic response to oral polio vaccine and enhanced-potency inactivated polio vaccines. Am J Epidemiol 128:615–628.
8. **Andre FE.** 1989. Summary of safety and efficacy data on a yeast-derived hepatitis B vaccine. Am J Med 87:14S-20S.
9. **Andrejeva J, Childs KS, Young DF, Carlos TS, Stock N, Goodbourn S, Randall RE.** 2004. The V proteins of paramyxoviruses bind the IFN-inducible RNA helicase, mda-5, and inhibit its activation of the IFN-β promoter. PNAS 101:17264–17269.
10. **Appannanavar SB, Mishra B.** 2011. An Update on Crimean Congo Hemorrhagic Fever. J Glob Infect Dis 3:285–292.
11. **Appel MJG, Shek WR, Shesberadaran H, Norrby E.** 1984. Measles virus and inactivated canine distemper virus induce incomplete immunity to canine distemper. Archives of Virology 82:73–82.
12. **Auwaerter PG, Rota PA, Elkins WR, Adams RJ, DeLozier T, Shi Y, Bellini WJ, Murphy BR, Griffin DE.** 1999. Measles Virus Infection in Rhesus Macaques: Altered Immune Responses and Comparison of the Virulence of Six Different Virus Strains. J Infect Dis. 180:950–958.
13. **Baccala R, Hoebe K, Kono DH, Beutler B, Theofilopoulos AN.** 2007. TLR-dependent and TLR-independent pathways of type I interferon induction in systemic autoimmunity. Nat Med 13:543–551.
14. **Bachmann MF, Zinkernagel RM.** 1997. Neutralising antiviral B cell responses. Annu Rev Immunol 15:235–270.
15. **Bailey-Elkin BA, Knaap RCM, Johnson GG, Dalebout TJ, Ninaber DK, van Kasteren PB, Bredenbeek PJ, Snijder EJ, Kikkert M, Mark BL.** 2014. Crystal Structure of the Middle East Respiratory Syndrome Coronavirus (MERS-CoV) Papain-like Protease Bound to Ubiquitin Facilitates Targeted Disruption of Deubiquitinating Activity to Demonstrate Its Role in Innate Immune Suppression. J. Biol. Chem. 289:34667–34682.
16. **Bajenoff M, Germain RN.** 2009. B-cell follicle development remodels the conduit system and allows soluble antigen delivery to follicular dendritic cells. Blood 114:4989–4997.
17. **Banchereau J, Briere F, Caux C, Davoust J, Lebecque S, Liu YJ, Pulendran B, Palucka K.** 2000. Immunobiology of dendritic cells. Annu Rev Immunol 18:767–811.
18. **Barchet W, Cella M, Odermatt B, Asselin-Paturel C, Colonna M, Kalinke U.** 2002. Virus-induced Interferon α Production by a Dendritic Cell Subset in the Absence of Feedback Signaling In Vivo. Journal of Experimental Medicine 195:507–516.
19. **Barouch DH.** 2008. Challenges in the development of an HIV-1 vaccine. Nature 455:613–619.
20. **Beare AS, Webster RG.** 1991. Replication of avian influenza viruses in humans. Archives of Virology 119:37–42.
21. **Becker G** de, **Moulin V, Tielemans F, Mattia F** de, **Urbain J, Leo O, Moser M.** 1998. Regulation of T helper cell differentiation in vivo by soluble and membrane proteins provided by antigen-presenting cells. Eur J Immunol 28:3161–3171.
22. **Belser JA, Gustin KM, Pearce MB, Maines TR, Zeng H, Pappas C, Sun X, Carney PJ, Villanueva JM, Stevens J, Katz JM, Tumpey TM.** 2013. Pathogenesis and transmission of avian influenza A (H7N9) virus in ferrets and mice. Nature 501:556–559.

23. **Bender BS, Croghan T, Zhang L, Small PA,** JR. 1992. Transgenic mice lacking class I major histocompatibility complex-restricted T cells have delayed viral clearance and increased mortality after influenza virus challenge. J Exp Med 175:1143–1145.
24. **Bereczky S, Lindegren G, Karlberg H, Åkerström S, Klingström J, Mirazimi A.** 2010. Crimean–Congo hemorrhagic fever virus infection is lethal for adult type I interferon receptor-knockout mice. Journal of General Virology 91:1473–1477.
25. **Bermingham A, Chand MA, Brown CS, Aarons E, Tong C, Langrish C, Hoschler K, Brown K, Galiano M, Myers R, Pebody RG, Green HK, Boddington NL, Gopal R, Price N, Newsholme W, Drosten C, Fouchier RA, Zambon M.** 2012. Severe respiratory illness caused by a novel coronavirus, in a patient transferred to the United Kingdom from the Middle East, September 2012. Euro Surveill 17:20290.
26. **Bertolotti-Ciarlet A, Smith J, Strecker K, Paragas J, Altamura LA, McFalls JM, Frias-Stäheli N, García-Sastre A, Schmaljohn CS, Doms RW.** 2005. Cellular Localization and Antigenic Characterization of Crimean-Congo Hemorrhagic Fever Virus Glycoproteins. J. Virol. 79:6152–6161.
27. **Billeter MA, Naim HY, Udem SA.** 2009. Reverse genetics of measles virus and resulting multivalent recombinant vaccines: applications of recombinant measles viruses. Curr Top Microbiol Immunol 329:129–162.
28. **Boehme KW, Guerrero M, Compton T.** 2006. Human cytomegalovirus envelope glycoproteins B and H are necessary for TLR2 activation in permissive cells. J Immunol 177:7094–7102.
29. **Bowie AG, Unterholzner L.** 2008. Viral evasion and subversion of pattern-recognition receptor signalling. Nature Reviews Immunology 8:911–922.
30. **Braciale TJ, La Morrison, Sweetser MT, Sambrook J, Gething MJ, Braciale VL.** 1987. Antigen presentation pathways to class I and class II MHC-restricted T lymphocytes. Immunol Rev 98:95–114.
31. **Brandler S, Ruffie C, Najburg V, Frenkiel M-P, Bedouelle H, Desprès P, Tangy F.** 2010. Pediatric measles vaccine expressing a dengue tetravalent antigen elicits neutralising antibodies against all four dengue viruses. Vaccine 28:6730–6739.
32. **Brandler S, Marianneau P, Loth P, Lacôte S, Combredet C, Frenkiel M-P, Desprès P, Contamin H, Tangy F.** 2012. Measles vaccine expressing the secreted form of West Nile virus envelope glycoprotein induces protective immunity in squirrel monkeys, a new model of West Nile virus infection. J. Infect. Dis. 206:212–219.
33. **Brandler S, Ruffié C, Combredet C, Brault J-B, Najburg V, Prevost M-C, Habel A, Tauber E, Desprès P, Tangy F.** 2013. A recombinant measles vaccine expressing chikungunya virus-like particles is strongly immunogenic and protects mice from lethal challenge with chikungunya virus. Vaccine 31:3718–3725.
34. **Brenner GJ, Cohen N, Moynihan JA.** 1994. Similar immune response to nonlethal infection with herpes simplex virus-1 in sensitive (BALB/c) and resistant (C57BL/6) strains of mice. Cell. Immunol. 157:510–524.
35. **Brochier B, Blancou J, Thomas I, Languet B, Artois M, Kieny MP, Lecocq JP, Costy F, Desmettre P, Chappuis G.** 1989. Use of recombinant vaccinia-rabies glycoprotein virus for oral vaccination of wildlife against rabies: innocuity to several non-target bait consuming species. J Wildl Dis 25:540–547.
36. **Buchschacher GL, Wong-Staal F.** 2000. Development of lentiviral vectors for gene therapy for human diseases. Blood 95:2499–2504.
37. **Budowsky EI, Friedman EA, Zheleznova NV, Noskov FS.** 1991. Principles of selective inactivation of viral genome. VI. Inactivation of the infectivity of the influenza virus by the action of beta-propiolactone. Vaccine 9:398–402.
38. **Bunde T, Kirchner A, Hoffmeister B, Habedank D, Hetzer R, Cherepnev G, Proesch S, Reinke P, Volk H-D, Lehmkuhl H, Kern F.** 2005. Protection from cytomegalovirus after transplantation is correlated with immediate early 1–specific CD8 T cells. Journal of Experimental Medicine 201:1031–1036.
39. **Burton, Williamson RA, Parren PW.** 2000. Antibody and virus: binding and neutralisation. Virology 270:1–3.
40. **Buttigieg KR, Dowall SD, Findlay-Wilson S, Miloszewska A, Rayner E, Hewson R, Carroll MW.** 2014. A Novel Vaccine against Crimean-Congo Haemorrhagic Fever Protects 100% of Animals against Lethal Challenge in a Mouse Model. PLoS ONE 9.
41. **Cameron MJ, Ran L, Xu L, Danesh A, Bermejo-Martin JF, Cameron CM, Muller MP, Gold WL, Richardson SE, Poutanen SM, Willey BM, DeVries ME, Fang Y, Seneviratne C, Bosinger SE, Persad D, Wilkinson P, Greller LD, Somogyi R, Humar A, Keshavjee S, Louie M, Loeb MB,**

Brunton J, McGeer AJ, Network, the Canadian SARS Research, Kelvin DJ. 2007. Interferon-Mediated Immunopathological Events Are Associated with Atypical Innate and Adaptive Immune Responses in Patients with Severe Acute Respiratory Syndrome. J. Virol. 81:8692–8706.
42. **Cattaneo R, Rebmann G, Baczko K, ter MV, Billeter MA.** 1987. Altered ratios of measles virus transcripts in diseased human brains. Virology 160:523–526.
43. **CDC.** 2009. H1N1: Overview of a Pandemic. https://www.cdc.gov/h1n1flu/yearinreview/yir5.htm. Accessed 9 December, 2010.
44. **Cervantes-Barragan L, Züst R, Weber F, Spiegel M, Lang KS, Akira S, Thiel V, Ludewig B.** 2007. Control of coronavirus infection through plasmacytoid dendritic-cell–derived type I interferon. Blood 109:1131–1137.
45. **Channappanavar R, Fehr AR, Vijay R, Mack M, Zhao J, Meyerholz DK, Perlman S.** 2016. Dysregulated Type I Interferon and Inflammatory Monocyte-Macrophage Responses Cause Lethal Pneumonia in SARS-CoV-Infected Mice. Cell Host & Microbe 19:181–193.
46. **Chan RWY, Chan MCW, Agnihothram S, Chan LLY, Kuok DIT, Fong JHM, Guan Y, Poon LLM, Baric RS, Nicholls JM, Peiris JSM.** 2013. Tropism of and Innate Immune Responses to the Novel Human Betacoronavirus Lineage C Virus in Human Ex Vivo Respiratory Organ Cultures. J. Virol. 87:6604–6614.
47. **Cheung CY, Poon LLM, Ng IHY, Luk W, Sia S-F, Wu MHS, Chan K-H, Yuen K-Y, Gordon S, Guan Y, Peiris JSM.** 2005. Cytokine Responses in Severe Acute Respiratory Syndrome Coronavirus-Infected Macrophages In Vitro: Possible Relevance to Pathogenesis. J. Virol. 79:7819–7826.
48. **Clementz MA, Chen Z, Banach BS, Wang Y, Sun L, Ratia K, Baez-Santos YM, Wang J, Takayama J, Ghosh AK, Li K, Mesecar AD, Baker SC.** 2010. Deubiquitinating and Interferon Antagonism Activities of Coronavirus Papain-Like Proteases. J. Virol. 84:4619–4629.
49. **Cockrell AS, Peck KM, Yount BL, Agnihothram SS, Scobey T, Curnes NR, Baric RS, Heise MT.** 2014. Mouse Dipeptidyl Peptidase 4 Is Not a Functional Receptor for Middle East Respiratory Syndrome Coronavirus Infection. J. Virol. 88:5195–5199.
50. **Coleman CM, Liu YV, Mu H, Taylor JK, Massare M, Flyer DC, Glenn GM, Smith GE, Frieman MB.** 2014. Purified coronavirus spike protein nanoparticles induce coronavirus neutralising antibodies in mice. Vaccine 32:3169–3174.
51. **Coleman CM, Matthews KL, Goicochea L, Frieman MB.** 2014. Wild-type and innate immune-deficient mice are not susceptible to the Middle East respiratory syndrome coronavirus. Journal of General Virology 95:408–412.
52. **Compton T, Kurt-Jones EA, Boehme KW, Belko J, Latz E, Golenbock DT, Finberg RW.** 2003. Human cytomegalovirus activates inflammatory cytokine responses via CD14 and Toll-like receptor 2. J Virol 77:4588–4596.
53. **Cooper NR, Nemerow GR.** 1983. Complement, viruses, and virus-infected cells. Springer Semin Immunopathol 6:327–347.
54. **Corman VM, Jores J, Meyer B, Younan M, Liljander A, Said MY, Gluecks I, Lattwein E, Bosch B-J, Drexler JF, Bornstein S, Drosten C, Müller MA.** 2014. Antibodies against MERS coronavirus in dromedary camels, Kenya, 1992-2013. Emerging Infect. Dis. 20:1319–1322.
55. **Coro ES, Chang WL, Baumgarth N.** 2006. Type I IFN receptor signals directly stimulate local B cells early following influenza virus infection. J Immunol 176:4343–4351.
56. **Couceiro JN, Paulson JC, Baum LG.** 1993. Influenza virus strains selectively recognize sialyloligosaccharides on human respiratory epithelium; the role of the host cell in selection of hemagglutinin receptor specificity. Virus Res. 29:155–165.
57. **Couzens L, Gao J, Westgeest K, Sandbulte M, Lugovtsev V, Fouchier R, Eichelberger M.** 2014. An optimized enzyme-linked lectin assay to measure influenza A virus neuraminidase inhibition antibody titers in human sera. J Virol Methods 210:7–14.
58. **Cowling BJ, Park M, Fang VJ, Wu P, Leung GM, Wu JT.** 2015. Preliminary epidemiologic assessment of MERS-CoV outbreak in South Korea, May–June 2015. Euro Surveill 20.
59. **Crotty S, Felgner P, Davies H, Glidewell J, Villarreal L, Ahmed R.** 2003. Cutting Edge: Long-Term B Cell Memory in Humans after Smallpox Vaccination. J Immunol 171:4969–4973.
60. **Crotty S, Ahmed R.** 2004. Immunological memory in humans. Anti-Viral Immunity 16:197–203.
61. **Cunningham AL, Garcon N, Leo O, Friedland LR, Strugnell R, Laupeze B, Doherty M, Stern P.** 2016. Vaccine development: From concept to early clinical testing. Vaccine.
62. **Dai B, Yang L, Yang H, Hu B, Baltimore D, Wang P.** 2009. HIV-1 Gag-specific immunity induced by a lentivector-based vaccine directed to dendritic cells. PNAS 106:20382–20387.
63. **Dandekar AA, Perlman S.** 2005. Immunopathogenesis of coronavirus infections: implications for SARS. Nature Reviews Immunology 5:917–927.

64. **Daszak P, Cunningham AA, Hyatt AD.** 2001. Anthropogenic environmental change and the emergence of infectious diseases in wildlife. Acta Trop 78:103–116.
65. **Davidkin I, Valle M.** 1998. Vaccine-induced measles virus antibodies after two doses of combined measles, mumps and rubella vaccine: a 12-year follow-up in two cohorts. Vaccine 16:2052–2057.
66. **Davidkin I, Jokinen S, Broman M, Leinikki P, Peltola H.** 2008. Persistence of Measles, Mumps, and Rubella Antibodies in an MMR-Vaccinated Cohort: A 20-Year Follow-up. J Infect Dis. 197:950–956.
67. **del Valle, Jorge Reyes, Devaux P, Hodge G, Wegner NJ, McChesney MB, Cattaneo R.** 2007. A vectored measles virus induces hepatitis B surface antigen antibodies while protecting macaques against measles virus challenge. J Virol 81:10597–10605.
68. **Demers KR, Reuter MA, Betts.** 2013. CD8+ T-cell effector function and transcriptional regulation during HIV pathogenesis. Immunol Rev 254:190–206.
69. **Desprès P, Combredet C, Frenkiel M-P, Lorin C, Brahic M, Tangy F.** 2005. Live measles vaccine expressing the secreted form of the West Nile virus envelope glycoprotein protects against West Nile virus encephalitis. J. Infect. Dis. 191:207–214.
70. **Devaraj SG, Wang N, Chen Z, Tseng M, Barretto N, Lin R, Peters CJ, Tseng CT, Baker SC, Li K.** 2007. Regulation of IRF-3-dependent innate immunity by the papain-like protease domain of the severe acute respiratory syndrome coronavirus. J Biol Chem 282:32208–32221.
71. **Deyde VM, Khristova ML, Rollin PE, Ksiazek TG, Nichol ST.** 2006. Crimean-Congo Hemorrhagic Fever Virus Genomics and Global Diversity. J. Virol. 80:8834–8842.
72. **Dhillon SS.** 1959. Incidence of Rinderpest in camels in Hissar district. Indian Vet. Jl 36:603–607.
73. **Diebold SS, Kaisho T, Hemmi H, Akira S, Sousa CRe.** 2004. Innate Antiviral Responses by Means of TLR7-Mediated Recognition of Single-Stranded RNA. Science 303:1529–1531.
74. **Donaldson LJ, Rutter PD, Ellis BM, Greaves FEC, Mytton OT, Pebody RG, Yardley IE.** 2009. Mortality from pandemic A/H1N1 2009 influenza in England: public health surveillance study. BMJ 339:b5213.
75. **Dormitzer PR, Tsai TF, Del GG.** 2012. New technologies for influenza vaccines. Hum Vaccin Immunother 8:45–58.
76. **Dowall SD, Buttigieg KR, Findlay-Wilson SJ, Rayner E, Pearson G, Miloszewska A, Graham VA, Carroll MW, Hewson R.** 2016. A Crimean-Congo hemorrhagic fever (CCHF) viral vaccine expressing nucleoprotein is immunogenic but fails to confer protection against lethal disease. Hum Vaccin Immunother 12:519–527.
77. **Dowall SD, Graham VA, Rayner E, Hunter L, Watson R, Taylor I, Rule A, Carroll MW, Hewson R.** 2016. Protective effects of a Modified Vaccinia Ankara-based vaccine candidate against Crimean-Congo Haemorrhagic Fever virus require both cellular and humoral responses. PLOS ONE 11:e0156637.
78. **Dowling PC, Blumberg BM, Menonna J, Adamus JE, Cook P, Crowley JC, Kolakofsky D, Cook SD.** 1986. Transcriptional map of the measles virus genome. J Gen Virol 67 (Pt 9):1987–1992.
79. **Drosten C, Seilmaier M, Corman VM, Hartmann W, Scheible G, Sack S, Guggemos W, Kallies R, Muth D, Junglen S, Muller MA, Haas W, Guberina H, Rohnisch T, Schmid-Wendtner M, Aldabbagh S, Dittmer U, Gold H, Graf P, Bonin F, Rambaut A, Wendtner C-M.** 2013. Clinical features and virological analysis of a case of Middle East respiratory syndrome coronavirus infection. Lancet Infect Dis 13:745–751.
80. **Du L, Kou Z, Ma C, Tao X, Wang L, Zhao G, Chen Y, Yu F, Tseng C-TK, Zhou Y, Jiang S.** 2013. A truncated receptor-binding domain of MERS-CoV spike protein potently inhibits MERS-CoV infection and induces strong neutralising antibody responses: implication for developing therapeutics and vaccines. PLoS ONE 8:e81587.
81. **Duprex WP, Rima BK.** 2002. Using green fluorescent protein to monitor measles virus cell-to-cell spread by time-lapse confocal microscopy. Methods Mol. Biol. 183:297–307.
82. **Edmondson WP, Rothenberg R, White PW, Gwaltney JM,** JR. 1971. A comparison of subcutaneous, nasal, and combined influenza vaccination. II. Protection against natural challenge. Am J Epidemiol 93:480–486.
83. **Elliott RM, Schmaljohn CS, Collett MS.** 1991. Bunyaviridae Genome Structure and Gene Expression. Springer Berlin Heidelberg. http://link.springer.com/content/pdf/10.1007%2F978-3-642-76018-1_4.pdf.
84. **Enders JF, Katz SL, Milovanovic MV, Holloway A.** 1960. Studies on an Attenuated Measles-Virus Vaccine. N Engl J Med 263:153–159.
85. **Enriquez-Rincon F, Klaus GG.** 1984. Differing effects of monoclonal anti-hapten antibodies on humoral responses to soluble or particulate antigens. Immunology 52:129–136.

86. **Ergonul O, Celikbas A, Dokuzoguz B, Eren S, Baykam N, Esener H.** 2004. Characteristics of patients with Crimean-Congo hemorrhagic fever in a recent outbreak in Turkey and impact of oral ribavirin therapy. Clin Infect Dis 39:284–287.
87. **Ergonul O.** 2006. Crimean-Congo haemorrhagic fever. Lancet Infect Dis 6:203–214.
88. **Estrada-Pena A.** 2001. Forecasting habitat suitability for ticks and prevention of tick-borne diseases. Vet Parasitol 98:111–132.
89. **Falzarano D, Wit Ed, Rasmussen AL, Feldmann F, Okumura A, Scott DP, Brining D, Bushmaker T, Martellaro C, Baseler L, Benecke AG, Katze MG, Munster VJ, Feldmann H.** 2013. Treatment with interferon-[alpha]2b and ribavirin improves outcome in MERS-CoV-infected rhesus macaques. Nat Med 19:1313–1317.
90. **FAO.** 2017. H7N9 situation update. http://www.fao.org/ag/AGAinfo/programmes/en/empres/H7N9/Situation_update.html. Accessed 09-02-17.
91. **Faure E, Poissy J, Goffard A, Fournier C, Kipnis E, Titecat M, Bortolotti P, Martinez L, Dubucquoi S, Dessein R, Gosset P, Mathieu D, Guery B.** 2014. Distinct Immune Response in Two MERS-CoV-Infected Patients: Can We Go from Bench to Bedside? PLOS ONE 9:e88716.
92. **Fenner F, Henderson DA, Arita I, Jezek Z, Ladnyi ID, Organization WH.** 1988. Smallpox and its eradication. Geneva : World Health Organization. http://www.who.int/iris/bitstream/10665/39485/1/9241561106.pdf.
93. **Ferguson NM, van Kerkhove MD.** 2014. Identification of MERS-CoV in dromedary camels. Lancet Infect Dis 14:93–94.
94. **Fink K, Lang KS, Manjarrez-Orduno N, Junt T, Senn BM, Holdener M, Akira S, Zinkernagel RM, Hengartner H.** 2006. Early type I interferon-mediated signals on B cells specifically enhance antiviral humoral responses. European Journal of Immunology 36:2094–2105.
95. **Forrest BD, Pride MW, Dunning AJ, Capeding MRZ, Chotpitayasunondh T, Tam JS, Rappaport R, Eldridge JH, Gruber WC.** 2008. Correlation of Cellular Immune Responses with Protection against Culture-Confirmed Influenza Virus in Young Children. Clin. Vaccine Immunol. 15:1042–1053.
96. **Fortenberry JD, Mariscalco MM, Louis PT, Stein F, Jones JK, Jefferson LS.** 1992. Severe Laryngotracheobronchitis Complicating Measles. Am J Dis Child 146:1040–1043.
97. **Frazer IH.** 2004. Prevention of cervical cancer through papillomavirus vaccination. Nat. Rev. Immunol. 4:46–54.
98. **Frieman M, Ratia K, Johnston RE, Mesecar AD, Baric RS.** 2009. Severe acute respiratory syndrome coronavirus papain-like protease ubiquitin-like domain and catalytic domain regulate antagonism of IRF3 and NF-kappaB signaling. J Virol 83:6689–6705.
99. **Funke S, Maisner A, Mühlebach MD, Koehl U, Grez M, Cattaneo R, Cichutek K, Buchholz CJ.** 2008. Targeted cell entry of lentiviral vectors. Mol. Ther. 16:1427–1436.
100. **Gao R, Cao B, Hu Y, Feng Z, Wang D, Hu W, Chen J, Jie Z, Qiu H, Xu K, Xu X, Lu H, Zhu W, Gao Z, Xiang N, Shen Y, He Z, Gu Y, Zhang Z, Yang Y, Zhao X, Zhou L, Li X, Zou S, Zhang Y, Li X, Yang L, Guo J, Dong J, Li Q, Dong L, Zhu Y, Bai T, Wang S, Hao P, Yang W, Zhang Y, Han J, Yu H, Li D, Gao GF, Wu G, Wang Y, Yuan Z, Shu Y.** 2013. Human Infection with a Novel Avian-Origin Influenza A (H7N9) Virus. N Engl J Med 368:1888–1897.
101. **Ghiasi SM, Salmanian AH, Chinikar S, Zakeri S.** 2011. Mice Orally Immunized with a Transgenic Plant Expressing the Glycoprotein of Crimean-Congo Hemorrhagic Fever Virus. Clin. Vaccine Immunol. 18:2031–2037.
102. **Griffin DE.** 2002. Measles Virus. *In* Wiley Encyclopedia of Molecular Medicine. John Wiley & Sons, Inc, Hoboken, NJ, USA.
103. **Griffin DE, Pan CH.** 2009. Measles: old vaccines, new vaccines. Curr Top Microbiol Immunol 330:191–212.
104. **Gubler DJ, Reiter P, Ebi KL, Yap W, Nasci R, Patz JA.** 2001. Climate variability and change in the United States: potential impacts on vector- and rodent-borne diseases. Environ Health Perspect 109:223–233.
105. **Guery B, Poissy J, Mansouf Le, Séjourné C, Ettahar N, Lemaire X, Vuotto F, Goffard A, Behillil S, Enouf V, Caro V, Mailles A, Che D, Manuguerra J-C, Mathieu D, Fontanet A, van der Werf S.** 2013. Clinical features and viral diagnosis of two cases of infection with Middle East Respiratory Syndrome coronavirus: a report of nosocomial transmission. The Lancet 381:2265–2272.
106. **Guidotti LG, Chisari FV.** 2001. Noncytolytic control of viral infections by the innate and adaptive immune response. Annu Rev Immunol 19:65–91.
107. **Guo X, Deng Y, Chen H, Lan J, Wang W, Zou X, Hung T, Lu Z, Tan W.** 2015. Systemic and mucosal immunity in mice elicited by a single immunization with human adenovirus type 5 or

41 vector-based vaccines carrying the spike protein of Middle East respiratory syndrome coronavirus. Immunology 145:476–484.
108. **Haagmans BL, Dhahiry, Said H S Al, Reusken, Chantal B E M, Raj VS, Galiano M, Myers R, Godeke G-J, Jonges M, Farag E, Diab A, Ghobashy H, AlHajri F, Al-Thani M, Al-Marri SA, Romaihi HEA, Khal AA, Bermingham A, Osterhaus, Albert D M E, AlHajri MM, Koopmans MPG.** 2014. Middle East respiratory syndrome coronavirus in dromedary camels: an outbreak investigation. The Lancet Infectious Diseases 14:140–145.
109. **Haagmans BL, van den Brand JMA, Raj VS, Volz A, Wohlsein P, Smits SL, Schipper D, Bestebroer TM, Okba N, Fux R.** 2016. An orthopoxvirus-based vaccine reduces virus excretion after MERS-CoV infection in dromedary camels. Science 351:77–81.
110. **Haferkamp S, Fernando L, Schwarz TF, Feldmann H, Flick R.** 2005. Intracellular localization of Crimean-Congo Hemorrhagic Fever (CCHF) virus glycoproteins. Virol J 2:42.
111. **Hale BG, Albrecht RA, García-Sastre A.** 2010. Innate immune evasion strategies of influenza viruses. Future Microbiol 5:23.
112. **Hashimoto G, Wright PF, Karzon DT.** 1983. Antibody-Dependent Cell-Mediated Cytotoxicity Against Influenza Virus-Infected Cells. J Infect Dis. 148:785–794.
113. **Haynes LM, Moore DD, Kurt-Jones EA, Finberg RW, Anderson LJ, Tripp RA.** 2001. Involvement of toll-like receptor 4 in innate immunity to respiratory syncytial virus. J Virol 75:10730–10737.
114. **Henderson DA, Witte JJ, Morris L, Langmuir AD.** 1964. Paralytic disease associated with oral polio vaccines. Jama 190:41–48.
115. **Hervas-Stubbs S, Perez-Gracia JL, Rouzaut A, Sanmamed MF, Le Bon A, Melero I.** 2011. Direct effects of type I interferons on cells of the immune system. Clin Cancer Res 17:2619–2627.
116. **Hewson R, Chamberlain J, Mioulet V, Lloyd G, Jamil B, Hasan R, Gmyl A, Gmyl L, Smirnova S, Lukashev A, Karganova G, Clegg C.** 2004. Crimean-Congo haemorrhagic fever virus: sequence analysis of the small RNA segments from a collection of viruses world wide. Virus Res. 102:185–189.
117. **Heymann DL, Weisfeld JS, Webb PA, Johnson KM, Cairns T, Berquist H.** 1980. Ebola Hemorrhagic Fever: Tandala, Zaire, 1977–1978. J Infect Dis. 142:372–376.
118. **Hobson D, Curry RL, Beare AS, Ward-Gardner A.** 1972. The role of serum haemagglutination-inhibiting antibody in protection against challenge infection with influenza A2 and B viruses. J Hyg (Lond) 70:767–777.
119. **Honda K, Yanai H, Negishi H, Asagiri M, Sato M, Mizutani T, Shimada N, Ohba Y, Takaoka A, Yoshida N, Taniguchi T.** 2005. IRF-7 is the master regulator of type-I interferon-dependent immune responses. Nature 434:772–777.
120. **Hoogstraal H.** 1979. The epidemiology of tick-borne Crimean-Congo hemorrhagic fever in Asia, Europe, and Africa. J Med Entomol 15:307–417.
121. **Hornung V, Schlender J, Guenthner-Biller M, Rothenfusser S, Endres S, Conzelmann K-K, Hartmann G.** 2004. Replication-Dependent Potent IFN-α Induction in Human Plasmacytoid Dendritic Cells by a Single-Stranded RNA Virus. The Journal of Immunology 173:5935–5943.
122. **Houtman JJ, Fleming JO.** 1996. Dissociation of demyelination and viral clearance in congenitally immunodeficient mice infected with murine coronavirus JHM. J Neurovirol 2:101–110.
123. **Huang DB, Wu JJ, Tyring SK.** 2004. A review of licensed viral vaccines, some of their safety concerns, and the advances in the development of investigational viral vaccines. Journal of Infection 49:179–209.
124. **Hussey GD, Clements CJ.** 1996. Clinical problems in measles case management. Annals of tropical paediatrics 16:307–318.
125. **Iankov ID, Haralambieva IH, Galanis E.** 2011. Immunogenicity of attenuated measles virus engineered to express Helicobacter pylori neutrophil-activating protein. Vaccine 29:1710–1720.
126. **Influenza WCC.** 1982. Concepts and procedures for laboratory-based influenza surveillance. US Department of Health and Human Services.
127. **Ivashkiv LB, Donlin LT.** 2014. Regulation of type I interferon responses. Nature Reviews Immunology 14:36–49.
128. **Jenner E.** 1801. An inquiry into the causes and effects of the variolae vaccinae, a disease discovered in some of the western counties of England, particularly Gloucestershire, and known by the name of the cow pox. printed for the author, by DN Shury.
129. **Jernigan DB, Cox NJ.** 2015. H7N9: Preparing for the Unexpected in Influenza. Annual review of medicine 66:361–371.

130. **Jiang L, Changsom D, Lerdsamran H, Wiriyarat W, Masamae W, Noisumdaeng P, Jongkaewwattana A, Puthavathana P.** 2016. Immunobiological properties of influenza A (H7N9) hemagglutinin and neuraminidase proteins. Arch Virol:1–12.
131. **Jing Y, Shaheen E, Drake RR, Chen N, Gravenstein S, Deng Y.** 2009. Aging is associated with a numerical and functional decline in plasmacytoid dendritic cells, whereas myeloid dendritic cells are relatively unaltered in human peripheral blood. Hum Immunol 70:777–784.
132. **Jones KE, Patel NG, Levy MA, Storeygard A, Balk D, Gittleman JL, Daszak P.** 2008. Global trends in emerging infectious diseases. Nature 451:990–993.
133. **Jones SM, Feldmann H, Stroher U, Geisbert JB, Fernando L, Grolla A, Klenk H-D, Sullivan NJ, Volchkov VE, Fritz EA, Daddario KM, Hensley LE, Jahrling PB, Geisbert TW.** 2005. Live attenuated recombinant vaccine protects nonhuman primates against Ebola and Marburg viruses. Nat Med 11:786–790.
134. **Jong MDd, Simmons CP, Thanh TT, Hien VM, Smith GJD, Chau TNB, Hoang DM, van Chau NV, Khanh TH, Dong VC, Qui PT, van Cam B, Ha DQ, Guan Y, Peiris JSM, Chinh NT, Hien TT, Farrar J.** 2006. Fatal outcome of human influenza A (H5N1) is associated with high viral load and hypercytokinemia. Nat Med 12:1203–1207.
135. **Kageyama T, Fujisaki S, Takashita E, Xu H, Yamada S, Uchida Y, Neumann G, Saito T, Kawaoka Y, Tashiro M.** 2013. Genetic analysis of novel avian A(H7N9) influenza viruses isolated from patients in China, February to April 2013. Euro Surveill 18:20453.
136. **Kapikian AZ, Mitchell RH, Chanock RM, Shvedoff RA, Stewart CE.** 1969. An epidemiologic study of altered clinical reactivity to respiratory syncytial (RS) virus infection in children previously vaccinated with an inactivated RS virus vaccine. Am J Epidemiol 89:405–421.
137. **Kaufman DR, Bivas-Benita M, Simmons NL, Miller D, Barouch DH.** 2010. Route of Adenovirus-Based HIV-1 Vaccine Delivery Impacts the Phenotype and Trafficking of Vaccine-Elicited CD8+ T Lymphocytes. J. Virol. 84:5986–5996.
138. **Kawai T, Sato S, Ishii KJ, Coban C, Hemmi H, Yamamoto M, Terai K, Matsuda M, Inoue J-i, Uematsu S, Takeuchi O, Akira S.** 2004. Interferon-|[alpha]| induction through Toll-like receptors involves a direct interaction of IRF7 with MyD88 and TRAF6. Nature Immunology 5:1061–1068.
139. **Khalafalla AI, Saeed IK, Ali YH, Abdurrahman MB, Kwiatek O, Libeau G, Obeida AA, Abbas Z.** 2010. An outbreak of peste des petits ruminants (PPR) in camels in the Sudan. Acta Trop 116:161–165.
140. **Khan KH.** 2013. DNA vaccines: roles against diseases. Germs 3:26–35.
141. **Kilbourne ED, Laver WG, Schulman JL, Webster RG.** 1968. Antiviral activity of antiserum specific for an influenza virus neuraminidase. J Virol 2:281–288.
142. **Kilbourne ED, Johansson BE, Grajower B.** 1990. Independent and disparate evolution in nature of influenza A virus hemagglutinin and neuraminidase glycoproteins. Proc Natl Acad Sci U S A 87:786–790.
143. **Kim DW, Kim YJ, Park SH, Yun, Yang JS, Kang HJ, Han YW, Lee HS, Man KH, Kim H, Kim AR, Heo, Kim SJ, Jeon JH, Park D, Kim JA, Cheong HM, Nam JG, Kim K, Kim SS.** 2016. Variations in Spike Glycoprotein Gene of MERS-CoV, South Korea, 2015. Emerging Infect. Dis. 22:100–104.
144. **Kim E, Okada K, Kenniston T, Raj VS, AlHajri MM, Farag, Elmoubasher A B A, AlHajri F, Osterhaus, Albert D M E, Haagmans BL, Gambotto A.** 2014. Immunogenicity of an adenoviral-based Middle East Respiratory Syndrome coronavirus vaccine in BALB/c mice. Vaccine 32:5975–5982.
145. **Kim TW, Lee JH, Hung C-F, Peng S, Roden R, Wang M-C, Viscidi R, Tsai Y-C, He L, Chen P-J, Boyd DAK, Wu T-C.** 2004. Generation and Characterization of DNA Vaccines Targeting the Nucleocapsid Protein of Severe Acute Respiratory Syndrome Coronavirus. J. Virol. 78:4638–4645.
146. **Kim Y, Cheon S, Min C-K, Sohn KM, Kang YJ, Cha Y-J, Kang J-I, Han SK, Ha N-Y, Kim G, Aigerim A, Shin HM, Choi M-S, Kim S, Cho H-S, Kim Y-S, Cho N-H.** 2016. Spread of Mutant Middle East Respiratory Syndrome Coronavirus with Reduced Affinity to Human CD26 during the South Korean Outbreak. mBio 7:e00019-16.
147. **Kindler E, Jónsdóttir HR, Muth D, Hamming OJ, Hartmann R, Rodriguez R, Geffers R, Fouchier RAM, Drosten C, Müller MA, Dijkman R, Thiel V.** 2013. Efficient Replication of the Novel Human Betacoronavirus EMC on Primary Human Epithelium Highlights Its Zoonotic Potential. mBio 4:e00611-12.
148. **Kindler E, Thiel V, Weber F.** 2016. Chapter Seven - Interaction of SARS and MERS Coronaviruses with the Antiviral Interferon Response, p. 219–243. *In* John Ziebuhr (ed), Advances in Virus Research : Coronaviruses, Volume 96. Academic Press.

149. **Kindler E, Thiel V.** 2016. SARS-CoV and IFN: Too Little, Too Late. Cell Host & Microbe 19:139–141.
150. **Klein U, Kuppers R, Rajewsky K.** 1997. Evidence for a large compartment of IgM-expressing memory B cells in humans. Blood 89:1288–1298.
151. **Knoops K, Kikkert M, Worm, Sjoerd H. E. van den, Zevenhoven-Dobbe JC, van der Meer Y, Koster AJ, Mommaas AM, Snijder EJ.** 2008. SARS-Coronavirus Replication Is Supported by a Reticulovesicular Network of Modified Endoplasmic Reticulum. PLOS Biology 6:e226.
152. **Kopecky-Bromberg SA, Martinez-Sobrido L, Frieman M, Baric RA, Palese P.** 2007. Severe acute respiratory syndrome coronavirus open reading frame (ORF) 3b, ORF 6, and nucleocapsid proteins function as interferon antagonists. J Virol 81:548–557.
153. **Krause PR.** 2015. Interim results from a phase 3 Ebola vaccine study in Guinea. The Lancet 386:831–833.
154. **Kreijtz JHCM, Wiersma LCM, Gruyter HLM** de, **Vogelzang-van Trierum SE, van Amerongen G, Stittelaar KJ, Fouchier RAM, Osterhaus, Albert D. M. E., Sutter G, Rimmelzwaan GF.** 2015. A single immunization with modified vaccinia virus Ankara-based influenza virus H7 vaccine affords protection in the influenza A(H7N9) pneumonia ferret model. J. Infect. Dis. 211:791–800.
155. **Kurosaki T, Kometani K, Ise W.** 2015. Memory B cells. Nature Reviews Immunology 15:149–159.
156. **Kurt-Jones EA, Popova L, Kwinn L, Haynes LM, Jones LP, Tripp RA, Walsh EE, Freeman MW, Golenbock DT, Anderson LJ, Finberg RW.** 2000. Pattern recognition receptors TLR4 and CD14 mediate response to respiratory syncytial virus. Nature Immunology 1:398–401.
157. **Lan J, Deng Y, Chen H, Lu G, Wang W, Guo X, Lu Z, Gao GF, Tan W.** 2014. Tailoring Subunit Vaccine Immunity with Adjuvant Combinations and Delivery Routes Using the Middle East Respiratory Coronavirus (MERS-CoV) Receptor-Binding Domain as an Antigen. PLoS ONE 9:e112602.
158. **Lanzavecchia A, Sallusto F.** 2002. Progressive differentiation and selection of the fittest in the immune response. Nature Reviews Immunology 2:982–987.
159. **Lemke A, Kraft M, Roth K, Riedel R, Lammerding D, Hauser AE.** 2016. Long-lived plasma cells are generated in mucosal immune responses and contribute to the bone marrow plasma cell pool in mice. Mucosal Immunology 9:83–97.
160. **Lindsey NP, Schroeder BA, Miller ER, Braun MM, Hinckley AF, Marano N, Slade BA, Barnett ED, Brunette GW, Horan K, Staples JE, Kozarsky PE, Hayes EB.** 2008. Adverse event reports following yellow fever vaccination. Vaccine 26:6077–6082.
161. **Liniger M, Zuniga A, Tamin A, Azzouz-Morin TN, Knuchel M, Marty RR, Wiegand M, Weibel S, Kelvin D, Rota PA, Naim HY.** 2008. Induction of neutralising antibodies and cellular immune responses against SARS coronavirus by recombinant measles viruses. Vaccine 26:2164–2174.
162. **Liu B, Havers F, Chen E, Yuan Z, Yuan H, Ou J, Shang M, Kang K, Liao K, Liu F, Li D, Ding H, Zhou L, Zhu W, Ding F, Zhang P, Wang X, Yao J, Xiang N, Zhou S, Liu X, Song Y, Su H, Wang R, Cai J, Cao Y, Wang X, Bai T, Wang J, Feng Z, Zhang Y, Widdowson M-A, Li Q.** 2014. Risk Factors for Influenza A(H7N9) Disease—China, 2013. Clin Infect Dis. 59:787–794.
163. **Liu MA.** 2003. DNA vaccines: a review. Journal of Internal Medicine 253:402–410.
164. **Lorin C, Mollet L, Delebecque F, Combredet C, Hurtrel B, Charneau P, Brahic M, Tangy F.** 2004. A Single Injection of Recombinant Measles Virus Vaccines Expressing Human Immunodeficiency Virus (HIV) Type 1 Clade B Envelope Glycoproteins Induces Neutralising Antibodies and Cellular Immune Responses to HIV. J Virol 78:146–157.
165. **Lorin C, Delebecque F, Labrousse V, Da Silva L, Lemonnier F, Brahic M, Tangy F.** 2005. A recombinant live attenuated measles vaccine vector primes effective HLA-A0201-restricted cytotoxic T lymphocytes and broadly neutralising antibodies against HIV-1 conserved epitopes. Vaccine 23:4463–4472.
166. **Ludwig S, Wang X, Ehrhardt C, Zheng H, Donelan N, Planz O, Pleschka S, García-Sastre A, Heins G, Wolff T.** 2002. The Influenza A Virus NS1 Protein Inhibits Activation of Jun N-Terminal Kinase and AP-1 Transcription Factors. J. Virol. 76:11166–11171.
167. **Lu G, Hu Y, Wang Q, Qi J, Gao F, Li Y, Zhang Y, Zhang W, Yuan Y, Bao J, Zhang B, Shi Y, Yan J, Gao GF.** 2013. Molecular basis of binding between novel human coronavirus MERS-CoV and its receptor CD26. Nature 500:227–231.
168. **Lu X, Pan J, Tao J, Guo D.** 2011. SARS-CoV nucleocapsid protein antagonizes IFN-beta response by targeting initial step of IFN-beta induction pathway, and its C-terminal region is critical for the antagonism. Virus Genes 42:37–45.

169. **Lu X, Rowe LA, Frace M, Stevens J, Abedi GR, Elnile O, Banassir T, Al-Masri M, Watson JT, Assiri A, Erdman DD.** 2017. Spike gene deletion quasispecies in serum of patient with acute MERS-CoV infection. Journal of Medical Virology 89:542–545.
170. **Ma C, Li Y, Wang L, Zhao G, Tao X, Tseng C-TK, Zhou Y, Du L, Jiang S.** 2014. Intranasal vaccination with recombinant receptor-binding domain of MERS-CoV spike protein induces much stronger local mucosal immune responses than subcutaneous immunization: Implication for designing novel mucosal MERS vaccines. Vaccine 32:2100–2108.
171. **Ma C, Wang L, Tao X, Zhang N, Yang Y, Tseng C-TK, Li F, Zhou Y, Jiang S, Du L.** 2014. Searching for an ideal vaccine candidate among different MERS coronavirus receptor-binding fragments--the importance of immunofocusing in subunit vaccine design. Vaccine 32:6170–6176.
172. **Malczyk AH, Kupke A, Prufer S, Scheuplein VA, Hutzler S, Kreuz D, Beissert T, Bauer S, Hubich-Rau S, Tondera C, Eldin HS, Schmidt J, Vergara-Alert J, Suzer Y, Seifried J, Hanschmann K-M, Kalinke U, Herold S, Sahin U, Cichutek K, Waibler Z, Eickmann M, Becker S, Muhlebach MD.** 2015. A Highly Immunogenic and Protective Middle East Respiratory Syndrome Coronavirus Vaccine Based on a Recombinant Measles Virus Vaccine Platform. J Virol 89:11654–11667.
173. **Malmgaard L.** 2004. Induction and regulation of IFNs during viral infections. J Interferon Cytokine Res 24:439–454.
174. **Marié I, Durbin JE, Levy DE.** 1998. Differential viral induction of distinct interferon-alpha genes by positive feedback through interferon regulatory factor-7. The Embo Journal 17:6660–6669.
175. **Martin A, Staeheli P, Schneider U.** 2006. RNA polymerase II-controlled expression of antigenomic RNA enhances the rescue efficacies of two different members of the Mononegavirales independently of the site of viral genome replication. J Virol 80:5708–5715.
176. **McElhaney JE, Xie D, Hager WD, Barry MB, Wang Y, Kleppinger A, Ewen C, Kane KP, Bleackley RC.** 2006. T cell responses are better correlates of vaccine protection in the elderly. J Immunol 176:6333–6339.
177. **McMichael AJ, Gotch FM, Noble GR, Beare PA.** 1983. Cytotoxic T-cell immunity to influenza. N. Engl. J. Med. 309:13–17.
178. **Mellman I, Turley SJ, Steinman RM.** 1998. Antigen processing for amateurs and professionals. Trends in Cell Biology 8:231–237.
179. **Memish ZA, Cotten M, Meyer B, Watson SJ, Alsahafi AJ, Al Rabeeah, Abdullah A, Corman VM, Sieberg A, Makhdoom HQ, Assiri A, Al Masri M, Aldabbagh S, Bosch B-J, Beer M, Müller MA, Kellam P, Drosten C.** 2014. Human infection with MERS coronavirus after exposure to infected camels, Saudi Arabia, 2013. Emerging Infect. Dis. 20:1012–1015.
180. **Menachery VD, Yount BL, Josset L, Gralinski LE, Scobey T, Agnihothram S, Katze MG, Baric RS.** 2014. Attenuation and Restoration of Severe Acute Respiratory Syndrome Coronavirus Mutant Lacking 2′-O-Methyltransferase Activity. J. Virol. 88:4251–4264.
181. **Miletic H, Fischer YH, Neumann H, Hans V, Stenzel W, Giroglou T, Hermann M, Deckert M, Laer D** von. 2004. Selective transduction of malignant glioma by lentiviral vectors pseudotyped with lymphocytic choriomeningitis virus glycoproteins. Hum Gene Ther 15:1091–1100.
182. **Mills CD, Kincaid K, Alt JM, Heilman MJ, Hill AM.** 2000. M-1/M-2 Macrophages and the Th1/Th2 Paradigm. The Journal of Immunology 164:6166–6173.
183. **Mirchamsy H, Bahrami B, Amighi M, Shafyi A.** 1970. Development of a Camel Kidney Cell Strain and Its Use in Virology. Appl Microbiol 20:276–278.
184. **Modjarrad K.** 2016. MERS-CoV vaccine candidates in development: The current landscape. WHO Product Development for Vaccines Advisory Committee (PDVAC) Pipeline Analyses for 25 Pathogens 34:2982–2987.
185. **Monath TP.** 1989. The arboviruses: epidemiology and ecology. Volume V. CRC Press, Inc.
186. **Mosmann TR, Coffman RL.** 1989. TH1 and TH2 cells: different patterns of lymphokine secretion lead to different functional properties. Annu Rev Immunol 7:145–173.
187. **Moss WJ, Ryon JJ, Monze M, Cutts F, Quinn TC, Griffin DE.** 2002. Suppression of Human Immunodeficiency Virus Replication during Acute Measles. J Infect Dis. 185:1035–1042.
188. **Mou H, Raj VS, van Kuppeveld, Frank J M, Rottier, Peter J M, Haagmans BL, Bosch BJ.** 2013. The receptor binding domain of the new Middle East respiratory syndrome coronavirus maps to a 231-residue region in the spike protein that efficiently elicits neutralising antibodies. J Virol 87:9379–9383.
189. **Mrkic B, Pavlovic J, Rulicke T, Volpe P, Buchholz CJ, Hourcade D, Atkinson JP, Aguzzi A, Cattaneo R.** 1998. Measles virus spread and pathogenesis in genetically modified mice. J Virol 72:7420–7427.

190. **Mühlebach MD, Mateo M, Sinn PL, Prüfer S, Uhlig KM, Leonard, Vincent H. J., Navaratnarajah CK, Frenzke M, Wong XX, Sawatsky B, Ramachandran S, McCray PB, Cichutek K, Messling V** von, **Lopez M, Cattaneo R.** 2011. Adherens junction protein nectin-4 (PVRL4) is the epithelial receptor for measles virus. Nature 480:530–533.
191. **Müller MA, Corman VM, Jores J, Meyer B, Younan M, Liljander A, Bosch B-J, Lattwein E, Hilali M, Musa BE, Bornstein S, Drosten C.** 2014. MERS Coronavirus Neutralising Antibodies in Camels, Eastern Africa, 1983-1997. Emerging Infect. Dis. 20.
192. **Munster VJ, Wit Ed, Feldmann H.** 2013. Pneumonia from Human Coronavirus in a Macaque Model. N Engl J Med 368:1560–1562.
193. **Murphy KP, Janeway CA, Travers P, Walport M, Mowat A, Weaver CT** (ed.). 2012. Janeway's Immunology. Janeway's immunobiology, 8. ed. Garland Science, London.
194. **Muth D, Corman VM, Meyer B, Assiri A, Al-Masri M, Farah M, Steinhagen K, Lattwein E, Al-Tawfiq JA, Albarrak A, Müller MA, Drosten C, Memish ZA.** 2015. Infectious Middle East Respiratory Syndrome Coronavirus Excretion and Serotype Variability Based on Live Virus Isolates from Patients in Saudi Arabia. J. Clin. Microbiol. 53:2951–2955.
195. **Muthumani K, Falzarano D, Reuschel EL, Kraynyak K, Ugen K, Kim P, Maslow J, Kim JJ, Sardesai NY, Kobinger G.** 2016. A synthetic consensus anti-Spike protein DNA vaccine induces protective immunity against Middle East Respiratory Syndrome Coronavirus in non-human primates. International Journal of Infectious Diseases:23.
196. **Nakamura K, Shirakura M, Suzuki Y, Naito T, Fujisaki S, Tashiro M, Nobusawa E.** 2016. Development of a high-yield reassortant influenza vaccine virus derived from the A/Anhui/1/2013 (H7N9) strain. Vaccine 34:328–333.
197. **Naniche D, Garenne M, Rae C, Manchester M, Buchta R, Brodine SK, Oldstone, Michael B A.** 2004. Decrease in measles virus-specific CD4 T cell memory in vaccinated subjects. J. Infect. Dis. 190:1387–1395.
198. **Nascimento I, Leite L.** 2012. Recombinant vaccines and the development of new vaccine strategies. Braz J Med Biol Res 45:1102–1111.
199. **Neuman BW, Adair BD, Yoshioka C, Quispe JD, Milligan RA, Yeager M, Buchmeier MJ.** 2006. Ultrastructure of SARS-CoV, FIPV, and MHV revealed by electron cryomicroscopy. Adv Exp Med Biol 581:181–185.
200. **Niemeyer D, Zillinger T, Muth D, Zielecki F, Horvath G, Suliman T, Barchet W, Weber F, Drosten C, Müller MA.** 2013. Middle East Respiratory Syndrome Coronavirus Accessory Protein 4a Is a Type I Interferon Antagonist. J Virol 87:12489–12495.
201. **Noad R, Roy P.** 2003. Virus-like particles as immunogens. Trends Microbiol. 11:438–444.
202. **Noyce RS, Richardson CD.** 2012. Nectin 4 is the epithelial cell receptor for measles virus. Trends Microbiol. 20:429–439.
203. **Okada H, Kobune F, Sato TA, Kohama T, Takeuchi Y, Abe T, Takayama N, Tsuchiya T, Tashiro M**. Extensive lymphopenia due to apoptosis of uninfected lymphocytes in acute measles patients. Arch. Virol. 145:905–920.
204. **Onoguchi K, Yoneyama M, Takemura A, Akira S, Taniguchi T, Namiki H, Fujita T.** 2007. Viral Infections Activate Types I and III Interferon Genes through a Common Mechanism. J. Biol. Chem. 282:7576–7581.
205. **Österlund PI, Pietilä TE, Veckman V, Kotenko SV, Julkunen I.** 2007. IFN Regulatory Factor Family Members Differentially Regulate the Expression of Type III IFN (IFN-λ) Genes. J Immunol 179:3434–3442.
206. **Palladino G, Mozdzanowska K, Washko G, Gerhard W.** 1995. Virus-neutralising antibodies of immunoglobulin G (IgG) but not of IgM or IgA isotypes can cure influenza virus pneumonia in SCID mice. J. Virol. 69:2075–2081.
207. **Papa A, Bozović B, Pavlidou V, Papadimitriou E, Pelemis M, Antoniadis A.** 2002. Genetic Detection and Isolation of Crimean-Congo hemorrhagic fever virus, Kosovo, Yugoslavia. Emerging Infect. Dis. 8:852–854.
208. **Pape KA, Catron DM, Itano AA, Jenkins MK.** 2007. The humoral immune response is initiated in lymph nodes by B cells that acquire soluble antigen directly in the follicles. Immunity 26:491–502.
209. **Perez O, Batista-Duharte A, Gonzalez E, Zayas C, Balboa J, Cuello M, Cabrera O, Lastre M, Schijns VE.** 2012. Human prophylactic vaccine adjuvants and their determinant role in new vaccine formulations. Braz J Med Biol Res 45:681–692.
210. **Petersen E, Hui DS, Perlman S, Zumla A.** 2015. Middle East Respiratory Syndrome– advancing the public health and research agenda on MERS- lessons from the South Korea outbreak. International Journal of Infectious Diseases 36:54–55.

211. **Peters PJ, Borst J, Oorschot V, Fukuda M, Krahenbuhl O, Tschopp J, Slot JW, Geuze HJ.** 1991. Cytotoxic T lymphocyte granules are secretory lysosomes, containing both perforin and granzymes. J Exp Med 173:1099–1109.
212. **Potter CW, Oxford JS.** 1979. Determinants of immunity to influenza infection in man. Br Med Bull 35:69–75.
213. **Poulet H, Minke J, Pardo MC, Juillard V, Nordgren B, Audonnet J-C.** 2007. Development and registration of recombinant veterinary vaccines: The example of the canarypox vector platform. 4th International Veterinary Vaccines and Diagnostics Conference, Oslo, 25-29 June 20064th International Veterinary Vaccines and Diagnostics Conference 25:5606–5612.
214. **Pozzi L-AM, Maciaszek JW, Rock KL.** 2005. Both Dendritic Cells and Macrophages Can Stimulate Naive CD8 T Cells In Vivo to Proliferate, Develop Effector Function, and Differentiate into Memory Cells. J Immunol 175:2071–2081.
215. **Provost A, Maurice Y, Borredon C.** 1971. Rinderpest protection of bovines by measles virus. II. Vaccination of calves born from cows vaccinated with the MB 113 strain. Rev Elev Med Vet Pays Trop 24:167–172.
216. **Pushko P, Pujanauski LM, Sun X, Pearce M, Hidajat R, Kort T, Schwartzman LM, Tretyakova I, Chunqing L, Taubenberger JK, Tumpey TM.** 2015. Recombinant H7 hemagglutinin forms subviral particles that protect mice and ferrets from challenge with H7N9 influenza virus. Vaccine 33:4975–4982.
217. **Qian Z, Dominguez SR, Holmes KV.** 2013. Role of the Spike Glycoprotein of Human Middle East Respiratory Syndrome Coronavirus (MERS-CoV) in Virus Entry and Syncytia Formation. PLOS ONE 8:e76469.
218. **Radecke F, Spielhofer P, Schneider H, Kaelin K, Huber M, Dötsch C, Christiansen G, Billeter MA.** 1995. Rescue of measles viruses from cloned DNA. The Embo Journal 14:5773–5784.
219. **Ramsauer K, Schwameis M, Firbas C, Müllner M, Putnak RJ, Thomas SJ, Desprès P, Tauber E, Jilma B, Tangy F.** 2015. Immunogenicity, safety, and tolerability of a recombinant measles-virus-based chikungunya vaccine: a randomised, double-blind, placebo-controlled, active-comparator, first-in-man trial. Lancet Infect Dis 15:519–527.
220. **Reed KD, Meece JK, Henkel JS, Shukla SK.** 2003. Birds, migration and emerging zoonoses: west nile virus, lyme disease, influenza A and enteropathogens. Clin Med Res 1:5–12.
221. **Reyes-del Valle J, de la Fuente, C, Turner MA, Springfeld C, Apte-Sengupta S, Frenzke ME, Forest A, Whidby J, Marcotrigiano J, Rice CM, Cattaneo R.** 2012. Broadly Neutralising Immune Responses against Hepatitis C Virus Induced by Vectored Measles Viruses and a Recombinant Envelope Protein Booster. J Virol 86:11558–11566.
222. **Riepenhoff-Talty M, Dharakul T, Kowalski E, Michalak S, Ogra PL.** 1987. Persistent rotavirus infection in mice with severe combined immunodeficiency. J. Virol. 61:3345–3348.
223. **Rimmelzwaan GF, Am Fouchier R, Osterhaus AD.** 2007. Influenza virus-specific cytotoxic T lymphocytes: a correlate of protection and a basis for vaccine development. Chemical biotechnology / Pharmaceutical biotechnology 18:529–536.
224. **Robert-Guroff M.** 2007. Replicating and non-replicating viral vectors for vaccine development. Chemical biotechnology / Pharmaceutical biotechnology 18:546–556.
225. **Robinson A, Irons LI, Ashworth L.** 1985. Pertussis vaccine. Present status and future prospects. Vaccine 3:11–22.
226. **Rollier CS, Reyes-Sandoval A, Cottingham MG, Ewer K, Hill AVS.** 2011. Viral vectors as vaccine platforms: deployment in sight. Current Opinion in Immunology 23:377–382.
227. **Rota PA, Oberste MS, Monroe SS, Nix WA, Campagnoli R, Icenogle JP, Peñaranda S, Bankamp B, Maher K, Chen M-h, Tong S, Tamin A, Lowe L, Frace M, DeRisi JL, Chen Q, Wang D, Erdman DD, Peret TCT, Burns C, Ksiazek TG, Rollin PE, Sanchez A, Liffick S, Holloway B, Limor J, McCaustland K, Olsen-Rasmussen M, Fouchier R, Günther S, Osterhaus, Albert D. M. E., Drosten C, Pallansch MA, Anderson LJ, Bellini WJ.** 2003. Characterization of a Novel Coronavirus Associated with Severe Acute Respiratory Syndrome. Science 300:1394–1399.
228. **Rouvier E, Luciani MF, Golstein P.** 1993. Fas involvement in Ca(2+)-independent T cell-mediated cytotoxicity. J Exp Med 177:195–200.
229. **Salk JE, Francis T.** 1946. Immunization against influenza. Annals of internal medicine 25:443–452.
230. **Sanchez AJ, Vincent MJ, Nichol ST.** 2002. Characterization of the Glycoproteins of Crimean-Congo Hemorrhagic Fever Virus. J. Virol. 76:7263–7275.
231. **Sanders B, Koldijk M, Schuitemaker H.** 2015. Inactivated Viral Vaccines. Springer Berlin Heidelberg.

232. **Sato M, Suemori H, Hata N, Asagiri M, Ogasawara K, Nakao K, Nakaya T, Katsuki M, Noguchi S, Tanaka N, Taniguchi T.** 2000. Distinct and Essential Roles of Transcription Factors IRF-3 and IRF-7 in Response to Viruses for IFN-α/β Gene Induction. Immunity 13:539–548.
233. **Scheuplein VA, Seifried J, Malczyk AH, Miller L, Hocker L, Vergara-Alert J, Dolnik O, Zielecki F, Becker B, Spreitzer I, Konig R, Becker S, Waibler Z, Muhlebach MD.** 2015. High secretion of interferons by human plasmacytoid dendritic cells upon recognition of Middle East respiratory syndrome coronavirus. J Virol 89:3859–3869.
234. **Schilte C, Couderc T, Chretien F, Sourisseau M, Gangneux N, Guivel-Benhassine F, Kraxner A, Tschopp J, Higgs S, Michault A, Arenzana-Seisdedos F, Colonna M, Peduto L, Schwartz O, Lecuit M, Albert ML.** 2010. Type I IFN controls chikungunya virus via its action on nonhematopoietic cells. Journal of Experimental Medicine 207:429–442.
235. **Schulman JL, Khakpour M, Kilbourne ED.** 1968. Protective Effects of Specific Immunity to Viral Neuraminidase on Influenza Virus Infection of Mice. J Virol 2:778–786.
236. **Schwartzman LM, Cathcart AL, Pujanauski LM, Qi L, Kash JC, Taubenberger JK.** 2015. An Intranasal Virus-Like Particle Vaccine Broadly Protects Mice from Multiple Subtypes of Influenza A Virus. mBio 6:e01044-15.
237. **Scott P.** 1993. Selective differentiation of CD4+ T helper cell subsets. Current Opinion in Immunology 5:391–397.
238. **Scott TF, Bonanno DE.** 1967. Reactions to live-measles-virus vaccine in children previously inoculated with killed-virus vaccine. N. Engl. J. Med. 277:248–250.
239. **Seo SH, Wang L, Smith R, Collisson EW.** 1997. The carboxyl-terminal 120-residue polypeptide of infectious bronchitis virus nucleocapsid induces cytotoxic T lymphocytes and protects chickens from acute infection. J Virol 71:7889–7894.
240. **Seth RB, Sun L, Chen ZJ.** 2006. Antiviral innate immunity pathways. Cell Res 16:141–147.
241. **Seto JT, Rott R.** 1966. Functional significance of sialidase during influenza virus multiplication. Virology 30:731–737.
242. **Shaw ML, Stone KL, Colangelo CM, Gulcicek EE, Palese P.** 2008. Cellular proteins in influenza virus particles. PLoS Pathog. 4:e1000085.
243. **Shikh MEE, Sayed RME, Sukumar S, Szakal AK, Tew JG.** 2010. Activation of B cells by antigens on follicular dendritic cells. Trends in Immunology 31:205–211.
244. **Shi L, Sings HL, Bryan JT, Wang B, Wang Y, Mach H, Kosinski M, Washabaugh MW, Sitrin R, Barr E.** 2007. GARDASIL: prophylactic human papillomavirus vaccine development--from bench top to bed-side. Clin Pharmacol Ther 81:259–264.
245. **Shodell M, Siegal FP.** 2002. Circulating, interferon-producing plasmacytoid dendritic cells decline during human ageing. Scand J Immunol 56:518–521.
246. **Shriner D, Shankarappa R, Jensen MA, Nickle DC, Mittler JE, Margolick JB, Mullins JI.** 2004. Influence of random genetic drift on human immunodeficiency virus type 1 env evolution during chronic infection. Genetics 166:1155–1164.
247. **Singh M, Billeter MA.** 1999. A recombinant measles virus expressing biologically active human interleukin-12. Journal of General Virology 80:101–106.
248. **Singh M, Cattaneo R, Billeter MA.** 1999. A recombinant measles virus expressing hepatitis B virus surface antigen induces humoral immune responses in genetically modified mice. J Virol 73:4823–4828.
249. **Siu KL, Yeung ML, Kok KH, Yuen KS, Kew C, Lui PY, Chan CP, Tse H, Woo PC, Yuen KY, Jin DY.** 2014. Middle east respiratory syndrome coronavirus 4a protein is a double-stranded RNA-binding protein that suppresses PACT-induced activation of RIG-I and MDA5 in the innate antiviral response. J Virol 88:4866–4876.
250. **Siu K-L, Kok K-H, Ng M-HJ, Poon VKM, Yuen K-Y, Zheng B-J, Jin D-Y.** 2009. Severe Acute Respiratory Syndrome Coronavirus M Protein Inhibits Type I Interferon Production by Impeding the Formation of TRAF3·TANK·TBK1/IKKε Complex. J. Biol. Chem. 284:16202–16209.
251. **Slifka MK, Matloubian M, Ahmed R.** 1995. Bone marrow is a major site of long-term antibody production after acute viral infection. J Virol 69:1895–1902.
252. **Slifka MK, Antia R, Whitmire JK, Ahmed R.** 1998. Humoral Immunity Due to Long-Lived Plasma Cells. Immunity 8:363–372.
253. **Smit JJ, Rudd BD, Lukacs NW.** 2006. Plasmacytoid dendritic cells inhibit pulmonary immunopathology and promote clearance of respiratory syncytial virus. J Exp Med 203:1153–1159.
254. **Somia NV, Zoppé M, Verma IM.** 1995. Generation of targeted retroviral vectors by using single-chain variable fragment: an approach to in vivo gene delivery. PNAS 92:7570–7574.

255. **Song F, Fux R, Provacia LB, Volz A, Eickmann M, Becker S, Osterhaus, Albert D M E, Haagmans BL, Sutter G.** 2013. Middle East respiratory syndrome coronavirus spike protein delivered by modified vaccinia virus Ankara efficiently induces virus-neutralising antibodies. J Virol 87:11950–11954.
256. **Spik K, Shurtleff A, McElroy AK, Guttieri MC, Hooper JW, SchmalJohn C.** 2006. Immunogenicity of combination DNA vaccines for Rift Valley fever virus, tick-borne encephalitis virus, Hantaan virus, and Crimean Congo hemorrhagic fever virus. Vaccine 24:4657–4666.
257. **Stärk CK, Morgan D.** 2015. Emerging zoonoses: tackling the challenges. Epidemiology and Infection 143:2015–2017.
258. **Steinman RM, Hemmi H.** 2006. Dendritic cells: translating innate to adaptive immunity. Curr Top Microbiol Immunol 311:17–58.
259. **Stephenne J.** 1990. Development and production aspects of a recombinant yeast-derived hepatitis B vaccine. Vaccine 8 Suppl:S69-73; discussion S79-80.
260. **Stohlman SA, Kyuwa S, Cohen M, Bergmann C, Polo JM, Yeh J, Anthony R, Keck JG.** 1992. Mouse hepatitis virus nucleocapsid protein-specific cytotoxic T lymphocytes are Ld restricted and specific for the carboxy terminus. Virology 189:217–224.
261. **Subbarao K, McAuliffe J, Vogel L, Fahle G, Fischer S, Tatti K, Packard M, Shieh W-J, Zaki S, Murphy B.** 2004. Prior infection and passive transfer of neutralising antibody prevent replication of severe acute respiratory syndrome coronavirus in the respiratory tract of mice. J Virol 78:3572–3577.
262. **Su S, Bi Y, Wong G, Gray GC, Gao GF, Li S.** 2015. Epidemiology, Evolution, and Recent Outbreaks of Avian Influenza Virus in China. J Virol 89:8671–8676.
263. **Swain SL, McKinstry KK, Strutt TM.** 2012. Expanding roles for CD4(+) T cells in immunity to viruses. Nat. Rev. Immunol. 12:136–148.
264. **Swiecki M, Gilfillan S, Vermi W, Wang Y, Colonna M.** 2010. Plasmacytoid dendritic cell ablation impacts early interferon responses and antiviral NK and CD8(+) T cell accrual. Immunity 33:955–966.
265. **Swiecki M, Colonna M.** 2010. Unraveling the functions of plasmacytoid dendritic cells during viral infections, autoimmunity, and tolerance. Immunol Rev 234:142–162.
266. **Sylte MJ, Suarez DL.** 2009. Influenza neuraminidase as a vaccine antigen. Curr Top Microbiol Immunol 333:227–241.
267. **Tahara M, Takeda M, Yanagi Y.** 2007. Altered interaction of the matrix protein with the cytoplasmic tail of hemagglutinin modulates measles virus growth by affecting virus assembly and cell-cell fusion. J Virol 81:6827–6836.
268. **Talon J, Horvath CM, Polley R, Basler CF, Muster T, Palese P, Garcia-Sastre A.** 2000. Activation of interferon regulatory factor 3 is inhibited by the influenza A virus NS1 protein. J Virol 74:7989–7996.
269. **Tatsuo H, Ono N, Tanaka K, Yanagi Y.** 2000. SLAM (CDw150) is a cellular receptor for measles virus. Nature 406:893–897.
270. **Taylor JJ, Pape KA, Jenkins MK.** 2012. A germinal center-independent pathway generates unswitched memory B cells early in the primary response. J Exp Med 209:597–606.
271. **Taylor LH, Latham SM, Woolhouse ME.** 2001. Risk factors for human disease emergence. Philos Trans R Soc Lond B Biol Sci 356:983–989.
272. **Terajima M, Cruz J, Co MDT, Lee J-H, Kaur K, Wilson PC, Ennis FA.** 2011. Complement-Dependent Lysis of Influenza A Virus-Infected Cells by Broadly Cross-Reactive Human Monoclonal Antibodies. J. Virol. 85:13463–13467.
273. **Thomas JK, Noppenberger J.** 2007. Avian influenza: a review. Am J Health Syst Pharm 64:149–165.
274. **Treanor JJ, Taylor DN, Tussey L, Hay C, Nolan C, Fitzgerald T, Liu G, Kavita U, Song L, Dark I, Shaw A.** 2010. Safety and immunogenicity of a recombinant hemagglutinin influenza-flagellin fusion vaccine (VAX125) in healthy young adults. Vaccine 28:8268–8274.
275. **Tsai S, Liaw Y, Chen M, Huang C, Kuo GC.** 1997. Detection of type 2-like T-helper cells in hepatitis C virus infection: Implications for hepatitis C virus chronicity. Hepatology 25:449–458.
276. **Uhlig KM, Schulke S, Scheuplein VAM, Malczyk AH, Reusch J, Kugelmann S, Muth A, Koch V, Hutzler S, Bodmer BS, Schambach A, Buchholz CJ, Waibler Z, Scheurer S, Muhlebach MD.** 2015. Lentiviral Protein Transfer Vectors Are an Efficient Vaccine Platform and Induce a Strong Antigen-Specific Cytotoxic T Cell Response. J Virol 89:9044–9060.
277. **van Hemert MJ, Worm, Sjoerd H. E. van den, Knoops K, Mommaas AM, Gorbalenya AE, Snijder EJ.** 2008. SARS-Coronavirus Replication/Transcription Complexes Are Membrane-Protected and Need a Host Factor for Activity In Vitro. PLOS Pathogens 4:e1000054.

278. **Versteeg GA, Bredenbeek PJ, van den Worm, Sjoerd H.E., Spaan WJ.** 2007. Group 2 coronaviruses prevent immediate early interferon induction by protection of viral RNA from host cell recognition. Virology 361:18–26.
279. **Voelkel C, Galla M, Maetzig T, Warlich E, Kuehle J, Zychlinski D, Bode J, Cantz T, Schambach A, Baum C.** 2010. Protein transduction from retroviral Gag precursors. PNAS 107:7805–7810.
280. **Volz A, Kupke A, Song F, Jany S, Fux R, Shams-Eldin H, Schmidt J, Becker C, Eickmann M, Becker S.** 2015. Protective efficacy of recombinant modified vaccinia virus Ankara delivering Middle East respiratory syndrome coronavirus spike glycoprotein. J Virol 89:8651–8656.
281. **Wang C, Zheng X, Gai W, Zhao Y, Wang H, Feng N, Chi H, Qiu B, Li N, Wang T.** 2016. MERS-CoV virus-like particles produced in insect cells induce specific humoural and cellular imminity in rhesus macaques. Oncotarget.
282. **Wang H, Peters N, Schwarze J.** 2006. Plasmacytoid dendritic cells limit viral replication, pulmonary inflammation, and airway hyperresponsiveness in respiratory syncytial virus infection. J Immunol 177:6263–6270.
283. **Wang L, Shi W, Joyce MG, Modjarrad K, Zhang Y, Leung K, Lees CR, Zhou T, Yassine HM, Kanekiyo M, Yang ZY, Chen X, Becker MM, Freeman M, Vogel L, Johnson JC, Olinger G, Todd JP, Bagci U, Solomon J, Mollura DJ, Hensley L, Jahrling P, Denison, Rao SS, Subbarao K, Kwong PD, Mascola,** JR, **Kong WP, Graham BS.** 2015. Evaluation of candidate vaccine approaches for MERS-CoV. Nature Communications 6:7712.
284. **Wang R, Song A, Levin J, Dennis D, Zhang NJ, Yoshida H, Koriazova L, Madura L, Shapiro L, Matsumoto A, Yoshida H, Mikayama T, Kubo RT, Sarawar S, Cheroutre H, Kato S.** 2008. Therapeutic potential of a fully human monoclonal antibody against influenza A virus M2 protein. Antiviral Res 80:168–177.
285. **Wang S-M, Lei H-Y, Liu C-C.** 2012. Cytokine Immunopathogenesis of Enterovirus 71 Brain Stem Encephalitis. Journal of Immunology Research 2012.
286. **Wang X, Li M, Zheng H, Muster T, Palese P, Beg AA, Garcia-Sastre A.** 2000. Influenza A virus NS1 protein prevents activation of NF-kappaB and induction of alpha/beta interferon. J Virol 74:11566–11573.
287. **Wang Z, Hangartner L, Cornu TI, Martin LR, Zuniga A, Billeter MA, Naim HY.** 2001. Recombinant measles viruses expressing heterologous antigens of mumps and simian immunodeficiency viruses. Vaccine 19:2329–2336.
288. **Wang Z, Wan Y, Qiu C, Quinones-Parra S, Zhu Z, Loh L, Tian D, Ren Y, Hu Y, Zhang X, Thomas PG, Inouye M, Doherty PC, Kedzierska K, Xu J.** 2015. Recovery from severe H7N9 disease is associated with diverse response mechanisms dominated by CD8(+) T cells. Nature Communications 6:6833.
289. **Wathelet MG, Orr M, Frieman MB, Baric RS.** 2007. Severe Acute Respiratory Syndrome Coronavirus Evades Antiviral Signaling: Role of nsp1 and Rational Design of an Attenuated Strain. J. Virol. 81:11620–11633.
290. **Webb GB.** 1929. Immunization against Tuberculosis by BacillusCalmette-Guérin (BCG). JAMA 93:1459–1461.
291. **Webby RJ, Andreansky S, Stambas J, Rehg JE, Webster RG, Doherty PC, Turner SJ.** 2003. Protection and compensation in the influenza virus-specific CD8+ T cell response. Proc Natl Acad Sci U S A 100:7235–7240.
292. **Whitehouse CA.** 2004. Crimean-Congo hemorrhagic fever. Antiviral Res 64:145–160.
293. **WHO.** 2003. Summary table of SARS cases by country, 1 November 2002 - 7 August 2003. http://www.who.int/csr/sars/country/2003_08_15/en/. Accessed 15 August, 2003.
294. **WHO.** 2015. WHO. 2015. Rabies, Fact Sheet #99. http://www.who.int/mediacentre/factsheets/fs099/en/. Accessed 1 March, 2016.
295. **WHO.** 2017. Annual review of the list of priority disease s for the WHO R&D Blueprint. http://www.who.int/csr/research-and-development/priority_disease_list_review_short_summary_25Jan2017.pdf?ua=1. Accessed 25 January, 2017.
296. **WHO.** 2017. Avian influenza A(H7N9) virus. http://www.who.int/influenza/human_animal_interface/influenza_h7n9/en/. Accessed 9 February, 2017.
297. **WHO.** 2017. Middle East respiratory syndrome coronavirus (MERS-CoV). http://www.who.int/emergencies/mers-cov/en/. Accessed 10 February, 2017.
298. **Wilde AHd, Raj VS, Oudshoorn D, Bestebroer TM, van Nieuwkoop S, Limpens, Ronald W. A. L., Posthuma CC, van der Meer Y, Bárcena M, Haagmans BL, Snijder EJ, Hoogen, Bernadette G. van den.** 2013. MERS-coronavirus replication induces severe in vitro cytopathology and is strongly inhibited by cyclosporin A or interferon-α treatment. Journal of General Virology 94:1749–1760.

299. **Wirblich C, Coleman CM, Kurup D, Abraham TS, Bernbaum JG, Jahrling PB, Hensley LE, Johnson RF, Frieman MB, Schnell MJ.** 2016. One-Health: A Safe, Efficient Dual-use Vaccine for Humans and Animals against MERS-CoV and Rabies Virus. J. Virol.:JVI.02040-16.
300. **Wit Ed, van Doremalen N, Falzarano D, Munster VJ.** 2016. SARS and MERS: recent insights into emerging coronaviruses. Nature Reviews Microbiology 14:523–534.
301. **Wohlbold TJ, Krammer F.** 2014. In the shadow of hemagglutinin: a growing interest in influenza viral neuraminidase and its role as a vaccine antigen. Viruses 6:2465–2494.
302. **Wolfson LJ, Strebel PM, Gacic-Dobo M, Hoekstra EJ, McFarland JW, Hersh BS.** 2007. Has the 2005 measles mortality reduction goal been achieved? A natural history modelling study. The Lancet 369:191–200.
303. **Wong SK, Lam CW, Wu AK, IP WK, Lee NL, Chan IH, Lit LC, Hui DS, Chan MH, Chung SS, Sung JJ.** 2004. Plasma inflammatory cytokines and chemokines in severe acute respiratory syndrome. Clin Exp Immunol 136:95–103.
304. **Wong SS, Yuen K-Y.** 2006. Avian Influenza Virus Infections in Humans. Chest 129:156–168.
305. **Woodall JP, Williams MC, Di Simpson.** 1967. Congo virus: a hitherto undescribed virus occurring in Africa. II. Identification studies. East Afr Med J 44:93–98.
306. **Xagorari A, Chlichlia K.** 2008. Toll-Like Receptors and Viruses: Induction of Innate Antiviral Immune Responses. Open Microbiol J 2:49–59.
307. **Xiao X, Feng Y, Zhu Z, Dimitrov DS.** 2011. Identification of a putative Crimean-Congo hemorrhagic fever virus entry factor. Biochem. Biophys. Res. Commun. 411:253–258.
308. **Xiao X, Feng Y, Zhu Z, Dimitrov DS.** 2011. Identification of a Putative Crimean-Congo Hemorrhagic Fever Virus Entry Factor. Biochem. Biophys. Res. Commun. 411:253–258.
309. **Yang L, Yang H, Rideout K, Cho T, Joo Ki, Ziegler L, Elliot A, Walls A, Yu D, Baltimore D, Wang P.** 2008. Engineered lentivector targeting of dendritic cells for in vivo immunization. Nature Biotechnology 26:326–334.
310. **Yang PL, Althage A, Chung J, Maier H, Wieland S, Isogawa M, Chisari FV.** 2010. Immune effectors required for hepatitis B virus clearance. PNAS 107:798–802.
311. **Yang Y, Zhang L, Geng H, Deng Y, Huang B, Guo Y, Zhao Z, Tan W.** 2013. The structural and accessory proteins M, ORF 4a, ORF 4b, and ORF 5 of Middle East respiratory syndrome coronavirus (MERS-CoV) are potent interferon antagonists. Protein Cell 4:951–961.
312. **Yang Y, Zhang Y, Fang L, Halloran ME, Ma M, Liang S, Kenah E, Britton T, Chen E, Hu J, Tang F, Cao W, Feng Z, Im Longini.** 2015. Household transmissibility of avian influenza A (H7N9) virus, China, February to May 2013 and October 2013 to March 2014. Euro Surveill 20.
313. **Yang Z-Y, Kong W-P, Huang Y, Roberts A, Murphy BR, Subbarao K, Nabel GJ.** 2004. A DNA vaccine induces SARS coronavirus neutralisation and protective immunity in mice. Nature 428:561–564.
314. **Yan J, Villarreal DO, Racine T, Chu JS, Walters JN, Morrow MP, Khan AS, Sardesai NY, Kim JJ, Kobinger GP, Weiner DB.** 2014. Protective immunity to H7N9 influenza viruses elicited by synthetic DNA vaccine. Vaccine Technology IV 32:2833–2842.
315. **Yoneyama M, Kikuchi M, Natsukawa T, Shinobu N, Imaizumi T, Miyagishi M, Taira K, Akira S, Fujita T.** 2004. The RNA helicase RIG-I has an essential function in double-stranded RNA-induced innate antiviral responses. Nature Immunology 5:730–737.
316. **Yoneyama M, Kikuchi M, Matsumoto K, Imaizumi T, Miyagishi M, Taira K, Foy E, Loo Y-M, Gale M, Akira S, Yonehara S, Kato A, Fujita T.** 2005. Shared and Unique Functions of the DExD/H-Box Helicases RIG-I, MDA5, and LGP2 in Antiviral Innate Immunity. J Immunol 175:2851–2858.
317. **Yuan J, Lau EH, Li K, Leung YH, Yang Z, Xie C, Liu Y, Liu Y, Ma X, Liu J, Li X, Chen K, Luo L, Di B, Cowling BJ, Tang X, Leung GM, Wang M, Peiris M.** 2015. Effect of live poultry market closure on avian influenza A(H7N9) virus activity in Guangzhou, China, 2014. Emerg Infect Dis:1784–1793.
318. **Yu L, Liu W, Schnitzlein WM, Tripathy DN, Kwang J.** 2001. Study of protection by recombinant fowl poxvirus expressing C-terminal nucleocapsid protein of infectious bronchitis virus against challenge. Avian Dis 45:340–348.
319. **Yun S-I, Lee Y-M.** 2014. Japanese encephalitis: The virus and vaccines. Hum Vaccin Immunother 10:263–279.
320. **Zaki AM, van Boheemen S, Bestebroer TM, Osterhaus, Albert D M E, Fouchier, Ron A M.** 2012. Isolation of a novel coronavirus from a man with pneumonia in Saudi Arabia. N. Engl. J. Med. 367:1814–1820.
321. **Zepp F.** 2010. Principles of vaccine design-Lessons from nature. Vaccine 28 Suppl 3:C14-24.

322. **Zhang N, Channappanavar R, Ma C, Wang L, Tang J, Garron T, Tao X, Tasneem S, Lu L, Tseng CT, Zhou Y, Perlman S, Jiang S, Du L.** 2016. Identification of an ideal adjuvant for receptor-binding domain-based subunit vaccines against Middle East respiratory syndrome coronavirus. Cell Mol Immunol 13:180–190.
323. **Zhang Q, Shi J, Deng G, Guo J, Zeng X, He X, Kong H, Gu C, Li X, Liu J, Wang G, Chen Y, Liu L, Liang L, Li Y, Fan J, Wang J, Li W, Guan L, Li Q, Yang H, Chen P, Jiang L, Guan Y, Xin X, Jiang Y, Tian G, Wang X, Qiao C, Li C, Bu Z, Chen H.** 2013. H7N9 Influenza Viruses Are Transmissible in Ferrets by Respiratory Droplet. Science 341:410–414.
324. **Zhao J, Li K, Wohlford-Lenane C, Agnihothram SS, Fett C, Zhao J, Gale MJ, Baric RS, Enjuanes L, Gallagher T, McCray PB, Perlman S.** 2014. Rapid generation of a mouse model for Middle East respiratory syndrome. Proc Natl Acad Sci U S A 111:4970–4975.
325. **Zhou J, Chu H, Li C, Wong BH, Cheng ZS, Poon VK, Sun T, Lau CC, Wong KK, Chan JY, Chan JF, To KK, Chan KH, Zheng BJ, Yuen KY.** 2014. Active replication of Middle East respiratory syndrome coronavirus and aberrant induction of inflammatory cytokines and chemokines in human macrophages: implications for pathogenesis. J. Infect. Dis. 209:1331–1342.
326. **Zhu FC, Zhang J, Zhang XF, Zhou C, Wang ZZ, Huang SJ, Wang H, Yang CL, Jiang HM, Cai JP, Wang YJ, Ai X, Hu YM, Tang Q, Yao X, Yan Q, Xian YL, Wu T, Li YM, Miao J, Ng MH, Shih JW, Xia NS.** 2010. Efficacy and safety of a recombinant hepatitis E vaccine in healthy adults: a large-scale, randomised, double-blind placebo-controlled, phase 3 trial. Lancet 376:895–902.
327. **Zhu H, Wang D, Kelvin DJ, Li L, Zheng Z, Yoon SW, Wong SS, Farooqui A, Wang J, Banner D, Chen R, Zheng R, Zhou J, Zhang Y, Hong W, Dong W, Cai Q, Roehrl MH, Huang SS, Kelvin AA, Yao T, Zhou B, Chen X, Leung GM, Poon LL, Webster RG, Webby RJ, Peiris JS, Guan Y, Shu Y.** 2013. Infectivity, transmission, and pathology of human-isolated H7N9 influenza virus in ferrets and pigs. Science 341:183–186.
328. **Zhu T, Korber BT, Nahmias AJ, Hooper E, Sharp PM, Ho DD.** 1998. An African HIV-1 sequence from 1959 and implications for the origin of the epidemic. Nature 391:594–597.
329. **Ziegler T, Matikainen S, Rönkkö E, Österlund P, Sillanpää M, Sirén J, Fagerlund R, Immonen M, Melén K, Julkunen I.** 2005. Severe Acute Respiratory Syndrome Coronavirus Fails To Activate Cytokine-Mediated Innate Immune Responses in Cultured Human Monocyte-Derived Dendritic Cells. J. Virol. 79:13800–13805.
330. **Zielecki F, Weber M, Eickmann M, Spiegelberg L, Zaki AM, Matrosovich M, Becker S, Weber F.** 2013. Human Cell Tropism and Innate Immune System Interactions of Human Respiratory Coronavirus EMC Compared to Those of Severe Acute Respiratory Syndrome Coronavirus. J. Virol. 87:5300–5304.
331. **Zinkernagel RM.** 2001. Maternal antibodies, childhood infections, and autoimmune diseases. N. Engl. J. Med. 345:1331–1335.
332. **Zinkernagel RM, LaMarre A, Ciurea A, Hunziker L, Ochsenbein AF, McCoy KD, Fehr T, Bachmann MF, Kalinke U, Hengartner H.** 2001. Neutralising antiviral antibody responses. Adv Immunol 79:1–53.
333. **Zuniga A, Wang Z, Liniger M, Hangartner L, Caballero M, Pavlovic J, Wild P, Viret JF, Glueck R, Billeter MA, Naim HY.** 2007. Attenuated measles virus as a vaccine vector. Vaccine 25:2974–2983.
334. **Züst R, Cervantes-Barragan L, Habjan M, Maier R, Neuman BW, Ziebuhr J, Szretter KJ, Baker SC, Barchet W, Diamond MS, Siddell SG, Ludewig B, Thiel V.** 2011. Ribose 2[prime]-O-methylation provides a molecular signature for the distinction of self and non-self mRNA dependent on the RNA sensor Mda5. Nature Immunology 12:137–143.

JVI Journals.ASM.org

High Secretion of Interferons by Human Plasmacytoid Dendritic Cells upon Recognition of Middle East Respiratory Syndrome Coronavirus

Vivian A. Scheuplein,[a] Janna Seifried,[a,e] Anna H. Malczyk,[a,f] Lilija Miller,[b] Lena Höcker,[b] Júlia Vergara-Alert,[c,h] Olga Dolnik,[c] Florian Zielecki,[c] Björn Becker,[d] Ingo Spreitzer,[d] Renate König,[e,f,g] Stephan Becker,[c,h] Zoe Waibler,[b,f] Michael D. Mühlebach[a,f]

Oncolytic Measles Viruses and Vaccine Vectors,[a] Novel Vaccination Strategies and Early Immune Responses,[b] Bacterial Safety,[d] and Host Pathogen Interactions,[e] Paul Ehrlich Institut, Langen, Germany; German Center for Infection Research, Langen, Germany[f]; Sanford-Burnham Medical Research Institute, Infectious and Inflammatory Disease Center, La Jolla, USA[g]; Institut für Virologie, Philipps Universität Marburg, Marburg, Germany[c]; German Centre for Infection Research, Marburg, Germany[h]

ABSTRACT

The Middle East respiratory syndrome coronavirus (MERS-CoV) emerged in 2012 as the causative agent of a severe respiratory disease with a fatality rate of approximately 30%. The high virulence and mortality rate prompted us to analyze aspects of MERS-CoV pathogenesis, especially its interaction with innate immune cells such as antigen-presenting cells (APCs). Particularly, we analyzed secretion of type I and type III interferons (IFNs) by APCs, i.e., B cells, macrophages, monocyte-derived/myeloid dendritic cells (MDDCs/mDCs), and by plasmacytoid dendritic cells (pDCs) of human and murine origin after inoculation with MERS-CoV. Production of large amounts of type I and III IFNs was induced exclusively in human pDCs, which were significantly higher than IFN induction by severe acute respiratory syndrome (SARS)-CoV. Of note, IFNs were secreted in the absence of productive replication. However, receptor binding, endosomal uptake, and probably signaling via Toll-like receptor 7 (TLR7) were critical for sensing of MERS-CoV by pDCs. Furthermore, active transcription of MERS-CoV N RNA and subsequent N protein expression were evident in infected pDCs, indicating abortive infection. Taken together, our results point toward dipeptidyl peptidase 4 (DPP4)-dependent endosomal uptake and subsequent infection of human pDCs by MERS-CoV. However, the replication cycle is stopped after early gene expression. In parallel, human pDCs are potent IFN-producing cells upon MERS-CoV infection. Knowledge of such IFN responses supports our understanding of MERS-CoV pathogenesis and is critical for the choice of treatment options.

IMPORTANCE

MERS-CoV causes a severe respiratory disease with high fatality rates in human patients. Recently, confirmed human cases have increased dramatically in both number and geographic distribution. Understanding the pathogenesis of this highly pathogenic CoV is crucial for developing successful treatment strategies. This study elucidates the interaction of MERS-CoV with APCs and pDCs, particularly the induction of type I and III IFN secretion. Human pDCs are the immune cell population sensing MERS-CoV but secrete significantly larger amounts of IFNs, especially IFN-α, than in response to SARS-CoV. A model for molecular virus-host interactions is presented outlining IFN induction in pDCs. The massive IFN secretion upon contact suggests a critical role of this mechanism for the high degree of immune activation observed during MERS-CoV infection.

In 2012 a novel human betacoronavirus associated with severe respiratory disease emerged in Saudi Arabia (1). Due to its geographic distribution, this new virus was classified as Middle East respiratory syndrome coronavirus (MERS-CoV) (2). MERS-CoV is associated with high fatality rates (3, 4), and case numbers globally have increased to 909 laboratory-confirmed cases with 331 fatalities (as of 21 November 2014 [http://www.who.int/csr/don/21-november-2014-mers/en/]). In parallel, the geographic distribution has expanded (4). MERS-CoV is the second emerging CoV with severe pathogenicity in humans within 10 years after the severe acute respiratory syndrome coronavirus (SARS-CoV) that infected approximately 8,000 people worldwide during its spread in 2003 (5). Human-to-human transmissions have been reported for MERS-CoV, but transmissibility seems to be inefficient (6, 7). MERS-CoV persists in animal reservoirs, i.e., dromedary camels (8), and transmission events between camels and contact persons have been reported (7–10). Thus, MERS-CoV infection of men has zoonotic origins, similar to SARS-CoV, but unlike SARS-CoV, where bats have been identified as the original virus reservoir, bats have been reported to host only closely related viruses of MERS-CoV (11). However, the only small-animal model developed so far involves type I interferon receptor (IFNAR)-deficient mice expressing human dipeptidyl peptidase 4 (huDPP4; CD26), the entry receptor of MERS-CoV (12), in the lung after intranasal administration of huDPP4-expressing adenoviral vectors (13). MERS-CoV causes symptoms in humans similar to those of SARS-CoV infection, such as severe pneumonia with acute respi-

Received 16 December 2014 **Accepted** 13 January 2015

Accepted manuscript posted online 21 January 2015

Citation Scheuplein VA, Seifried J, Malczyk AH, Miller L, Höcker L, Vergara-Alert J, Dolnik O, Zielecki F, Becker B, Spreitzer I, König R, Becker S, Waibler Z, Mühlebach MD. 2015. High secretion of interferons by human plasmacytoid dendritic cells upon recognition of Middle East respiratory syndrome coronavirus. J Virol 89:3859–3869. doi:10.1128/JVI.03607-14.

Editor: S. Perlman

Address correspondence to Zoe Waibler, Zoe.Waibler@pei.de, or Michael D. Mühlebach, Michael.Muehlebach@pei.de.

J.S. and A.H.M. contributed equally to this work.

doi:10.1128/JVI.03607-14

ratory distress syndrome, leukopenia and lymphopenia (14), septic shock, and multiorgan failure. A special feature of MERS-CoV infection is that it can cause renal complications which may end in renal failure (15). The unusual tropism of MERS-CoV has been related to the wide tissue distribution of DPP4, e.g., on renal epithelial cells or leukocytes (16).

MERS-CoV replication is sensitive to type I and type III interferons (IFN) *in vitro* (17, 18), and macaques can be protected by administration of IFN-β in combination with ribavirin (19). However, a benefit of IFN-β treatment could not be confirmed in five severely ill human patients in whom disease had presumably progressed too far (20, 21). Sensitivity of MERS-CoV to IFNs indicates that innate immunity and IFN secretion are critical parameters for the outcome of MERS-CoV infection. Type I IFNs, particularly IFN-β, can be produced by most stromal cell types upon viral infection. Indeed, MERS-CoV actively suppresses type I IFN production in a variety of infected cell types, such as primary airway epithelial cells (18, 22). Additionally, professional antigen-presenting cells (APCs) are an important source of type I IFNs upon recognition of pathogen-associated molecular patterns (PAMPs) (23). Particularly, plasmacytoid dendritic cells (pDCs) have been shown to secrete large amounts of IFN-α after contact with virus (e.g., HIV-1 [24] or SARS-CoV [25]). Type I IFNs have a significant bystander effect on uninfected neighboring cells by inducing an antiviral state, activating innate immune cells, and priming adaptive immunity. On the other hand, over shooting secretion of IFN can result in cytokine dysregulation and immune pathogenesis (26).

To analyze the role of primary innate immune cells, especially their IFN secretion levels during MERS-CoV infection, we inoculated a range of professional APCs and pDCs with MERS-CoV. No type I or type III IFNs were produced by murine myeloid DCs (mDCs), pDCs, or peritoneal exudate cells (PECs) after contact with MERS-CoV. Most interestingly, this was also the case for all human APC cell types, which did not react to MERS-CoV with IFN secretion. Human pDCs, however, produced large amounts of IFN-α and IFN-β and moderate amounts of IFN-λ upon contact with MERS-CoV without virus amplification. The observed IFN induction was dependent on the availability of the MERS-CoV receptor DPP4, endosomal maturation, or partially on PAMP recognition via Toll-like receptor 7 (TLR7) and correlated with *de novo* expression of MERS-CoV N protein. The large amounts of type I IFNs which are secreted by pDCs during MERS-CoV infection suggest that type I IFNs hold a key position in MERS-CoV infection.

MATERIALS AND METHODS

Cell lines and viruses. Vero cells (ATCC CCL-81) and BHK-21 cells (C-13) (ATCC CCL-10) were purchased from the ATCC (Manassas, VA, USA) and cultured in Dulbecco's modified Eagle's medium (DMEM; Lonza, Cologne, Germany) supplemented with 2 mM glutamine and 10% fetal bovine serum (FBS; Biochrom, Berlin, Germany) at 37°C in a humidified atmosphere containing 6% CO_2 for no longer than 6 months of culture after thawing of the original stock. MERS-CoV (EMC/2012) (14) and SARS-CoV (strain Frankfurt-1) (27) were propagated in Vero cells. Titers were determined by 50% tissue culture infection dose ($TCID_{50}$) titration on Vero cells (28). Virus stocks were stored in aliquots at −80°C. Inactivated MERS-CoV was generated by UV inactivation (120,000 μJ/cm^2 UV light [254 nm] for 90 min) (Stratalinker UV Cross-linker; Stratagene, La Jolla, CA) of 0.1 ml of virus suspension in 48-well plates on ice. Thogoto virus, an influenza-like orthomyxovirus inducing type I IFNs in murine mDCs, lacking an elongated matrix protein [THOV(ΔML)] (29), and vesicular stomatitis virus M2 (VSV-M2) (30), a variant of VSV with defects in M protein functionality that induces high IFN responses in cells (31), were propagated on BHK-21 cells and titrated via plaque assay on Vero cells as described previously (30).

Isolation and generation of human professional antigen-presenting cells and pDCs. Human peripheral blood mononuclear cells (PBMCs) were isolated by Ficoll (Biochrom) density gradient centrifugation from buffy coats (Blutspendedienst, Frankfurt am Main, Germany) or citrate-blood samples of anonymized healthy human volunteers. Human B cells were purified by negative selection using a B-Cell Isolation Kit II (Miltenyi Biotec, Bergisch Gladbach, Germany) and cultured as described before (32). Monocytes were purified by positive selection using CD14 MicroBeads (Miltenyi Biotec). For generation of monocyte-derived DCs (MDDCs), 2×10^5 $CD14^+$ monocytes were cultured in 96-well flat-bottom tissue culture plates using X-VIVO 15 medium (Lonza) in the presence of granulocyte-macrophage colony-stimulating factor (GM-CSF; 1,000 U/ml) (CellGenix, Freiburg, Germany) and interleukin-4 (IL-4; 1,000 U/ml) (CellGenix) for 5 days (33). For generation of GM-CSF-derived (M1) macrophages, monocytes were cultured in X-VIVO 15 medium supplemented with 10 ng/ml GM-CSF. For macrophage colony-stimulating factor (M-CSF)-derived (M2) macrophage generation, monocytes were cultured in RPMI 1640 medium containing 10% FBS, 10 mM L-glutamine, 0.5 mM penicillin-streptomycin (PAA Laboratories, Egelsbach, Germany), 0.1 mM nonessential amino acids (Biochrom), and 30 ng/ml M-CSF (R&D Systems, Wiesbaden-Nordendstadt, Germany) (34). Untouched human plasmacytoid dendritic cells (pDCs) were isolated by negative selection from PBMCs using a plasmacytoid dendritic cell isolation kit (Miltenyi Biotec) and cultured in RPMI 1640 medium (Biowest, Nuaillé, France) containing 10% fetal calf serum (FCS; Lonza), 10 mM L-glutamine, and 100 ng/ml recombinant IL-3 (R&D Systems). For subsequent experiments, all APCs were seeded at a density of 2.5×10^5 APCs/well, and pDCs were seeded at a density of 2×10^4 pDCs/well in 96-well plates in 200 μl of medium.

Generation of murine professional antigen-presenting cells. Murine bone marrow-derived myeloid dendritic cells (mDCs) and plasmacytoid dendritic cells (pDCs) were generated from bone marrow cells isolated from femurs and tibias of sacrificed 6- to 10-week-old C57BL/6N mice by differentiation with GM-CSF (R&D Systems) or Flt-3L (R&D Systems) for 8 days, as described before (35). Peritoneal exudate cells (PECs) were isolated from sacrificed 6- to 10-week-old C57BL/6N mice by flushing out cells from the abdominal cavity with 5 ml of phosphate-buffered saline (PBS) and seeding at 2×10^5 cells/ml in 200 μl of RPMI 1640 medium (Biowest).

Virus growth kinetics. Vero cells, APCs, or pDCs were infected at a multiplicity of infection (MOI) of 0.01 or 5. Cells were washed once at 1 h postinfection (hpi) and incubated in the respective cell culture medium. At the time points indicated in the figures, cell-free supernatants were sampled and stored at −80°C. Titers were determined by $TCID_{50}$ titration on Vero cells as described above.

Analysis of type I and III interferon secretion. Innate immune cells were inoculated with MERS-CoV, SARS-CoV, or UV-inactivated MERS-CoV. VSV-M2 (MOI of 0.1), THOV (MOI of 0.1), CpG 2216 (5 μg/ml), or CpG 2006 (5 μg/ml) (Invitrogen Life Technologies) (36) was used as a control. Cell-free supernatant was collected at 24 hpi and stored at −80°C. Supernatants of human cells were analyzed for secreted IFNs using a human IFN-α enzyme-linked immunosorbent assay (ELISA) (Mabtech AB, Nacka Strand, Sweden), human IFN-β ELISA (R&D Systems), human IL-29 (IFN-λ1) ELISA (eBioscience, Frankfurt, Germany), or a human IL-6 DuoSet ELISA development system (R&D Systems) according to the manufacturers' instructions. Supernatants of murine cells were analyzed using a mouse IFN-α or mouse IFN-β ELISA (PBL Biomedical Laboratories, Piscataway, NJ) kit. To inhibit endosomal maturation or TLR7 signaling, pDCs were preincubated for 30 min at 37°C with 5 μM chloroquine (Sigma) or 5.6 μM inhibitory oligonucleotide (ODN) IRS661

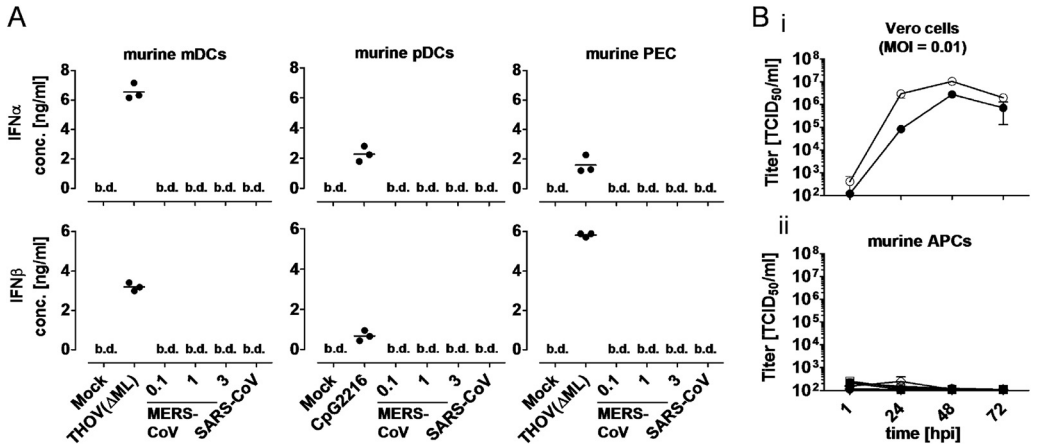

FIG 1 Inoculation of murine cells with MERS-CoV. (A) Type I IFN secretion by murine immune cells. Cells were inoculated with MERS-CoV (MOIs as indicated), SARS-CoV, or the indicated positive controls. Single dots, individual experiments; horizontal lines, means. IFNs were measured at 24 hpi. b.d., below detection. Limits of detection were 12.5 pg/ml for IFN-α and 15.6 pg/ml for IFN-β. (B) Growth kinetics of MERS-CoV on Vero cells or murine APCs (MOI of 0.01). Indicated cell types were inoculated with virus, and sampled supernatants were titrated. Filled symbols, MERS-CoV; open symbols, SARS-CoV; ◇, PECs; ○, mDCs; □, pDCs. Values are means of three independent experiments; error bars indicate standard deviations. conc, concentration.

(Invitrogen Life Technologies), respectively, and infected with MERS-CoV (MOI of 1) in the presence of inhibitors. To inhibit receptor binding of MERS-CoV, pDCs were preincubated for 30 min at 37°C with the recombinant receptor binding domain (RBD) consisting of residues 358 to 588 of the MERS-CoV spike protein (S) or with IgG1-Fc control protein (40 ng/ml) (37) before infection (MOI of 1).

qRT-PCR. A total of 2×10^4 pDCs were infected with MERS-CoV (MOI of 3) and washed once with medium at 1 hpi. Total RNA of infected cells was isolated using an RNeasy Plus minikit (QIAgen, Hilden, Germany) according to the manufacturer's instructions. Isolated RNA (10 μl) was subjected to quantitative reverse-transcription PCR (qRT-PCR) using a SuperScript III Platinum OneStep qRT-PCR System (Invitrogen Life Technologies) with primers N2-Forward and N2-Reverse and probe N2-Probe (labeled 5′ with 6-carboxyfluorescein and 3′ with Black Hole Quencher 1) as described previously (38) utilizing an ABI7900 HT Fast Real-Time PCR System (Invitrogen Life Technologies). The amplification protocol was as follows: RT at 50°C for 30 min, initial denaturation at 95°C for 2 min, and PCR consisting of 40 cycles at 95°C for 15 s and 55°C for 1 min, with a final elongation at 55°C for 5 min. Data were normalized to cellular glyceraldehyde-3-phosphate dehydrogenase (GAPDH) mRNA, which was quantified using a SuperScript III Platinum SYBR green OneStep qRT-PCR System (Invitrogen Life Technologies) with primers GapdH fwd (5′-GGCGATGCTGGCGCTGAGTAC-3′) and GapdH rev (5′-TGGTCCACACCCATGACGA-3′) for human GAPDH and mGAPDH fwd (5′-CACCAACTGCTTAGCCCC-3′) and mGAPDH rev (5′-TCTTCTGGGTGGCAGTGATG-3′) for murine GAPDH. The amplification protocol was as follows: 50°C for 30 min and 95°C for 15 min, followed by 40 cycles of 94°C for 15 s, 56°C for 1 min, 72°C for 30 s, and 95°C for 15 min. The normalized change in the cycle threshold (C_T) value [$\Delta C_T = C_{T(\text{MERS vRNA})} - C_{T(\text{GAPDH mRNA})}$, where vRNA is viral RNA] thus describes the difference between threshold cycle numbers for qRT-PCR signals of viral RNA and cellular mRNA for a given sample. Therefore, the lower the ΔC_T, the higher is the relative amount of vRNA in the sample. Due to exponential amplification of DNA during PCR, differences (n) between ΔC_T values were converted to x-fold ratios using the formula $x = 2^{-n}$, assuming optimal amplification for all samples.

Immunoblotting. For detection of CoV N protein expression, 5×10^4 pDCs were incubated with MERS-CoV (MOI of 3) and washed once with medium at 1 hpi or 8 hpi. For blocking experiments, cells were preincubated with the respective blocking agents as described above or with human DPP4/CD26 affinity-purified polyclonal antibody (R&D Systems) or goat IgG control (R&D Systems) (40 μg/ml) (12) for 30 min at 37°C before infection. Subsequently, washed pDCs were lysed and subjected to immunoblot analysis as described previously (39). MERS-CoV N protein was detected using polyclonal rabbit anti-MERS-CoV serum (1:1,000) with donkey horseradish peroxidase (HRP)-conjugated anti-rabbit IgG(H+L) (1:10,000) (Rockland, Gilbertsville, PA); β-actin was detected by mouse monoclonal anti-β-actin antibody (AC-15; 1:5,000) (ab6276; Abcam, Cambridge, United Kingdom) with HRP-conjugated rabbit anti-mouse secondary antibody (Invitrogen Life Technologies). Pierce ECL 2 Western blotting substrate (Thermo Scientific) on Amersham Hyperfilm ECL (GE Healthcare) was used for detection of specific bands.

Flow cytometry analysis. Flow cytometry was performed on an LSRII-SORP fluorescence-activated cell sorter (FACS; BD, Heidelberg, Germany), and data were analyzed using FACSDiva, version 6.1.3, or FCS Express, version 3 (De Novo Software, Los Angeles, CA). Cells were stained and analyzed as described previously (39) using the following antibodies: murine anti-human CD26-phycoerythrin (PE) (BA5b; Biolegend, San Diego, CA), murine anti-human CD14-fluorescein isothiocyanate (FITC) (M5E2; BD), murine anti-human CD19-PE (HIB19; BD Bioscience), murine anti-human CD123-PE (9F5; BD Bioscience), or murine anti-human DC303-allophycocyanin (APC) (BD Bioscience) according to the manufacturers' instructions. Fc block was performed with Gammagard (1.25 mg/m; Baxter, Deerfield, IL). Viability was checked by Fixable Viability Dye eFluor 780 (eBioscience).

RESULTS

Analysis of type I IFN secretion in murine immune cells. Due to the sensitivity of MERS-CoV to IFNs and the important role of innate immune cells in pathogen recognition and IFN secretion, we were interested in which innate immune cell subsets produce type I or type III IFNs upon contact with MERS-CoV. Therefore, type I IFN secretion by murine APCs and pDCs inoculated with MERS-CoV was analyzed first. Murine PECs (mainly macrophages), mDCs, or pDCs were inoculated with MERS-CoV or SARS-CoV. For murine mDCs and PECs, THOV(ΔML) served as a positive control for IFN secretion (29). Murine pDCs were inoculated with CpG 2216 oligonucleotide to test the cells' reactivity. All murine immune cells revealed robust IFN-α and IFN-β responses to the adequate positive controls but no induction of type I IFN after contact with MERS-CoV or with SARS-CoV (Fig. 1A). Next, viral replication of MERS-CoV in murine APCs was

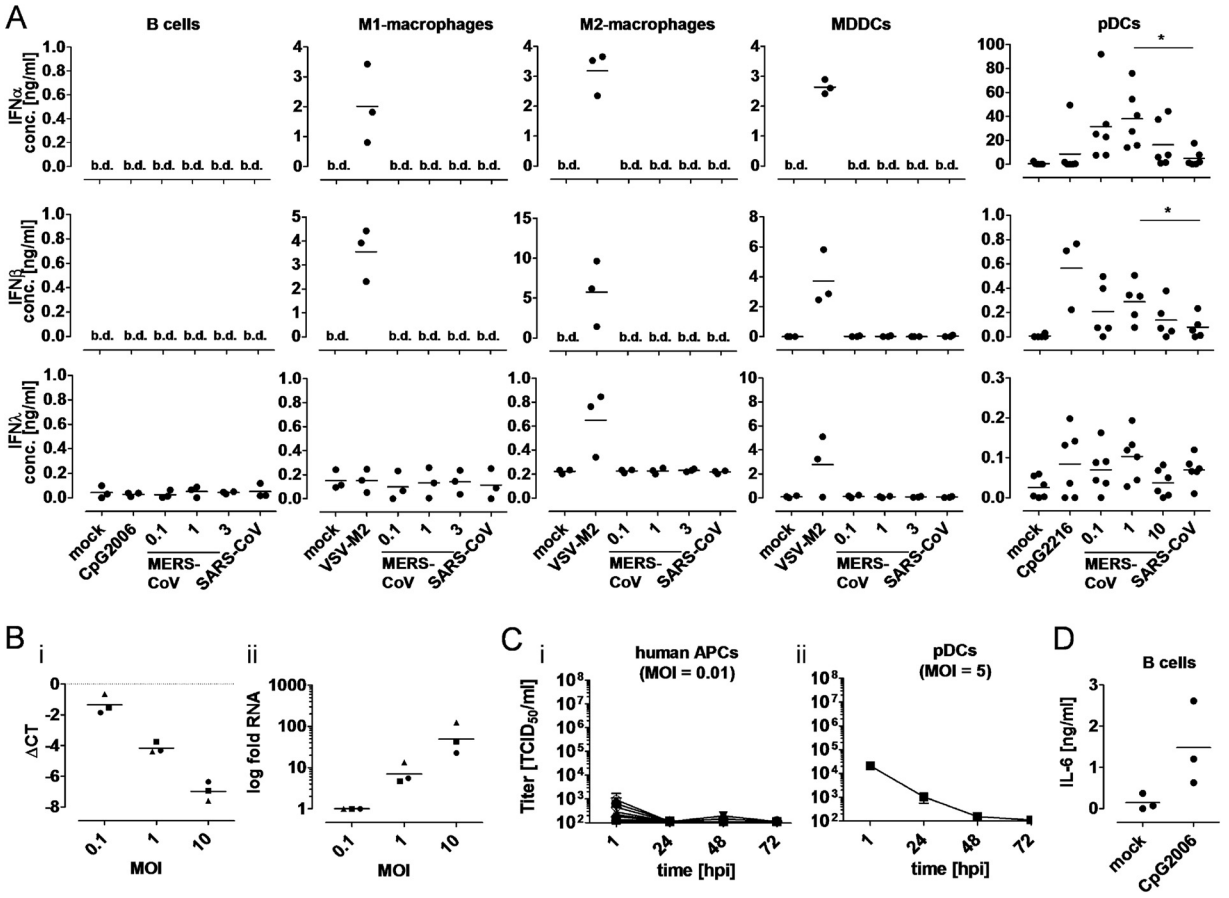

FIG 2 Inoculation of human immune cells with MERS-CoV. (A) Type I and III IFN secretion by human immune cells. Human cells were inoculated with MERS-CoV (MOIs indicated), SARS-CoV (MOI of 1), or the indicated positive control (CpG 2006, VSV-M2, or CpG 2216). Supernatants were sampled at 24 hpi, and secreted IFNs were determined by specific ELISAs. (B) Isolated RNA was used for qRT-PCR. MERS RNA signals were normalized to cellular GAPDH mRNA [$\Delta C_T = C_{T(\text{MERS RNA})} - C_{T(\text{GAPDH mRNA})}$]. ΔC_T values and respectively calculated *x*-fold amounts of RNA normalized to an MOI of 0.1 were determined. (C) Titers of MERS-CoV or SARS-CoV (control) in human immune cells (APCs) infected at an MOI of 0.01 or on pDCs infected at an MOI of 5. (D) IL-6 secretion by human B cells upon inoculation with stimulating CpG 2006. Supernatants were sampled at 24 h after inoculation with CpG 2006, and secreted IFNs were determined by ELISA. Individual donors are displayed as single dots, and horizontal lines indicate means. Limits of detection were 7 pg/ml for IFN-α, 50 pg/ml for IFN-β, and 8 pg/ml for IFN-λ. b.d., below detection; filled symbols, MERS-CoV; open symbols, SARS-CoV; ◇, B cells; △, M1 macrophages; ▽, M2 macrophages; ○, MDDCs; □, pDCs. Growth in human APCs (MOI of 0.01) (i, left), or in human pDCs (MOI of 5) (ii, right) was determined. Values are means of three independent experiments; error bars indicated standard deviation. *, $P < 0.05$.

controlled since inhibition of type I IFN production in MERS-CoV-infected cells has been described previously (17), potentially decoupling replication from IFN secretion. Productive viral replication in immune cells was quantified by titration of the supernatant of inoculated cells to detect released infectious progeny virus (Fig. 1B). Two days postinfection, permissive Vero cells produced high peak titers of 5×10^6 $TCID_{50}$s/ml and 1×10^7 $TCID_{50}$s/ml of MERS- and SARS-CoV, respectively (Fig. 1B, panel i). In contrast, no infectious virus considerably above the limit of detection (1×10^2 $TCID_{50}$s/ml) was detected in the supernatants of any murine cell population for both MERS- and SARS-CoV (Fig. 1B, panel ii).

Interferon production by human APCs upon contact with MERS-CoV. Although MERS-CoV did not induce any reactivity in murine immune cells, reactivity of human immune cells seemed not too unlikely as SARS-CoV exhibited such a pattern of IFN induction (25). Therefore, we analyzed next if and which human innate immune cell subset(s) produces type I or type III IFNs upon inoculation with MERS-CoV. Human B cells, M1 and M2 type macrophages, MDDCs, and pDCs were inoculated with MERS-CoV or SARS-CoV. As positive controls for IFN secretion, M1 and M2 macrophages and MDDCs were inoculated with VSV-M2 (30), B cells were inoculated with the B cell-stimulating CpG oligonucleotide CpG2006 (40), and pDCs were inoculated with pDC-stimulating CpG oligonucleotide CpG2216 (41). Untreated cells served as mock controls. Human B cells, M1 macrophages, M2 macrophages, and MDDCs did not secrete type I or type III IFNs upon inoculation with MERS-CoV, despite being responsive to appropriate stimuli (Fig. 2A). General responsiveness of B cells was confirmed by IL-6 secretion after stimulation with CpG 2006 (Fig. 2D) (40). In contrast, human pDCs secreted large amounts of IFN-α, IFN-β, or IFN-λ (up to 40, 0.3, or 0.1 ng/ml, respectively) upon contact with MERS-CoV (Fig. 2A), with the highest secretion at an intermediate MOI of 1. Interestingly, this did not correlate with rates of infection. pDCs inoculated with increasing MOIs of MERS-CoV revealed an approximately linear correlation of viral RNA detectable in infected pDCs, as determined by calculating the normalized ΔC_T values of qRT-PCR analysis and converting the detected differences into fold changes (Fig. 2B). The

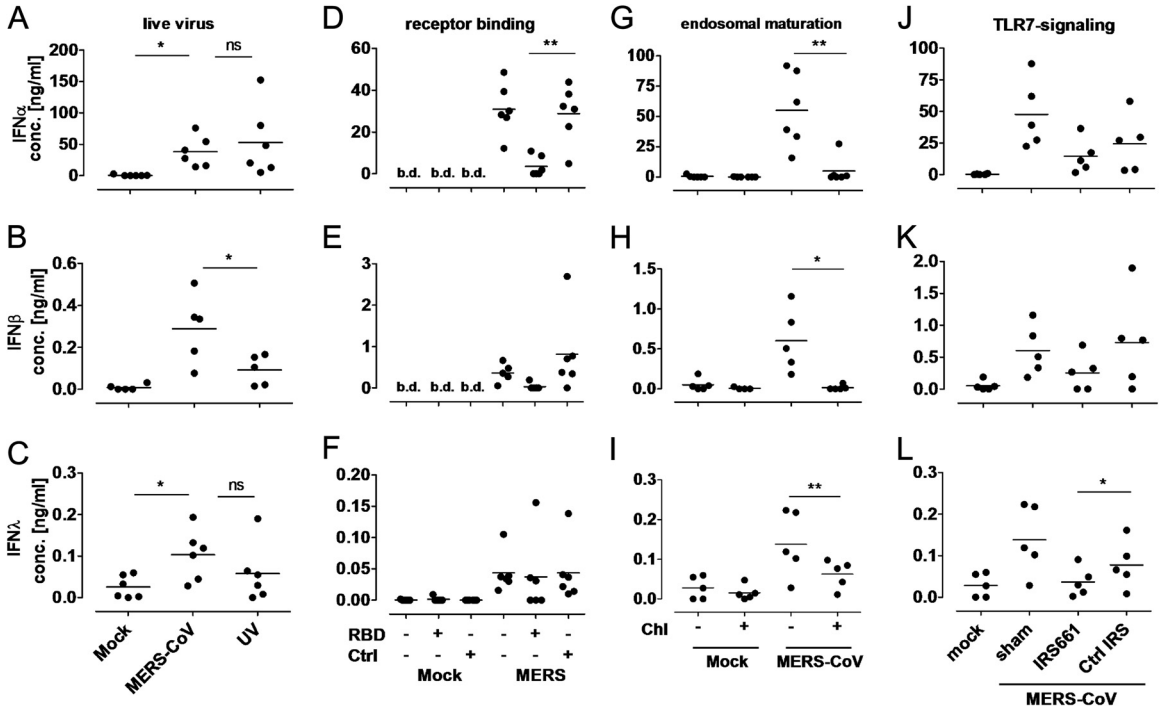

FIG 3 Dissecting type I and III IFN induction in human pDCs. Impact of different parameters on IFN induction in pDCs after inoculation of MERS-CoV (MOI of 1). (A to C) Live virus. pDCs were incubated with UV-inactivated virus (UV) or live virus (MERS-CoV). (D to F) Entry receptor. Infection was performed in the presence or absence of the MERS-CoV S receptor binding domain (RBD) or IgG1-Fc control protein (Ctrl). (G to I) Endosomal maturation. Infection was performed in the presence of chloroquine. (J to L) TLR recognition. Infection was performed in the presence of TLR7 inhibitor (IRS661). IFNs were sampled at 24 hpi. Mock and MERS-CoV data for live virus experiments are the same as displayed in Fig. 2. Mock, uninfected cells; sham, infected but untreated cells. Single dots, individual donors; horizontal lines, means. *, $P < 0.05$; **, $P < 0.01$; ns, not significant.

largest amounts of secreted IFNs at an MOI of 1 were about 8-, 4-, or 1.5-fold higher, respectively, than IFN levels measured after inoculation with SARS-CoV (5 ng/ml IFN-α, 0.07 ng/ml IFN-β, and 0.07 ng/ml IFN-λ). In addition, responses of human pDCs to CpG 2216 (8.6 ng/ml IFN-α, 600 pg/ml IFN-β, and 80 pg/ml IFN-λ) were remarkably less strong than to MERS-CoV but clearly detectable (41).

MERS-CoV replication in human innate immune cells. To analyze whether production of IFNs corresponds to productive replication of MERS-CoV in the respective human innate immune cell subsets, we inoculated cells with MERS-CoV and SARS-CoV at a low MOI of 0.01. Productive viral replication was quantified by titration of the supernatant of inoculated cells to detect released infectious progeny virus (Fig. 2C). Similar to findings with murine APCs (Fig. 1B, panel ii), no infectious virus considerably above the limit of detection (1×10^2 $TCID_{50}$s/ml) was detected in the supernatants of any human cell population for both MERS- and SARS-CoV (Fig. 2C). Thus, no productive replication of MERS-CoV in APCs and pDCs became evident after infection at a low MOI. Since replication of MERS-CoV in M1 macrophages or MDDCs after infection at a high MOI has been reported (42, 43), human pDCs were additionally infected at an MOI of 5 to test, if, e.g., putative antiviral cellular restriction factors may be overcome by infection at high MOIs, and infectious virus in supernatants was titrated. A slowly decreasing titer with an initial set point (1 hpi) of 2×10^4 $TCID_{50}$s/ml was detected in the supernatant (Fig. 2C, panel ii). This indicates only inefficient replication of MERS-CoV in pDCs in our hands even after inoculation at a high MOI. Thus, IFN secretion by pDCs is not linked to virus amplification.

Inhibition of IFN production by pDCs upon MERS-CoV contact. Next, we aimed to study the recognition of MERS-CoV in human pDCs. Therefore, human pDCs were inoculated with UV-inactivated MERS-CoV particles (corresponding to an MOI of 1 before inactivation).

UV-inactivated MERS-CoV induced secretion of similar amounts of IFN-α (50 ng/ml) and IFN-λ (0.06 ng/ml) but significantly reduced amounts of IFN-β (0.08 ng/ml) compared to values with untreated MERS-CoV (Fig. 3A to C). These results indicate the requirement for replication-competent virus particles (even if no productive replication was evident in pDCs) to induce IFN-β secretion, whereas IFN-α and IFN-λ are induced by replication-defective virus particles as well, as evident by similar differences in induction between UV-inactivated and untreated MERS-CoV compared to mock controls.

To determine the route of MERS-CoV cell entry necessary for viral replication, we first analyzed the role of the virus receptor DPP4. Analysis of DPP4 surface expression by flow cytometry indicated surface expression of DPP4 on human pDCs (Fig. 4A). Indeed, preincubation of human pDCs with the receptor binding domain (RBD) of MERS-CoV (37) to block active MERS-CoV entry reduced secretion of IFNs by pDCs. Secretion of IFN-α was reduced 10-fold (3 ng/ml versus 30 ng/ml), that of IFN-β was reduced 26-fold (0.03 ng/ml versus 0.8 ng/ml), but that of IFN-λ was reduced only slightly (37 pg/ml versus 43 pg/ml) compared to levels in control-treated cells (Fig. 3D to F). For IFN-λ the impact of one outlier data point with high IFN-λ secretion within this experiment influenced the data. In an additional data set, RBD

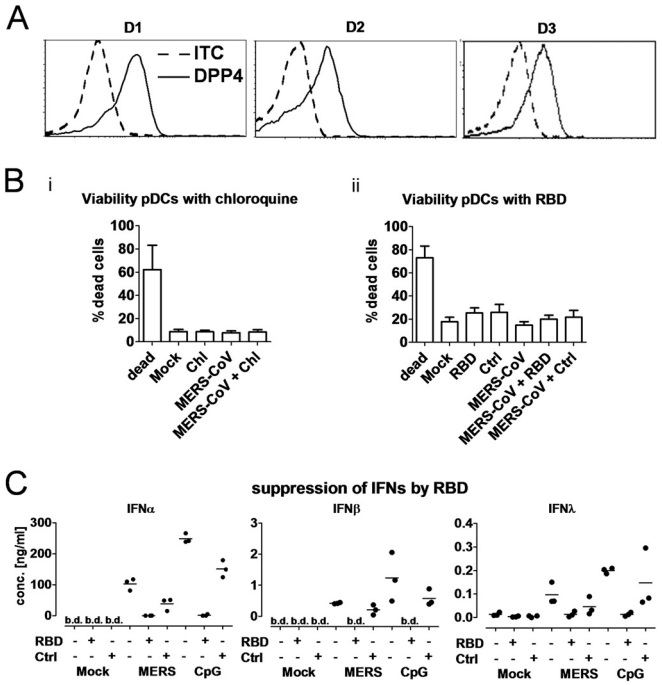

FIG 4 CD26 expression and functionality of human pDCs. (A) Expression of MERS-CoV receptor DPP4 on human pDCs. pDCs were stained with anti-DPP4 antibody and analyzed via flow cytometry. ITC, isotype control antibody. (B) Viability of pDCs of three different donors (D1 to D3) treated with inhibitors. pDCs were treated as indicated. At 24 hpi, cells were stained for viability and analyzed via flow cytometry. Dead, cells killed by osmotic shock. (C) Block of CpG 2216-induced IFN secretion by MERS-CoV RBD. Secretion of the indicated IFNs was determined in the presence or absence of the MERS-CoV S receptor binding domain (RBD) or IgG1-Fc control protein (Ctrl) upon MERS-CoV infection or the DPP4-independent stimulus CpG 2216. IFNs were sampled at 24 hpi. Single dots, individual donors; horizontal lines, means. b.d., below detection.

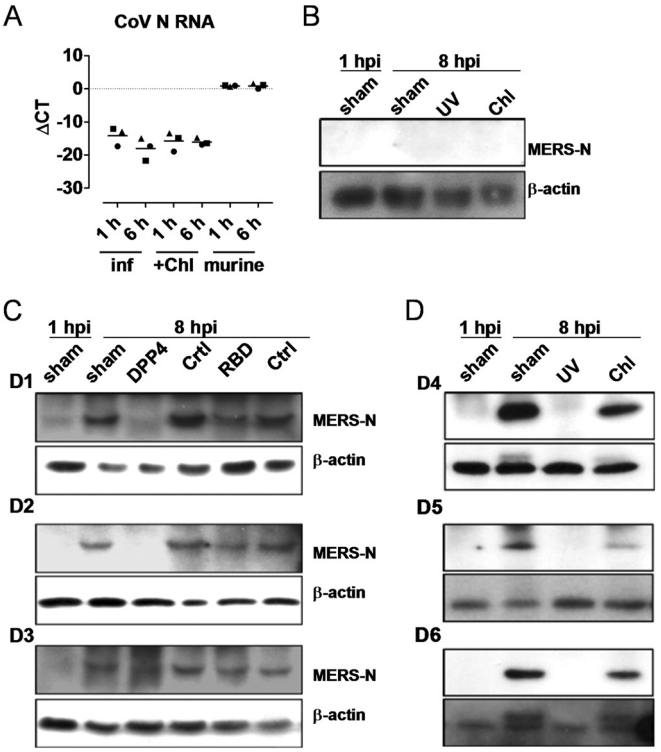

FIG 5 Infection of human pDCs by MERS-CoV. (A) Quantification of viral N RNA in human or murine pDCs by qRT-PCR in the presence or absence of chloroquine, normalized to cellular GAPDH mRNA [$\Delta C_T = C_{T(\text{MERS vRNA})} - C_{T(\text{GAPDH mRNA})}$] at indicated time points after inoculation. (B to D) Immunoblot analysis of N protein expression in murine pDCs (B) or human pDCs (C and D) after inoculation with MERS-CoV (MOI of 3). pDCs of three different donors (D1 to D3 and D4 to D6) were infected in the presence of blocking anti-DPP4 serum (DPP4), the receptor binding domain of MERS-CoV S protein (RBD), or respective controls (Ctrl) or with UV-inactivated (UV) or live MERS-CoV in the presence (Chl) or absence (sham) of chloroquine. Cells were lysed at the indicated time points and subjected to analyses.

blocked IFN-λ, again, for each of the three studied donors (Fig. 4C). However, also after stimulation by CpG2216 the secretion of all IFNs was strongly reduced in the presence of RBD protein (1.5 ng/ml versus 150 ng/ml IFN-α, <50 pg/ml versus 0.16 ng/ml IFN-β, 4 pg/ml versus 40 pg/ml IFN-λ), indicating general immune-suppressive properties of the RBD protein (Fig. 4C).

To evaluate if MERS-CoV particles are endocytosed and if MERS-CoV is recognized in the endosome, endosomal maturation and, thus, the endosomal route of entry and IFN induction (44) were inhibited by chloroquine. Of note, 24 h after cotreatment with chloroquine or RBD and MERS-CoV, viability of pDCs was not impaired (Fig. 4B). When pDCs were infected with MERS-CoV (MOI of 1) in the presence of chloroquine, the secretion of IFNs was reduced by factors of 11 for IFN-α (5 ng/ml versus 55 ng/ml), 35 for IFN-β (0.6 ng/ml versus 0.016 ng/ml), and 2.3 for IFN-λ (60 pg/ml versus 140 pg/ml) (Fig. 3G to I). These data indicate that the endosomal route is critical for sensing of MERS-CoV infection by human pDCs. Since viral RNA can be recognized as a PAMP in the endosomes of pDCs by TLR7, we inhibited TLR7 via the inhibitory ODN IRS661. IFN-α production was 1.5-fold decreased upon TLR7 inhibition (15 ng/ml versus 25 ng/ml) compared to infection in the presence of a noninhibiting control oligonucleotide. IFN-β production was 3-fold decreased (0.25 ng/ml versus 0.73 ng/ml), and IFN-λ production was 2-fold decreased upon TLR7 inhibition (36 pg/ml versus 77 pg/ml) (Fig. 3J to L). Thus, secretion of all IFNs analyzed was reduced upon inhibition of TLR7. These data indicate involvement of TLR7 in sensing MERS-CoV RNA and in IFN induction upon MERS-CoV infection of pDCs.

Transcription of MERS-CoV N RNA in infected pDCs. Even though no significant productive viral replication was observed, initial steps of viral infection and replication may take place in pDCs and could be responsible for triggering cytosolic pattern recognition receptors (PRRs). To analyze MERS-CoV infection of pDCs, onset of viral transcription was monitored by qRT-PCR of N protein RNA in infected pDCs. For this purpose, total RNA of human pDCs infected with MERS-CoV (MOI of 3) was isolated, and amounts of MERS-CoV N RNA was quantified at 1 hpi and 6 hpi and normalized to cellular housekeeping gene mRNA (GAPDH) (Fig. 5A). The relative amount of N RNA increased from 1 hpi to 6 hpi by 14-fold, indicating onset of viral gene transcription. In line with IFN-blocking experiments, only a minimal increase in relative N RNA levels was detected when human pDCs were pretreated with chloroquine (1.2-fold) or when murine pDCs were used as the substrate (no increase) (Fig. 5A).

Expression of MERS-CoV nucleocapsid protein in infected human pDCs. To back up mRNA expression data, the onset of viral protein translation was monitored by immunoblot analysis

of viral N protein expression in infected pDCs. For this purpose, human pDCs were infected with MERS-CoV (MOI of 3), and N protein expression was checked (Fig. 5C and D). As expected, no CoV N protein was detected in murine pDCs (Fig. 5B) and human pDCs at 1 hpi (Fig. 5C and D). However, at 8 hpi CoV N protein expression was clearly demonstrated in human pDCs, indicating the onset of viral gene expression in infected human pDCs. In contrast, using polyclonal anti-DPP4 antibody or the RBD, MERS-CoV N protein expression was decreased in comparison to that in the respective control, indicating infection of pDCs via DPP4 (Fig. 5C). Moreover, when human pDCs were inoculated with UV-inactivated MERS-CoV, no expression of N protein was detected, thus indicating that intact viral genomes are crucial for N protein expression (Fig. 5D). In addition, inhibition of endosomal maturation was accompanied by considerably less N protein expression in infected cells at 8 hpi (Fig. 5D). Therefore, expression of MERS-CoV N depends on receptor binding and endosomal maturation, arguing for the endosomal pathway as a primary route of MERS-CoV entry into human pDCs.

DISCUSSION

Our data reveal that primary human pDCs produce large amounts of type I and type III IFNs in response to MERS-CoV infection. Sensing depends on receptor availability, endosomal uptake, and, at least partially, functionality of TLR7. Moreover, we detected expression of MERS-CoV N mRNA and protein in the absence of progeny virus, suggesting unproductive infection of human pDCs. Similar to data obtained upon SARS-CoV infection, secretion of IFNs was exclusively found in pDCs (25), but the amounts of IFNs induced by MERS-CoV were significantly higher.

In parallel, stimulation with CpG 2216 also resulted in lower, but clearly detectable, amounts of IFNs. Thereby, integrity of pDCs can be assumed since the amounts of secreted IFNs were comparable to those in previously published data (25, 41) considering the fact that in the present study only one-third the amount of pDCs was used and that IFN-containing supernatants were harvested after 24 h.

When human B cells, macrophages, or MDDCs were inoculated with MERS-CoV, no type I or III IFNs were detected in the supernatant of infected cells. In line with these data, Zhou et al. (42) could not detect upregulation of type I IFN mRNA upon infection of human macrophages. Also in infected human MDDCs, only minor induction of IFN-α mRNA was detected, and no induction of IFN-β mRNA synthesis was detected (43).

In contrast, large amounts of IFN-α were detected when human pDCs were inoculated with MERS-CoV. IFN-α can be induced in pDCs after recognition of PAMPs in the endosome, e.g., via TLR7 (45). In our experiments, secretion of IFN-α was strongly inhibited by chloroquine treatment. Indeed, chloroquine is an inhibitor of endosomal maturation and can inhibit IFN production induced by viruses (e.g., HIV) via PRRs within the endosome (46). When the endosomal PRR of pDCs for viral RNA, TLR7, was inhibited, secretion of IFN-α also decreased. Taken together, these data argue for endosomal recognition of MERS-CoV and potentially recognition via TLR7 in mature endosomes of pDCs. The pattern of IFN-λ secretion by human pDCs after MERS-CoV inoculation followed that of IFN-α, as expected, since IFN-λ is induced by stimuli similar to those that induce IFN-α (47).

IFN-β was also secreted in significant amounts by human pDCs upon MERS-CoV inoculation. IFN-β can be induced after recognition of PAMPs by cytosolic PRRs such as MDA-5 or RIG-I (48). Indeed, we demonstrated the onset of viral gene expression in human pDCs. In line with this, UV inactivation of MERS-CoV, which damages the viral genome and thereby inhibits transcription and amplification of viral RNA, significantly reduced IFN-β secretion, but secretion of IFN-α or IFN-λ remained on similar levels. Thus, cytoplasmic recognition of viral replication intermediates seems to be responsible for IFN-β induction. However, MERS-CoV-induced IFN-β secretion was also blocked by chloroquine, an effect that cannot be explained if we postulate direct viral entry across the plasma membrane after contact of the viral spike glycoprotein S with its receptor CD26/DPP4, as assumed for MERS-CoV entry into lung epithelial cells (49). To use this entry pathway, MERS-CoV S has to be activated by cellular exopeptidases; mainly, transmembrane protease serine 2 (TMPRSS2) has been demonstrated to be responsible for cleavage during MERS-CoV entry into Calu-3 cells (49). In contrast, we demonstrate that endosomal maturation is crucial for MERS-CoV entry into pDCs. Interestingly, uptake of MERS-CoV via the endosomal route has already been described as an alternative pathway for entry into, e.g., Vero cells (49). Here, lysosomal proteases such as cathepsin L are required to activate the MERS-CoV S protein (50), but their activity depends on endosomal maturation (51). Hence, chloroquine-mediated inhibition of IFN-β secretion by pDCs after contact with MERS-CoV argues for receptor-mediated endocytosis of MERS-CoV particles and activation of MERS-CoV S protein by endosomal proteases, such as cathepsin L, finally resulting in cytosolic entry of MERS-CoV across the endosomal membrane. Indeed, expression of mRNA and MERS-CoV N protein was considerably decreased in the presence of chloroquine, indicating chloroquine-mediated inhibition of infection.

Furthermore, we blocked cell attachment of MERS-CoV to pDCs by blocking DPP4 with recombinant viral RBD. Block of receptor binding led to a significant reduction of IFN production following virus inoculation. However, CpG-stimulated IFN induction was blocked by recombinant RBD as well, indicating the immune suppressive properties of the MERS-CoV RBD in human pDCs. DPP4 is described as an activating receptor on T lymphocytes (52–54), but its function in DCs has thus far been linked only to T cell stimulation (55). Thus, the reasons for the eventually immune-suppressive properties of the RBD remain to be elucidated. Nevertheless, the remarkable inhibition of N protein expression by both RBD and anti-DPP4 serum indicates the necessity of DPP4 as an entry receptor for endocytotic uptake and subsequent infection on human pDCs. Receptor-dependent endocytosis as an uptake pathway for MERS-CoV may also explain the absence of IFN induction in murine pDCs after contact with the virus. In contrast to human DPP4, murine DPP4 is no suitable receptor for promoting infection with MERS-CoV (56). Thus, lack of binding of MERS-CoV to murine DPP4 should reduce endosomal uptake of virus particles, thereby reducing the amount of PAMPs which can be sensed by PRRs, resulting in strongly reduced IFN induction in murine pDCs.

To summarize the data, a model explaining the mechanism how of MERS-CoV induces type I IFN in human pDCs may be proposed (Fig. 6). MERS-CoV binds to its entry receptor DPP4 on the surface of pDCs, triggering receptor-mediated endocytosis of viral particles. In the mature endosome, MERS-CoV RNA is sensed by TLR7, inducing IFN-α secretion. Furthermore, MERS-

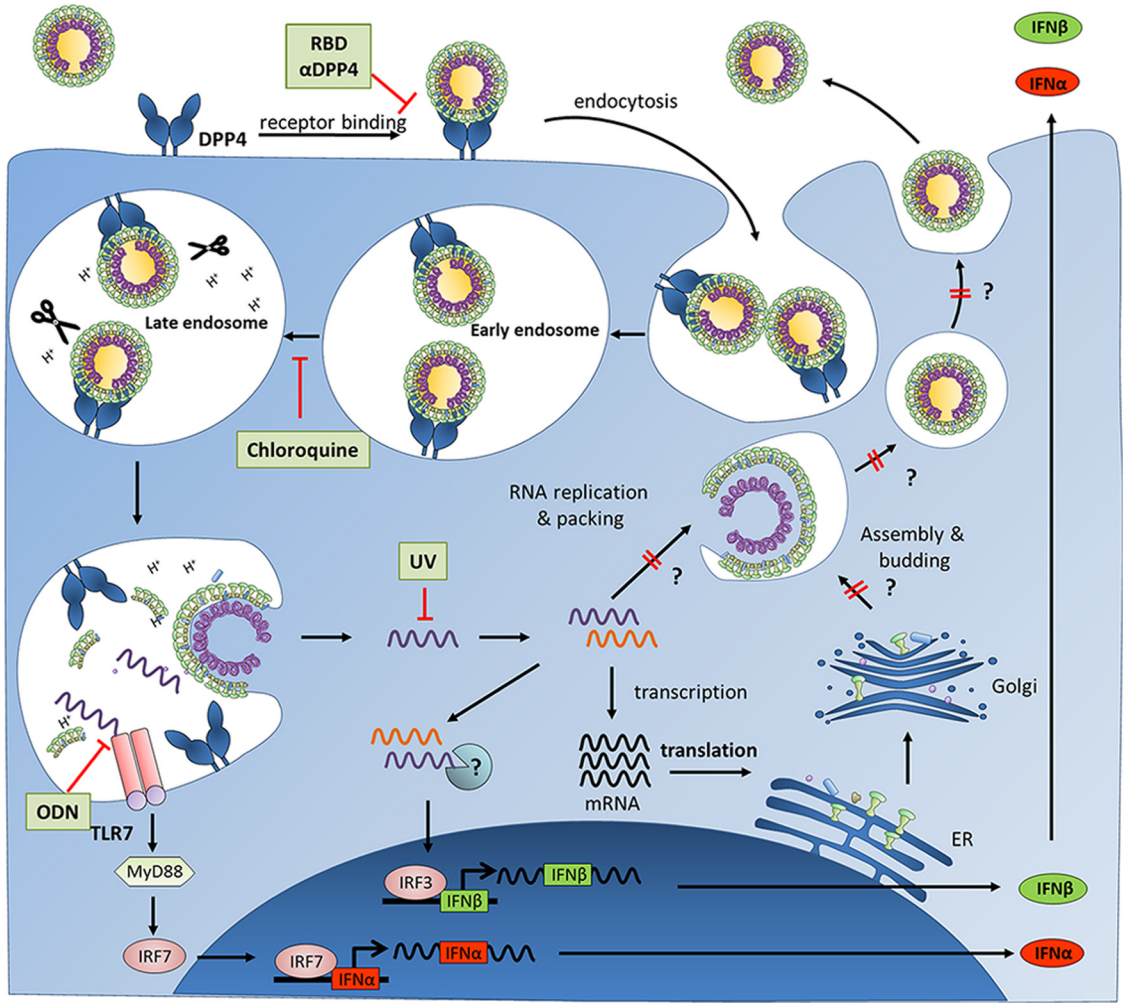

FIG 6 Model for MERS-CoV-induced type I IFN secretion in human pDCs. The figure schematically depicts the life cycle of MERS-CoV in human pDCs and events triggering secretion or infection of type I IFNs. Successful inhibition of IFN secretion at single steps is indicated. Inhibitors or proteins which have been analyzed are depicted in bold. Question marks point out steps during assembly or release of viral particles, the block of which could be responsible for absence of significant viral replication in pDCs. α, anti.

CoV spike proteins become cleaved by endosomal proteases during or after endosome maturation. This cleavage allows fusion of viral and endosomal membranes, causing release of the viral genome into the cytoplasm. In the cytoplasm, expression of viral proteins starts. We hypothesize that MERS-CoV RNA replication intermediates are recognized by cytosolic PRRs, resulting in full-blown induction of IFN-β. However, assembly or release of new progeny viral particles is impaired by yet unknown mechanisms in stages subsequent to viral gene expression. This absence of significant MERS-CoV replication in pDCs in contrast with the virus's replication in MDDCs (43) or macrophages (42) may be explained by the significant (biological and functional) differences between pDCs and other DC subsets (57). In line with this hypothesis, influenza A virus replication was also demonstrated in mDCs but shown to be blocked at postentry steps in pDCs (58).

Entry receptors are crucial for MERS-CoV recognition by pDCs, and lack of functional entry receptors in mice leads to lack of IFN production in murine cells. Meanwhile, it has been shown that murine DPP4 cannot be used as a MERS-CoV entry receptor; as demonstrated by expression of human DPP4 in mouse lungs via adenoviral vectors, this is sufficient to gain (partial) susceptibility to MERS-CoV infection (13).

Moreover, type I (59) and type III (17) IFNs inhibit MERS-CoV replication *in vitro*. A characteristic feature of type I IFNs is that effects are seen at small concentrations. In previous studies replication of MERS-CoV was inhibited by type I and III IFNs in different cell types *in vitro* already starting at a ng/ml concentration range (17, 59, 60). The IFN-α levels obtained in the experiments surpassed such amounts at least 40-fold; thus, the amounts of IFNs produced by pDCs upon MERS-CoV infection can be supposed to be relevant. The release of type I and III IFNs may protect against MERS-CoV-induced pathogenicity. It is therefore counterintuitive that MERS-CoV induces significantly higher secretion of IFNs than SARS-CoV when infecting pDCs, but clinically recorded MERS patients having a worse prognosis than SARS patients (5). However, secretion of extraordinarily large amounts of type I IFNs can result in aberrant immune activation. Zhou et al. already speculated that an induced cytokine storm could be the reason for the severity of illness on the basis of large amounts of proinflammatory cytokines and chemokines such as IL-12 or

IP-10 secreted by human macrophages upon MERS-CoV infection (42). In human SARS patients, aberrant IFN-stimulated gene expression and cytokine responses, compared to those of healthy individuals, were indeed observed (61). Patients that had such kinds of hyperimmune activation were more likely to succumb to the infection (62). Furthermore, the severity of SARS correlated with large amounts of inflammatory cytokines in serum (63), and symptoms of disease became usually worse after virus clearance (64). For these reasons, immune-mediated pathogenesis has been proposed for SARS-CoV infection (62). Whether such a pathomechanism also applies to MERS and whether pDCs are really the major source of IFNs in such a setting remain to be demonstrated in further studies. However, the up to 8-fold-enhanced IFN type I secretion upon MERS-CoV infection compared to SARS-CoV infection might then hint at overshooting immune reactions being potentially one factor for the higher mortality rate observed in MERS patients.

ACKNOWLEDGMENTS

We thank Heike Schmitz, Steffen Prüfer, Stefanie Bauer, and Christiane Tondera for excellent technical assistance and Kay-Martin Hanschmann for statistical analysis. The authors are indebted to Ron Fouchier for providing MERS-CoV strain EMC/2012, to Christian Drosten and Doreen Muth for SARS-CoV strain Frankfurt-1 and PCR protocols, and to Berend Jan Bosch for the MERS-CoV RBD and control IgG1 Fc protein.

REFERENCES

1. **Bermingham A, Chand MA, Brown CS, Aarons E, Tong C, Langrish C, Hoschler K, Brown K, Galiano M, Myers R, Pebody RG, Green HK, Boddington NL, Gopal R, Price N, Newsholme W, Drosten C, Fouchier RA, Zambon M.** 2012. Severe respiratory illness caused by a novel coronavirus, in a patient transferred to the United Kingdom from the Middle East, September 2012. Euro Surveill **17:**20290. http://www.eurosurveillance.org/ViewArticle.aspx?ArticleId=20290.
2. **de Groot RJ, Baker SC, Baric RS, Brown CS, Drosten C, Enjuanes L, Fouchier RA, Galiano M, Gorbalenya AE, Memish ZA, Perlman S, Poon LL, Snijder EJ, Stephens GM, Woo PC, Zaki AM, Zambon M, Ziebuhr J.** 2013. Middle East respiratory syndrome coronavirus (MERS-CoV): announcement of the Coronavirus Study Group. J Virol **87:**7790–7792. http://dx.doi.org/10.1128/JVI.01244-13.
3. **van Boheemen S, de Graaf M, Lauber C, Bestebroer TM, Raj VS, Zaki AM, Osterhaus AD, Haagmans BL, Gorbalenya AE, Snijder EJ, Fouchier RA.** 2012. Genomic characterization of a newly discovered coronavirus associated with acute respiratory distress syndrome in humans. mBio **3**(6):e00473–12. http://dx.doi.org/10.1128/mBio.00473-12.
4. **Al-Tawfiq JA, Memish ZA.** 2014. Middle East respiratory syndrome coronavirus: epidemiology and disease control measures. Infect Drug Resist **7:**281–287. http://dx.doi.org/10.2147/IDR.S51283.
5. **Peiris JS, Guan Y, Yuen KY.** 2004. Severe acute respiratory syndrome. Nat Med **10:**S88–97. http://dx.doi.org/10.1038/nm1143.
6. **Breban R, Riou J, Fontanet A.** 2013. Interhuman transmissibility of Middle East respiratory syndrome coronavirus: estimation of pandemic risk. Lancet **382:**694–699. http://dx.doi.org/10.1016/S0140-6736(13)61492-0.
7. **Drosten C, Meyer B, Müller MA, Corman VM, Al-Masri M, Hossain R, Madani H, Sieberg A, Bosch BJ, Lattwein E, Alhakeem RF, Assiri AM, Hajomar W, Albarrak AM, Al-Tawfiq JA, Zumla AI, Memish ZA.** 2014. Transmission of MERS-coronavirus in household contacts. N Engl J Med **371:**828–835. http://dx.doi.org/10.1056/NEJMoa1405858.
8. **Haagmans BL, Dhahiry Al, Said HS, Reusken, Chantal BE, Raj VS, Galiano M, Myers R, Godeke G, Jonges M, Farag E, Diab A, Ghobashy H, Alhajri F, Al-Thani M, Al-Marri SA, Al Romaihi, Hamad E, Al Khal A, Bermingham A, Osterhaus, Albert DME, Alhajri MM, Koopmans, Marion PG.** 2014. Middle East respiratory syndrome coronavirus in dromedary camels: an outbreak investigation. Lancet Infect Dis **14:**140–145. http://dx.doi.org/10.1016/S1473-3099(13)70690-X.
9. **Azhar EI, El-Kafrawy SA, Farraj SA, Hassan AM, Al-Saeed MS, Hashem AM, Madani TA.** 2014. Evidence for camel-to-human transmission of MERS coronavirus. N Engl J Med **370:**2499–2505. http://dx.doi.org/10.1056/NEJMoa1401505.
10. **Madani TA, Azhar EI, Hashem AM.** 2014. Evidence for camel-to-human transmission of MERS coronavirus. N Engl J Med **371:**1360. http://dx.doi.org/10.1056/NEJMc1409847.
11. **Corman VM, Ithete NL, Richards LR, Schoeman MC, Preiser W, Drosten C, Drexler JF.** 2014. Rooting the phylogenetic tree of Middle East respiratory syndrome coronavirus by characterization of a conspecific virus from an African bat. J Virol **88:**11297–11303. http://dx.doi.org/10.1128/JVI.01498-14.
12. **Raj VS, Mou H, Smits SL, Dekkers DH, Müller MA, Dijkman R, Muth D, Demmers JA, Zaki A, Fouchier RA, Thiel V, Drosten C, Rottier PJ, Osterhaus AD, Bosch BJ, Haagmans BL.** 2013. Dipeptidyl peptidase 4 is a functional receptor for the emerging human coronavirus-EMC. Nature **495:**251–254. http://dx.doi.org/10.1038/nature12005.
13. **Zhao J, Li K, Wohlford-Lenane C, Agnihothram SS, Fett C, Zhao J, Gale MJ, Baric RS, Enjuanes L, Gallagher T, McCray PB, Perlman S.** 2014. Rapid generation of a mouse model for Middle East respiratory syndrome. Proc Natl Acad Sci U S A **111:**4970–4975. http://dx.doi.org/10.1073/pnas.1323279111.
14. **Zaki AM, van Boheemen S, Bestebroer TM, Osterhaus AD, Fouchier RAM.** 2012. Isolation of a novel coronavirus from a man with pneumonia in Saudi Arabia. N Engl J Med **367:**1814–1820. http://dx.doi.org/10.1056/NEJMoa1211721.
15. **Drosten C, Seilmaier M, Corman VM, Hartmann W, Scheible G, Sack S, Guggemos W, Kallies R, Muth D, Junglen S, Müller MA, Haas W, Guberina H, Röhnisch T, Schmid-Wendtner M, Aldabbagh S, Dittmer U, Gold H, Graf P, Bonin F, Rambaut A, Wendtner C.** 2013. Clinical features and virological analysis of a case of Middle East respiratory syndrome coronavirus infection. Lancet Infect Dis **13:**745–751. http://dx.doi.org/10.1016/S1473-3099(13)70154-3.
16. **Schütz F, Hackstein H.** 2014. Identification of novel dendritic cell subset markers in human blood. Biochem Biophys Res Commun **443:**453–457. http://dx.doi.org/10.1016/j.bbrc.2013.11.112.
17. **Kindler E, Jónsdóttir HR, Muth D, Hamming OJ, Hartmann R, Rodriguez R, Geffers R, Fouchier RAM, Drosten C, Müller MA, Dijkman R, Thiel V.** 2013. Efficient replication of the novel human betacoronavirus EMC on primary human epithelium highlights its zoonotic potential. mBio **4**(1):e00611–12. http://dx.doi.org/10.1128/mBio.00611-12.
18. **Zielecki F, Weber M, Eickmann M, Spiegelberg L, Zaki AM, Matrosovich M, Becker S, Weber F.** 2013. Human cell tropism and innate immune system interactions of human respiratory coronavirus EMC compared to those of severe acute respiratory syndrome coronavirus. J Virol **87:**5300–5304. http://dx.doi.org/10.1128/JVI.03496-12.
19. **Falzarano D, de Wit E, Rasmussen AL, Feldmann F, Okumura A, Scott DP, Brining D, Bushmaker T, Martellaro C, Baseler L, Benecke AG, Katze MG, Munster VJ, Feldmann H.** 2013. Treatment with interferon-α2b and ribavirin improves outcome in MERS-CoV-infected rhesus macaques. Nat Med **19:**1313–1317. http://dx.doi.org/10.1038/nm.3362.
20. **Al-Tawfiq JA, Momattin H, Dib J, Memish ZA.** 2014. Ribavirin and interferon therapy in patients infected with the Middle East respiratory syndrome coronavirus: an observational study. Int J Infect Dis **20:**42–46. http://dx.doi.org/10.1016/j.ijid.2013.12.003.
21. **Khalid M, Al Rabiah F, Khan B, Al Mobeireek A, Butt TS, Al Mutairy E.** 15 May 2014. Ribavirin and interferon (IFN)-alpha-2b as primary and preventive treatment for Middle East respiratory syndrome coronavirus (MERS-CoV): a preliminary report of two cases. Antivir Ther http://dx.doi.org/10.3851/IMP2792.
22. **Chan RW, Chan MC, Agnihothram S, Chan LL, Kuok DI, Fong JH, Guan Y, Poon LL, Baric RS, Nicholls JM, Peiris JS.** 2013. Tropism of and innate immune responses to the novel human betacoronavirus lineage C virus in human ex vivo respiratory organ cultures. J Virol **87:**6604–6614. http://dx.doi.org/10.1128/JVI.00009-13.
23. **Siegal FP, Kadowaki N, Shodell M, Fitzgerald-Bocarsly PA, Shah K, Ho S, Antonenko S, Liu YJ.** 1999. The nature of the principal type 1 interferon-producing cells in human blood. Science **284:**1835–1837. http://dx.doi.org/10.1126/science.284.5421.1835.
24. **Beignon A, McKenna K, Skoberne M, Manches O, DaSilva I, Kavanagh DG, Larsson M, Gorelick RJ, Lifson JD, Bhardwaj N.** 2005. Endocytosis of HIV-1 activates plasmacytoid dendritic cells via Toll-like receptor-viral RNA interactions. J Clin Invest **115:**3265–3275. http://dx.doi.org/10.1172/JCI26032.
25. **Cervantes-Barragan L, Züst R, Weber F, Spiegel M, Lang KS, Akira S,**

Thiel V, Ludewig B. 2007. Control of coronavirus infection through plasmacytoid dendritic-cell-derived type I interferon. Blood **109:**1131–1137. http://dx.doi.org/10.1182/blood-2006-05-023770.

26. **Haller O, Kochs G, Weber F.** 2006. The interferon response circuit: induction and suppression by pathogenic viruses. Virology **344:**119–130. http://dx.doi.org/10.1016/j.virol.2005.09.024.
27. **Drosten C, Günther S, Preiser W, van der Werf S, Brodt HR, Becker S, Rabenau H, Panning M, Kolesnikova L, Fouchier RA, Berger A, Burguière AM, Cinatl J, Eickmann M, Escriou N, Grywna K, Kramme S, Manuguerra JC, Müller S, Rickerts V, Stürmer M, Vieth S, Klenk HD, Osterhaus AD, Schmitz H, Doerr HW.** 2003. Identification of a novel coronavirus in patients with severe acute respiratory syndrome. N Engl J Med **348:**1967–1976. http://dx.doi.org/10.1056/NEJMoa030747.
28. **Kärber G.** 1931. Beitrag zur kollektiven Behandlung pharmakologischer Reihenversuche. Arch Exp Pathol Pharmakol **162:**480–483. http://dx.doi.org/10.1007/BF01863914.
29. **Kochs G, Bauer S, Vogt C, Frenz T, Tschopp J, Kalinke U, Waibler Z.** 2010. Thogoto virus infection induces sustained type I interferon responses that depend on RIG-I-like helicase signaling of conventional dendritic cells. J Virol **84:**12344–12350. http://dx.doi.org/10.1128/JVI.00931-10.
30. **Waibler Z, Detje CN, Bell JC, Kalinke U.** 2007. Matrix protein mediated shutdown of host cell metabolism limits vesicular stomatitis virus-induced interferon-alpha responses to plasmacytoid dendritic cells. Immunobiology **212:**887–894. http://dx.doi.org/10.1016/j.imbio.2007.09.003.
31. **Stojdl DF, Lichty BD, ten Oever BR, Paterson JM, Power AT, Knowles S, Marius R, Reynard J, Poliquin L, Atkins H, Brown EG, Durbin RK, Durbin JE, Hiscott J, Bell JC.** 2003. VSV strains with defects in their ability to shutdown innate immunity are potent systemic anti-cancer agents. Cancer Cell **4:**263–275. http://dx.doi.org/10.1016/S1535-6108(03)00241-1.
32. **Weissmüller S, Semmler LY, Kalinke U, Christians S, Müller-Berghaus J, Waibler Z.** 2012. ICOS-LICOS interaction is critically involved in TGN1412-mediated T-cell activation. Blood **119:**6268–6277. http://dx.doi.org/10.1182/blood-2011-12-401083.
33. **Sender LY, Gibbert K, Suezer Y, Radeke HH, Kalinke U, Waibler Z.** 2010. CD40 ligand-triggered human dendritic cells mount interleukin-23 responses that are further enhanced by danger signals. Mol Immunol **47:**1255–1261. http://dx.doi.org/10.1016/j.molimm.2009.12.008.
34. **Neu C, Sedlag A, Bayer C, Förster S, Crauwels P, Niess J, van Zandbergen G, Frascaroli G, Riedel CU.** 2013. CD14-dependent monocyte isolation enhances phagocytosis of *Listeria monocytogenes* by proinflammatory, GM-CSF-derived macrophages. PLoS One **8:**e66898. http://dx.doi.org/10.1371/journal.pone.0066898.
35. **Waibler Z, Anzaghe M, Ludwig H, Akira S, Weiss S, Sutter G, Kalinke U.** 2007. Modified vaccinia virus Ankara induces Toll-like receptor-independent type I interferon responses. J Virol **81:**12102–12110. http://dx.doi.org/10.1128/JVI.01190-07.
36. **Kerkmann M, Rothenfusser S, Hornung V, Towarowski A, Wagner M, Sarris A, Giese T, Endres S, Hartmann G.** 2003. Activation with CpG-A and CpG-B oligonucleotides reveals two distinct regulatory pathways of type I IFN synthesis in human plasmacytoid dendritic cells. J Immunol **170:**4465–4474. http://dx.doi.org/10.4049/jimmunol.170.9.4465.
37. **Mou H, Raj VS, van Kuppeveld FJ, Rottier PJ, Haagmans BL, Bosch BJ.** 2013. The receptor binding domain of the new Middle East respiratory syndrome coronavirus maps to a 231-residue region in the spike protein that efficiently elicits neutralizing antibodies. J Virol **87:**9379–9383. http://dx.doi.org/10.1128/JVI.01277-13.
38. **Lu X, Whitaker B, Sakthivel SK, Kamili S, Rose LE, Lowe L, Mohareb E, Elassal EM, Al-sanouri T, Haddadin A, Erdman DD.** 2014. Real-time reverse transcription-PCR assay panel for Middle East respiratory syndrome coronavirus. J Clin Microbiol **52:**67–75. http://dx.doi.org/10.1128/JCM.02533-13.
39. **Funke S, Maisner A, Mühlebach MD, Koehl U, Grez M, Cattaneo R, Cichutek K, Buchholz CJ.** 2008. Targeted cell entry of lentiviral vectors. Mol Ther **16:**1427–1436. http://dx.doi.org/10.1038/mt.2008.128.
40. **Hartmann G, Krieg AM.** 2000. Mechanism and function of a newly identified CpG DNA motif in human primary B cells. J Immunol **164:**944–953. http://dx.doi.org/10.4049/jimmunol.164.2.944.
41. **Krug A, Rothenfusser S, Hornung V, Jahrsdörfer B, Blackwell S, Ballas ZK, Endres S, Krieg AM, Hartmann G.** 2001. Identification of CpG oligonucleotide sequences with high induction of IFN-alpha/beta in plasmacytoid dendritic cells. Eur J Immunol **31:**2154–2163. http://dx.doi.org/10.1002/1521-4141(200107)31:7<2154::AID-IMMU2154>3.0.CO;2-U.
42. **Zhou J, Chu H, Li C, Wong BH, Cheng Z, Poon VK, Sun T, Lau CC, Wong KK, Chan JY, Chan JF, To KK, Chan K, Zheng B, Yuen K.** 2014. Active replication of Middle East respiratory syndrome coronavirus replication and aberrant induction of inflammatory cytokines and chemokines in human macrophages: implications for pathogenesis. J Infect Dis **209:**1331–1342. http://dx.doi.org/10.1093/infdis/jit504.
43. **Chu H, Zhou J, Wong BH, Li C, Cheng Z, Lin X, Poon VK, Sun T, Lau CC, Chan JF, To KK, Chan K, Lu L, Zheng B, Yuen K.** 2014. Productive replication of Middle East respiratory syndrome coronavirus in monocyte-derived dendritic cells modulates innate immune response. Virology **454-455:**197–205. http://dx.doi.org/10.1016/j.virol.2014.02.018.
44. **Lee J, Chuang T, Redecke V, She L, Pitha PM, Carson DA, Raz E, Cottam HB.** 2003. Molecular basis for the immunostimulatory activity of guanine nucleoside analogs: activation of Toll-like receptor 7. Proc Natl Acad Sci U S A **100:**6646–6651. http://dx.doi.org/10.1073/pnas.0631696100.
45. **Birmachu W, Gleason RM, Bulbulian BJ, Riter CL, Vasilakos JP, Lipson KE, Nikolsky Y.** 2007. Transcriptional networks in plasmacytoid dendritic cells stimulated with synthetic TLR 7 agonists. BMC Immunol **8:**26. http://dx.doi.org/10.1186/1471-2172-8-26.
46. **Martinson JA, Montoya CJ, Usuga X, Ronquillo R, Landay AL, Desai SN.** 2010. Chloroquine modulates HIV-1-induced plasmacytoid dendritic cell alpha interferon: implication for T-cell activation. Antimicrob Agents Chemother **54:**871–881. http://dx.doi.org/10.1128/AAC.01246-09.
47. **Coccia EM, Severa M, Giacomini E, Monneron D, Remoli ME, Julkunen I, Cella M, Lande R, Uzé G.** 2004. Viral infection and Toll-like receptor agonists induce a differential expression of type I and lambda interferons in human plasmacytoid and monocyte-derived dendritic cells. Eur J Immunol **34:**796–805. http://dx.doi.org/10.1002/eji.200324610.
48. **Li J, Liu Y, Zhang X.** 2010. Murine coronavirus induces type I interferon in oligodendrocytes through recognition by RIG-I and MDA5. J Virol **84:**6472–6482. http://dx.doi.org/10.1128/JVI.00016-10.
49. **Shirato K, Kawase M, Matsuyama S.** 2013. Middle East respiratory syndrome coronavirus infection mediated by the transmembrane serine protease TMPRSS2. J Virol **87:**12552–12561. http://dx.doi.org/10.1128/JVI.01890-13.
50. **Gierer S, Bertram S, Kaup F, Wrensch F, Heurich A, Krämer-Kühl A, Welsch K, Winkler M, Meyer B, Drosten C, Dittmer U, von Hahn T, Simmons G, Hofmann H, Pöhlmann S.** 2013. The spike protein of the emerging betacoronavirus EMC uses a novel coronavirus receptor for entry, can be activated by TMPRSS2, and is targeted by neutralizing antibodies. J Virol **87:**5502–5511. http://dx.doi.org/10.1128/JVI.00128-13.
51. **Guha S, Padh H.** 2008. Cathepsins: fundamental effectors of endolysosomal proteolysis. Indian J Biochem Biophys **45:**75–90.
52. **Dong RP, Kameoka J, Hegen M, Tanaka T, Xu Y, Schlossman SF, Morimoto C.** 1996. Characterization of adenosine deaminase binding to human CD26 on T cells and its biologic role in immune response. J Immunol **156:**1349–1355.
53. **Ohnuma K, Dang NH, Morimoto C.** 2008. Revisiting an old acquaintance: CD26 and its molecular mechanisms in T cell function. Trends in immunology **29:**295–301. http://dx.doi.org/10.1016/j.it.2008.02.010.
54. **Dang NH, Torimoto Y, Deusch K, Schlossman SF, Morimoto C.** 1990. Comitogenic effect of solid-phase immobilized anti-1F7 on human CD4 T cell activation via CD3 and CD2 pathways. J Immunol **144:**4092–4100.
55. **Zhong J, Rao X, Deiuliis J, Braunstein Z, Narula V, Hazey J, Mikami D, Needleman B, Satoskar AR, Rajagopalan S.** 2013. A potential role for dendritic cell/macrophage-expressing DPP4 in obesity-induced visceral inflammation. Diabetes **62:**149–157. http://dx.doi.org/10.2337/db12-0230.
56. **Cockrell AS, Peck KM, Yount BL, Agnihothram SS, Scobey T, Curnes NR, Baric RS, Heise MT.** 2014. Mouse dipeptidyl peptidase 4 is not a functional receptor for Middle East respiratory syndrome coronavirus infection. J Virol **88:**5195–5199. http://dx.doi.org/10.1128/JVI.03764-13.
57. **Dalod M, Chelbi R, Malissen B, Lawrence T.** 2014. Dendritic cell maturation: functional specialization through signaling specificity and transcriptional programming. EMBO J **33:**1104–1116. http://dx.doi.org/10.1002/embj.201488027.
58. **Smed-Sörensen A, Chalouni C, Chatterjee B, Cohn L, Blattmann P, Nakamura N, Delamarre L, Mellman I.** 2012. Influenza A virus infection of human primary dendritic cells impairs their ability to cross-present antigen to CD8 T cells. PLoS Pathog **8:**e1002572. http://dx.doi.org/10.1371/journal.ppat.1002572.

59. **Falzarano D, de Wit E, Martellaro C, Callison J, Munster VJ, Feldmann H.** 2013. Inhibition of novel β coronavirus replication by a combination of interferon-α2b and ribavirin. Sci Rep **3:**1686. http://dx.doi.org/10.1038/srep01686.
60. **Hart BJ, Dyall J, Postnikova E, Zhou H, Kindrachuk J, Johnson RF, Olinger GG, Frieman MB, Holbrook MR, Jahrling PB, Hensley L.** 2014. Interferon-β and mycophenolic acid are potent inhibitors of Middle East respiratory syndrome coronavirus in cell-based assays. J Gen Virol **95:**571–577. http://dx.doi.org/10.1099/vir.0.061911-0.
61. **Huang K, Su I, Theron M, Wu Y, Lai S, Liu C, Lei H.** 2005. An interferon-gamma-related cytokine storm in SARS patients. J Med Virol **75:**185–194. http://dx.doi.org/10.1002/jmv.20255.
62. **Cameron MJ, Ran L, Xu L, Danesh A, Bermejo-Martin JF, Cameron CM, Muller MP, Gold WL, Richardson SE, Poutanen SM, Willey BM, DeVries ME, Fang Y, Seneviratne C, Bosinger SE, Persad D, Wilkinson P, Greller LD, Somogyi R, Humar A, Keshavjee S, Louie M, Loeb MB, Brunton J, McGeer AJ, Kelvin DJ.** 2007. Interferon-mediated immunopathological events are associated with atypical innate and adaptive immune responses in patients with severe acute respiratory syndrome. J Virol **81:**8692–8706. http://dx.doi.org/10.1128/JVI.00527-07.
63. **Wong CK, Lam CW, Wu AK, Ip WK, Lee NL, Chan IH, Lit LC, Hui DS, Chan MH, Chung SS, Sung JJ.** 2004. Plasma inflammatory cytokines and chemokines in severe acute respiratory syndrome. Clin Exp Immunol **136:**95–103. http://dx.doi.org/10.1111/j.1365-2249.2004.02415.x.
64. **Perlman S, Dandekar AA.** 2005. Immunopathogenesis of coronavirus infections: implications for SARS. Nat Rev Immunol **5:**917–927. http://dx.doi.org/10.1038/nri1732.

JVI Journals.ASM.org

Lentiviral Protein Transfer Vectors Are an Efficient Vaccine Platform and Induce a Strong Antigen-Specific Cytotoxic T Cell Response

Katharina M. Uhlig,[a] Stefan Schülke,[b] Vivian A. M. Scheuplein,[a] Anna H. Malczyk,[a] Johannes Reusch,[a] Stefanie Kugelmann,[a] Anke Muth,[c] Vivian Koch,[a] Stefan Hutzler,[a] Bianca S. Bodmer,[a] Axel Schambach,[d] Christian J. Buchholz,[c,e] Zoe Waibler,[f] Stephan Scheurer,[b] Michael D. Mühlebach[a]

Oncolytic Measles Viruses and Vaccine Vectors,[a] Molecular Allergology,[b] Molecular Biotechnology and Gene Therapy,[c] and Novel Vaccination Strategies and Early Immune Responses,[f] Paul-Ehrlich-Institut, Langen, Germany; Institute of Experimental Hematology, Hannover Medical School, Hannover, Germany[d]; German Cancer Consortium, Heidelberg, Germany[e]

ABSTRACT

To induce and trigger innate and adaptive immune responses, antigen-presenting cells (APCs) take up and process antigens. Retroviral particles are capable of transferring not only genetic information but also foreign cargo proteins when they are genetically fused to viral structural proteins. Here, we demonstrate the capacity of lentiviral protein transfer vectors (PTVs) for targeted antigen transfer directly into APCs and thereby induction of cytotoxic T cell responses. Targeting of lentiviral PTVs to APCs can be achieved analogously to gene transfer vectors by pseudotyping the particles with truncated wild-type measles virus (MV) glycoproteins (GPs), which use human SLAM (signaling lymphocyte activation molecule) as a main entry receptor. SLAM is expressed on stimulated lymphocytes and APCs, including dendritic cells. SLAM-targeted PTVs transferred the reporter protein green fluorescent protein (GFP) or Cre recombinase with strict receptor specificity into SLAM-expressing CHO and B cell lines, in contrast to broadly transducing vesicular stomatitis virus G protein (VSV-G) pseudotyped PTVs. Primary myeloid dendritic cells (mDCs) incubated with targeted or nontargeted ovalbumin (Ova)-transferring PTVs stimulated Ova-specific T lymphocytes, especially $CD8^+$ T cells. Administration of Ova-PTVs into SLAM-transgenic and control mice confirmed the observed predominant induction of antigen-specific $CD8^+$ T cells and demonstrated the capacity of protein transfer vectors as suitable vaccines for the induction of antigen-specific immune responses.

IMPORTANCE

This study demonstrates the specificity and efficacy of antigen transfer by SLAM-targeted and nontargeted lentiviral protein transfer vectors into antigen-presenting cells to trigger antigen-specific immune responses *in vitro* and *in vivo*. The observed predominant activation of antigen-specific $CD8^+$ T cells indicates the suitability of SLAM-targeted and also nontargeted PTVs as a vaccine for the induction of cytotoxic immune responses. Since cytotoxic $CD8^+$ T lymphocytes are a mainstay of antitumoral immune responses, PTVs could be engineered for the transfer of specific tumor antigens provoking tailored antitumoral immunity. Therefore, PTVs can be used as safe and efficient alternatives to gene transfer vectors or live attenuated replicating vector platforms, avoiding genotoxicity or general toxicity in highly immunocompromised patients, respectively. Thereby, the potential for easy envelope exchange allows the circumventing of neutralizing antibodies, e.g., during repeated boost immunizations.

Vaccination is the administration of one or more immunogens, the vaccine, into patients to trigger antigen-specific adaptive immune responses to prevent (prophylactic vaccination) or to treat (therapeutic vaccination) disease. Vaccines can be classified into several subtypes. Among these are live attenuated replicating vaccines, inactivated vaccines, subunit vaccines, DNA vaccines, or recombinant vector vaccines (for review, see reference 1). Well-known live attenuated vaccines are, e.g., those against measles (2) or mumps (3). These vaccines replicate but have been attenuated to become apathogenic. The immune responses triggered by live attenuated vaccines are similar to those induced by the pathogenic form of the microbe (4, 5) and involve both the cellular and humoral arms of the immune system. However, attenuated replicating pathogens may carry an inherent risk of reversion to the parental virulent form by *in vivo* passaging during vaccination, as observed for the Sabin strain used as a polio vaccine (6), or may still be pathogenic in highly immunocompromised patients (7), depending on the respective degree of attenuation of the vaccine strains. On the other hand, inoculation of solely proteinaceous antigens (such as the hepatitis B virus vaccine [8]) or antigen-encoding genes (as a DNA vaccine) is regarded as safe but relatively inefficient (9).

As an alternative to such vaccines, the genes encoding an antigen can be transferred into cells and thereby presented to the immune system by using recombinant vaccine vectors. For that purpose, an attenuated vector is utilized as a carrier for the antigen-encoding sequences of another pathogen. Thereby, they are

Received 30 March 2015 **Accepted** 14 June 2015

Accepted manuscript posted online 17 June 2015

Citation Uhlig KM, Schülke S, Scheuplein VAM, Malczyk AH, Reusch J, Kugelmann S, Muth A, Koch V, Hutzler S, Bodmer BS, Schambach A, Buchholz CJ, Waibler Z, Scheurer S, Mühlebach MD. 2015. Lentiviral protein transfer vectors are an efficient vaccine platform and induce a strong antigen-specific cytotoxic t cell response. J Virol 89:9044–9060. doi:10.1128/JVI.00844-15.

Editor: F. Kirchhoff

Address correspondence to Michael D. Mühlebach, Michael.Muehlebach@pei.de.

doi:10.1128/JVI.00844-15

sound triggers of immune responses due to stimulation of innate immunity by the pathogen-associated molecular patterns (PAMPs) of the vector backbone's structure. This vaccine subtype is relatively easy to generate and to manipulate; heterologous proteins can be encoded, and the vector vaccine's safety is comparable to the safety of the chosen vector backbone. Among other vector backbones tested for such applications are human immunodeficiency virus type 1 (HIV-1)-derived lentiviral vectors (LVs). These vectors do not replicate but support only a single round of infection of a target cell. Their potential to reconstitute the pathogenic parental virus is excluded by the split-vector-genome approach separating essential components of the virus on at least three different plasmids. Receptor specificity depends on the glycoproteins (GPs) used for pseudotyping the vector particles. A variety of cell types can be transduced by LVs, even nondividing cells (10, 11), but especially myeloid cells reveal a considerable degree of resistance to HIV-1-derived gene transfer due to a postentry block of replication steps (12). Among these are dendritic cells (DCs) (13), one of the most potent types of antigen-presenting cells (APCs) (14). As such, the main function of DCs is to activate naive, antigen-specific T cells upon uptake, processing, and presentation of antigens in the context of costimulatory molecules. Besides inducing T cell immune responses, humoral immunity is closely linked to activation and antigen processing by APCs, especially DCs, either by direct B cell-DC interactions (15) or indirectly via activation of $CD4^+$ T helper cells.

Due to the important function of DCs, considerable effort has been made to target the transfer of antigen-encoding sequences to DCs. Several surface molecules on DCs have been used for targeting approaches, e.g., the C-type lectin DC-SIGN interacting with the Sindbis virus envelope protein used to pseudotype LVs (16). Also the glycoproteins of the measles virus (MV) strain Edmonston with its natural tropism for the receptors CD46, nectin-4, and SLAM (signaling lymphocyte activation molecule), the last expressed on activated immune cells such as DCs (17), have been shown to be highly suited for targeting of DCs (18). Moreover, engineered MV-GPs displaying a single-chain antibody fragment directed against major histocompatibility complex class II (MHC-II) have been successfully used for targeting of APCs (19). The transduced DCs then express the transferred antigen-encoding genes, process the antigens, present the antigen-derived peptides on MHC-I and MHC-II, and consequently activate antigen-specific $CD4^+$ and $CD8^+$ T cells (20). Consequently, antibody production is induced. Usually, the genetic information for the antigen transferred by LVs is stably integrated into the host cells' genome, potentially causing issues with genomic integrity of the transduced cells. Alternatively, nonintegrating LVs have been tested in which a defective integrase prevents genomic integration of the transferred vector genomes (21). However, a relatively large amount of vectors or complementation with HIV-2 Vpx has to be used to overcome the postentry block to gene transfer preventing antigen expression *in situ*.

Nevertheless, lenti- and other retroviral vectors transfer not only their genomes during transduction but also their structural proteins into the target cell's cytoplasm. This feature can be utilized to shuttle foreign cargo proteins into transduced cells when the cargo is genetically fused to the structural vector proteins (22). This protein transfer is independent from gene transfer and, if a carefully chosen pretested fusion site is used, does not impair the genomic integrity of the transduced target cells. Thus, a risk of insertional mutagenesis by these so-called protein transfer vectors (PTVs) does not exist. Furthermore, blocks in postentry steps of genome replication do not impair protein transfer in any way and thus should be no hindrance for the application of such vectors under otherwise limiting conditions.

We reasoned that, besides marker proteins or enzymes, PTVs may be constructed in which antigenic proteins of specific pathogens or antigens associated to tumor cells are genetically fused to the structural vector proteins. In this study, we aimed to evaluate if lentiviral PTVs could be used as such antigen carriers to induce antigen-specific immune responses. We assessed the performance of vectors pseudotyped with GPs of SLAM-tropic wild-type MV_{wt323} (here, MV_{wt}) (23) enabling direct targeting of APCs in comparison to vectors pseudotyped with the standard glycoprotein VSV-G, which broadly transduces a large variety of cells but gives rise to high-titer vector preparations. As proof of principle, we demonstrated highly selective protein transfer into MV_{wt} receptor-positive cell lines by MV_{wt}-GP pseudotyped green fluorescent protein (GFP)- and ovalbumin (Ova)-transferring PTVs (GFP-PTVs and Ova-PTVs, respectively), which matched with gene transfer of cotransduced red fluorescent protein Katushka (TurboFP635)-encoding vector genomes. Cytoplasmic release of cargo proteins was confirmed for both tested pseudotypes. *Ex vivo* treatment of myeloid DCs (mDCs) with Ova-PTVs resulted in stimulation of Ova-specific $CD8^+$ T lymphocytes, evident by secretion of interleukin-2 (IL-2) and gamma interferon (IFN-γ). In contrast, $CD4^+$ T cells were stimulated most by mDCs incubated with "bald" vector particles, which did not incorporate viral glycoproteins and were thus not able to actively enter a target cell. *In vivo*, ovalbumin-transferring PTVs triggered a predominantly cellular immune response in mice expressing the respective receptor, stimulating especially $CD8^+$ cytotoxic T cells. Thus, SLAM-targeted PTVs have demonstrated specificity and, as well as nontargeted PTVs, efficacy of antigen transfer into primary APCs to trigger antigen-specific immune activation. Since especially $CD8^+$ T cells were activated *ex vivo* and *in vivo*, SLAM-targeted PTVs represent a suitable and, due to the absence of integration, safe vaccine especially for inducing cytotoxic immune responses. Since cytotoxic $CD8^+$ T lymphocytes are a mainstay of antitumoral immune responses, SLAM-targeted PTVs could be engineered for the transfer of specific tumor antigens provoking tailored antitumoral immunity.

MATERIALS AND METHODS

Cells. CHO-K1 (ATCC CCL-61), 293T (CRL-11268), HT1080 (CCL-121), and Raji (CCL-86) cells were purchased from the American Type Culture Collection (ATCC, Manassas, VA, USA) and cultured for no longer than 6 months after initial thawing. CHO cells expressing human SLAM (CHO-hSLAM) (24), CHO-CD46 (25), CHO-Nectin 4 (26), B95a (27), and HT1080-Cre (28) are described elsewhere. CHO-K1, CHO-CD46, CHO-Nectin 4, 293T, HT1080, and HT1080-Cre cells were grown in Dulbecco's modified Eagle's medium (DMEM) supplemented with 10% fetal bovine serum (FBS) (PAA, Cölbe, Germany) and 2 mM L-Gln. Geneticin (Life Technologies, Darmstadt, Germany) was additionally added for the cultivation of CHO-CD46 (1.2 mg/ml) or CHO-Nectin 4 (0.5 mg/ml) cells. Raji and CHO-hSLAM cells were maintained in RPMI 1640 medium supplemented with 10% FBS, 2 mM L-Gln, and, for CHO-hSLAM cells, 0.5 mg/ml Geneticin. CHO-K1-blue, CHO-hSLAM-blue, and Raji-blue cells were generated by stable transduction with VSV-G pseudotyped HIV-1-derived lentiviral vectors encoding an expression cassette for a floxed cerulean gene (LeGO-Cer2, plasmid 27338; Addgene)

(29). Single clones were selected by limiting dilution. The cells were maintained as described for the parental cell lines. JAWSII dendritic cells (ATCC CRL-11904) were purchased from ATCC. JAWSII-Ova are JAWSII cells stably expressing Ova after lentiviral transduction. Both were cultured in minimal essential medium alpha (MEM-α) with ribonucleosides and deoxyribonucleosides (Gibco BRL, Eggenstein, Germany) supplemented with 20% FBS, 2 mM L-Gln, 1 mM sodium pyruvate (Biochrom), and 5 ng/ml murine granulocyte-macrophage colony-stimulating factor (GM-CSF) (Peprotech, Hamburg, Germany). All cells were cultured at 37°C with 6% CO_2 and 96% humidity.

Plasmids. For cloning of pcHIV1_MA_P_Ova, the 3′ end of the matrix (MA) [primers HIVgag-ClaI(+) and MA-Prot(−)] and the 5′ end of capsid (CA) [primers Prot-CA(+) and HIVgag-BaeI(−)] genes were amplified by PCR using pCMVΔR8.9 as the template. The ovalbumin gene was amplified by PCR [primers MA-Prot-Ova(+) and CA-Prot-Ova(−)] with template pET15b-Ova (30). Thereby, the sequence encoding an additional HIV-1 protease cleavage site (amino acid sequence VSQNYPI VQN) was inserted between the matrix and Ova genes with primers MA-Prot(−) and MA-Prot-Ova(+). The three resulting PCR fragments were joined by primer extension PCR (31) using primers HIVgag-ClaI(+) and CA-Prot-Ova(−). Primer sequences and detailed PCR protocols are available upon request. PCR products were ligated into pCR2.1-TOPO (Life Technologies), resulting in pCR2.1HIV1_MA_P_Ova, and the absence of mutations was confirmed by sequencing (Eurofins MWG Operon, Ebersberg, Germany). To enable directed cloning, the 3′ end of pCR2.1HIV1_MA_P_Ova was elongated by a 1.64-kb *gag* fragment obtained from NsiI-cleaved pcDNA3.GP+GFP.4xCTE (22, 32) to yield pCR2.1-gag-Ova.NsiI. The desired sequence from the resulting plasmid was cloned via ClaI and SbfI with the intended insert orientation into pcDNA3.GP+GFP.4xCTE to yield pcHIV1_MA_P_Ova.

To generate pcHIV1_MA_P_Cre, pUC18 (Life Technologies) was linearized by BamHI/EcoRI, and blunt ends were generated by Klenow fill-in to yield pUC18-mod. The cargo protein-encoding cassette was isolated from pcHIV1_MA_P_GFP (identical to pcHIV1_MA_P_Ova with GFP instead of Ova sequence) via EcoRV/EcoRI and inserted into pUC18-mod to yield pUC18-gag/pol-P. BamHI/AvaI restriction sites flanking the cargo sequence were introduced by PCR (primers GGS-linker + P fwd; GGS-linker + P rev; LGG, AvaI fwd; LGG, AvaI rev) to yield pUC18-gag/pol-P-mod. The *cre* gene was amplified by PCR with flanking BamHI/AvaI sites (primers Cre-BamHI fwd and Cre-AvaI rev) using pSEW-Cre (33) as the template. Primer sequences and detailed PCR protocols are available upon request. The amplified *cre* fragment was ligated into pCR2.1-TOPO (Life Technologies) to yield pCR2.1-Cre-inv and sequenced. The *cre* gene was subsequently cloned into pUC18-gag/pol-P-mod via AvaI/BamHI to yield pUC18-gag/pol-P-Cre. Finally, the matrix-Cre-capsid fragment was inserted into pcHIV1_MA_P_GFP via ClaI/SbfI to yield pcHIV1_MA_P_Cre.

Plasmids pMD.G2 (34), pCG-Hwt323Δ18 (35), pCG-Fwt323Δ30 (35), pSEW-TurboFP635 (36), and pCMVΔR8.9 (37) have been described previously.

Transfection of cells. A total of 7×10^5 293T cells were seeded in six-well plates (Nunc, Wiesbaden, Germany). The next day, cells (approximately 80% confluent) were transiently transfected with 5 μg of plasmid DNA using Lipofectamine 2000 reagent (Life Technologies) according to the manufacturer's instructions.

Vector production. HIV-1-derived lentiviral vector particles were produced by transfection of 293T cells as described previously (38). To produce VSV-G or MV_{wt}-GP pseudotyped PTVs, 3.98 μg of Env expression plasmid(s) (pMD.G2 or 1.49 μg of pCG-Hwt323Δ18 plus 2.49 μg of pCG-Fwt323Δ30), 12.73 μg of transfer vector plasmid (pSEW-TurboFP635), and 18.3 μg of packaging plasmid(s) (pCMVΔR8.9 and respective cargo protein-encoding constructs in a 1:1 or, for Cre-encoding constructs, 2:1 ratio) were transfected per T175 flask. Bald particles were produced by cotransfecting 14.36 μg of transfer vector plasmid and 20.64 μg of packaging plasmid(s). Two days after transfection, cell debris was removed using 0.45-μm-pore-size filters and subsequently concentrated by ultracentrifugation through a 20% sucrose cushion (100,000 × *g*, 4°C, 3 h). Pelleted vector particles were resuspended in Opti-MEM (Life Technologies) and stored in aliquots at −80°C.

Lentiviral transduction of cells. For transduction, cells were seeded in 24-, 48-, or 96-well plates (Nunc). The next day, when cells reached 70 to 80% confluence, 250 μl (24-well plates) or 150 μl (48-well plates) of vector-containing medium was added to the cells. In gene transfer experiments, vector-containing supernatant was replaced by normal growth medium at 6 h posttransduction. Protein transfer was assessed at 4 h posttransduction, whereas gene transfer was analyzed at 72 h posttransduction.

Lysis of cells. Cells were lysed 48 h after transient transfection or 4 h after transduction. First, cells were washed once with ice-cold phosphate-buffered saline (PBS). After transduction with protein transfer vectors, surface-bound particles were removed by incubation with citric acid buffer (40 mM citric acid [Sigma-Aldrich], 135 mM NaCl, 10 mM KCl) for 2 min at room temperature, where indicated in the text and on the figure. Then, cells were washed once with ice-cold PBS and lysed with radioimmunoprecipitation assay (RIPA) lysis buffer (50 mM Tris, 150 mM NaCl, 1% NP-40, 0.5% sodium desoxycholate, 0.1% SDS) supplemented with protease inhibitor cocktail (Roche, Mannheim, Germany). Either 500 μl or 100 μl of RIPA lysis buffer was used per 6- or 48-well plate, respectively.

Immunoblotting. Cell lysates or suspensions of purified vector particles were denatured using equal volumes of 2× urea sample buffer (200 mM Tris-HCl, 8 M urea, 5% SDS, 0.1 mM EDTA, 0.03% bromophenol blue, 1.5% dithiothreitol) and incubated for 10 min at 95°C. Proteins were separated by polyacrylamide gel electrophoresis on 10% SDS-PAGE gels and blotted onto polyvinylidene difluoride (PVDF) membranes (Hybond P; GE Healthcare, Freiburg, Germany). The membranes were incubated with rabbit anti-GFP (1:2,000; Life Technologies), rabbit anti-Cre (1:20,000; Merck Millipore, Darmstadt, Germany), rabbit anti-chicken ovalbumin (1:40,000; Novus Biologicals, Cambridge, United Kingdom), mouse anti-HIV-1 p24 (1:1,000; Gentaur, Aachen, Germany), rabbit anti-MV hemagglutinin protein (MV-H) (1:1,000; clone 606), rabbit anti-MV fusion protein (MV-F) (1:4,000; clone 1034; Abcam, Cambridge, United Kingdom), rabbit anti-VSV-G (1:2,000), or mouse anti-α-tubulin (1:50,000; Sigma-Aldrich) primary antibody in 5% milk or horse serum in TBS-T (50 mM Tris, 150 mM NaCl, pH 7.4, 0.1% Tween 20). As secondary antibody, horseradish peroxidase (HRP)-conjugated donkey anti-rabbit IgG(H+L) (1:10,000; Rockland, Limerick, PA, USA) or rabbit anti-mouse IgG-IgA-IgM(H+L) (1:10,000; Life Technologies) was used as appropriate. Probed membranes were stripped with Restore Plus Western blot stripping buffer (Thermo Fisher Scientific, Dreieich, Germany) for 20 min at room temperature and washed once with TBS-T before being reprobed.

Flow cytometry analysis. Adherent cell lines were detached using trypsin-EDTA, and DCs were detached by vigorous pipetting. A total of 5×10^5 cells per staining were washed thoroughly with fluorescence-activated cell sorter (FACS) wash buffer (PBS, 1% FBS, 0.1% NaN_3). To stain DCs, cells were incubated first with Fc-blocking reagent (1:100; Miltenyi Biotec, Bergisch-Gladbach, Germany) for 15 min at room temperature. Then, antibodies were added, and samples were incubated for 20 min at 4°C in the dark. For flow cytometry, anti-mouse CD11c-allophycocyanin (APC) (1:500; BD, Heidelberg, Germany), anti-mouse CD69-phycoerythrin (PE)-Cy7, or anti-mouse CD86-Pacific Blue (each 1:100; BioLegend, London, United Kingdom) was used. After staining, all cells were washed twice with FACS wash buffer before fixation with 100 μl of FACS Fix buffer (PBS, 1% paraformaldehyde [PFA]). Cells expressing fluorophores, e.g., after transduction, were subjected to flow cytometry after being washed thoroughly and fixed with FACS Fix buffer. All samples were analyzed using an LSRII SORP cytometer (BD). Data were analyzed using FACSDiva (BD) or FCS Express software (De Novo Software, Glendale, CA, USA).

Electron microscopy. At 48 h posttransfection, vector-producing packaging cells were fixed by addition of 10% (vol/vol) glutaraldehyde to the culture medium. After a 10-min incubation at room temperature, the medium was removed, and cells were gently washed twice with PBS without Ca^{2+}/Mg^{2+}. The fixed cells were stored in PBS lacking Ca^{2+}/Mg^{2+} at 4°C until ultrathin sections were prepared as described previously (38). In short, fixed cells were scraped from the plastic surface and embedded in agarose. Then, cells were stained and subjected to secondary fixation with 1% osmium tetroxide (Sigma-Aldrich), contrasted with 2% uranyl acetate (Merck, Darmstadt, Germany), and finally dehydrated by consecutive use of 30%, 50%, 70%, 80%, 90%, 96%, and 100% ethanol (EtOH). In a last step, cells were embedded into epoxy, and ultrathin sections were cut. Samples were placed on Formvar-coated mesh copper grids (Athene; Agar Scientific, Essex, United Kingdom) and analyzed with an EM109 transmission electron microscope (Zeiss, Jena, Germany).

NanoSight particle analysis. NanoSight particle analysis of concentrated vector particles by a liquid-phase Stokes diffusion particle-tracking system was performed using a NanoSight NS500 device and NTA2.3 software (both, NanoSight, Ltd., Amesbury, United Kingdom). Prior to analysis, samples were diluted in sterile filtered PBS without Ca^{2+}/Mg^{2+} to obtain suspensions with a particle concentration of 1×10^7 to 1×10^9 particles/ml. The paths of 20 to 40 particles were followed per measurement. Each sample was measured in triplicate (75 s each) at a constant temperature of 25°C, and the mean of the single measurements was calculated. The device was cleaned thoroughly before and after each measurement.

Generation and transduction of bone marrow-derived myeloid dendritic cells. Myeloid dendritic cells (mDCs) were generated by cultivating bone marrow cells from IFNAR$^{-/-}$ and IFNAR$^{-/-}$-SLAM^{ki} (where ki is knock-in) mice in the presence of GM-CSF (100 ng/ml) as described previously (30). A total of 3.2×10^5 mDCs were seeded per well into 24-well plates and stimulated by addition of 100 ng/ml lipopolysaccharide (LPS; Sigma-Aldrich) overnight to upregulate SLAM on mDCs of IFNAR$^{-/-}$-SLAM^{ki} mice (39). Subsequently, mDCs were transduced with the respective PTVs. For inhibition of transduction using the MV-specific fusion inhibitor FIP (2-D-Phe-Phe-Gly-OH; Bachem, Bubendorf, Switzerland) (40), medium containing FIP (200 μM) was added 30 min before transduction. Inhibitor-supplemented medium was used in all further steps. mDCs were incubated with protein transfer vectors for 4 h. Then, transduced mDCs were coincubated with 8×10^5 primary T cells isolated from splenocytes of OT-I (41) or OT-II (42) mice by magnetic cell separation using CD4$^+$ T Cell Isolation Kit II (mouse) or a CD8a$^+$ T cell isolation kit (mouse) (both, Miltenyi Biotec) and suspended in DC medium (RPMI 1640 medium, 10% FBS, 2 mM L-glutamine, 100 U/ml penicillin, 100 μg/ml streptomycin, 10 mM HEPES, 1 mM sodium pyruvate, 0.1 mM 2-mercaptoethanol). At 24 h and 72 h after addition of T cells, supernatants of the cocultures were sampled and stored at −20°C for analysis of secreted cytokines by enzyme-linked immunosorbent assay (ELISA).

ELISA. Murine IL-2 or IFN-γ was quantified with BD OptEIA Set Mouse IL-2 or BD OptEIA Set Mouse IFN-γ (BD Biosciences), respectively, according to the manufacturer's instructions. Ovalbumin concentration was determined using a chicken egg ovalbumin ELISA kit (Alpha Diagnostic International, San Antonio, TX, USA); HIV-1 p24 concentration was determined by an HIV-1 p24 antigen ELISA (Gentaur, Aachen, Germany) according to the manufacturer's instructions.

ELISpot assay. Antigen-specific IFN-γ secretion of splenocytes in mice was analyzed using a mouse IFN-γ enzyme-linked immunosorbent spot (ELISpot) assay (Ready-Set-Go! kit; eBioscience). One day before the assay, MultiScreen-IP filter plates (Merck Millipore) were activated with 70% EtOH and immediately washed three times with sterile water and once with PBS before further processing was done according to the manufacturer's protocol. A total of 5×10^5 splenocytes per well were incubated with plain medium (negative control), 10 μg/ml concanavalin A ([ConA] positive control; Sigma-Aldrich), 10 μg/ml recombinant Ova (30), 5 μg/ml of an Ova peptide consisting of residues 257 to 264 ($Ova_{257–264}$; SIINFEKL), or 5 μg/ml $Ova_{323–339}$ (ISQAVHAAHAEINEAGR) (both, Invivogen, Toulouse, France). The plates were subsequently incubated, without movement, for 36 h at 37°C and 6% CO_2 in a humidified incubator. IFN-γ-secreting cells were detected according to the manufacturer's instructions. The spots were counted using an ELISpot reader (Eli.Scan; A.EL.VIS, Hannover, Germany) with the software ELI.Analyse (A.EL.VIS). Wells with too many spots to be counted were set to 1,500 spots (maximum spot count reliably determined).

Animal experiments. Animal experiments were performed in compliance with the regulations of the German animal protection law. All animals used were bred in-house at Paul-Ehrlich-Institut, and genotypes were confirmed by PCR-based genotyping. Six- to 8-week-old IFNAR$^{-/-}$ (43) or IFNAR$^{-/-}$-SLAM^{ki} (39) mice were injected intraperitoneally (i.p.) with 200 μl of vector suspension diluted in Opti-MEM adjusted to a total content of 1 μg of ovalbumin. MV_{wt}-GP pseudotyped HIV-derived vectors transferring GFP protein and cotransducing the *katushka* gene [HIV-$GFP_{Katushka}(MV_{wt})$] were normalized by p24 content to HIV-$Ova_{Katushka}(MV_{wt})$. Four weeks later, mice were boosted. The animals were sacrificed on day 32, spleens were harvested, and splenocytes were isolated by mashing the spleens through a 70-μm-pore-size filter. After lysis of red blood cells (155 mM NH_4Cl, 10 mM Tris, pH 7.5) and one wash step, splenocytes were either used directly for IFN-γ ELISpot assays or stored at −80°C in freezing medium (90% FBS, 10% dimethyl sulfoxide [DMSO]) before use.

Statistical analysis. To evaluate the statistical significance between data sets, statistical analysis was done using the analyzing software GraphPad Prism (GraphPad Software, Inc., La Jolla, CA) with tests indicated in the respective figure legends.

RESULTS

Generation and characterization of lentiviral protein transfer vectors. To establish the generation of cargo protein-transferring particles, VSV-G pseudotyped vector particles were produced using different ratios of packaging plasmids expressing unmodified Gag/Pol and a construct where GFP was genetically fused to the C terminus of the matrix (MA) protein coding region of *gag* (Fig. 1A). While protein transfer can thus be detected by GFP fluorescence, gene transfer into HT1080 cells was monitored in parallel by packaging of a transfer vector (pSEW-TurboFP635) encoding the red-fluorescing Katushka protein into these vector particles. Increasing the amount of *gag* fused to *gfp* relative to the amount of unmodified *gag* in packaging cells enhanced both the percentage and mean fluorescence intensity (MFI) of GFP-positive (GFP$^+$) cells after transduction of target cells, thereby indicating that more GFP had been packaged into protein transfer vector particles (Fig. 1B). However, if only GFP-tagged Gag/Pol was used for particle production, protein transfer was strongly reduced (Fig. 1B). Interestingly, gene transfer by the produced PTVs reciprocally correlated with protein transfer, and this correlation was even stronger in terms of the MFI than of the percentage of transduced cells, indicating multiple transduction events of target cells for "optimal" ratios (Fig. 1B). Thus, the higher the ratio was of Gag-GFP to Gag expressed during vector production, the lower the gene transfer efficacy of the generated particles was. When solely Gag-GFP fusion protein was used for particle production, no transducing particles were generated at all. The optimal relation of protein and gene transfer was determined in packaging cells transfected with a 1:1 ratio of Gag-GFP/Pol-to-Gag/Pol packaging plasmids [Gag(-GFP)/Pol] (Fig. 1B). While greater GFP transfer by particles generated in cells that express more GFP-Gag than Gag is expected, a reduction in gene transfer by larger amounts of the GFP-Gag fusion protein may argue for impairment of vector particle

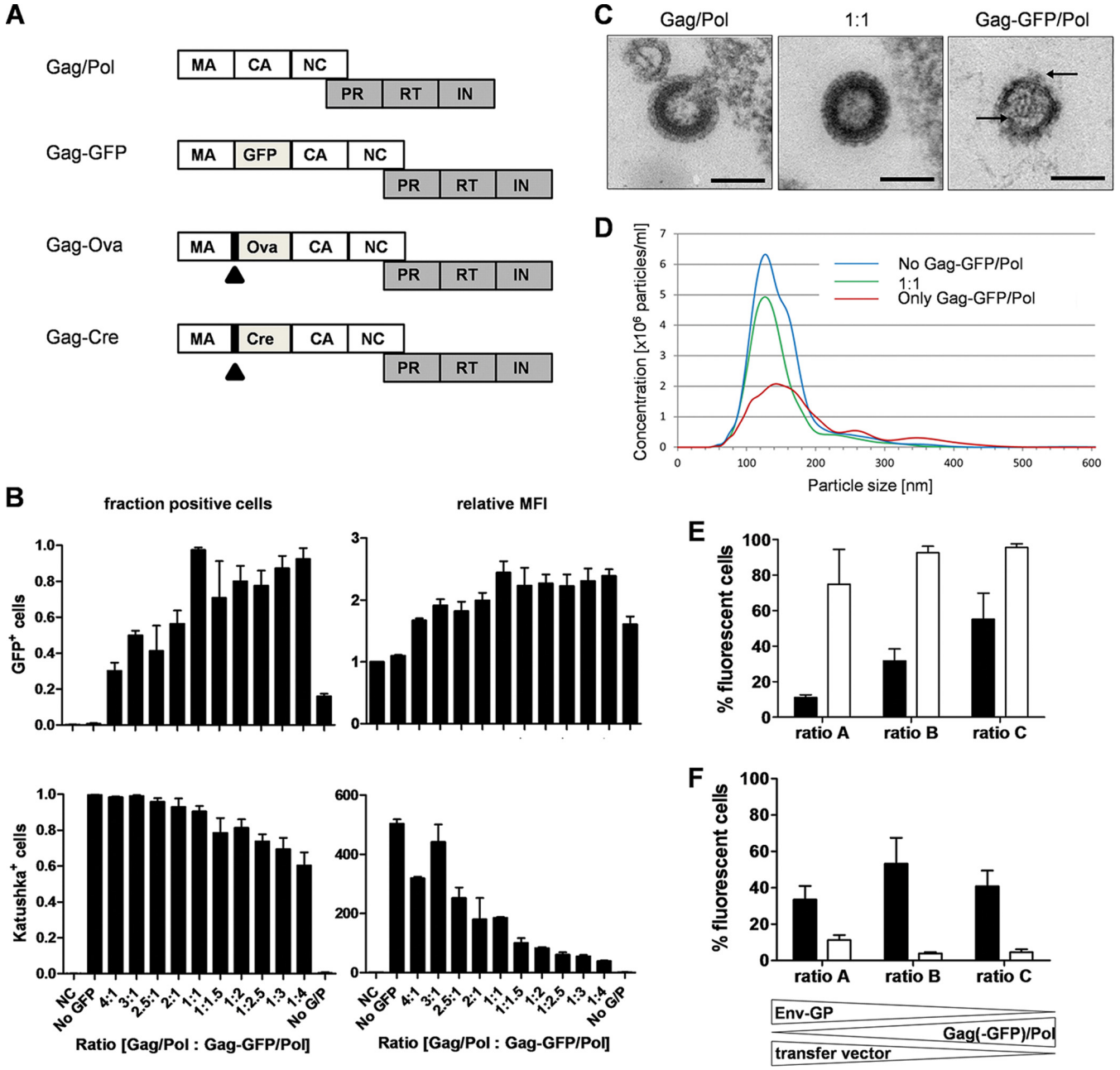

FIG 1 Optimization of lentiviral protein transfer vector production. (A) Schematic depiction of Gag-cargo/Pol constructs. MA, matrix; CA, capsid; NC, nucleocapsid; PR, protease; RT, reverse transcriptase; IN, integrase. The arrowhead indicates HIV-1 protease cleavage motif. (B) Titration of Gag/Pol to Gag-GFP/Pol used for PTV production. VSV-G pseudotyped PTVs transferring the *katushka* transgene were produced in 293T cells transfected with the indicated ratios of Gag/Pol to Gag-GFP/Pol packaging constructs. GFP transfer or Katushka expression (gene transfer) by flow cytometry 3 h or 72 h posttransduction, respectively, was assessed in HT1080 cells after transduction with similar volumes of vector-containing supernatant, analyzed both for the fraction of positive cells or relative MFI. The maximal fraction of cells positive for protein or gene transfer was normalized to 1. For relative MFI, the MFI of untransduced cells was set to 1. Values are means ± standard errors of the means ($n = 3$). No GFP, vector lacking GFP cargo; No G/P, vectors composed of Gag-GFP/Pol only. (C) Particle morphology. Ultrathin sections of 293T cells releasing the indicated PTVs were analyzed by electron microscopy. Arrows depict disrupted MA layer and irregularities of envelope. Scale bar, 100 nm. (D) Particle size. Analysis of PTV particles produced as indicated by real-time single-particle tracking analysis. (E and F) Optimization of protein and gene transfer during PTV production for PTVs pseudotyped by VSV-G (E) or PTVs pseudotyped by MV glycoproteins (F). Vectors harvested from 293T cells transfected with the indicated relative plasmid ratios (Gag-Pol/Gag-cargo-Pol to Env to transfer vector; ratio A, 1.62:0.87:2.5; ratio B, 2.1:0.7:2.1; ratio C, 2.3:0.5:1.6) were used for transduction of CHO-hSLAM cells with same volume of PTVs. GFP protein transfer (black) or Katushka gene transfer (white) were assessed by flow cytometry at 3 h or 3 days after transduction, respectively. Values are means ± standard errors of the means ($n = 3$).

structure due to the changed steric requirements of the Gag-GFP polyprotein in these vector particles.

To test this hypothesis, the morphology of PTV particles produced with only GFP-Gag or with GFP-Gag/Gag in a 1:1 ratio was characterized by electron microscopy of ultrathin sections of corresponding packaging cells. In parallel, purified vector particles were analyzed in comparison to the respective vector particles with no additional cargo protein using the NanoSight system. Electron microscopy revealed no morphological differences between lentiviral gene transfer vectors and protein transfer vectors produced with a 1:1 ratio of Gag-GFP/Pol-to-Gag/Pol packaging plasmids (Fig. 1C). In contrast, fewer particles were detected when only Gag-GFP/Pol was used for particle production. These particles also revealed structural abnormalities such as a disrupted MA layer and the presence of fewer and irregularly arranged envelope protein complexes (Fig. 1C, right panel).

Real-time single-particle tracking analysis of the three particle types confirmed the different structure of particles produced with only Gag-GFP/Pol (Fig. 1D). Gene transfer vectors and PTVs produced with a 1:1 ratio of packaging constructs did not differ essentially in particle diameter, which was determined to be 125 nm for both vector types. A few aggregates were detected in both particle stocks. In contrast, in vector particle stocks produced with GFP-tagged Gag only, at least four particle populations with diameters of approximately 110 nm, 140 nm, 260 nm, and 355 nm could be distinguished (Fig. 1D). These data clearly demonstrate the presence of aggregates and irregularly formed particles when only GFP-Gag was used for packaging, explaining the lack of transducing vector particles (Fig. 1B, right column). Therefore, a 1:1 ratio of Gag-GFP/Pol to Gag/Pol packaging constructs was chosen for the generation of PTV particles in all subsequent experiments.

Finally, the ratio of Gag(-GFP)/Pol packaging plasmids to transfer vector and envelope expression constructs required for PTV production was varied, and the resulting particles were analyzed as described above. When the relative fraction of packaging plasmids (Gag/Pol and Gag-GFP/Pol) was increased and the fractions of envelope protein (VSV-G or MV-F plus MV-H) and transfer vector plasmids (pSEW-TurboFP635) were reduced, the efficacy of gene and protein transfer became affected (Fig. 1E and F). For VSV-G pseudotyped vectors, employing a ratio of 2.3 to 0.5 to 1.6 (sum of Gag/Gag-cargo to Env to vector) (Fig. 1E and F, ratio C), efficiency of protein transfer by the resulting particles could be increased from 11.0% ± 2.8% to 55.2% ± 25.5%, which was also accompanied by an increase of gene transfer from 74.9% ± 34.1% to 95.5% ± 3.8% (Fig. 1E). For MV glycoproteins (Fig. 1F), the best protein transfer (53.3% ± 28.3% positive cells) was achieved at a ratio of 2.1 to 0.7 to 2.1 (Fig. 1E and F, ratio B), but gene transfer was slightly reduced to 4% ± 1.3% in this setting. Taken together, these data show a positive correlation between the amount of packaging plasmids transfected into 293T packaging cells for vector production and the capability of the originating particles to transfer cargo proteins. In essence, the greater the amount of Gag-GFP/Pol and Gag/Pol packaging plasmids that was transfected for vector production, the greater was the amount of GFP protein transferred into transduced target cells by VSV-G pseudotyped vector particles, as expected. For MV_{wt}-GP pseudotyped particles, however, this was less stringent, most likely due to more complex Env-GP organization. Obviously, the nature of the glycoproteins codetermines functionality of the respective pseudotyped PTV particles.

Transfer of different cargo proteins by PTVs. In addition to PTVs transferring GFP, Cre recombinase- or ovalbumin (Ova)-transferring PTVs were used in this study. For this purpose, packaging plasmids encoding Cre recombinase or Ova within the *gag* open reading frame (ORF) were cloned (Fig. 1A). To assess whether the cargo proteins encoded by these packaging plasmids were expressed, Cre or Ova expression was analyzed in addition to GFP expression in transfected 293T cells by Western blot analysis. In both Cre- and Ova-encoding packaging constructs, an HIV-1 protease site (VSQNY ↓ PIVQN)-encoding amino acid sequence was inserted between matrix- and cargo protein-encoding DNA sequences (Fig. 1A). This cleavage site (indicated by the down arrow) enables release of the respective cargo proteins into the cytoplasm of transduced cells after fusion of particle and plasma membranes during cell entry due to processing of the respective MA-cargo precursor protein during particle maturation. All cargo proteins were efficiently expressed (Fig. 2A to C) and were detected as fusion proteins within the 55-kDa Gag polyprotein precursor and/or with the 17-kDa MA protein. Gag-GFP (82 kDa) and MA-GFP (44 kDa) fusion proteins were detected in cells transfected with pcDNA3.GP+GFP.4xCTE, and expression of Gag-Ova (98 kDa) was visible in pcHIV1_MA_P_Ova-transfected cells, whereas Gag-Cre (93 kDa) and MA-Cre (55 kDa) were detected in lysates of 293T cells transfected with pcHIV1_Ma_P_Cre. Additionally, the respective released cargo proteins Ova (43 kDa) and Cre (38 kDa) were detected with the expected molecular masses as well, indicating functionality of the inserted protease cleavage site. Taken together, these data demonstrate expression of all Gag-cargo fusion proteins and release of Ova or Cre recombinase by proteolytic cleavage during particle maturation.

These plasmids were used for production of PTVs pseudotyped with VSV-G or truncated MV_{wt} glycoproteins, i.e., the hemagglutinin (H) and fusion protein (F). Vector particles were produced in 293 T cells and concentrated via ultracentrifugation. Subsequently, incorporation of cargo proteins into the respective concentrated vector particles was analyzed by Western blot analysis (Fig. 2D to F). GFP, Cre, and Ova were detected in purified PTV lysates, indicating efficient incorporation of cargo proteins into PTV particles. In PTVs generated using Gag-cargo/Pol constructs with the additional protease cleavage site between MA and cargo, complete release of Ova from matrix fusion proteins was observed (Fig. 2F). Also Cre was completely released from the Gag-Cre polyprotein, but in addition to free Cre recombinase, degradation products of the enzyme were also observed (Fig. 2E, lower bands). If no cleavage site was encoded, the cargo protein was detected as a fusion protein with MA, as demonstrated for vectors incorporating the MA-GFP fusion protein (Fig. 2D). Additionally, incorporation of the envelope glycoproteins VSV-G, MV-H, or MV-F correlated with p24 incorporation irrespective of the payload of the different vector particles (Fig. 2D to F). In contrast, no cellular cytoplasmic proteins seem to be incorporated into PTVs, as demonstrated by the lack of α-tubulin in all PTV preparations (Fig. 2G to I).

To analyze whether incorporation of different cargo proteins into lentiviral particles causes structural alterations of vectors, the morphology of PTVs was assessed by electron microscopy of ultrathin sections of vector-producing packaging cells. No remark-

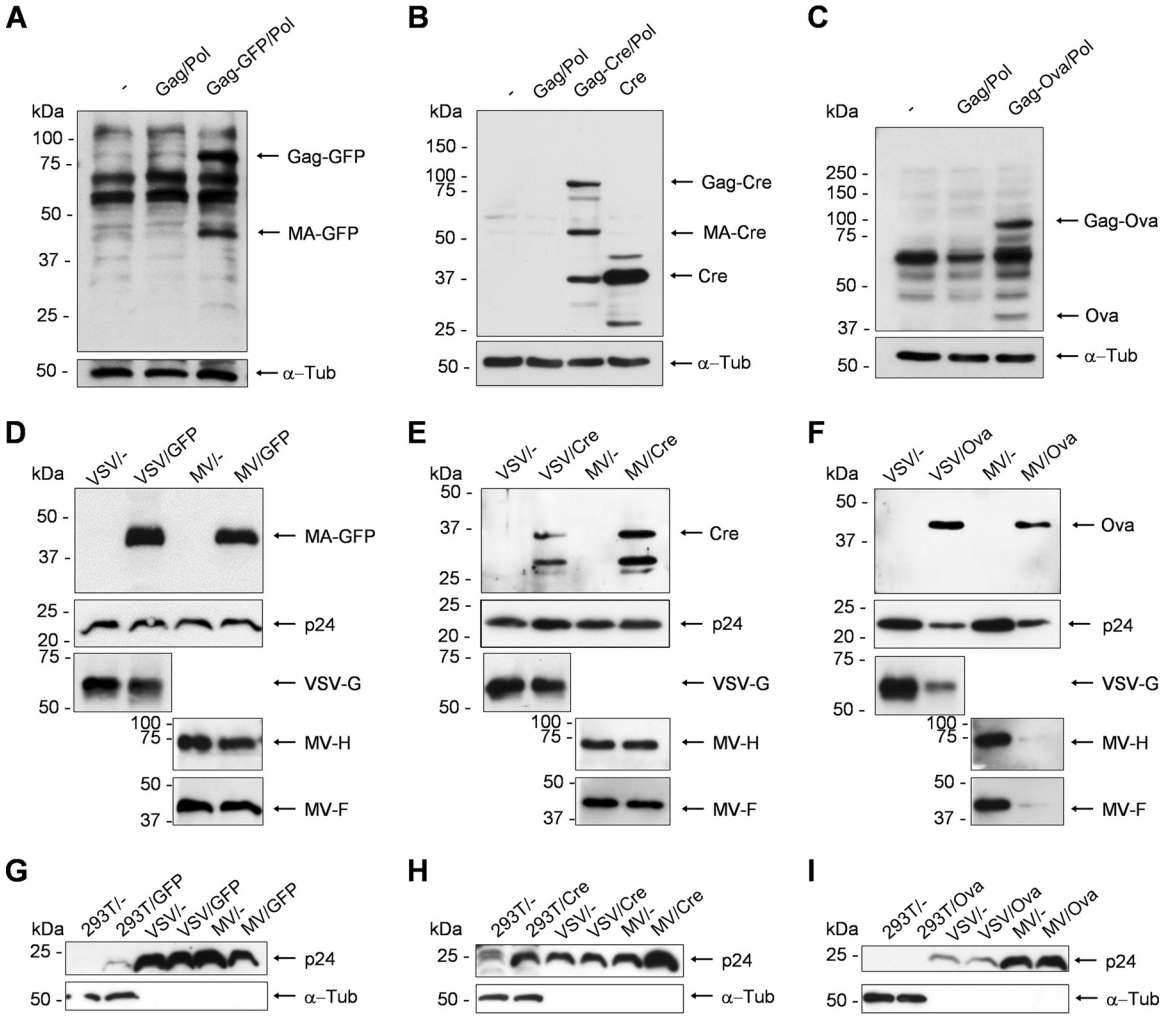

FIG 2 Expression of cargo proteins by packaging constructs and efficient incorporation into PTV particles. (A to C) Expression of GFP, Cre, or Ova by packaging constructs. Immunoblot analysis was performed of 293T cells left untransfected (−) or transfected with Gag/Pol, the indicated Gag-cargo/Pol packaging plasmids, or pSEW-Cre (transfer vector encoding Cre recombinase). At 48 h after transfection blots were probed for GFP (A), Cre (B), or Ova (C). (D to I) Protein incorporation into PTVs. PTV particles produced in 293T packaging cells were purified and concentrated by ultracentrifugation from supernatants and subjected to immunoblot analysis probing for GFP (D), Cre (E), or Ova (F) to detect cargo protein content. Lentiviral gene transfer vectors, pseudotyped with VSV-G (VSV/−) or MV_{wt}-GPs (MV/−), served as negative controls. All particle preparations were further probed for incorporation of envelope glycoproteins (lower panels, D to F) or α-tubulin (lower panels, G to I). Lysates of unmodified 293T cells or 293T cells transfected with the indicated Gag/Pol packaging plasmids served as positive controls, as well as p24 detection in vector preparations (different from those used in the experiments shown in panels D to F). α-Tub, α-tubulin.

able differences between GFP or other protein transfer vectors and the respective lentiviral gene transfer vectors were observed (Fig. 3). All PTV particles revealed a regularly shaped core structure, which was indistinguishable between PTVs and gene transfer vectors. However, particles with different envelope proteins could clearly be discriminated. VSV-G pseudotyped vectors were characterized by a high density of an ordered envelope glycoprotein shell (Fig. 3B). MV_{wt}-GPs were less abundant on PTV surfaces (Fig. 3C) but clearly detectable as distinct envelope protein complexes protruding from the particles' surfaces (marked by arrows) while such structures were not detectable on bald particles (Fig. 3A).

Receptor specificity of pseudotyped PTVs. Next, we aimed to assess receptor specificity, i.e., the tropism of pseudotyped PTVs, and thereby to analyze their potential for targeting specific cell types of interest. A receptor-transgenic CHO cell panel expressing MV_{wt} receptors (CHO-hSLAM and CHO-Nectin 4), controls (CHO-K1 and CHO-CD46), and naturally SLAM-positive B95a and Raji cells were used. These cells were transduced in parallel with GFP-transferring PTVs additionally mediating gene transfer of the Katushka marker gene at a multiplicity of infection (MOI) of 1 (all vectors were previously titrated by gene transfer in CHO-hSLAM cells). As depicted in Fig. 4A and B, flow cytometry revealed specific delivery of GFP by PTVs pseudotyped with MV_{wt} glycoproteins (MV_{wt}-GP) exclusively into SLAM- or nectin-4-positive cells, as expected. In parallel, transfer of vector genomes encoding Katushka was demonstrated into the same cells, which had been susceptible for protein transfer. In contrast, VSV-G pseudotyped PTVs revealed the expected broad tropism, as indicated by gene transfer into all CHO lines and human Raji cells, but

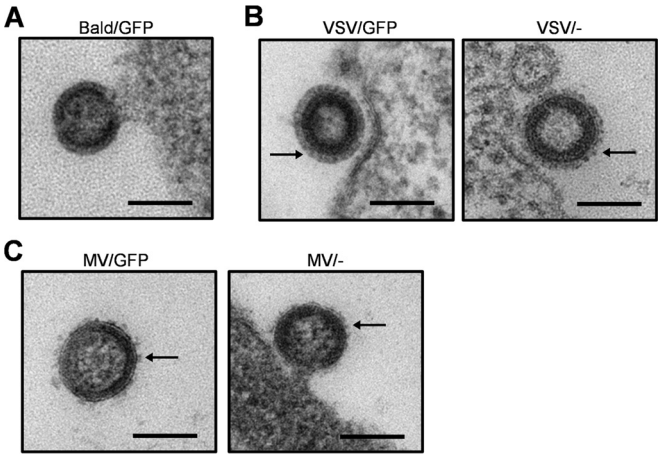

FIG 3 Analysis of vector particle morphology by electron microscopy. Ultrathin sections of 293T packaging cells transfected to produce GFP-PTV particles harboring no envelope glycoproteins (Bald/GFP) (A), GFP-PTV or lentiviral gene transfer particles pseudotyped with VSV-G (VSV/GFP and VSV/−, respectively) (B), or GFP-PTV or lentiviral gene transfer particles pseudotyped with MV_{wt}-GPs (MV/GFP and MV/−, respectively) (C) were analyzed by electron microscopy. Representative pictures of each vector particle type are shown. Arrows point at envelope glycoprotein complexes. Scale bar, 100 nm.

the protein transfer was significantly less efficient and sometimes (e.g., in CHO-K1 cells) very scarce. Results in the simian cell line B95a differed from those in the other analyzed cell lines since gene transfer was absent in these cells using VSV-G pseudotyped PTVs. Also gene transfer by MV_{wt}-GP pseudotyped PTVs was drastically reduced in B95a cells. In contrast, efficient protein transfer especially using MV_{wt}-GP pseudotyped PTVs was unimpaired in these cells. Taken together, analysis of lentiviral GFP-PTVs on receptor-transgenic CHO and B cell lines revealed specific delivery of cargo protein by MV_{wt}-GP pseudotyped vectors only into SLAM- and nectin-4-positive cells, in contrast to broadly transducing VSV-G pseudotyped vector particles.

PTVs mediate cytoplasmic transfer of their cargo protein. To exclude that the observed fluorescence of target cells after transduction by GFP-transferring PTVs was caused by adhesion of the individual particles to cellular surfaces, we aimed to confirm cell entry of vectors using Cre recombinase-transferring PTVs in combination with receptor-transgenic cell lines. These target cells were modified to incorporate a protein expression cassette for the blue fluorescent marker protein cerulean (44), in which the cerulean ORF is flanked by Cre recognition sites (Fig. 5A). Thus, expression of Cre recombinase results in loss of blue fluorescence due to inactivation of the cerulean ORF by recombination.

Cre indicator cell lines harboring a floxed cerulean cassette but differing in their receptor status (CHO-K1-blue, $SLAM^-$; CHO-hSLAM-blue, $SLAM^+$; Raji-blue, $SLAM^+$) were transduced with Cre PTVs pseudotyped with VSV-G [HIV-$Cre_{Katushka}$(VSV)] or MV_{wt}-GPs [HIV-$Cre_{Katushka}$(MV_{wt})] at an MOI of 15 or, as a positive control, VSV-G pseudotyped Cre gene transfer vectors [HIV_{Cre}(VSV)] at an MOI of 10. Blue fluorescence of transduced cells and controls was analyzed 2 weeks after transduction to allow fading of fluorescence after inactivation of the cerulean ORF (Fig. 5B). Transduction with HIV_{Cre}(VSV) gene transfer vectors resulted in complete (CHO-K1-blue and CHO-hSLAM-blue) or at least significant loss of cerulean fluorescence (Raji-blue), as expected (Fig. 5B, right column). Transduction with HIV-$Cre_{Katushka}$(MV_{wt}) PTVs resulted in fading of cerulean fluorescence in a significant fraction of transduced cells (Fig. 5B, middle and right columns). With the exception of MV receptor-negative CHO-K1-blue cells, this fraction of cells was bigger than after transduction of the same indicator cell lines by HIV-$Cre_{Katushka}$(VSV) particles. Accordingly, we observed 0% versus 3.4% loss of fluorescence in CHO-K1-blue cells, 13.0% versus 3.0% fading of blue fluorescence in CHO-hSLAM-blue cells, and 1.9% versus 0.8% inactivation of cerulean fluorescence in Raji-blue cells after transduction with HIV-$Cre_{Katushka}$(MV_{wt}) or HIV-$Cre_{Katushka}$(VSV) PTVs. Thus, HIV-$Cre_{Katushka}$(MV_{wt}) selectively diminished blue fluorescence in only MV_{wt} receptor-positive indicator cell lines, whereas HIV-$Cre_{Katushka}$(VSV) led to inactivation of cerulean fluorescence in all three cell lines, independent of the presence of SLAM. These data thus confirmed cytoplasmic release of functional proteins into transduced cells and confirmed the receptor specificity of the generated PTVs.

SLAM-targeted transfer of ovalbumin is feasible by MV_{wt}-GP pseudotyped PTVs. Since the final aim of this study has been the analysis of the suitability of PTVs for use in vaccines, the immunologically well-characterized protein ovalbumin (Ova) was chosen as a model antigen for subsequent analyses. As described above for GFP-PTVs, the target receptor specificity of Ova-PTVs was determined using the same cell panel expressing the different receptor(s) of interest. Although we were aware of the challenge in using a small quantity of transferred protein, i.e., 723 fg of Ova per transducing unit (TU) in HIV-$Ova_{Katushka}$(MV_{wt}) vector preparations as determined by ELISA (data not shown), lysates of cells transduced with Ova-PTVs were subjected to anti-Ova immunoblot analysis. Analysis of lysates of transduced cells revealed clearly detectable Ova signals in receptor-positive CHO-hSLAM, B95a, and Raji cells transduced with MV_{wt} pseudotyped Ova-PTVs (Fig. 4C). These signals were still detectable after citric acid buffer treatment (to remove surface-bound particles) of transduced cells before lysis, thus indicating that Ova was transferred into the cytoplasm of the transduced target cells, as expected. Moreover, selective Katushka transgene expression, as detected by flow cytometry analysis, confirmed transduction of the SLAM-positive cells by HIV-$Ova_{Katushka}$(MV_{wt}) (Fig. 4D). In contrast, in cell lysates obtained from cells transduced by HIV-$Ova_{Katushka}$(VSV) vectors at the same MOI, no Ova was detectable by Western blot analysis. Gene transfer, however, was observed for all HIV-$Ova_{Katushka}$(VSV)-transduced cells, except, again, for the monkey cell line B95a (Fig. 4D). In conclusion, receptor-dependent transduction was demonstrated also for Ova-PTVs.

***Ex vivo* transduction of murine mDCs with Ova-PTVs.** In the next step, myeloid dendritic cells (mDCs) were generated from bone marrow of MV receptor-negative $IFNAR^{-/-}$ and receptor-positive $IFNAR^{-/-}$-$SLAM^{ki}$ mice (parental strain of both, C57BL/6) as prototypic antigen-presenting cells (APCs) (Fig. 6A). PTVs, especially those targeted to APCs, may constitute a well-suited agent for the induction of APC-initiated immune responses due to their ability to transfer antigenic protein into these cells. However, activation of APCs requires additional costimulation. As PTVs are derived from virus particles, interaction of PTVs with APCs might stimulate APCs *per se*. Thus, stimulation of APCs by PTVs was analyzed 24 h after transduction by analysis of expression of the activation markers CD69 and CD86 on mDCs. None of the tested PTVs induced upregulation of CD69 or CD86 in trans-

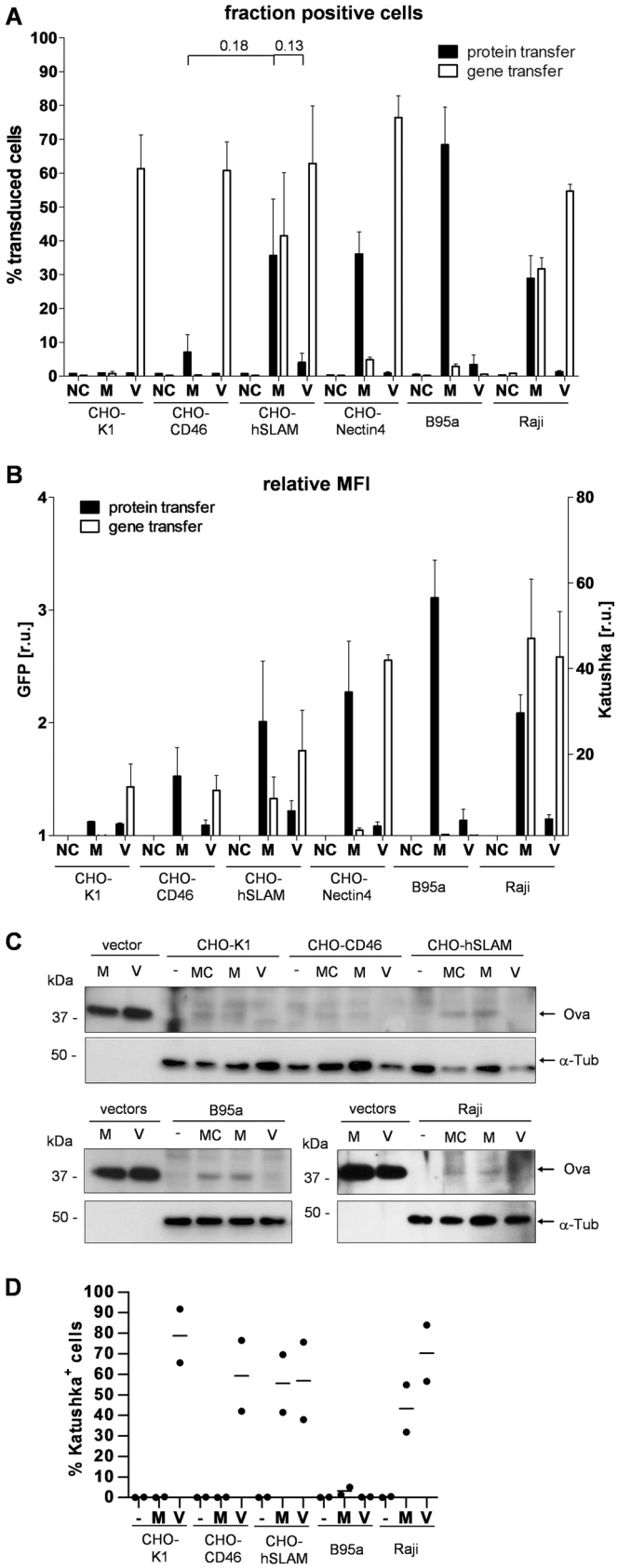

FIG 4 Receptor specificity of GFP and Ova protein transfer by PTV particles. (A and B) Receptor-dependent transduction of cell lines by GFP-PTVs. Transgenic CHO cells expressing either MV_{wt} receptors (CHO-hSLAM and CHO-Nectin 4), MV vaccine strain receptor (CHO-CD46), or no receptors (CHO-K1) or naturally SLAM-expressing B95a and Raji cells were mock transduced (negative control, NC), or transduced with concentrated GFP-PTV, pseudotyped with VSV-G (V) or MV_{wt}-GPs (M), at an MOI of 1. Protein and gene transfer were monitored at 3 h or 3 days posttransduction for the fraction of positive cells or relative MFI. Values are means ± standard errors of the means ($n = 3$). (C and D) Receptor-dependent transduction of cell lines by Ova-PTVs. Cell lines as described for panel A were transduced with Ova-PTVs at an MOI of 1 and subjected to immunoblot analysis at 3 h posttransduction (C). MC indicates citric acid buffer treatment 3 h after transduction with HIV-$Ova_{Katushka}(MV_{wt})$. Katushka fluorescence was analyzed at 72 h post-transduction by flow cytometry (D). Values are means ($n = 2$). Statistical significance was determined by a two-tailed unpaired Student's t test.

duced mDCs (Fig. 6B) despite the general responsiveness of those cells, as demonstrated by the addition of LPS (Fig. 6B).

To assess the immune-stimulatory capacity of mDCs transduced by Ova-PTVs, transduced mDCs were cocultured with Ova-specific $CD8^+$ or $CD4^+$ T cells isolated from spleens of T cell receptor (TCR)-transgenic mice (OT-I or OT-II mice, respectively) (Fig. 6A). Stimulation of T cells was assessed by quantifying the secretion of IL-2 or IFN-γ (Fig. 6C and D). $CD8^+$ T cells were stimulated to secrete only IL-2 and IFN-γ in coculture with $IFNAR^{-/-}$ mouse-derived mDCs preincubated with endotoxin-depleted recombinant Ova or HIV-$Ova_{Katushka}$(VSV) PTVs. Preincubation of mDCs with HIV-$Ova_{Katushka}$(bald), HIV-$Ova_{Katushka}(MV_{wt})$, or GFP-PTVs [HIV-$GFP_{Katushka}(MV_{wt})$ and HIV-$GFP_{Katushka}$(VSV)] did not induce activation of OT-I T cells. Similarly, $CD8^+$ Ova-specific T cells were stimulated by $IFNAR^{-/-}$-$SLAM^{ki}$ mDCs preincubated with recombinant Ova or HIV-$Ova_{Katushka}$(VSV). However, IL-2 and IFN-γ release was additionally detected for OT-I cells in coculture with mDCs transduced by HIV-$Ova_{Katushka}(MV_{wt})$ PTVs. Thus, PTVs pseudotyped with MV_{wt}-GPs revealed highly selective transduction of SLAM-positive APCs only. Cytokine secretion was also dependent on the number of infectious HIV-$Ova_{Katushka}(MV_{wt})$ particles as IFN-γ release correlated with the MOI (Fig. 6C). In line with these data, activation of $CD8^+$ T cells by mDCs transduced with HIV-$Ova_{Katushka}(MV_{wt})$ was completely ablated upon addition of the fusion-inhibiting peptide FIP (data not shown), which inhibits MV_{wt}-GP-mediated membrane fusion. These data indicate GP-mediated transfer of the cargo protein into the cytosols of mDCs by PTVs. Obviously, transferred cargo proteins were proteasomally processed and presented on MHC-I molecules via the endogenous antigen presentation pathway. Interestingly, the amount of secreted IL-2 in cocultures of cytotoxic T cells with HIV-$Ova_{Katushka}$(VSV)- or HIV-$Ova_{Katushka}(MV_{wt})$-transduced mDCs was comparable to the cytokine level released by $CD8^+$ T cells in culture with mDCs incubated with 50 μg of recombinant Ova, albeit only approximately 230 ng of protein was transferred by PTVs. Thus, transduction of mDCs by PTVs is significantly more efficient in stimulating antigen-specific T cells than incubation with purified protein.

In contrast to the efficient activation of $CD8^+$ T cells by mDCs transduced with pseudotyped PTVs, $CD4^+$ T cells were most vigorously stimulated by mDCs when incubated with HIV-$Ova_{Katushka}$(bald) vector particles without envelope GPs, irrespective of receptor status (Fig. 6D). Moreover, also MV_{wt}-GP pseudotyped PTVs [HIV-$Ova_{Katushka}(MV_{wt})$] triggered activation of Ova-specific $CD4^+$ T cells when MV-receptor-negative mDCs (from $IFNAR^{-/-}$ mice) were incubated with these vectors

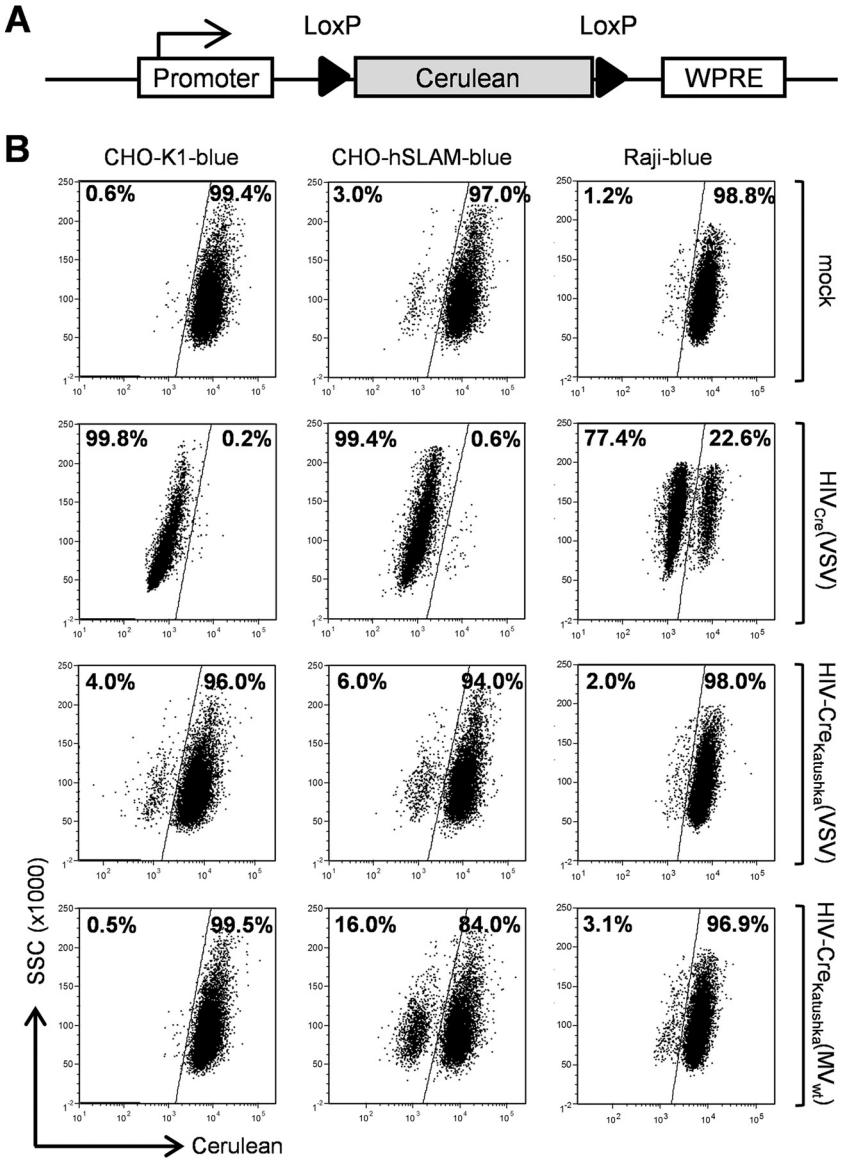

FIG 5 Demonstration of cytoplasmic protein transfer by PTV particles. (A) Schematic depiction of the marker gene expression cassette present in indicator cell lines. The *cerulean* ORF, encoding the blue-fluorescing cerulean protein, is flanked by two LoxP sites. Cre recombinase thus excises the *cerulean* ORF and induces fading of blue fluorescence over time. WPRE, woodchuck hepatitis virus posttranscriptional regulatory element. (B) Receptor-dependent Cre protein transfer into indicator cell lines. MV_{wt} receptor-negative CHO-K1-blue and MV_{wt} receptor-positive CHO-hSLAM-blue and Raji-blue indicator cells were mock transduced (mock) or transduced with HIV_{Cre}(VSV), transferring the *cre* gene (MOI of 10), or with the Cre protein transfer vector HIV-$Cre_{Katushka}$(VSV) or HIV-$Cre_{Katushka}$(MV_{wt}) (MOI of 15). At 14 days after transduction, fading of blue fluorescence was assessed by flow cytometry. Results of one representative experiment are shown ($n = 3$). SSC, side scatter.

(Fig. 6D). Together, these data indicate endocytotic uptake of vector particle-associated Ova in the absence of the corresponding cell entry receptor, followed by MHC class II presentation, as expected for the classic route for receptor-independent internalization by antigen presentation.

Immunogenic properties of Ova-PTVs *in vivo*. After demonstration of the immune-stimulatory properties (especially activation of $CD8^+$ T lymphocytes) of PTVs *in vitro*, nontargeted VSV-G- and SLAM-targeted MV_{wt}-GP pseudotyped PTVs were analyzed *in vivo* for induction of cytotoxic antigen-specific immune responses. For this purpose, $IFNAR^{-/-}$ and $IFNAR^{-/-}$-$SLAM^{ki}$ mice were inoculated with HIV-$Ova_{Katushka}$(bald), HIV-$GFP_{Katushka}$(MV_{wt}), HIV-$Ova_{Katushka}$(MV_{wt}), and HIV-$Ova_{Katushka}$(VSV), as well as with recombinant Ova or with medium (mock control). The amount of particles administered i.p. was adjusted to 1 μg of Ova per injection. The particle number of HIV-$GFP_{Katushka}$(MV_{wt}) was normalized to that of HIV-$Ova_{Katushka}$(MV_{wt}) by capsid protein (p24) content. Mice were primed and boosted 4 weeks later. Four days after boosting, the animals were sacrificed, and splenocytes were isolated (Fig. 7A). Then, the number of antigen-specific T cells among splenocytes of vaccinated mice was determined by IFN-γ ELISpot analysis.

No IFN-γ-secreting splenocytes were found in $IFNAR^{-/-}$ mice injected with Opti-MEM (mock), recombinant Ova, HIV-

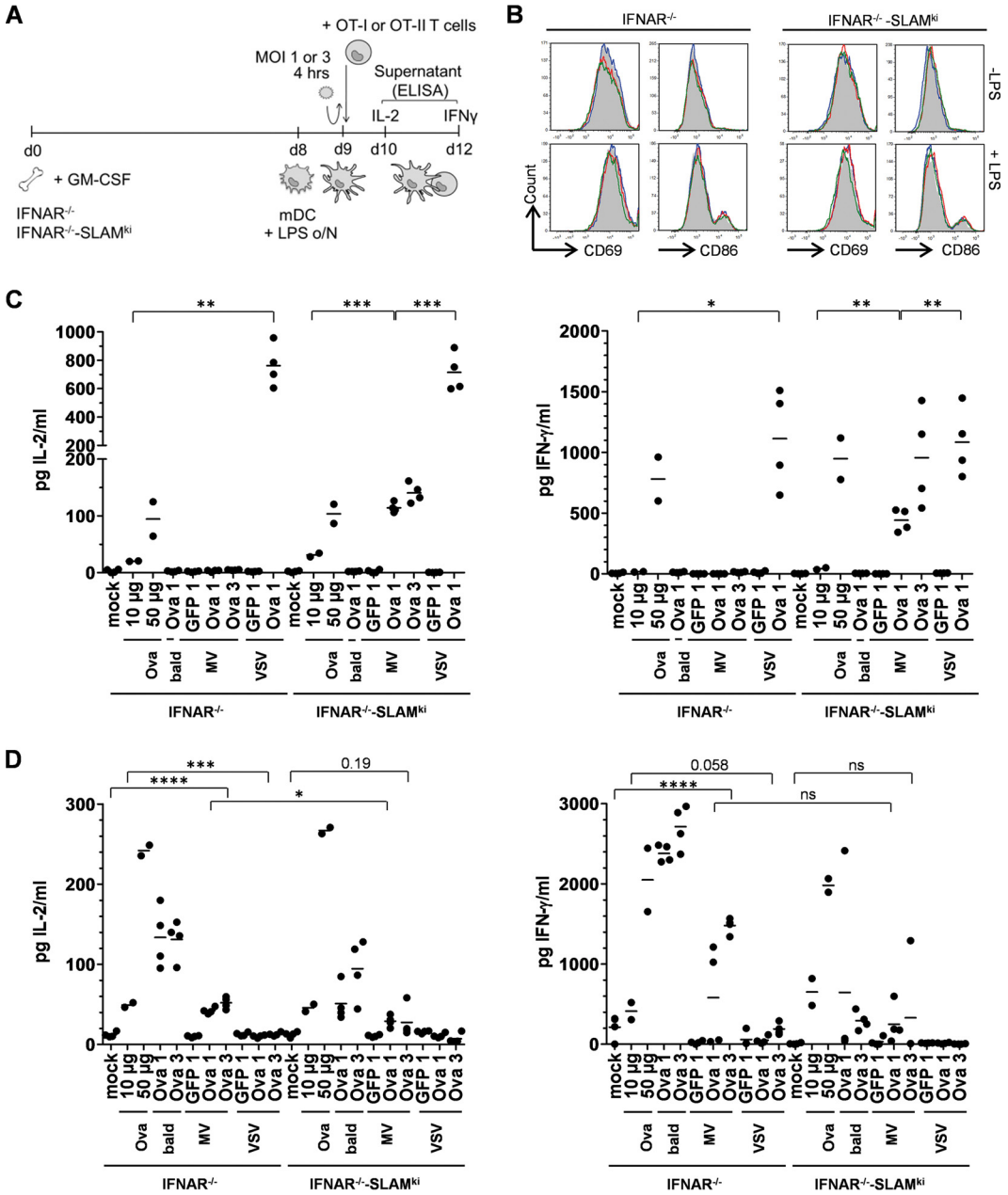

FIG 6 Immunostimulatory properties of *ex vivo*-transduced myeloid dendritic cells. (A) Schematic depiction of experimental procedures. (B) Analysis of immune stimulation by Ova-PTVs. Prestimulated (+LPS) or unstimulated (−LPS) mDCs were mock transduced (gray area) or transduced with HIV-$Ova_{Katushka}$(bald) (green line), HIV-$Ova_{Katushka}$(MV_{wt}) (red line), or HIV-$Ova_{Katushka}$(VSV) (blue line) vector preparations. Expression of CD69 or CD86 among the CD11c-positive DC population was analyzed by flow cytometry at 24 h posttransduction. (C and D) IL-2 or IFN-γ secretion by Ova-specific OT-I (C) or OT-II T cells (D) after incubation with mDCs transduced *ex vivo* with PTV particles transferring either GFP or Ova (MOI of 1 or 3) without envelope GPs (bald) or MV_{wt}-GFPs (MV) or VSV-G (VSV), as indicated, or untransduced mDCs in the presence of 10 µg or 50 µg of recombinant Ova, as indicated. Results of one representative experiment are shown ($n = 4$ for panel C or 2 for panel D). Statistical significance was determined by a two-tailed unpaired Student's *t* test. ns, not significant; *, $P < 0.05$; **, $P < 0.01$; ***, $P < 0.001$; ****, $P < 0.0001$.

$Ova_{Katushka}$(bald), or HIV-$Ova_{Katushka}$(MV_{wt}), thus revealing the absence of Ova-specific T cell induction under these conditions (Fig. 7B). In contrast, splenocytes of IFNAR$^{-/-}$ mice vaccinated with HIV-$Ova_{Katushka}$(VSV) showed a significant release of IFN-γ, i.e., 685.9 ± 750.84 reactive T cells/10^6 splenocytes (restimulated with Ova). Surprisingly, recall of IFN-γ-producing T cells was largely independent of the stimuli used. In line with these findings, no IFN-γ-secreting Ova-specific T cells were observed among splenocytes from mock-vaccinated IFNAR$^{-/-}$-SLAM^{ki} mice and animals vaccinated with HIV-$GFP_{Katushka}$(MV_{wt}) or recombinant soluble Ova (Fig. 7C). In contrast, IFN-γ-secreting T cells were found in splenocytes from IFNAR$^{-/-}$-SLAM^{ki} mice inoculated with HIV-$Ova_{Katushka}$(bald) (101.0 ± 118.0 reactive T cells/10^6 splenocytes), HIV-$Ova_{Katushka}$(MV_{wt}) (212.8 ± 288.2 reactive T

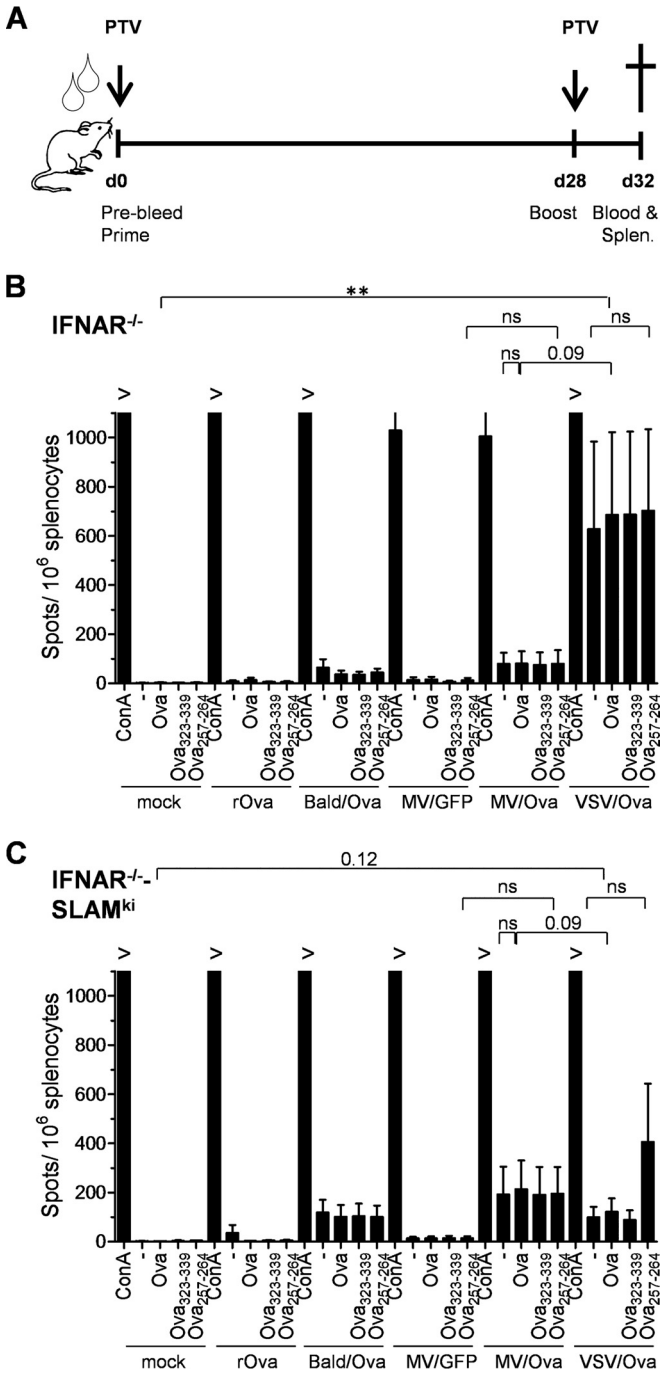

FIG 7 Analysis of immune-stimulatory properties of Ova-PTVs *in vivo*. (A) Schematic depiction of experimental procedures. d, day; Splen., splenocytes. (B and C) IFNAR$^{-/-}$ or IFNAR$^{-/-}$-SLAM^{ki} mice were vaccinated, and freshly isolated splenocytes were subjected to IFN-γ ELISpot analysis. Ova, $Ova_{323–339}$, and $Ova_{257–264}$ were added for antigen-specific recall, whereas ConA-supplemented or pure medium served as a control. >, the number of IFN-γ secreting spots is >1,000. Values are means ± standard errors of the means per group (n = 5 to 6). Statistical significance was determined by a two-tailed Mann-Whitney test (unpaired values between different animal groups) or two-tailed Wilcoxon test (paired values of one animal group). ns, not significant; **, $P < 0.01$.

cells/10^6 splenocytes), or HIV-$Ova_{Katushka}$(VSV) (121.4 ± 134.9 reactive T cells/10^6 splenocytes) but, again, largely independent of the stimuli used for recall.

To identify the cause for the stimulus-independent recall, pooled splenocytes were subsequently fractionated into untouched T cells and other cell types, the latter group containing splenic APCs, by magnetic cell sorting. After overnight incubation in medium containing no IL-2, purified T cells were coincubated with mDCs (generated from nonvaccinated syngeneic IFNAR$^{-/-}$ or IFNAR$^{-/-}$-SLAM^{ki} mice) pulsed with recombinant Ova or Ova-derived immune-dominant peptides for CD8$^+$ or CD4$^+$ T cell responses ($Ova_{257–264}$ or $Ova_{323–339}$, respectively). Alternatively, purified T cells were coincubated with JAWSII and JAWSII-Ova dendritic cells, the latter expressing ovalbumin. T cell reactivity was then determined by IFN-γ ELISpot analysis again. In line with the results obtained for freshly isolated splenocytes, no IFN-γ secretion was observed for cocultures of pulsed mDCs with T cells derived from IFNAR$^{-/-}$ mice injected with Opti-MEM (mock), recombinant Ova, HIV-$Ova_{Katushka}$(bald), HIV-$GFP_{Katushka}$(MV_{wt}), or HIV-$Ova_{Katushka}$(MV_{wt}) (Fig. 8A). As expected, T cells from HIV-$Ova_{Katushka}$(VSV)-injected mice in coculture with pulsed syngeneic mDCs secreted IFN-γ. However, IFN-γ secretion was observed only upon addition of recombinant Ova or $Ova_{257–264}$ peptide, characterizing Ova-specific T cell responses (Fig. 8A). In addition, JAWSII-Ova dendritic cells stimulated cytokine secretion by T cells obtained from HIV-$Ova_{Katushka}$(VSV)-vaccinated IFNAR$^{-/-}$ mice while causing no IFN-γ release by T cells from other experimental cohorts (Fig. 8A). T cells derived from IFNAR$^{-/-}$-SLAM^{ki} mice immunized with Opti-MEM (mock), recombinant soluble Ova, HIV-$Ova_{Katushka}$(bald), and HIV-$GFP_{Katushka}$(MV_{wt}) were not activated upon cocultivation with pulsed mDCs or JAWSII-Ova cells (Fig. 8B). However, IFN-γ was secreted by T cells from HIV-$Ova_{Katushka}$(MV_{wt})- or HIV-$Ova_{Katushka}$(VSV)-vaccinated animals (Fig. 8B). Thus, by comparing IFN-γ secretion by T cells from MV receptor-negative IFNAR$^{-/-}$ (Fig. 8A) and MV receptor-positive IFNAR$^{-/-}$-SLAM^{ki} mice (Fig. 8B), receptor specificity of HIV-$Ova_{Katushka}$(MV_{wt}) could also be demonstrated *in vivo*. T cells from HIV-$Ova_{Katushka}$(VSV)-injected animals were exclusively stimulated by mDCs pulsed with $Ova_{257–264}$. No protein stimulus-dependent recall was observed for T cells from HIV-$Ova_{Katushka}$(MV_{wt})-injected mice, but cocultivation of JAWSII-Ova cells selectively induced IFN-γ production by T cells derived from both HIV-$Ova_{Katushka}$(VSV)- and HIV-$Ova_{Katushka}$(MV_{wt})-vaccinated mice. No IFN-γ secretion was detected by the same T cells upon coculture with JAWSII cells (Fig. 8B), confirming antigen specificity of the T cells.

The retentate fraction of the magnetic cell separation (which contained APCs) was incubated with splenocytes isolated from C57BL/6, OT-I, or OT-II mice that contained no, CD8$^+$, or CD4$^+$ Ova-specific T cells, respectively. These cocultures were subjected to IFN-γ ELISpot analysis to provide evidence for Ova-peptide presentation by APCs from vaccinated animals even 4 days after booster vaccination, cell isolation, storage, and reculture. Interestingly, IFN-γ secretion was indeed observed for at least OT-I T cells in coculture with the retentate of HIV-$Ova_{Katushka}$(VSV)-immunized IFNAR$^{-/-}$ mice (Fig. 8C). These data provide evidence that a singular PTV-mediated antigen transfer induces antigen presentation over a couple of days by transduced APCs. Thereby, the potency of these vectors for prolonged antigen presentation

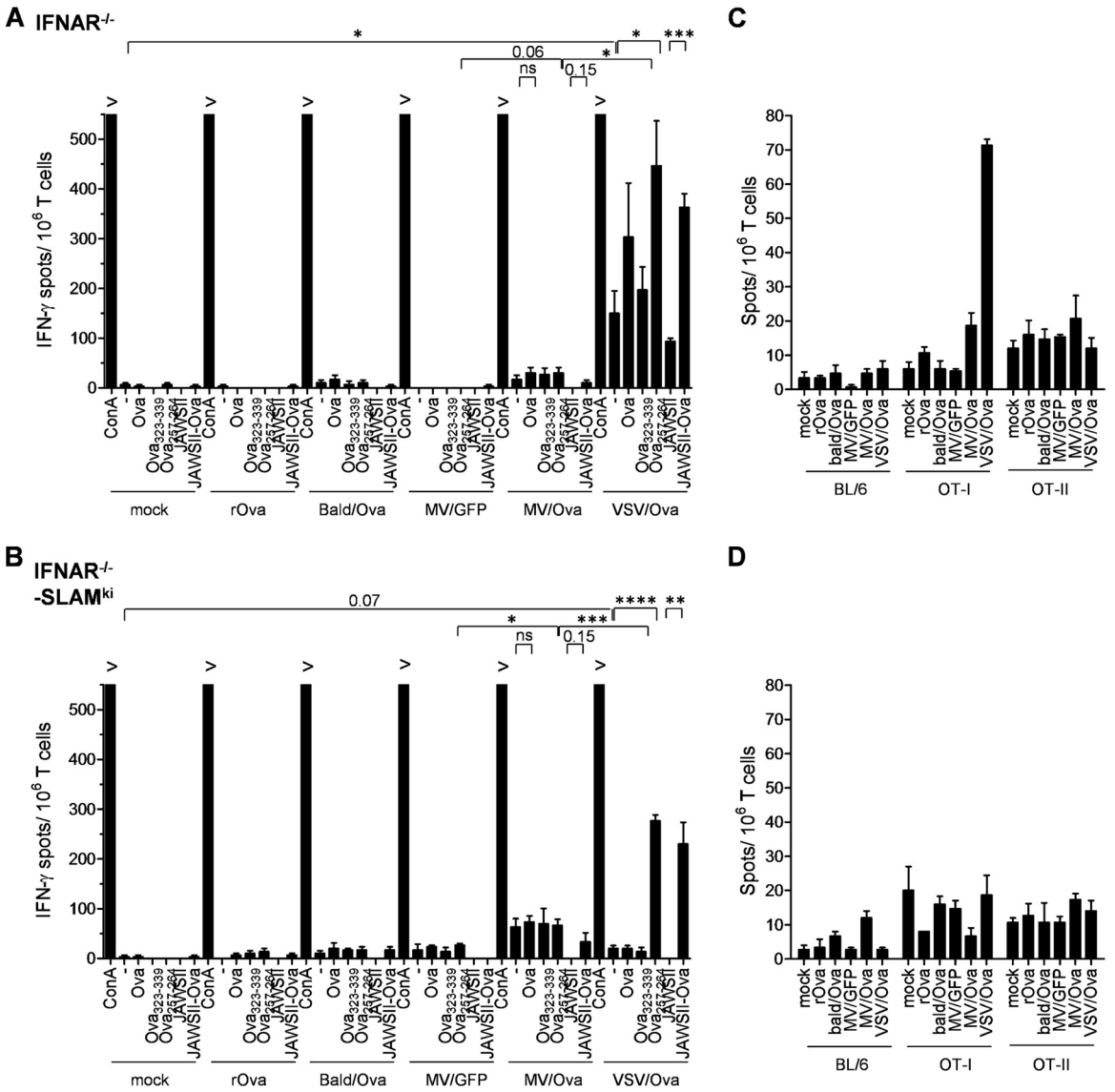

FIG 8 Analysis of splenocytes from vaccinated mice after magnetic bead cell sorting separation into T cells and APC-containing retentate. (A and B) T cells from IFNAR$^{-/-}$ mice or IFNAR$^{-/-}$-SLAM^{ki} mice were cocultivated with syngeneic mDCs pulsed with Ova or immunodominant Ova peptides for CD4$^+$ or CD8$^+$ T cell responses (Ova$_{323–339}$ or Ova$_{257–264}$, respectively). ConA or medium served as a control. In parallel, separated T cells were cocultured with JAWSII or JAWSII-Ova DCs. Stimulation of T cells derived from animals injected with Opti-MEM (mock), recombinant ovalbumin (rOva), HIV-Ova$_{Katushka}$(bald), HIV-GFP$_{Katushka}$(MV$_{wt}$), HIV-Ova$_{Katushka}$(MV$_{wt}$), and HIV-Ova$_{Katushka}$(VSV) was assessed by IFN-γ ELISpot analysis. (C and D) The APC-containing retentate fraction from immunized IFNAR$^{-/-}$ mice (C) or IFNAR$^{-/-}$-SLAM^{ki} mice (D) was cocultured with splenocytes isolated from C57BL/6 (BL/6), OT-I, or OT-II mice. Stimulation of T cells by retentate was analyzed by IFN-γ ELISpot assay. Statistical significance was determined by a two-tailed unpaired Student's *t* test. ns, not significant; *, $P < 0.05$; **, $P < 0.01$; ***, $P < 0.001$; ****, $P < 0.0001$.

and immune stimulation by transduced APCs *in vivo* is indicated. Moreover, these data suggest that the T cell activation by residual Ova-presenting APCs among splenocyte preparations is the reason for the initially observed stimulation-independent recall of T cell activity derived from animals vaccinated with HIV-Ova$_{Katushka}$(VSV), HIV-Ova$_{Katushka}$(MV$_{wt}$), or HIV-Ova$_{Katushka}$(bald).

DISCUSSION

This study demonstrates for the first time the potential of antigen transfer by lentiviral PTVs for the induction of substantial cellular immune responses and thereby the potential for their use as vaccines. Initial characterization of GFP- and Ova-PTVs for receptor specificity on receptor-transgenic CHO cells and B cell lines revealed that vectors pseudotyped with MV$_{wt}$-GPs mediated specific delivery into SLAM-positive cells only, in contrast to broadly transducing VSV-G pseudotyped vectors. Cytoplasmic protein transfer and functionality of the cargo protein were demonstrated by Cre recombinase transfer, which mediated excision of a LoxP-flanked cerulean ORF in receptor-positive indicator cell lines. Moreover, *ex vivo* treatment of primary APCs, i.e., myeloid dendritic cells (mDCs), with Ova-PTVs resulted in stimulation of Ova-specific T lymphocytes upon cocultivation with transduced

mDCs. The immunogenicity of PTVs in mice correlated with the capacity of PTV-inoculated myeloid DCs to stimulate antigen-specific T cells *in vitro*.

Initially, the optimal ratio of Gag/Pol to Gag-cargo/Pol for production of lentiviral PTVs was assessed in order to obtain maximum protein and gene transfer in transduced cells. In principle, PTVs can be used for transient cell modification (22). Nevertheless, it is feasible to generate PTVs which additionally transfer a vector genome encoding, e.g., a marker gene to facilitate detection of transduction and titration of vector stocks (22; this study). In the present study, gene transfer was shown to be ablated when solely Gag-cargo/Pol packaging constructs were used for particle generation. This dysfunction correlated with morphological changes, i.e., disrupted Gag core and the presence of fewer and irregularly arranged envelope proteins. Such morphological changes have been described before and were attributed to discontinuities in the Gag-GFP layer induced by the GFP polypeptide (45). Only GFP-PTV particles containing at least 50% unmodified structural proteins were shown to be infective and indistinguishable by electron microscopy from LV particles transferring no cargo protein. This composition of similar amounts of Gag-cargo/Pol and wild-type Gag/Pol allowing successful particle production has been described also for gammaretroviral particles (22). By successfully generating PTVs transferring ovalbumin or Cre recombinase (in addition to GFP), the variety of proteins introduced into Gag by retroviral particles was expanded. Before, only GFP, cyan fluorescent protein (CFP), monomeric red fluorescent protein (mRFP), yellow fluorescent protein (YFP), Flp recombinase, and β-lactamase had been demonstrated to be amendable for protein transfer by retroviral vectors (46). These cargo proteins were transferred into cells in considerable amounts, as, e.g., demonstrated by Ova-specific immunoblot analysis of PTV-transduced indicator cell lines in this study.

During budding of an HIV-1 particle, approximately 5,000 Gag and Gag/Pol polyproteins assemble (47). Thus, using a 1:1 ratio of untagged *gag* to cargo-tagged *gag* in packaging plasmids, approximately 2,500 cargo protein molecules should be incorporated per vector particle. However, when SLAM-targeted PTV particle preparations were analyzed, only approximately 100 ng of Ova/μg p24 protein and approximately 720 fg of Ova/transducing unit were measured. These data indicate that only about 5.3% of Gag molecules in PTV particles are tagged with Ova, which might reflect increased incorporation of wild-type Gag/Pol in vector particles due to steric requirements. However, 723 fg of Ova corresponds to 9.7×10^6 Ova molecules per transducing unit of HIV-$Ova_{Katushka}(MV_{wt})$. A labeling efficiency of 5.3% indicates the presence of 1.8×10^8 Gag molecules in such preparations, which is sufficient to generate approximately 3.7×10^4 particles given the incorporation of 5,000 Gag molecules per particle. Thus, just 1 in 3.7×10^4 MV_{wt}-GP pseudotyped particles would be infectious. This infectivity is clearly lower than that usually observed for retroviral particles, where 1 in 100 to 1,000 particles is infective (46). Nevertheless, infectivity is clearly codetermined by the glycoproteins used for pseudotyping retroviral vector particles (48, 49) and may vary by at least two logs (49). Accordingly, glycoprotein-specific differences have been observed also in this study when VSV-G or MV-H/F expression plasmids were titrated against the other constituents of PTVs during establishment of PTV generation (Fig. 1F), further strengthening the impact of the comparably low infectivity of MV_{wt} pseudotyped PTV particles when this is assessed by gene transfer. For VSV-G pseudotypes, much higher infectivity can be expected. This, as well as the different entry pathway used, potentially causes degradation of cargo proteins in endocytotic vesicles after VSV-G-triggered endocytosis, thus accounting for the relatively lower protein transfer efficiency mediated by HIV-$GFP_{Katushka}$(VSV) on different target cell lines.

Targeting of PTVs to APCs was accomplished by pseudotyping with modified wild-type MV-GPs due to their natural tropism for SLAM and nectin-4 (24, 50, 51). This tropism was found to be conserved in pseudotyped PTVs, as expected in analogy to lentiviral gene transfer vectors (33–35). Indeed, the similar specificities of protein and gene transfer were also confirmed using CHO cells expressing the MV receptors and naturally receptor-positive cells, with one exception. The marmoset cell line B95a was susceptible for protein transfer but highly resistant to gene transfer at an MOI of 1. This may be explained by expression of the antiviral restriction factor Trim5α in cotton-top tamarin cells (52) such as B95a. Trim5α is well known to cause species-specific premature uncoating of incoming retroviral capsids, thereby interrupting reverse transcription (53), and indeed restricts foamy virus in B95-8 cells (54), the parental cells of the B95a line. In contrast to gene transfer, incoming structural viral proteins are not impeded by this restriction factor.

Interestingly, MV-GPs provide the opportunity to retarget PTV tropism to a plethora of other targets of choice by utilizing engineered MV-GPs with mutations ablating the natural MV receptor tropism but fused with binding domains like single-chain antibodies (scFv) (55) or designed ankyrin repeat proteins (DARPins) (56). With respect to APCs, successful targeting of lentiviral gene transfer vectors to MHC-II molecules has been demonstrated (19) and may be employed for retargeting of PTVs also. On the other hand, inherently stable VSV-G confers very high titers to pseudotyped lentiviral particles (57). This stability may be utilized to achieve protein transfer with overall higher transduction efficacy *in vivo*, as already demonstrated for gene transfer vectors (19). Indeed, when the vectors for vaccination are normalized to protein amounts only, VSV-G pseudotyped Ova-PTVs were shown to be most efficient in inducing Ova-specific immune responses, supporting this hypothesis. MV_{wt}-GP pseudotyped PTVs lagged behind in this setting since infectivity is up to 200-fold lower when vector titers are compared to particle numbers based on p24 ELISA or NanoSight analysis (data not shown). Nevertheless, this method of normalization was used to allow fair comparison of vector particle preparations not only with each other but also with recombinant proteins. Here, PTVs turned out to be much more immunogenic, especially with respect to induction of $CD8^+$ T cells. This phenomenon has already been described for other antigens, e.g., HIV-1 Env presented by virus-like particles (VLPs) eliciting a higher cellular response than soluble forms of Env (58). This could be due to the stimulatory context of the presented antigens in the VLP structure (albeit we did not find evidence of a stimulatory nature of PTV preparations *per se* in our experiments) or due to better uptake of particulate antigen into the APCs (59). Which pseudotype particle will be superior *in vivo* when applied at similar numbers of infectious particles remains to be elucidated in future analyses.

For lentiviral gene transfer vectors transferring antigen-encoding sequences, transduction of APCs *in vivo* has been shown to trigger predominantly $CD8^+$ T cells, irrespective of entry targeting (16, 19) or no entry targeting (60, 61). Predominant induction

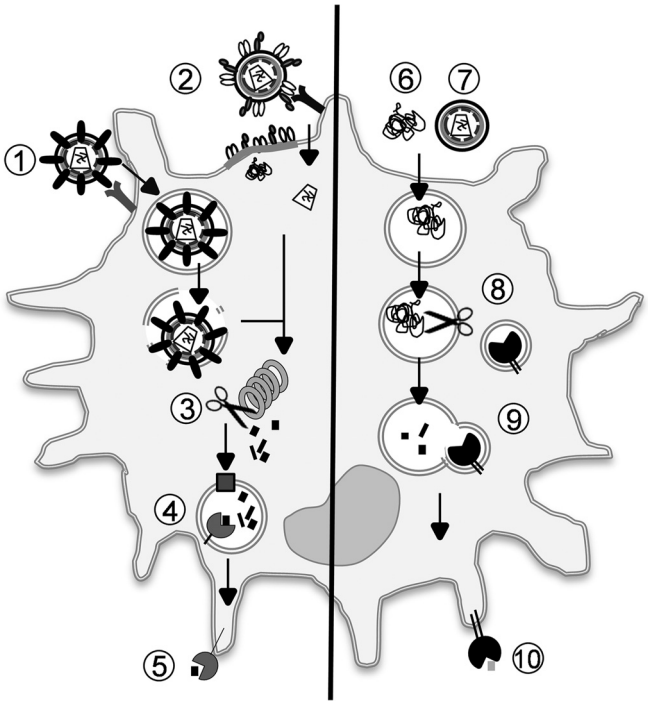

FIG 9 Model for uptake and presentation of PTV-associated antigens. PTV particles incorporating the antigen as a fusion protein with structural proteins of the vector release the antigen from capsids following receptor-dependent, glycoprotein-mediated membrane fusion into the cytoplasm. Thereby, VSV-G pseudotyped particles utilize the endosomal entry pathway (1), whereas pH-neutral entry is catalyzed by MV-GPs at the cellular membrane after receptor contact (2). The released cytoplasmic antigen is then proteasomally processed (3), loaded (4), and presented on MHC class I molecules via the endogenous antigen-presenting pathway (5). In contrast, in the absence of specific glycoprotein-receptor interactions, soluble antigen (6) or particle-associated antigen (7) is taken up by APCs via the endosomal/lysosomal route, followed by lysosomal degradation (8), MHC-II loading (9), and presentation via the exogenous pathway (10).

of $CD8^+$ T cell responses indicates cytoplasmic antigen transfer by PTVs. This is in line with our strategy to release the cargo protein into the target cell's cytosol by insertion of the additional HIV-1 protease cleavage motif, as described before (22) and as demonstrated in our study by cytosolic transfer and subsequent function of Cre recombinase in the respective indicator cell lines. Moreover, Ova protein transfer also occurred exclusively in receptor-positive cells, as assessed by immunoblot analysis after removal of surface-bound virions by citric acid buffer treatment (32). Both experiments indicate cytoplasmic protein transfer and exclude passive surface adhesion of PTV particles. This receptor specificity determined *in vitro* was reflected by receptor-dependent induction of $CD8^+$ T cell responses in *ex vivo* cocultures of PTV-transduced mDCs with Ova-specific T cells and *in vivo* after vaccination of mice with PTVs. In the presence of the cognate cellular receptor, PTVs thus demonstrated the capacity for cytoplasmic antigen transfer and the subsequent stimulation of cellular immune responses by antigen presentation via MHC-I molecules (Fig. 9, left). However, the observed induction of $CD4^+$ T cell responses in the absence of receptor expression indicates receptor-independent, nonspecific uptake of the particulate antigen via the endosomal route, followed by lysosomal antigen processing and presentation by MHC-II (Fig. 9, right). Such pseudotype-independent nonspecific uptake of gammaretroviral and lentiviral particles into human cells has been reported before also for particles pseudotyped with the MV vaccine strain GPs (32). Taken together, these data can be used for proposing a model of PTV interaction with APCs after inoculation and subsequent presentation of peptides via MHC-I or MHC-II (Fig. 9).

Surprisingly, T cell reactivity among splenocytes of vaccinated animals was initially found to be independent of stimuli used for recall 4 days after booster immunization. When isolated T cells tranquilized by overnight cultivation in medium without IL-2 were used, this reactivity vanished but was recalled by antigen-specific stimuli. Interestingly, persisting activation of T cells for a few days after boost vaccination has already been demonstrated, e.g., when activated $CD8^+$ T cells directed against HIV-1 Env were detected 5 days after boosting (62). On the other hand, APCs of PTV-vaccinated mice proved capable of stimulating Ova-specific T cells of nonvaccinated, TCR-transgenic mice. This may be explained by intracellular storage of particle-associated Ova, followed by rather constant processing and antigen presentation, thus resulting in long-lasting T cell activation. Lysosome-like antigen storage organelles, distinct from MHC class I and MHC class II compartments, have been described in mature DCs, which provide an internal antigen source for several days, thereby facilitating a prolonged cytotoxic T cell cross-priming capacity of DCs (63). It will be interesting to elucidate how and why PTV-associated antigens may be processed differently than proteinaceous antigens after uptake by APCs.

In conclusion, we have demonstrated the capacity of PTVs to efficiently mediate (targeted) transfer antigens into APCs, thereby effectively triggering antigen-specific T cell responses *in vitro* and *in vivo*. Thus, PTVs are an effective vaccine, the protective capacity of which will be demonstrated in future studies. Furthermore, the exact mode of action will be a matter of interest, giving room for future enhancement of these vectors.

ACKNOWLEDGMENTS

We thank Y. Yanagi for kindly providing $IFNAR^{-/-}$-$SLAM^{ki}$ mice and CHO-hSLAM cells, M. Lopez for CHO-Nectin 4, R. Cattaneo for CHO-CD46 and B95a, C. Stocking for HT1080-Cre, D. Trono for VSV-G expression plasmid pMD.G2, and B. Fehse for providing LeGO-Cer2. We are indebted to K. Boller and R. Eberle for help with electron microscopy and K.-M. Hanschmann for help with statistical analysis.

This work was supported by BMG grant 2510-FSB-705 to M.D.M. and C.J.B., the LOEWE Center for Cell and Gene Therapy Frankfurt, funded by Hessisches Ministerium für Wissenschaft und Kunst (III L 4-518/17.004; 2010), to C.J.B, and DFG-funded SFB738 to A.S.

REFERENCES

1. **Clem AS.** 2011. Fundamentals of vaccine immunology. J Glob Infect Dis **3:**73–78. http://dx.doi.org/10.4103/0974-777X.77299.
2. **Hilleman MR, Buynak EB, Weibel RE, Stokes J, Whitman JE, Leagus MB.** 1968. Development and evaluation of the Moraten measles virus vaccine. JAMA **206:**587–590. http://dx.doi.org/10.1001/jama.1968.03150030043009.
3. **Buynak EB, Hilleman MR.** 1966. Live attenuated mumps virus vaccine. 1. Vaccine development. Proc Soc Exp Biol Med **123:**768–775. http://dx.doi.org/10.3181/00379727-123-31599.
4. **van Binnendijk RS, van der Heijden RW, van Amerongen G, Uytde-Haag FG, Osterhaus AD.** 1994. Viral replication and development of specific immunity in macaques after infection with different measles virus strains. J Infect Dis **170:**443–448. http://dx.doi.org/10.1093/infdis/170.2.443.
5. **Naim HY.** 2013. Applications and challenges of multivalent recombinant vaccines. Hum Vaccin Immunother **9:**457–461. http://dx.doi.org/10.4161/hv.23220.

6. **Cann AJ, Stanway G, Hughes PJ, Minor PD, Evans DM, Schild GC, Almond JW.** 1984. Reversion to neurovirulence of the live-attenuated Sabin type 3 oral poliovirus vaccine. Nucleic Acids Res **12:**7787–7792. http://dx.doi.org/10.1093/nar/12.20.7787.
7. **Centers for Disease Control and Prevention.** 1996. Measles pneumonitis following measles-mumps-rubella vaccination of a patient with HIV infection, 1993. MMWR Morb Mortal Wkly Rep **45:**603–606.
8. **McAleer WJ, Buynak EB, Maigetter RZ, Wampler DE, Miller WJ, Hilleman MR.** 1992. Human hepatitis B vaccine from recombinant yeast. 1984. Biotechnology **24:**500–502.
9. **Bolhassani A, Yazdi SR.** 2009. DNA immunization as an efficient strategy for vaccination. Avicenna J Med Biotechnol **1:**71–88.
10. **Lewis P, Hensel M, Emerman M.** 1992. Human immunodeficiency virus infection of cells arrested in the cell cycle. EMBO J **11:**3053–3058.
11. **Weinberg JB, Matthews TJ, Cullen BR, Malim MH.** 1991. Productive human immunodeficiency virus type 1 (HIV-1) infection of nonproliferating human monocytes. J Exp Med **174:**1477–1482. http://dx.doi.org/10.1084/jem.174.6.1477.
12. **Neil S, Martin F, Ikeda Y, Collins M.** 2001. Postentry restriction to human immunodeficiency virus-based vector transduction in human monocytes. J Virol **75:**5448–5456. http://dx.doi.org/10.1128/JVI.75.12.5448-5456.2001.
13. **Pion M, Granelli-Piperno A, Mangeat B, Stalder R, Correa R, Steinman RM, Piguet V.** 2006. APOBEC3G/3F mediates intrinsic resistance of monocyte-derived dendritic cells to HIV-1 infection. J Exp Med **203:**2887–2893. http://dx.doi.org/10.1084/jem.20061519.
14. **Banchereau J, Steinman RM.** 1998. Dendritic cells and the control of immunity. Nature **392:**245–252. http://dx.doi.org/10.1038/32588.
15. **Wykes M, Pombo A, Jenkins C, MacPherson GG.** 1998. Dendritic cells interact directly with naive B lymphocytes to transfer antigen and initiate class switching in a primary T-dependent response. J Immunol **161:**1313–1319.
16. **Yang L, Yang H, Rideout K, Cho T, Joo KI, Ziegler L, Elliot A, Walls A, Yu D, Baltimore D, Wang P.** 2008. Engineered lentivector targeting of dendritic cells for in vivo immunization. Nat Biotechnol **26:**326–334. http://dx.doi.org/10.1038/nbt1390.
17. **Bleharski JR, Niazi KR, Sieling PA, Cheng G, Modlin RL.** 2001. Signaling lymphocytic activation molecule is expressed on CD40 ligand-activated dendritic cells and directly augments production of inflammatory cytokines. J Immunol **167:**3174–3181. http://dx.doi.org/10.4049/jimmunol.167.6.3174.
18. **Humbert J, Frecha C, Amirache Bouafia F, N′Guyen TH, Boni S, Cosset F, Verhoeyen E, Halary F.** 2012. Measles virus glycoprotein-pseudotyped lentiviral vectors are highly superior to vesicular stomatitis virus G pseudotypes for genetic modification of monocyte-derived dendritic cells. J Virol **86:**5192–5203. http://dx.doi.org/10.1128/JVI.06283-11.
19. **Ageichik A, Buchholz CJ, Collins MK.** 2011. Lentiviral vectors targeted to MHC II are effective in immunization. Hum Gene Ther **22:**1249–1254. http://dx.doi.org/10.1089/hum.2010.184.
20. **Dai B, Yang L, Yang H, Hu B, Baltimore D, Wang P.** 2009. HIV-1 Gag-specific immunity induced by a lentivector-based vaccine directed to dendritic cells. Proc Natl Acad Sci U S A **106:**20382–20387. http://dx.doi.org/10.1073/pnas.0911742106.
21. **Banasik MB, McCray PB.** 2010. Integrase-defective lentiviral vectors: progress and applications. Gene Ther **17:**150–157. http://dx.doi.org/10.1038/gt.2009.135.
22. **Voelkel C, Galla M, Maetzig T, Warlich E, Kuehle J, Zychlinski D, Bode J, Cantz T, Schambach A, Baum C.** 2010. Protein transduction from retroviral Gag precursors. Proc Natl Acad Sci U S A **107:**7805–7810. http://dx.doi.org/10.1073/pnas.0914517107.
23. **Takeda M, Takeuchi K, Miyajima N, Kobune F, Ami Y, Nagata N, Suzaki Y, Nagai Y, Tashiro M.** 2000. Recovery of pathogenic measles virus from cloned cDNA. J Virol **74:**6643–6647. http://dx.doi.org/10.1128/JVI.74.14.6643-6647.2000.
24. **Tatsuo H, Ono N, Tanaka K, Yanagi Y.** 2000. SLAM (CDw150) is a cellular receptor for measles virus. Nature **406:**893–897. http://dx.doi.org/10.1038/35022579.
25. **Nakamura T, Peng K, Vongpunsawad S, Harvey M, Mizuguchi H, Hayakawa T, Cattaneo R, Russell SJ.** 2004. Antibody-targeted cell fusion. Nat Biotechnol **22:**331–336. http://dx.doi.org/10.1038/nbt942.
26. **Fabre-Lafay S, Garrido-Urbani S, Reymond N, Gonçalves A, Dubreuil P, Lopez M.** 2005. Nectin-4, a new serological breast cancer marker, is a substrate for tumor necrosis factor-alpha-converting enzyme (TACE)/ADAM-17. J Biol Chem **280:**19543–19550. http://dx.doi.org/10.1074/jbc.M410943200.
27. **Kobune F, Sakata H, Sugiura A.** 1990. Marmoset lymphoblastoid cells as a sensitive host for isolation of measles virus. J Virol **64:**700–705.
28. **Galla M, Will E, Kraunus J, Chen L, Baum C.** 2004. Retroviral pseudotransduction for targeted cell manipulation. Mol Cell **16:**309–315. http://dx.doi.org/10.1016/j.molcel.2004.09.023.
29. **Weber K, Thomaschewski M, Warlich M, Volz T, Cornils K, Niebuhr B, Täger M, Lütgehetmann M, Pollok J, Stocking C, Dandri M, Benten D, Fehse B.** 2011. RGB marking facilitates multicolor clonal cell tracking. Nat Med **17:**504–509. http://dx.doi.org/10.1038/nm.2338.
30. **Schülke S, Waibler Z, Mende M, Zoccatelli G, Vieths S, Toda M, Scheurer S.** 2010. Fusion protein of TLR5-ligand and allergen potentiates activation and IL-10 secretion in murine myeloid DC. Mol Immunol **48:**341–350. http://dx.doi.org/10.1016/j.molimm.2010.07.006.
31. **Horton RM, Hunt HD, Ho SN, Pullen JK, Pease LR.** 1989. Engineering hybrid genes without the use of restriction enzymes: gene splicing by overlap extension. Gene **77:**61–68. http://dx.doi.org/10.1016/0378-1119(89)90359-4.
32. **Voelkel C, Galla M, Dannhauser PN, Maetzig T, Sodeik B, Schambach A, Baum C.** 2012. Pseudotype-independent nonspecific uptake of gammaretroviral and lentiviral particles in human cells. Hum Gene Ther **23:**274–286. http://dx.doi.org/10.1089/hum.2011.011.
33. **Anliker B, Abel T, Kneissl S, Hlavaty J, Caputi A, Brynza J, Schneider IC, Münch RC, Petznek H, Kontermann RE, Koehl U, Johnston Ian CD, Keinänen K, Müller UC, Hohenadl C, Monyer H, Cichutek K, Buchholz CJ.** 2010. Specific gene transfer to neurons, endothelial cells and hematopoietic progenitors with lentiviral vectors. Nat Methods **7:**929–935. http://dx.doi.org/10.1038/nmeth.1514.
34. **Funke S, Maisner A, Mühlebach MD, Koehl U, Grez M, Cattaneo R, Cichutek K, Buchholz CJ.** 2008. Targeted cell entry of lentiviral vectors. Mol Ther **16:**1427–1436. http://dx.doi.org/10.1038/mt.2008.128.
35. **Funke S, Schneider IC, Glaser S, Mühlebach MD, Moritz T, Cattaneo R, Cichutek K, Buchholz CJ.** 2009. Pseudotyping lentiviral vectors with the wild-type measles virus glycoproteins improves titer and selectivity. Gene Ther **16:**700–705. http://dx.doi.org/10.1038/gt.2009.11.
36. **Bach P, Abel T, Hoffmann C, Gal Z, Braun G, Voelker I, Ball CR, Johnston Ian CD, Lauer UM, Herold-Mende C, Mühlebach MD, Glimm H, Buchholz CJ.** 2013. Specific elimination of $CD133^+$ tumor cells with targeted oncolytic measles virus. Cancer Res **73:**865–874. http://dx.doi.org/10.1158/0008-5472.CAN-12-2221.
37. **Zufferey R, Nagy D, Mandel RJ, Naldini L, Trono D.** 1997. Multiply attenuated lentiviral vector achieves efficient gene delivery in vivo. Nat Biotechnol **15:**871–875. http://dx.doi.org/10.1038/nbt0997-871.
38. **Rasbach A, Abel T, Münch RC, Boller K, Schneider-Schaulies J, Buchholz CJ.** 2013. The receptor attachment function of measles virus hemagglutinin can be replaced with an autonomous protein that binds Her2/neu while maintaining its fusion-helper function. J Virol **87:**6246–6256. http://dx.doi.org/10.1128/JVI.03298-12.
39. **Ohno S, Ono N, Seki F, Takeda M, Kura S, Tsuzuki T, Yanagi Y.** 2007. Measles virus infection of SLAM (CD150) knockin mice reproduces tropism and immunosuppression in human infection. J Virol **81:**1650–1659. http://dx.doi.org/10.1128/JVI.02134-06.
40. **Richardson CD, Scheid A, Choppin PW.** 1980. Specific inhibition of paramyxovirus and myxovirus replication by oligopeptides with amino acid sequences similar to those at the N-termini of the F1 or HA2 viral polypeptides. Virology **105:**205–222. http://dx.doi.org/10.1016/0042-6822(80)90168-3.
41. **Hogquist KA, Jameson SC, Heath WR, Howard JL, Bevan MJ, Carbone FR.** 1994. T cell receptor antagonist peptides induce positive selection. Cell **76:**17–27. http://dx.doi.org/10.1016/0092-8674(94)90169-4.
42. **Barnden MJ, Allison J, Heath WR, Carbone FR.** 1998. Defective TCR expression in transgenic mice constructed using cDNA-based alpha- and beta-chain genes under the control of heterologous regulatory elements. Immunol Cell Biol **76:**34–40. http://dx.doi.org/10.1046/j.1440-1711.1998.00709.x.
43. **Gerlach N, Schimmer S, Weiss S, Kalinke U, Dittmer U.** 2006. Effects of type I interferons on Friend retrovirus infection. J Virol **80:**3438–3444. http://dx.doi.org/10.1128/JVI.80.7.3438-3444.2006.
44. **Rizzo MA, Springer GH, Granada B, Piston DW.** 2004. An improved cyan fluorescent protein variant useful for FRET. Nat Biotechnol **22:**445–449. http://dx.doi.org/10.1038/nbt945.
45. **Pornillos O, Higginson DS, Stray KM, Fisher RD, Garrus JE, Payne M,**

He G, Wang HE, Morham SG, Sundquist WI. 2003. HIV Gag mimics the Tsg101-recruiting activity of the human Hrs protein. J Cell Biol **162:**425–434. http://dx.doi.org/10.1083/jcb.200302138.

46. **Maetzig T, Baum C, Schambach A.** 2012. Retroviral protein transfer: falling apart to make an impact. Curr Gene Ther **12:**389–409. http://dx.doi.org/10.2174/156652312802762581.
47. **Briggs John AG, Simon MN, Gross I, Kräusslich H, Fuller SD, Vogt VM, Johnson MC.** 2004. The stoichiometry of Gag protein in HIV-1. Nat Struct Mol Biol **11:**672–675. http://dx.doi.org/10.1038/nsmb785.
48. **Steidl S.** 2004. Genetic engineering of onco/lentivirus hybrids results in formation of infectious but not of replication-competent viruses. J Gen Virol **85:**665–678. http://dx.doi.org/10.1099/vir.0.19479-0.
49. **Kahl CA, Marsh J, Fyffe J, Sanders DA, Cornetta K.** 2004. Human immunodeficiency virus type 1-derived lentivirus vectors pseudotyped with envelope glycoproteins derived from Ross River virus and Semliki Forest virus. J Virol **78:**1421–1430. http://dx.doi.org/10.1128/JVI.78.3.1421-1430.2004.
50. **Mühlebach MD, Mateo M, Sinn PL, Prüfer S, Uhlig KM, Leonard Vincent HJ, Navaratnarajah CK, Frenzke M, Wong XX, Sawatsky B, Ramachandran S, McCray PB, Cichutek K, Messling V von, Lopez M, Cattaneo R.** 2011. Adherens junction protein nectin-4 is the epithelial receptor for measles virus. Nature **480:**530–533. http://dx.doi.org/10.1038/nature10639.
51. **Noyce RS, Bondre DG, Ha MN, Lin L, Sisson G, Tsao M, Richardson CD.** 2011. Tumor cell marker PVRL4 (nectin 4) is an epithelial cell receptor for measles virus. PLoS Pathog **7:**e1002240. http://dx.doi.org/10.1371/journal.ppat.1002240.
52. **Goldschmidt V, Ciuffi A, Ortiz M, Brawand D, Muñoz M, Kaessmann H, Telenti A.** 2008. Antiretroviral activity of ancestral TRIM5α. J Virol **82:**2089–2096. http://dx.doi.org/10.1128/JVI.01828-07.
53. **Stremlau M, Perron M, Lee M, Li Y, Song B, Javanbakht H, Diaz-Griffero F, Anderson DJ, Sundquist WI, Sodroski J.** 2006. Specific recognition and accelerated uncoating of retroviral capsids by the TRIM5α restriction factor. Proc Natl Acad Sci U S A **103:**5514–5519. http://dx.doi.org/10.1073/pnas.0509996103.
54. **Yap MW, Lindemann D, Stanke N, Reh J, Westphal D, Hanenberg H, Ohkura S, Stoye JP.** 2008. Restriction of foamy viruses by primate Trim5α. J Virol **82:**5429–5439. http://dx.doi.org/10.1128/JVI.02462-07.
55. **Nakamura T, Peng K, Harvey M, Greiner S, Lorimer Ian AJ, James CD, Russell SJ.** 2005. Rescue and propagation of fully retargeted oncolytic measles viruses. Nat Biotechnol **23:**209–214. http://dx.doi.org/10.1038/nbt1060.
56. **Friedrich K, Hanauer JR, Prüfer S, Münch RC, Völker I, Filippis C, Jost C, Hanschmann K, Cattaneo R, Peng K, Plückthun A, Buchholz CJ, Cichutek K, Mühlebach MD.** 2013. DARPin-targeting of measles virus: unique bispecificity, effective oncolysis, and enhanced safety. Mol Ther **21:**849–859. http://dx.doi.org/10.1038/mt.2013.16.
57. **Burns JC, Friedmann T, Driever W, Burrascano M, Yee JK.** 1993. Vesicular stomatitis virus G glycoprotein pseudotyped retroviral vectors: concentration to very high titer and efficient gene transfer into mammalian and nonmammalian cells. Proc Natl Acad Sci U S A **90:**8033–8037. http://dx.doi.org/10.1073/pnas.90.17.8033.
58. **McBurney SP, Young KR, Ross TM.** 2007. Membrane embedded HIV-1 envelope on the surface of a virus-like particle elicits broader immune responses than soluble envelopes. Virology **358:**334–346. http://dx.doi.org/10.1016/j.virol.2006.08.032.
59. **Bachmann MF, Jennings GT.** 2010. Vaccine delivery: a matter of size, geometry, kinetics and molecular patterns. Nat Rev Immunol **10:**787–796. http://dx.doi.org/10.1038/nri2868.
60. **Esslinger C, Romero P, MacDonald HR.** 2002. Efficient transduction of dendritic cells and induction of a T-cell response by third-generation lentivectors. Hum Gene Ther **13:**1091–1100. http://dx.doi.org/10.1089/104303402753812494.
61. **Palmowski MJ, Lopes L, Ikeda Y, Salio M, Cerundolo V, Collins MK.** 2004. Intravenous injection of a lentiviral vector encoding NY-ESO-1 induces an effective CTL response. J Immunol **172:**1582–1587. http://dx.doi.org/10.4049/jimmunol.172.3.1582.
62. **Haglund K, Leiner I, Kerksiek K, Buonocore L, Pamer E, Rose JK.** 2002. Robust recall and long-term memory T-cell responses induced by prime-boost regimens with heterologous live viral vectors expressing human immunodeficiency virus type 1 Gag and Env proteins. J Virol **76:**7506–7517. http://dx.doi.org/10.1128/JVI.76.15.7506-7517.2002.
63. **van Montfoort N, Camps MG, Khan S, Filippov DV, Weterings JJ, Griffith JM, Geuze HJ, van Hall T, Verbeek JS, Melief CJ, Ossendorp F.** 2009. Antigen storage compartments in mature dendritic cells facilitate prolonged cytotoxic T lymphocyte cross-priming capacity. Proc Natl Acad Sci U S A **106:**6730–6735. http://dx.doi.org/10.1073/pnas.0900969106.

JVI Journals.ASM.org

A Highly Immunogenic and Protective Middle East Respiratory Syndrome Coronavirus Vaccine Based on a Recombinant Measles Virus Vaccine Platform

Anna H. Malczyk,[a,b] Alexandra Kupke,[c,d] Steffen Prüfer,[a] Vivian A. Scheuplein,[a] Stefan Hutzler,[a] Dorothea Kreuz,[e] Tim Beissert,[f] Stefanie Bauer,[e] Stefanie Hubich-Rau,[g] Christiane Tondera,[a] Hosam Shams Eldin,[c,d] Jörg Schmidt,[c,d] Júlia Vergara-Alert,[c,d] Yasemin Süzer,[a] Janna Seifried,[a] Kay-Martin Hanschmann,[h] Ulrich Kalinke,[i,j] Susanne Herold,[k] Ugur Sahin,[f,g] Klaus Cichutek,[a,b] Zoe Waibler,[b,e] Markus Eickmann,[c,d] Stephan Becker,[c,d] Michael D. Mühlebach[a,b]

Oncolytic Measles Viruses and Vaccine Vectors,[a] Novel Vaccination Strategies and Early Immune Responses,[e] and Biostatistics,[h] Paul-Ehrlich-Institut, Langen, Germany; German Center for Infection Research, Langen, Germany[b]; Institut für Virologie, Philipps Universität Marburg, Marburg, Germany[c]; Universities Gießen & Marburg Lung Center, Department of Internal Medicine II, Section of Infectious Diseases, Giessen, Germany[k]; German Center for Infection Research, Marburg, Germany[d]; TRON gGmbH, Mainz, Germany[f]; Universitätsmedizin Mainz, Mainz, Germany[g]; Institute for Experimental Infection Research, TWINCORE, Centre for Experimental and Clinical Infection Research, Hannover, Germany[i]; German Center for Infection Research, Hannover, Germany[j]

ABSTRACT

In 2012, the first cases of infection with the Middle East respiratory syndrome coronavirus (MERS-CoV) were identified. Since then, more than 1,000 cases of MERS-CoV infection have been confirmed; infection is typically associated with considerable morbidity and, in approximately 30% of cases, mortality. Currently, there is no protective vaccine available. Replication-competent recombinant measles virus (MV) expressing foreign antigens constitutes a promising tool to induce protective immunity against corresponding pathogens. Therefore, we generated MVs expressing the spike glycoprotein of MERS-CoV in its full-length (MERS-S) or a truncated, soluble variant of MERS-S (MERS-solS). The genes encoding MERS-S and MERS-solS were cloned into the vaccine strain MV_{vac2} genome, and the respective viruses were rescued (MV_{vac2}-CoV-S and MV_{vac2}-CoV-solS). These recombinant MVs were amplified and characterized at passages 3 and 10. The replication of MV_{vac2}-CoV-S in Vero cells turned out to be comparable to that of the control virus MV_{vac2}-GFP (encoding green fluorescent protein), while titers of MV_{vac2}-CoV-solS were impaired approximately 3-fold. The genomic stability and expression of the inserted antigens were confirmed via sequencing of viral cDNA and immunoblot analysis. *In vivo*, immunization of type I interferon receptor-deficient ($IFNAR^{-/-}$)-CD46Ge mice with 2×10^5 50% tissue culture infective doses of MV_{vac2}-CoV-S(H) or MV_{vac2}-CoV-solS(H) in a prime-boost regimen induced robust levels of both MV- and MERS-CoV-neutralizing antibodies. Additionally, induction of specific T cells was demonstrated by T cell proliferation, antigen-specific T cell cytotoxicity, and gamma interferon secretion after stimulation of splenocytes with MERS-CoV-S presented by murine dendritic cells. MERS-CoV challenge experiments indicated the protective capacity of these immune responses in vaccinated mice.

IMPORTANCE

Although MERS-CoV has not yet acquired extensive distribution, being mainly confined to the Arabic and Korean peninsulas, it could adapt to spread more readily among humans and thereby become pandemic. Therefore, the development of a vaccine is mandatory. The integration of antigen-coding genes into recombinant MV resulting in coexpression of MV and foreign antigens can efficiently be achieved. Thus, in combination with the excellent safety profile of the MV vaccine, recombinant MV seems to constitute an ideal vaccine platform. The present study shows that a recombinant MV expressing MERS-S is genetically stable and induces strong humoral and cellular immunity against MERS-CoV in vaccinated mice. Subsequent challenge experiments indicated protection of vaccinated animals, illustrating the potential of MV as a vaccine platform with the potential to target emerging infections, such as MERS-CoV.

In November 2012, a novel coronavirus was identified for the first time in a patient from Saudi Arabia who presented with severe respiratory disease. Later, this virus was termed Middle East respiratory syndrome coronavirus (MERS-CoV) (1). By 26 December 2014, 938 laboratory-confirmed cases of MERS-CoV, mostly from Saudi Arabia and neighboring countries, had been diagnosed and had resulted in 343 casualties (2). A few cases of MERS-CoV were also detected in the United States, the United Kingdom, Netherlands, Austria, France, Greece, Italy, and Germany, indicating the virus's principal potential for spread (2). Fortunately, direct transmission upon contact with human patients seems to be limited, yet is still possible, as determined by analysis of household contact infections among MERS patients' families (3) and as evidenced by a recent cluster of MERS infections in South Korea, with 166 cases between 20 May and 19 June 2015, including 106 third-generation and 11 fourth-generation cases (4, 5). As a natural reservoir, dromedary camels have been identified as the most likely source, based on partially identical genomes detected in viruses isolated from humans or camels (6, 7). Additionally, antibodies against the spike glycoprotein of MERS-CoV with virus-neutralizing capacity were detected in camels (8–10), and infection of humans with MERS-CoV have been reported after contact with infected camels (11, 12). Interestingly, while all other members of the C lineage of the *Betacoronavirus* genus have been found in different bat species (13, 14), only closely related, most likely precursor viruses of MERS-CoV

have been identified in *Neoromicia capensis* bats (15). Thus, MERS-CoV has a zoonotic origin, but sustained infections, the severity of the disease, and the risk of virus adaption to gain efficient human-to-human transmission mandates the development of effective vaccines to combat local infections and to be prepared for the eventual occurrence of a global pandemic, as previously observed with severe acute respiratory syndrome coronavirus (SARS-CoV) in 2003 (16).

Occurring 10 years before the current MERS-CoV epidemic, SARS-CoV was the first *Betacoronavirus* of zoonotic origin with potentially fatal outcomes in human patients (1). Experimental vaccines protecting animal models against SARS have been developed (17–19), and the properties of such SARS vaccines may be applicable to vaccines that should protect against MERS-CoV infections. Both neutralizing antibodies and T cell responses are essential for prevention of SARS-CoV infection (17, 18). The spike protein (S), a coronavirus class I fusion protein (20, 21), has been identified as the most immunogenic antigen of SARS-CoV, as it induces a strong humoral as well as cellular immune response (17, 19). Similarly, MERS-S constructs expressed by recombinant modified vaccinia virus Ankara or recombinant adenoviral vectors have already been demonstrated to induce neutralizing antibodies (22, 23). The detected neutralizing capacity of induced antibodies is expected, since the receptor-binding domain (RBD) in the S1 domain of both SARS-CoV and MERS-CoV S proteins mediate host-cell receptor binding as a prerequisite for cell entry (24, 25). Thus, S1 is the main target of neutralizing antibodies (26). Also the RBD of MERS-CoV-S alone has been demonstrated to induce strong neutralizing antibody titers (23, 27–31). In combination with different adjuvants, even induction of T cell responses by the recombinant RBD has been described (31). Thus, a prototypic MERS vaccine should be based on MERS-S expression, since the induction of neutralizing antibodies has been shown to be a direct correlate of protection in cases of SARS-CoV (32).

The measles vaccine is an efficient, live attenuated, replicating virus that induces both humoral and cellular immune responses, has an excellent safety record, and probably provides lifelong protection (33, 34). The vaccine's manufacturing process is extremely well established (35), and millions of doses can be generated quite easily and quickly. Generation of recombinant measles virus (MV) from DNA via reverse genetics is feasible (35) and allows the insertion of additional transcription units (ATU) by duplication of sequences terminated by start and stop sequences (36). Hence, genes expressing foreign antigens up to 6 kb can be cloned into the MV backbone (36) and elicit coexpression of MV proteins and inserted genes. Besides marker genes (37) or immune modulators (38), expression of antigens from foreign pathogens like hepatitis B or C virus (39, 40), HIV (41), West Nile virus (WNV) (42, 43), dengue virus (44), Chikungunya virus (CHIKV) (45), or SARS-CoV (19) by recombinant MVs has already been demonstrated. Thereby, robust immune responses against vector and foreign antigens are induced after vaccination of transgenic, MV-susceptible type I interferon receptor-deficient (IFNAR$^{-/-}$)-CD46Ge mice (46) or nonhuman primates with recombinant MVs, in general. In particular, protection of vaccinated animals from lethal challenge with WNV (42) or CHIKV (45) was demonstrated and indicated the high efficacy of the system. Interestingly, prevaccinated animals with protective immunity against measles were still amendable to vaccination with the recombinant MV, since significant immune responses against the foreign antigen(s) are consistently induced (41, 45), and the MV-based CHIKV vaccine demonstrated efficacy in phase I trials irrespective of measles virus immunity (47).

Here, we aimed to utilize the efficacy of the MV vaccine platform to generate a live attenuated vaccine against MERS-CoV based on recombinant MV_{vac2}. This recombinant virus reflects the MV vaccine strain Moraten (48), which has been authorized for vaccination against measles. As the antigen, we choose the MERS-CoV S glycoprotein to induce neutralizing antibodies and robust cellular immunity. Two variants of the glycoprotein were analyzed as antigen: the full-length, membrane-anchored MERS-S, and a truncated, soluble form lacking the transmembrane domain (MERS-solS). Both variants include the S1 domain as a target structure. The soluble protein variant should be taken up better by B cells (49–51) and thus should induce humoral immune responses more efficiently (52), potentially boosting virus-neutralizing antibody titers (VNTs). The respective genes were inserted into two different positions of the MV genome to modulate expression of the antigens, and all recombinant MVs were successfully rescued. Cells infected with such viruses expressed the desired antigens. Indeed, immunization of IFNAR$^{-/-}$-CD46Ge mice induced strong humoral and cellular immune responses directed against MV and MERS-CoV S which were sufficient to protect vaccinated animals from MERS-CoV infection. Thus, MV platform-based vaccines are a powerful option to develop a prepandemic vaccine against MERS-CoV.

MATERIALS AND METHODS

Cells. Vero cell (African green monkey kidney cells; ATCC CCL-81), 293T cell (ATCC CRL-3216), and EL4 mouse T cell (ATCC TIB-39) lines were purchased from ATCC (Manassas, VA, USA) and cultured in Dulbecco's modified Eagle's medium (DMEM) supplemented with 10% fetal bovine serum (FBS; Biochrom, Berlin, Germany) and 2 mM L-glutamine (L-Gln; Biochrom). JAWSII dendritic cells (ATCC CRL-11904) were purchased from ATCC and cultured in minimal essential medium alpha (MEM-α) with ribonucleosides and deoxyribonucleosides (Gibco BRL, Eggenstein, Germany) supplemented with 20% FBS, 2 mM L-Gln, 1 mM sodium pyruvate (Biochrom), and 5 ng/ml murine granulocyte-macrophage colony-stimulating factor (GM-CSF; Peprotech, Hamburg, Germany). DC2.4 and DC3.2 murine dendritic cell lines (53) were cultured in RPMI containing 10% FBS, 2 mM L-Gln, 1% nonessential amino acids (Biochrom), 10 mM HEPES (pH 7,4), and 50 μM 2-mercaptoethanol (Sigma-Aldrich, Steinheim, Germany). All cells were cultured at 37°C in a humidified atmosphere containing 6% CO_2 for a maximum of 6 months of culture after thawing of the original stock.

Received 16 July 2015 **Accepted** 3 September 2015

Accepted manuscript posted online 9 September 2015

Citation Malczyk AH, Kupke A, Prüfer S, Scheuplein VA, Hutzler S, Kreuz D, Beissert T, Bauer S, Hubich-Rau S, Tondera C, Eldin HS, Schmidt J, Vergara-Alert J, Süzer Y, Seifried J, Hanschmann K-M, Kalinke U, Herold S, Sahin U, Cichutek K, Waibler Z, Eickmann M, Becker S, Mühlebach MD. 2015. A highly immunogenic and protective Middle East respiratory syndrome coronavirus vaccine based on a recombinant measles virus vaccine platform. J Virol 89:11654–11667. doi:10.1128/JVI.01815-15.

Editor: S. Perlman

Address correspondence to Michael D. Mühlebach, Michael.Muehlebach@pei.de.

A.K. and S.P. contributed equally.

Plasmids. The codon-optimized gene encoding MERS-CoV-S (GenBank accession number JX869059) flanked with AatII/MluI binding sites in plasmid pMA-RQ-MERS-S was obtained by gene synthesis (Invitrogen Life Technologies, Regensburg, Germany). A truncated form of MERS-S lacking the transmembrane domain was amplified by PCR, flanked with AatII/MluI binding sites, and fully sequenced. Both antigens, as well as the immediate early cytomegalovirus (CMV) promoter (54), were inserted into p(+)BR-MV_{vac2}-GFP(H) or p(+)MV_{vac2}-ATU(P) (48) via AatII/MluI or SfiI/SacII, respectively, to generate p(+)PolII-MV_{vac2}-MERS-S(H), p(+)PolII-MV_{vac2}-MERS-S(P), p(+)PolII-MV_{vac2}-MERS-solS(H), and p(+)PolII-MV_{vac2}-MERS-solS(P), respectively. For construction of lentiviral transfer vectors encoding the MERS-CoV antigens, the open reading frame (ORF) of MERS-S was amplified by PCR with primers encompassing flanking NheI/XhoI restriction sites and template pMA-RQ-MERS-S. Details on primers and PCR procedures are available upon request. PCR products were cloned into pCR2.1-TOPO (Invitrogen Life Technologies) and fully sequenced. Intact antigen ORF was cloned into pCSCW2gluc-IRES-GFP (55) by using NheI/XhoI restriction sites to yield pCSCW2-MERS-S-IRES-GFP.

Production of lentiviral vectors. Viral vectors were produced using 293T cells and polyethylenimine (PEI; Sigma-Aldrich) transfection (56). A total of 1×10^7 293T cells were seeded per 175-cm^2 cell culture flask and cultured overnight. To produce lentivirus vectors pseudotyped with the G protein of vesicular stomatitis virus (VSV-G), these cells were transfected using a standard three-plasmid lentivirus vector system. Cells were transfected with 17.5 μg pCSCW2-MERS-S-IRES-GFP transfer vector, 6.23 μg pMD2.G, and 11.27 μg pCMVΔR8.9 (57), as described previously (58). The medium was exchanged 1 day posttransfection, and $HIV_{MERS\text{-}S\text{-}IRES\text{-}GFP}$ (VSV-G) vector particles were harvested 2 and 3 days after transfection. For harvest of vector particles, the supernatants of three culture flasks were filtered (0.45-μm pore size), pooled, and concentrated by centrifugation (100,000 × *g*, 3 h, 4°C). Pellets were resuspended in DMEM and stored at −80°C.

Generation of antigen-expressing cell lines. Syngeneic target cells based on the C57BL/6-derived DC lines JAWSII, DC2.4, and DC3.2, as well as T cell line EL-4 were transduced with $HIV_{MERS\text{-}S\text{-}IRES\text{-}GFP}$(VSV-G) vector-containing supernatant to express MERS-S and the green marker protein GFP ($JAWSII_{green}$-MERS-S, $EL\text{-}4_{green}$-MERS-S, $DC2.4_{green}$-MERS-S, and $DC3.2_{green}$-MERS-S), thereby presenting respective peptides via major histocompatibility complex class I (MHC-I). EL-4 cells were alternatively transduced with $HIV_{TurboFP635}$(VSV-G) vectors (59) to express red fluorescent Katushka protein as a negative control ($EL\text{-}4_{red}$). For this purpose, 1×10^5 target cells were seeded in 24-well plates and transduced with 0.1, 1, or 10 μl of concentrated vector suspension. For analysis of transduction efficiencies, cells were fixed in 1% paraformaldehyde (Merck Millipore, Darmstadt, Germany), and the percentages of GFP-positive or Katushka-positive cells were quantified by flow cytometry using an LSRII flow cytometer (BD, Heidelberg, Germany). Cell populations revealing a 1 to 10% fraction of GFP-positive cells were used for single-cell cloning by limiting dilution. For that purpose, cell dilutions with 50 μl conditioned medium statistically containing 0.3 cells were seeded per well in 96-well plates. Single-cell clones were cultured and analyzed by flow cytometry. GFP-positive clones were selected for further analysis.

Viruses. The viruses were rescued as described previously (54). In brief, 5 μg of MV genome plasmids with MERS-CoV antigen ORFs were cotransfected with plasmids pCA-MV-N (0.4 μg), pCA-MV-P (0.1 μg), and pCA-MV-L (0.4 μg) encoding MV proteins necessary for genome replication and expression. These plasmids were cotransfected into 293T cells cultured in 6-well plates by using Lipofectamine 2000 (Invitrogen Life Technologies). The transfected 293T cells were overlaid 2 days after transfection onto 50% confluent Vero cells seeded in 10 cm-dishes. Overlay cultures were closely monitored for isolated syncytia, which indicated monoclonal replicative centers. Single syncytia were picked and overlaid onto 50% confluent Vero cells cultured in 6-well plates and harvested as passage 0 (P0) by scraping and a freeze-thaw cycle of cells at the time of maximal infection. Subsequent passages were generated after titration to determine the 50% tissue culture infective dose ($TCID_{50}$) of infectious virus according to the method of Kaerber and Spaerman (60) and infection of Vero cells at a multiplicity of infeciton (MOI) of 0.03. The viruses were passaged up to P10. MERS vaccine viruses and control viruses $MV\text{-}_{vac2}$-GFP(H) and MV_{vac2}-GFP(P) in P3 were used for characterization, and viruses in P4 were used for vaccination. MERS-CoV (isolate EMC/2012) (1) was used for neutralization assays, and challenge virus was propagated in Vero cells and titrated as described above for recombinant MV. All virus stocks were stored in aliquots at −80°C.

Measles virus genome sequence analysis. The RNA genomes of recombinant MV in P3 or P10 were isolated using the QIAamp RNeasy kit (QIAgen, Hilden, Germany) according to the manufacturer's instructions and resuspended in 50 μl RNase-free water. Viral cDNA was reverse transcribed using the SuperScript II reverse transcription (RT) kit (Invitrogen) with 2 μl viral RNA (vRNA) as the template and random hexamer primers, according to manufacturer's instructions. For specific amplification of antigen ORFs, the respective genomic regions of recombinant MVs were amplified by PCR with primers binding to sequences flanking the regions of interest and cDNA as the template. Detailed descriptions of primers and procedures are available upon request. The PCR products were directly sequenced (Eurofins Genomics, Ebersberg, Germany).

Western blot analysis. For Western blot analysis, cells were lysed and immunoblotted as previously described (61). A rabbit anti-MERS-CoV serum (1:1,000) was used as the primary antibody for MERS-CoV-S, and a rabbit anti-MV-N polyclonal antibody (1:25,000; Abcam, Cambridge, United Kingdom) was used for MV-N detection. A donkey horseradish peroxidase (HRP)-coupled anti-rabbit IgG (H&L) polyclonal antibody (1:10,000; Rockland, Gilbertsville, PA) served as the secondary antibody for both. Peroxidase activity was visualized with an enhanced chemiluminescence (ECL) detection kit (Thermo Scientific, Bremen, Germany) on Amersham ECL hyperfilm (GE Healthcare, Freiburg, Germany).

Production of recombinant soluble MERS-CoV spike protein. The S protein lacking the transmembrane domain was genetically tagged with six His residues at its carboxy terminus. The resulting construct was inserted into a Semliki forest virus-derived self-replicating RNA vector (SFV replicon) downstream of the subgenomic promoter. These replicons were transcribed *in vitro* and purified as previously described (62, 63). The integrity of purified replicon was assessed by on-chip electrophoresis (2100 BioAnalyzer; Agilent, Santa Clara, CA). To produce SFV vector particles, replicon RNA and helper RNA were coelectroporated into BHK21 cells by using a square-wave electroporator (one pulse, 750 V/cm for 16 ms; BTX ECM 830; Harvard Apparatus, Holliston, MA). Particles were harvested after 24 h, frozen in N_2 (liquid), and stored at −80°C. For protein production, 2×10^7 BHK21 cells were transduced with SFV particles (MOI, 40) and harvested after 24 h. Cell pellets were lysed (phosphate-buffered saline [PBS], 0.2% Triton X-100, protease inhibitor cocktail [Roche]) for 30 min at 4°C. Afterwards, cells were sonicated, and lysates were cleared by centrifugation (30 min, 21,000 × *g*, 4°C). The supernatant was filtered (0.2 μm), loaded on a HisTrap high-performance (HP) column (17-5247-01; GE Healthcare), and washed with 10 volumes of binding buffer (20 mM Na_2HPO_4, 0.5 M NaCl, 10 mM imidazole). S protein was eluted with a gradient of binding buffer containing 0.5 M imidazole followed by buffer exchange to PBS. Protein integrity was checked by Western blotting with a mouse anti-His monoclonal antibody (MAb; 1:50; Dianova, Germany).

Animal experiments. All animal experiments were carried out in compliance with the regulations of German animal protection laws and as authorized by the RP Darmstadt. Six- to 12-week-old $IFNAR^{-/-}$-CD46Ge mice expressing human CD46 were inoculated intraperitoneally (i.p.) with 1×10^5 $TCID_{50}$ of recombinant MV or 200 μl Opti-MEM on days 0 and 28 and bled via the retrobulbar route on days 7, 28, 32, and 49 postinfection (p.i.) under anesthesia. Serum samples were stored at −20°C. Mice were euthanized on day 32 or 49 p.i., and spleens were isolated. For challenge

experiments, immunized mice were transduced intranasally (i.n.) on day 63 with 20 μl of an adenovirus vector encoding human DPP4 and mCherry with a final titer of 2.5×10^8 PFU per inoculum (AdV-hDPP4; ViraQuest Inc.) and challenged i.n. with 20 μl of MERS-CoV at a final titer of 7×10^4 $TCID_{50}$ on day 68. The mice were euthanized 4 days after challenge, and representative left lobe lung samples were prepared for RNA isolation.

Antibody ELISA. MV bulk antigens (10 μg/ml; Virion Serion, Würzburg, Germany) or recombinant MERS-S protein (20 μg/ml) in 50 μl carbonate buffer (Na_2CO_3 at 30 mM, $NaHCO_3$ at 70 mM; pH 9.6) was used to coat wells of Nunc Maxisorp 96-well enzyme-linked immunosorbent assay (ELISA) plates (eBioscience) and incubated overnight at 4°C. The plates were washed three times with 150 μl ELISA washing buffer (PBS, 0.1% [wt/vol]Tween 20) and blocked with 50 μl blocking buffer (PBS, 5% bovine serum albumin [BSA], 0.1% Tween 20) for 2 h at room temperature. Mice sera sampled on days −7 or 49 were serially diluted in ELISA dilution buffer (PBS, 1% BSA, 0.1% Tween 20), and 50 μl/well was used for the assay. The plates were incubated at 37°C for 2 h and washed again with ELISA washing buffer. Plates were incubated with 50 μl/well of HRP-conjugated rabbit anti-mouse IgG (Dako; 1:1,000 in ELISA dilution buffer) at room temperature for 1 h. Subsequently, the plates were washed and 100 μl tetramethylbenzidine substrate (eBioscience) was added per well. The reaction was stopped by addition of 50 μl/well H_2SO_4 (1 N), and the absorbance at 405 nm was measured.

Neutralization assays. For quantification of VNTs, mouse sera were serially diluted in 2-fold dilutions in DMEM. A total of 50 PFU of MV_{vac2}-GFP(P) or 200 $TCID_{50}$ of MERS-CoV was mixed with serum dilutions and incubated at 37°C for 1 h. Virus suspensions were added to 1×10^4 Vero cells seeded 4 h prior to assay in 96-well plates and incubated for 4 days at 37°C. VNTs were calculated as the reciprocal of the highest dilution that abolished infection.

ELISpot assays. Murine gamma interferon (IFN-γ) enzyme-linked immunosorbent spot (ELISpot) assays (eBioscience, Frankfurt, Germany) were performed according to the manufacturer's instructions using multiscreen immunoprecipitation (IP) ELISpot polyvinylidene difluoride 96-well plates (Millipore, Darmstadt, Germany). A total of 5×10^5 splenocytes isolated 4 days after boost immunization were cocultured with 5×10^4 $JAWSII_{green}$-MERS-S, $DC2.4_{green}$-MERS-S, or $DC3.2_{green}$-MERS-S, or untransduced DC cell lines for 36 h in 200 μl RPMI (10% fetal bovine serum [FBS], 2 nM L-Gln, 1% penicillin-streptomycin). Medium alone served as the negative control. Concanavalin A (ConA; Sigma-Aldrich) at 10 μg/ml was used for demonstration of splenocyte reactivity. Recombinant MV bulk antigens (Virion Serion) at 10 μg/ml were used to analyze MV-specific immune responses in vaccinated animals. Cells were removed from the plates, and the plates were incubated with biotin-conjugated anti-IFN-γ antibodies and avidin-HRP according to the manufacturer's instructions. 3-Amino-9-ethyl-carbazole (AEC; Sigma-Aldrich) substrate solution for development of spots was prepared according to the manufacturer's instructions using AEC dissolved in *N*,*N*-dimethylformamide (Merck Millipore). Spots were counted using an Eli.Scan ELISpot scanner (AE.L.VIS, Hamburg, Germany) and ELISpot analysis software (AE.L.VIS).

T cell proliferation assay. Splenocytes isolated 3 weeks after booster immunization were labeled with 0.5 μM carboxyfluorescein succinimidyl ester (CFSE; eBioscience) as previously described (64). In brief, 5×10^5 labeled cells were seeded in RPMI 1640 supplemented with 10% mouse serum, 2 nM L-glutamine, 1 mM HEPES, 1% penicillin-streptomycin, and 100 μM 2-mercaptoethanol in 96-well plates. Aliquots of 200 μl of medium containing ConA (10 μg/ml), MV bulk antigens (10 μg/ml), or 5×10^3 $JAWSII_{green}$-MERS-S cells were added to each well, and cells were cultured for 6 days. Medium and untransduced JAWSII cells served as controls. Stimulated cells were subsequently stained with CD3-PacBlue (1:50; clone 500A2; Invitrogen Life Technologies) and CD8-allophycocyanin (1:100; clone 53-6.7; eBioscience) antibodies and fixed with 1% paraformaldehyde (PFA) in PBS. Stained cells were analyzed by flow cytometry using an LSR II flow cytometer (BD) and FACSDiva software (BD).

Cytotoxic T lymphocyte (CTL) killing assay. For restimulation of T cells isolated 4 days after booster immunization, 5×10^6 splenocytes were cocultured with 5×10^4 $JAWSII_{green}$-MERS-S cells for 6 days in 12-well plates in RPMI 1640 supplemented with 10% FBS, 2 nM L-glutamine, 1 mM HEPES, 1% penicillin-streptomycin, 2-mercaptoethanol (100 μM), and 100 U/ml recombinant interleukin-2 (rIL-2; murine, Peprotech). A total of 2×10^3 $EL\text{-}4_{red}$ cells were labeled with 0.5 μM CFSE and mixed with 8×10^3 $EL\text{-}4_{green}$-MERS-S cells per well. Splenocytes were counted and cocultured with EL-4 target cells at the indicated ratios for 4 h. Afterwards, EL-4 cells were labeled with the fixable viability dye eFluor 780 (eBioscience), fixed with 1% PFA, and analyzed by flow cytometry using an LSR II flow cytometer (BD) and FACSDiva software (BD). For determination of the antigen:NC EL-4 ratio, cell counts of living MERS-S-expressing cells were divided by the counts for living negative controls.

Determination of viral RNA copy numbers and infectious virus in mouse tissue. Samples of immunized and challenged mice (6- by 6-mm tissue slices of approximately 0.035 ± 0.011 g [mean ± standard deviation]) excised from the centers of left lung lobes were homogenized in 1 ml DMEM with ceramic beads (diameter, 1.4 mm) in a FastPrep SP120 instrument three times for 40 s at 6.5 m/s. The homogenate was centrifuged for 3 min at 2,400 rpm in a Mikro 200R centrifuge (Hettich Lab Technology) to remove tissue debris. Live virus titers in supernatant (in $TCID_{50}$ per milliliter) were determined on Vero cells as described above. Aliquots of 100 μl of the supernatants were used for RNA isolation with the RNeasy minikit (Qiagen) according to the manufacturer's instructions. The RNA amount was measured with the NanoDrop ND-100 spectrophotometer. Total RNA was reverse transcribed and quantified by real-time PCR using the SuperScript III OneStep RT-PCR System (Invitrogen Life Technologies) as described previously (65) with the primer pair upE-Fwd and upE-Rev and the probe upE-Prb on an ABI7900 high-throughput fast real-time PCR system (Life Technologies Instruments).

Additionally, for every sample of the transduced and infected mice, evidence for successful hDPP4 transduction was determined by real-time RT-PCR for mCherry with the OneStep RT-PCR kit on a Rotor Gene Q apparatus (both from Qiagen). Primers and probe (Tib-Molbiol, Berlin, Germany) were as follows: mCherry forward, CATGGTAACGATGAGT TAG; mCherry reverse, GTTGCCTTCCTAATAAGG; mCherry probe, 6-carboxyfluorescein (FAM)–TACCACCTTACTTCCACCAATCGG–BBQ (BlackBerry quencher). Primers and probe were used at final concentrations of 0.4 μM and 0.2 μM, respectively. The quantitative reverse transcription-PCR (qRT-PCR) program was as follows: 50°C for 30 min; 95°C for 15 min; 40 cycles of 95°C for 15 s, 48°C for 30 s, and 72°C for 20 s. All samples for mCherry were evaluated in one run to exclude an impact of different conditions on the results in different runs. Quantification was carried out using a standard curve based on 10-fold serial dilutions of appropriate cloned RNA ranging from 10^2 to 10^5 copies. Briefly, PCR fragments were generated using the primers described above. For cloning, the TOPO TA cloning kit with pCR2.1-TOPO plasmid (Invitrogen) and *Escherichia coli* were used. Inserts were examined for correct orientation and length, amplified with plasmid-specific primers, purified, and transcribed into RNA by using the SP6/T7 transcription kit (Roche).

Histopathological and immunohistochemical examination of lung tissue. Lungs of vaccinated and mock-vaccinated mice transduced with AdV-hDPP4 were collected on day 4 postchallenge with MERS-CoV. Tissue was fixed in 4% PFA and embedded in paraffin. Sections were cut with a Leica RM2255 microtome (Leica Biosystems) and stained with hematoxylin and eosin (H&E). For detection of MERS-CoV, a rabbit polyclonal antibody against MERS-CoV spike protein S1 (100208-RP; Sino Biological Inc., Beijing, China) diluted 1:50 was used. To monitor adenovirus transduction, a mouse monoclonal antibody against mCherry (ab125096; Abcam) diluted 1:250 was used after antigen retrieval with target retrieval solution (Dako) for 23 min at 97°C. To block unspecific binding, slides were incubated for 10 min with 20% nonimmune pig serum (MERS-

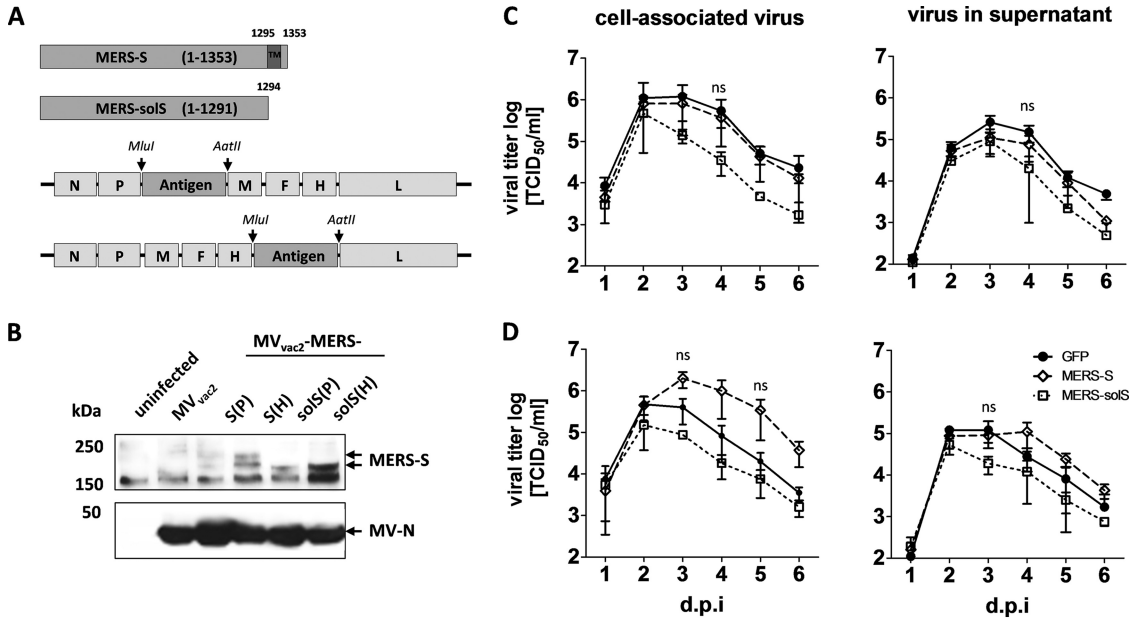

FIG 1 Generation and characterization of MV_{vac2}-MERS-S and MV_{vac2}-MERS-solS. (A) Schematic depiction of full-length MERS-S and a soluble variant lacking the transmembrane and cytoplasmatic region (MERS-solS) (upper schemes) and recombinant MV_{vac2} genomes used for their expression (lower schemes). Antigen or antigen-encoding genes are depicted in dark gray; MV viral gene cassettes (light gray) are annotated. MluI and AatII restriction sites used for cloning of antigen-encoding genes into post-P or post-H ATU are highlighted (B) Immunoblot analysis of Vero cells infected at an MOI of 0.03 with MV_{vac2}-MERS-S, MV_{vac2}-MERS-solS, or MV_{vac2}-GFP(H) (MV_{vac2}), as depicted above the lanes. Uninfected cells served as mock controls. Blots were probed using rabbit serum reactive against MERS-CoV (upper blot) or mAb reactive against MV-N (lower blot). Arrows indicate specific bands. (C and D) Growth kinetics of recombinant MV on Vero cells infected at an MOI of 0.02 with MV_{vac2}-MERS-S (MERS-S), MV_{vac2}-MERS-solS (MERS-solS), or MV_{vac2}-GFP encoding extra genes in post-H (C) or post-P (D) ATU. Titers of samples prepared at the indicated time points postinfection were determined on Vero cells. Means and standard deviations of three independent experiments are presented. ns, not significant.

CoV) or for 30 min with 20% nonimmune horse serum (mCherry). Primary antibodies were incubated overnight at 4°C. A pig anti-rabbit IgG and a biotinylated horse anti-mouse IgG served as secondary antibodies for MERS-CoV and mCherry, respectively. For detection of antigen-antibody complexes, the ABC method for mCherry and the rabbit PAP method for MERS-CoV were used in combination with diaminobenzidine for staining. Papanicolaou stain was used for counterstaining.

Statistical analysis. To compare the means of different groups from growth curves, neutralization assays, and ELISpot assays, a nonparametric one-way analysis of variance (one-way ANOVA) was performed. For the proliferation assay, the mean differences between control and vaccinated groups were calculated and analyzed by using an unpaired *t* test. To all three groups in the CTL killing assays, a linear curve was fitted for antigen versus the log-transformed effector-target ratio (E:T). The *P* values for differences in slopes were calculated, and MV_{vac2}-MERS-S(H) or MV_{vac2}-MERS-solS(H) was compared with the control, MV_{vac2}-ATU(P). For analysis of challenge data, mean ratios and 95% confidence intervals were calculated based on log-transformed and back-transformed data. The ratio, instead of the difference, was chosen due to the rather log-normal distribution of the data. The widths of the confidence intervals caused high variability of the data, and limited sample sizes were used ($n = 10$ observations each). For comparisons between groups, the Wilcoxon two-sample test was used. *P* values were not adjusted for multiple comparisons due to the explorative character of the study.

RESULTS

Generation and expression of MERS-CoV-S by recombinant MV_{vac2}. Since the spike protein (S) of SARS-CoV has been shown to potently induce humoral and cellular immune responses, MERS-S was chosen as the appropriate antigen to be expressed by the recombinant MV vaccine platform. In addition to full-length MERS-S, a truncated form lacking the transmembrane and cytoplasmic domains (MERS-solS), was cloned into two different ATUs either behind P (post-P) or H (post-H) cassettes of the vaccine strain MV_{vac2} genome (Fig. 1A). Virus clones of all recombinant genomes were successfully rescued and amplified up to P10 in Vero cells, with titers of up to 6×10^7 $TCID_{50}$/ml. The stability of the viral genomes was demonstrated via sequencing of viral genomes after RT-PCR (data not shown). Besides the exclusion of mutations or deletions of the antigen-encoding genes, the verification of antigen expression is essential for vaccine function and, thus, virus characterization. Western blot analysis of Vero cells infected with the different MV_{vac2}-MERS vaccines revealed expression of the antigen (Fig. 1B). Interestingly, the expression of both S and solS was higher when cells were infected with viruses encoding antigens in post-H ATU compared to the post-P constructs. Therefore, growth kinetics were analyzed to check if the insertion or expression of the S antigen variants into or by recombinant MV, respectively, impaired the vaccines' replication (Fig. 1C and D). For that purpose, the vaccine viruses containing the MERS-S or MERS-solS gene in post-H (Fig. 1C) or post-P (Fig. 1D) positions were analyzed in parallel to the corresponding MV_{vac2}-GFP control viruses. MV_{vac2} encoding full-length, membrane-bound MERS-S grew comparably to the control viruses; only MV_{vac2}-MERS-solS(P) (Fig. 1D) and MV_{vac2}-MERS-solS(H) (Fig. 1C) revealed an approximately 3-fold-reduced maximal virus titer, albeit no statistical significance was observed [1.5×10^5 $TCID_{50}$/ml for MV_{vac2}-MERS-solS(P) and 4.7×10^5 $TCID_{50}$/ml for MV_{vac2}-MERS-solS(H) versus 4.7×10^5 for MV_{vac2}-GFP(P)

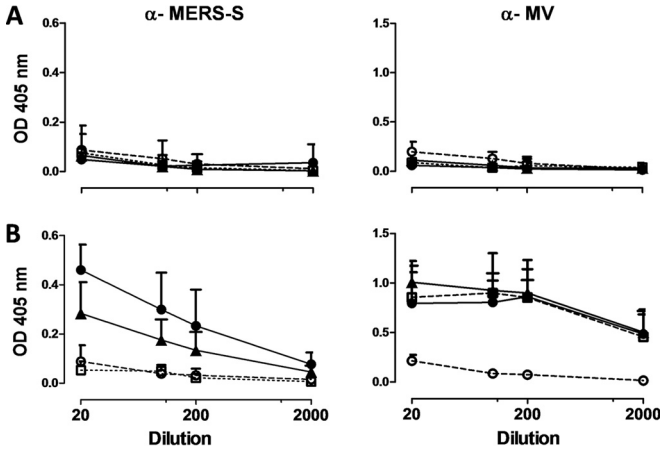

FIG 2 Induction of antibodies that specifically bind MERS-S (α-MERS-S) or MV (α-MV) antigens. Sera of mice vaccinated on days 0 and 28 with indicated viruses were sampled on days −7 (prebleed, A) and 49 (B) and analyzed for antibodies that bound MERS-S or MV bulk antigens by ELISA. Medium-inoculated mice served as mock controls. Antibodies binding to recombinant MERS-S or MV bulk antigens were detected at an optical density of 405 nm in the ELISA. Means and standard deviations of each group are depicted ($n = 6$). Filled triangles, MV_{vac2}-MERS-S(H); filled circles, MV_{vac2}-MERS-solS(H); open circles, mock controls; open squares, MV_{vac2}-ATU(P).

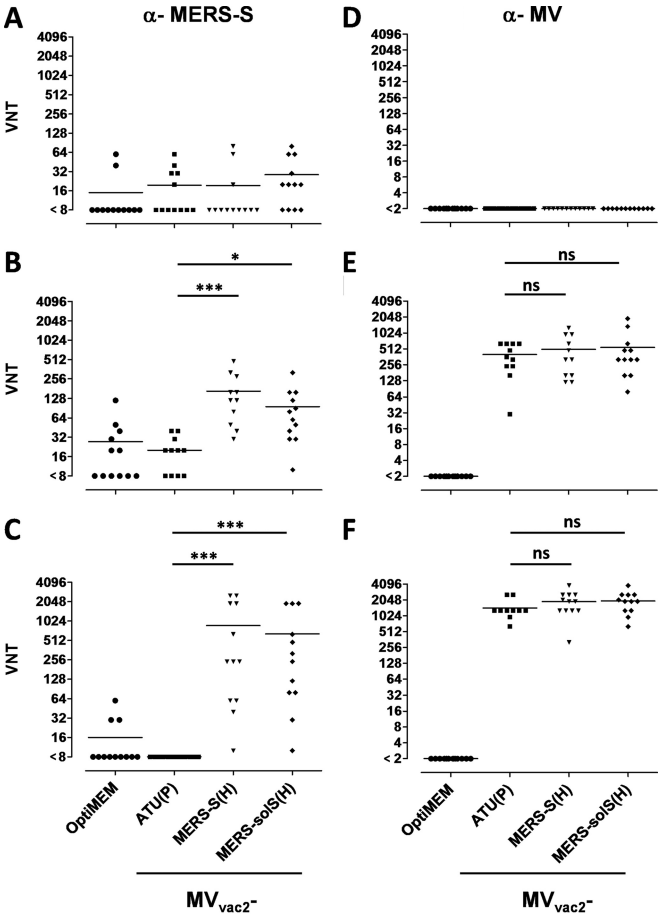

FIG 3 Analysis of neutralizing antibodies. VNTs for animals vaccinated on days 0 and 28 with the indicated viruses and sampled on day −7 (A and D), 28 (B and E), or 49 (C and F) for complete neutralization of 200 $TCID_{50}$ of MERS-CoV or 50 PFU of MV. Medium-inoculated mice served as mock controls. VNTs were calculated as reciprocals of the highest dilution abolishing infectivity. Dots represent single animals ($n = 10$); horizontal lines represents mean per group. The *y* axis starts at the detection limit; all mice with VNTs at the detection limit had no detectable VNT. ns, not significant; *, $P < 0.05$; ***, $P < 0.0001$.

and 1.2×10^6 $TCID_{50}$/ml for MV_{vac2}-GFP(H)] (Fig. 1C). Thus, cloning and rescue of MVs expressing MERS-CoV antigens, even at the cost of an 4,049 bp additional genome length, were achieved easily and relative quickly. All constructs expressed the inserted antigens without significant impact on viral replication.

Antibodies with neutralizing capacity directed against MV or MERS-CoV are induced by MV_{vac2}-MERS-S and MV_{vac2}-MERS-solS. To test the efficacy of the MV_{vac2}-MERS vaccines *in vivo*, genetically modified $IFNAR^{-/-}$-CD46Ge mice were chosen, since they are the prime small animal model for analysis of MV-derived vaccines (46). Based on the higher antigen expression of MERS-S and MERS-solS if cloned into the post-H position of the MV genome, the respective viruses were used for vaccination. Thus, 6 mice per group were inoculated via the i.p. route on days 0 and 28, each time with 1×10^5 $TCID_{50}$ of MV_{vac2}-MERS-S(H), MV_{vac2}-MERS-solS(H), or MV_{vac2}-ATU(P), the latter a recombinant control virus without an insertion of a foreign antigen-encoding gene cassette into an otherwise-empty additional transcription unit. Medium-inoculated mice served as negative controls. At 21 days after boost immunization, sera of immunized mice were compared to prebleed sera by ELISA on antigen-coated plates for antibodies binding to MV bulk antigens or MERS-S (Fig. 2A and B). Indeed, sera of mice vaccinated with MV_{vac2}-MERS-S(H) or MV_{vac2}-MERS-solS(H) clearly encompassed IgG binding to MERS-S (Fig. 2B), whereas no antibodies were found in mice before vaccination (Fig. 2A) or in control mice. Moreover, sera of mice vaccinated with any recombinant MV had IgG in the serum that bound to MV bulk antigens, as expected, indicating successful vaccination with MVs and general mouse reactivity. To determine the neutralizing capacity of the induced antibodies, the potential of serum dilutions to neutralize 200 $TCID_{50}$ of MERS-CoV or 50 PFU of MV_{vac2}-GFP(H) (Fig. 3A to C) was assayed. All mice immunized with recombinant MV (including the control virus) indeed developed MV VNTs already after the first immunization (Fig. 3B). These titers were boosted approximately 6-fold upon the second immunization (512 to 3,072 VNT) (Fig. 3C). Evidence for induction of neutralizing antibodies against MERS-CoV was only found in mice vaccinated with MV_{vac2}-MERS-S(H) or MV_{vac2}-MERS-solS(H), as expected. The VNT against MERS-CoV reached a titer of 96 to 167 after the first immunization (Fig. 3B) and was boosted about 5- to 7-fold by the second immunization (Fig. 3C). Mice immunized with MV_{vac2}-MERS-S(H) induced slightly higher MERS-CoV VNTs than did MV_{vac2} expressing the truncated form of the spike protein (167 versus 96 after the first and 874 versus 640 after the second immunization) (Fig. 3B and C). However, this difference was not statistically significant. No VNTs against MV or MERS-CoV were detected in control mice inoculated with medium alone. In summary, both recombinant MVs expressing MERS-S or MERS-solS specifically induced significant amounts of antibodies in immunized mice capable of neutralizing MV as well as MERS-CoV.

Splenocytes of animals vaccinated with MV_{vac2}-MERS-S or MV_{vac2}-MERS-solS secrete IFN-γ upon MERS-S-specific stimulation. To analyze the ability of MV-based vaccine viruses to in-

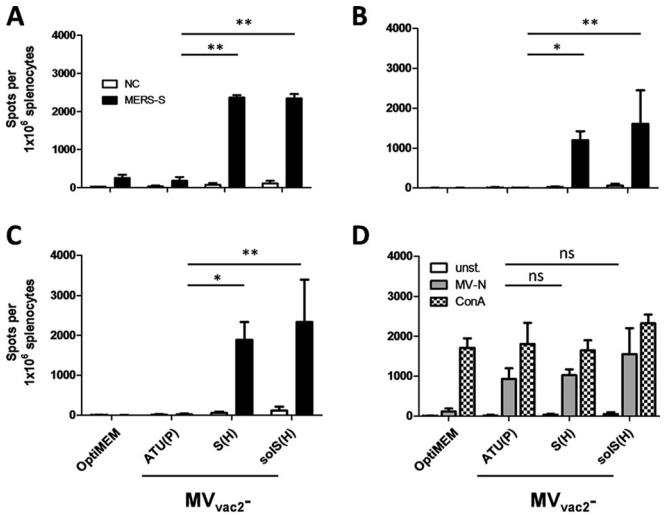

FIG 4 Secretion of IFN-γ after antigen-specific restimulation of splenocytes. (A to C) IFN-γ ELISpot analysis results with splenocytes of mice vaccinated on days 0 and 28 with indicated viruses, isolated 4 days after boost immunization and after coculture with JAWSII (A), DC2.4 (B), or DC3.2 (C) dendritic cell lines transgenic for MERS-S or untransduced controls (NC). (D) To analyze cellular responses directed against MV, splenocytes were stimulated with 10 μg/ml MV bulk antigens (MV-N) or left unstimulated (unst.). The reactivity of splenocytes was confirmed by ConA treatment (10 μg/ml). Presented are means and standard deviation per group ($n = 6$). ns, not significant; *, $P < 0.05$; **, $P < 0.01$.

duce MERS-CoV-specific cellular immune responses, splenocytes of animals vaccinated with MV_{vac2}-MERS-S(H) or MV_{vac2}-MERS-solS(H), or control animals inoculated with medium or MV_{vac2}-ATU(P), were analyzed for antigen-specific IFN-γ secretion by ELISpot assay. For this purpose, mice were immunized following the described prime-boost scheme, and splenocytes were isolated 4 days after the second immunization. To restimulate the antigen-specific T cells *in vitro*, syngeneic murine DC cell lines (JAWSII, DC2.4, and DC3.2) had been genetically modified by lentiviral vector transduction to stably express MERS-S protein and thereby presented the respective T cell MHC epitopes. Single-cell clones were derived by flow cytometric sorting of single GFP-positive cells. Antigen expression by transduced DCs was verified by Western blot analysis (data not shown).

ELISpot assays using splenocytes of vaccinated animals in coculture with JAWSII-MERS-S revealed about 2,400 IFN-γ-secreting cells per 1×10^6 splenocytes after immunization with MV_{vac2}-MERS-S or MV_{vac2}-MERS-solS (Fig. 4A). In contrast, control mice revealed a background response of about 200 IFN-γ-producing cells per 1×10^6 splenocytes. As expected, restimulation of T cells by JAWSII presenting no exogenous antigen revealed only reactivity in the background range (Fig. 4A). To rule out clonal or cell line-associated artifacts, antigen-specific IFN-γ secretion by splenocytes of MV_{vac2}-MERS-S- or MV_{vac2}-MERS-solS-vaccinated mice was confirmed by stimulation with transgenic DC2.4 (Fig. 4B) or DC3.2 (Fig. 4C) cell clones expressing MERS-S. These cell lines stimulated 1,200 to 2,300 IFN-γ-secreting cells per 1×10^6 splenocytes in animals receiving the recombinant MERS vaccines, whereas no background stimulation of respective controls was observed. The differences between MV control and MV_{vac2}-MERS-S- or MV_{vac2}-MERS-solS-vaccinated mice were significant for all cell lines. Additionally, cellular immune responses targeting MV antigens were detected upon stimulation with MV bulk antigens in vaccinated mice that had received any recombinant virus, as expected. However, MV bulk antigens stimulated only about 930 to 1,500 IFN-γ-secreting cells per 1×10^6 splenocytes of MV-vaccinated animals. Finally, splenocytes of all mice revealed a similar basic reactivity to unspecific T cell stimulation, as confirmed by similar numbers of IFN-γ-secreting cells upon ConA treatment (Fig. 4D). Remarkably, both stimulation by ConA or MV bulk antigens resulted in lower numbers of IFN-γ^+ cells than stimulation by DCs expressing MERS-S, indicating an extremely robust induction of cellular immunity against this antigen. Thus, the generated MV-based vaccine platform expressing MERS-S or MERS-solS not only induces humoral but also strong MERS S-specific cellular immune responses.

MV_{vac2}-MERS-S(H) or MV_{vac2}-MERS-solS(H) induce antigen-specific $CD8^+$ CTLs. While ELISpot analyses revealed antigen-specific IFN-γ secretion by vaccinated mice's T cells, we next aimed at detecting antigen-specific $CD8^+$ CTLs, which would be important for clearance of virus-infected cells. For that purpose, proliferation of $CD8^+$ T cells upon stimulation with MERS-S was analyzed 3 weeks after the boost via a flow cytometric assay. Mice were immunized as described above, and splenocytes were isolated 21 days after the boost. JAWSII cells expressing MERS-S were used for restimulation of MERS-S-specific T cells. The splenocytes were labeled with CFSE and subsequently cocultured with JAWSII-MERS-S cells or, as a control, with parental JAWSII cells for 6 days and finally stained for CD3 and CD8 before being analyzed by fluorescence-activated cell sampling for proliferation, detectable by the dilution of the CFSE stain due to cell division.

T cells of mice vaccinated with MV_{vac2}-MERS-S or MV_{vac2}-MERS-solS revealed an increase in the population of $CD3^+$ $CD8^+$ $CFSE^{low}$ cells after restimulation with JAWSII-MERS-S cells compared to restimulation with parental JAWSII without MERS antigens (Fig. 5A). In contrast, T cells of control mice did not reveal this pattern, but the $CFSE^{low}$ population remained rather constant, as expected. This specific increase in $CD3^+$ $CD8^+$ $CFSE^{low}$ cells, which was significant for MV_{vac2}-MERS-S-vaccinated and nearly significant ($P = 0.0505$) for MV_{vac2}-MERS-solS-vaccinated mice, indicated that $CD3^+$ $CD8^+$ CTLs specific for MERS-S proliferated upon respective stimulation. Thus, MERS-specific cytotoxic memory T cells are induced in mice after vaccination with MV_{vac2}-MERS-S(H) or MV_{vac2}-MERS-solS(H).

Induced T cells revealed antigen-specific cytotoxicity. To demonstrate the effector ability of induced CTLs, a killing assay was performed to directly analyze antigen-specific cytotoxicity (Fig. 5B). Splenocytes of immunized mice isolated 4 days post-booster vaccination were cocultured with JAWSII-MERS-S or the nontransduced control JAWSII cells for 6 days to restimulate antigen-specific T cells. When these restimulated T cells were coincubated with a defined mixture of $EL\text{-}4_{green}$-MERS-S target and $EL\text{-}4_{red}$ control cells (ratio, 4:1), only T cells from MV_{vac2}-MERS-S(H)-vaccinated or MV_{vac2}-MERS-solS(H)-vaccinated mice significantly shifted the ratio of live MERS-S-expressing target cells to control cells in a dose-dependent manner (Fig. 5B). This antigen-dependent killing was also dependent on restimulation with JAWSII-CoV-S cells, since naive T cells did not shift significantly the ratios of target to nontarget cells.

These results indicated that CTLs isolated from MV_{vac2}-MERS-S(H)- or MV_{vac2}-MERS-solS(H)-vaccinated mice are capable of lysing cells expressing MERS-S. Neither splenocytes of

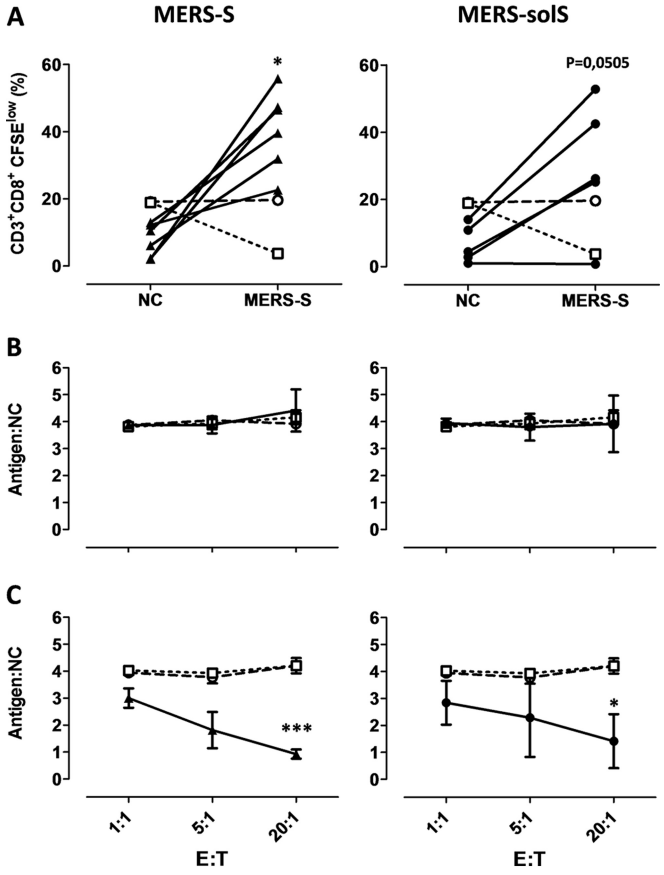

FIG 5 Induction of MERS-S-specific CTLs. (A) Proliferation assay using splenocytes of mice vaccinated on days 0 and 28 with MV_{vac2}-MERS-S(H) or MV_{vac2}-MERS-solS(H) and isolated 21 days after boost immunization, after coculture with JAWSII dendritic cell lines transgenic for MERS-S (right, filled triangles), or untransduced controls (left, filled circles). Depicted are the percentages of $CD8^+$ T cells with low CFSE staiing, indicating proliferation in the samples. Results for splenocytes of vaccinated mice are displayed individually and the trend between paired unstimulated and restimulated samples is outlined. Splenocytes of control vaccinated mice [open circles, mock; open squares, MV_{vac2}-ATU(P)] were pooled. (B and C) Killing assay using splenocytes of mice vaccinated on days 0 and 28 and isolated 4 days after boost immunization. Splenocytes were cocultured with untransduced JAWSII (B) or with antigen-presenting JAWSII-MERS-S (C) or for 6 days. Activated CTLs were then cocultured with EL-4-MERS-S target cells (antigen) and EL-4_{red} control cells (NC) at the indicated effector:target (E:T) ratios for 4 h. Ratios of living target versus nontarget cells (antigen:NC) were determined by flow cytometry. Filled triangles, MV_{vac2}-MERS-S(H); filled circles, MV_{vac2}-MERS-solS(H); open circles, mock; open squares, MV_{vac2}-ATU(P). Results shown are means and standard deviation of each group ($n = 6$). ns, not significant; *, $P < 0.05$; ***, $P < 0.0001$.

control mice restimulated with JAWSII-MERS-S nor splenocytes of MERS-S-vaccinated mice restimulated with control JAWSII cells showed such an antigen-specific killing activity. These results demonstrated that the MV-based vaccine platform induces fully functional antigen-specific $CD8^+$ CTLs in vaccinated mice when applied as a MERS-CoV vaccine.

Vaccination of mice with MV_{vac2}-MERS-S(H) or MV_{vac2}-MERS-solS(H) rescues animals from challenge with MERS-CoV. The induction of strong humoral and cellular immune responses directed against MERS-CoV in mice vaccinated with MV_{vac2}-MERS-S(H) or MV_{vac2}-MERS-solS(H) indicated that those animals are possibly protected against a challenge with MERS-CoV. To investigate the efficacy of the candidate vaccines, two independent experiments were performed in which groups of five mice were either vaccinated with MV_{vac2}-MERS-S(H), MV_{vac2}-MERS-solS(H), or control MV [MV_{vac2}-ATU(P)] or left untreated. All mice immunized with MV_{vac2}-MERS-S(H) or MV_{vac2}-MERS-solS(H) showed VNTs directed against MERS-CoV, with titers up to 1,280 for MERS-S and up to 960 for MERS-solS. No MERS-CoV-neutralizing antibodies were detected in control mice (data not shown). Since the murine DPP4 does not serve as a functional MERS-CoV entry receptor (66) and mice are therefore not susceptible to MERS-CoV infection, the vaccinated mice were i.n. transduced with a recombinant adenoviral vector to express human DPP4 (AdV-hDPP4) in murine airways. At 5 days after airway transduction with AdV-hDPP4, mice were infected i.n. with 7×10^4 $TCID_{50}$ MERS-CoV. Four days later, animals were euthanized, lungs were isolated, the tissue was homogenized, and homogenates were used for purification of total RNA and virus titration. In the lungs of mock-infected control mice, MERS-CoV RNA was detected by qRT-PCR (9,649 ± 3,045 MERS-CoV genome copies/ng RNA) (Fig. 6A). Mice vaccinated with control MV_{vac2}-ATU(P) showed slightly lower copy numbers of viral RNA (5,923 ± 3,045 MERS-CoV genome copies/ng RNA) (Fig. 6A). Vaccination with MV_{vac2}-MERS-S(H) or MV_{vac2}-MERS-solS(H) resulted in near-complete reduction of viral loads to 74 ± 60 genome copies/ng RNA or 51 ± 32 genome copies/ng RNA, respectively (Fig. 6A). Next, titers of infectious virus were determined in the lung tissue. While the titers were generally low, they corresponded to the qRT-PCR data. In mock-treated control mice, titers of up to 5,000 $TCID_{50}$/ml were determined (mean, 868 ± 692 $TCID_{50}$/ml) and in lungs of mice vaccinated with the vaccine backbone without MERS antigen [MV_{vac2}-ATU(P)], 1,673 ± 866 $TCID_{50}$/ml were detected. A considerable albeit statistically not significant reduction of infectious virus titers was found in mice vaccinated with MV_{vac2}-MERS-S(H) or MVvac2-MERS-solS(H) compared to mock control mice (Fig. 6B). These results revealed that, indeed, vaccination with the recombinant measles viruses was able to protect mice against a challenge with MERS-CoV.

MERS-CoV infection of transduced mice was not always successful, which was indicated by a completely negative PCR result for viral genomes in about 40% of all animals. In approximately 30% of MERS-CoV-negative animals, PCR for the mCherry gene was negative, indicating that transduction was not successful and explaining why these mice were not susceptible. Why the remaining transduced mice were not infected is currently unclear. However, even when the dropout animals were included in statistical analysis, the difference between mean viral loads of the medium control group and MV_{vac2}-MERS-solS(H)-treated mice (ratio, 278.2; 95% confidence interval, 1.52 to 50,904) stayed significant ($P = 0.0329$). Protection of the MV_{vac2}-MERS-S(H)-vaccinated group was close to significance ($P = 0.057$) compared to mock-treated animals (ratio, 149.2; 95% CI, 0.82 to 27,301).

Histological analyses were performed to analyze if the reduced viral load in mice vaccinated with MV_{vac2}-MERS-solS(H) or MV_{vac2}-MERS-S(H) was matched by decreased pathological changes in mouse lungs (Fig. 7). For this purpose, lungs were examined with H&E staining to visualize inflammation. Additionally, MERS-S and mCherry expression was determined by immunohistochemistry using antigen-specific antibodies. Consistent with the qRT-PCR results, all mice that were positive in the

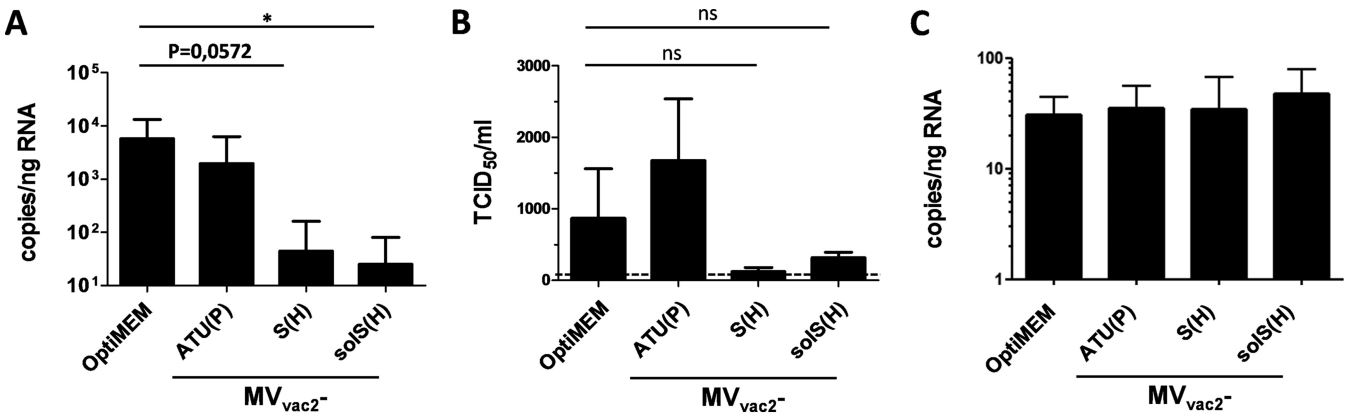

FIG 6 Viral loads after MERS-CoV challenge *in vivo*. (A and B) Viral loads, determined as genome copies per nanogram of RNA (A) or infectious virus titers (B) in the lungs of prevaccinated mice after transduction with DPP4-encoding AdV 21 days after boost and challenge with MERS-CoV 25 days after boost. Two independent experiments ($n = 4$ to 5 per group). Error bars, standard errors of the means (SEM). Dotted line, limit of detection (LOD of qPCR, <1.7 copies/ng RNA). ns, not significant; *, $P < 0.05$. (C) AdV transduction control mCherry mRNA results (in copies per nanogram of RNA). Error bars, SEM.

qRT-PCR for the mCherry gene expressed mCherry in epithelia of the lungs, demonstrating successful transduction (Fig. 7, right column). The histopathological examination of H&E-stained lung tissues clearly showed differences between the vaccinated mice and controls (Fig. 7, left column). In the mock (Opti-MEM) as well as vector control [MV_{vac2}-ATU(P)] groups, large areas of inflamed tissue were observed to be densely packed with lymphocytes, macrophages and, to a lesser extent, neutrophils and eosinophils. Moreover, hyperplasia of the bronchus-associated lymphoid tissue was present to various degrees. These inflamed areas colocalized with expression of MERS-CoV spike protein (Fig. 7, middle column). Mice that were vaccinated with recombinant MV expressing MERS-S showed fewer signs of inflammation and consistently lower MERS-S expression after challenge with MERS. These differences were most obvious in lungs of MV_{vac2}-MERS-solS(H)-vaccinated animals, where only small foci of inflammation could be observed. These results revealed that vaccination with recombinant MV expressing MERS S reduced pathological changes in the lungs of MERS-CoV-infected mice.

DISCUSSION

In this study, we have demonstrated the capacity of recombinant MV encoding different forms of the MERS-CoV S glycoprotein to induce both strong humoral and cellular immune responses that revealed a protective capacity in a challenge model of mice vaccinated with these stable live-attenuated vaccines. So far, different strategies to develop vaccines against MERS-CoV have been proposed, including recombinant full-length S protein (67) or the receptor-binding domain (RBD) of MERS-S (27, 28, 30, 31, 68), as well as platform-based approaches using modified vaccinia virus Ankara (MVA) (22) or adenoviral vectors (AdV) (23) encoding MERS-S. Similar to our MV-based vaccine, these experimental vaccines induced humoral immune responses with virus-neutralizing capacities. Among vectored vaccines, immunization with MVA- or AdV-expressing MERS-S resulted in VNTs of approximately 1,800 or 1,024, respectively, when used to immunize BALB/c mice. Vaccination with MV_{vac2}-MERS-S or MV_{vac2}-MERS-solS induced somewhat lower VNTs of about 840, which is an extremely robust titer if it is taken into account that mice were immunized with 10^3-fold fewer virus particles than with MVA and 10^6-fold lower particles than with replication-deficient AdV. Moreover, transgenic IFNAR$^{-/-}$-CD46Ge mice have been used in our study with defects in type I IFN receptor signaling. Knockout of the type I IFN receptor results in reduced adaptive immune responses (68–70), since type I IFNs are an important link between the innate and adaptive immunity via, among others factors, activation of DCs (71), leading to a disadvantage for the mouse adaptive immune system. Nevertheless, these mice have to be used routinely to analyze efficacy of MV-based vaccines in a small animal model (46), since wild-type mice are not susceptible to MV infection for mainly two reasons. First, murine homologues of MV receptors cannot be used for cell entry (69), with the exception of nectin-4 (70). Second, MV replication is strongly impaired by type I IFN responses (71, 72), and mice with an intact IFNAR feedback loop failed to be susceptible to MV infection (46). Therefore, the IFNAR$^{-/-}$-CD46Ge mouse strain transgenic for human MV vaccine receptor CD46 and with a knockout of the IFNAR is used to analyze MV-based vaccines. Additionally, the mouse strain backgrounds (BALB/c versus C57BL/6) differ in T helper cell responses (BALB/c, predominantly Th2; C57BL/6, predominantly Th1 responses [73]), which reflects the different balance of cellular versus humoral immunity (74, 75). Thus, the mouse model which had to be used in this study certainly is disadvantageous with respect to VNTs. To directly compare efficacy of the different vector systems, all vectors should ideally be used side by side in the same animal model. This may be a focus of future studies. The VNTs of about 1,000 induced by three immunizations with recombinant RBD are hardly comparable to our results, since other protocols for determination of VNTs were used in the other studies (27, 31). Interestingly, the expression of the soluble version of S by MV did not enhance VNTs. This is consistent with humoral immunity induced by DNA vaccines targeting SARS-CoV. Plasmids encoding soluble SARS-S lacking the transmembrane domain provoked lower VNTs than membrane-bound variants (32). An altered, less physiological conformation of the S protein has been proposed to result from deletion of the transmembrane domain, which should be responsible for worse immune recognition and lower antibody titers binding to the native, correctly folded S proteins in virus particles. In contrast, the soluble S1 domain of MERS-S expressed by AdV actually induced

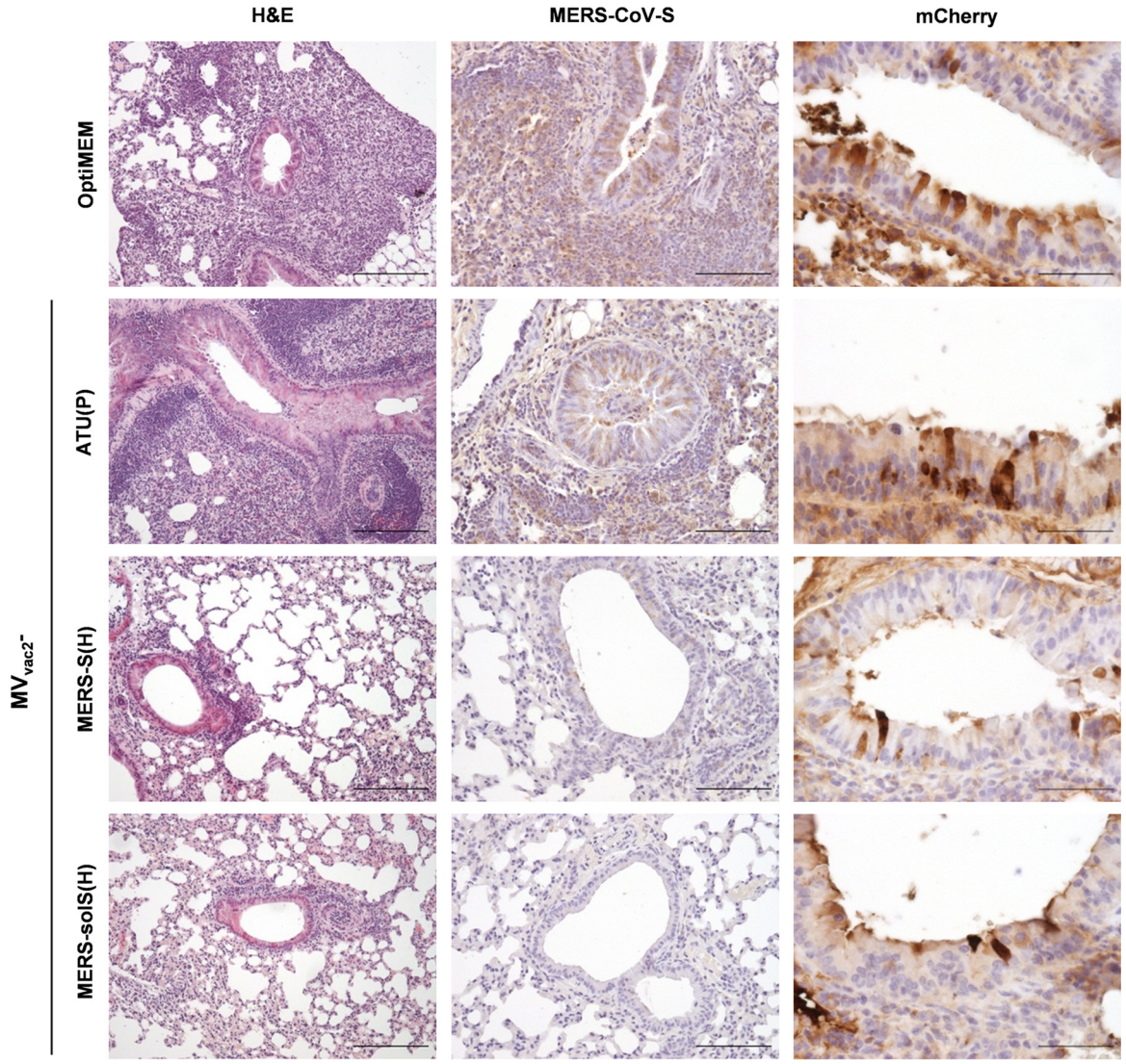

FIG 7 Histopathological changes and immunohistochemical analysis of lungs after challenge. Analysis of lung tissue of representative prevaccinated mice (as indicated) after transduction with hDPP4-encoding AdV and challenge with MERS-CoV. Pictures arranged in a row were from samples of the same individual mouse. Paraffin-fixed tissue was stained with H&E (first column; scale bar, 200 μm), with Ab against MERS-CoV-S antigen (middle column; scale bar, 100 μm), and as a control of AdV transduction against mCherry (right column; scale bar, 50 μm).

slightly higher VNTs than did full-length S (23). However, soluble constructs consisting of the MERS S1 and S2 domains have not been compared to the soluble S1 domain yet. Interestingly, recombinant MV expressing soluble MERS-S revealed slightly impaired replication in comparison to control MV, in contrast to MV expressing full-length MERS-S. This impaired viral replication might be based on cytotoxicity of MERS-solS, probably as a result of an altered folding or the solubility of the S protein. Cytotoxic effects of the S protein have already been observed for the S2 domain of SARS-S (76–80), but not for other coronaviruses, like mouse hepatitis coronavirus (81). However, both MV-based vaccines encoding either the soluble or the full-length variant of MERS-S did induce strong VNTs and cellular immune responses.

The protective capacity of humoral immune responses against CoV infection is controversial. Neutralizing antibodies have been identified as correlates of protection against SARS-CoV challenge, since passive serum transfer was sufficient to rescue animals from challenge (32, 82) and T cell depletion did not impair protection (32). In contrast, immunization with the nucleocapsid protein resulted in protection against the coronavirus infectious bronchitis virus (IBV) without induction of neutralizing antibodies (83, 84), indicating the capacity of cellular immune responses for IBV protection. Anyway, the antigenic potential of S for induction of $CD4^+$ or $CD8^+$ T cell immunity has already been demonstrated for SARS-CoV (32, 85) by using recombinant protein or DNA vaccines. Also for MERS-CoV, application of RBD protein together with adjuvants has been shown to induce cellular immunity (27, 31). We demonstrated in this study that induction of cellular immunity by a vectored vaccine works independently from adjuvants or the application strategy. The MV-based vaccine induced very strong MERS-S-specific $CD8^+$ T cell responses, revealed by ELISpot, killing, and proliferation assays. The broad repertoire of

reactivity, in the case of antigen-specific proliferation also 21 days after the booster immunization, indicated induction of both a functional effector and memory T cell repertoire by MV_{vac2}-MERS-S and MV_{vac2}-MERS-solS. Thereby, the extraordinary high number of IFN-γ-secreting T cells in vaccinated mice both stresses the potential of the vaccine platform and underlines the immunogenicity of MERS-S.

On top, the present study tested whether the induced immune responses protected mice against a challenge infection with MERS-CoV. Indeed, vaccination with MV_{vac2}-MERS-S or MV_{vac2}-MERS-solS significantly reduced viral loads in the lungs of vaccinated mice after challenge with MERS-CoV. As expected, this reduction of viral load correlated with reduced pathological alterations in the lung, indicating that MV-derived MERS vaccines were able to confer protection against MERS-CoV infection. At least 4 mice out of each group did not reveal any MERS-CoV infection nor any pathological lung alterations indicating failure of infection in these individuals. In 30% of those mice, transduction with the recombinant adenovirus expressing human DPP4 did not appear to be successful. However, the majority of mice with no signs of MERS-CoV infection at all showed expression of mCherry, indicating that transduction was successful. Currently, the reason for the failure to infect these animals is unclear.

The direct correlates of protection in the vaccinated mice remain to be determined in future studies. Most recently, mice transgenic for human DPP4 have been developed that allow analysis of MERS-CoV infection on a more robust and physiologic basis (86). These could only be used for analysis of MV-based vaccines after intercrossing them with $IFNAR^{-/-}$-CD46Ge or similar mouse strains to obtain mice simultaneously susceptible to MV and MERS-CoV, which may also be a focus of future work.

Efficacy of MV_{vac2}-based MERS vaccines has been demonstrated in MV-naive mice. Theoretically, preexisting antivector immunity against the MV backbone may be considered a potential limitation both for the specific MERS vaccines tested in this study and for use of recombinant MV as a vaccine platform, in general, for MV-immunized patients (87). However, it has been clearly demonstrated both in mice (41, 45) and nonhuman primates (41) with humoral immune responses regarded to be protective against measles that vaccination with recombinant MVs encoding antigens of HIV-1 (41) or Chikungunya virus (45) still induced surprisingly robust antigen-specific immune responses. Most interestingly, when the efficacy of recombinant MV-CHIKV vaccine in a phase I trial in human volunteers was analyzed, the vaccine was recently shown to be effective in inducing anti-CHIKV immune responses irrespective of preexisting antimeasles immunity (47). These data question the "sterilizing" character of measles immunity and clearly indicate the potential of recombinant MV as a promising vaccine platform for vaccination against MERS-CoV or other infectious agents, in general. Indeed, the efficacy of MV-based recombinant vaccines has been demonstrated preclinically with quite a range of different pathogen antigens, e.g., HBV (39), dengue virus (44), WNV (42), and CHIKV (45). Additionally, the efficacy of MV to induce immune responses against coronaviruses has been shown for the S protein and nucleocapsid protein of SARS-CoV (19). All these recombinant vaccines have in common that they are based on a very-well-known platform: MV vaccines have been shown to exhibit an extremely beneficial safety profile in light of the millions of applied doses over the last 40 years. Only heavily immune-suppressed patients are excluded from measles vaccination campaigns, but the protection holds over decades and is thought to be most likely for life (33, 34).

Most interestingly, a quite similar recombinant vaccine based on a rhabdovirus, a member of another family within the *Mononegavirales* order, is currently being tested in the clinic as an experimental vaccine against Ebola virus (EBOV) infection. Recombinant VSV encoding the Ebola Zaire strain glycoprotein. replacing VSV-G (VSV-ZEBOV) was shown to be effective in animal models (88, 89) and is now being tested in phase I trials for safety in human patients (90), in preparation to being moved to the field to combat current EBOV epidemics. Thereby, the potential interest in such platform-based vaccines to combat emerging or reemerging infections is impressively highlighted.

Taken together, MV vaccine strain Moraten-derived recombinant MV_{vac2} vaccines are effective vaccines against MERS-CoV, inducing both humoral and cellular immune responses protective for vaccinated animals. Thereby, the capacity of the recombinant MV-based vaccine platform for fast generation of effective vaccines has been demonstrated also with a more general view to future emerging or reemerging infections, but also with a view on MERS-CoV. MV-MERS-S provides an opportunity for further development of this experimental vaccine to be prepared especially to reduce the risk of pandemic spread of this disease.

ACKNOWLEDGMENTS

We thank Vivian Koch, Daniela Müller, Michael Schmidt, and Gotthard Ludwig for excellent technical assistance, Sonja Witzel, Manuel Gimmel, Tina Hempel, Aileen Laubenheimer, and Tobias Blödel for excellent technical support in production of recombinant MERS-S protein, and Roland Plesker for assistance in animal experiments. We thank Lucie Sauerhering and Erik Dietzel for help with animal studies under biosafety level 4 conditions. We are indebted to Ron Fouchier for providing MERS-CoV strain EMC/2012, to Kenneth Rock for DC2.4 and DC3.2 cells, and to Christian Drosten and Doreen Muth for PCR protocols. We further thank Bakhos Tannous for providing pCSCW2gluc-IRES-GFP and Kenneth Lundström for the SFV vector system.

TWINCORE is a joint venture between the Hannover Medical School and the Helmholtz Centre for Infection Research, in Hannover, Germany.

This work was supported by the German Center for Infection Research (DZIF; TTU 01.802, TTU 01.904) and the Deutsche Forschungsgemeinschaft (SFB1021, SFB593).

REFERENCES

1. **Zaki AM, van Boheemen S, Bestebroer TM, Osterhaus AD, Fouchier RM.** 2012. Isolation of a novel coronavirus from a man with pneumonia in Saudi Arabia. N Engl J Med **367:**1814–1820. http://dx.doi.org/10.1056/NEJMoa1211721.
2. **World Health Organization.** 2014. Middle East respiratory syndrome coronavirus (MERS-CoV)—Saudi Arabia. World Health Organization, Geneva, Switzerland. http://www.who.int/csr/don/17-december-2014-mers/en/.
3. **Drosten C, Meyer B, Müller MA, Corman VM, Al-Masri M, Hossain R, Madani H, Sieberg A, Bosch BJ, Lattwein E, Alhakeem RF, Assiri AM, Hajomar W, Albarrak AM, Al-Tawfiq JA, Zumla AI, Memish ZA.** 2014. Transmission of MERS-coronavirus in household contacts. N Engl J Med **371:**828–835. http://dx.doi.org/10.1056/NEJMoa1405858.
4. **Petersen E, Hui DS, Perlman S, Zumla A.** 2015. Middle East respiratory syndrome: advancing the public health and research agenda on MERS. Lessons from the South Korea outbreak. Int J Infect Dis **36:**54–55. http://dx.doi.org/10.1016/j.ijid.2015.06.004.
5. **Cowling BJ, Park M, Fang VJ, Wu P, Leung GM, Wu JT.** 2015. Preliminary epidemiological assessment of MERS-CoV outbreak in South Korea, May to June. Euro Surveill **20:**pii=2113. http://dx.doi.org/10.2807/1560-7917.ES2015.25.21163.
6. **Raj VS, Farag EA, Reusken CB, Lamers MM, Pas SD, Voermans J,**

Smits SL, Osterhaus AD, Al-Mawlawi N, Al-Romaihi HE, Al Hajri MM, El-Sayed AM, Mohran KA, Ghobashy H, Al Hajri F, Al-Thani M, Al-Marri SA, El-Maghraby MM, Koopmans MP, Haagmans BL. 2014. Isolation of MERS coronavirus from a dromedary camel, Qatar, 2014. Emerg Infect Dis **20:**1339–1342. http://dx.doi.org/10.3201/eid2008.140663.

7. **Ferguson NM, Van Kerkhove MD.** 2014. Identification of MERS-CoV in dromedary camels. Lancet Infect Dis **14:**93–94. http://dx.doi.org/10.1016/S1473-3099(13)70691-1.
8. **Müller MA, Corman VM, Jores J, Meyer B, Younan M, Liljander A, Bosch B, Lattwein E, Hilali M, Musa BE, Bornstein S, Drosten C.** 2014. MERS coronavirus neutralizing antibodies in camels, Eastern Africa, 1983-1997. Emerg Infect Dis **20:**2093–2095. http://dx.doi.org/10.3201/eid2012.141026.
9. **Meyer B, Müller MA, Corman VM, Reusken CB, Ritz D, Godeke G, Lattwein E, Kallies S, Siemens A, van Beek J, Drexler JF, Muth D, Bosch B, Wernery U, Koopmans MP, Wernery R, Drosten C.** 2014. Antibodies against MERS coronavirus in dromedary camels, United Arab Emirates, 2003 and 2013. Emerg Infect Dis **20:**552–559. http://dx.doi.org/10.3201/eid2004.131746.
10. **Corman VM, Jores J, Meyer B, Younan M, Liljander A, Said MY, Gluecks I, Lattwein E, Bosch B, Drexler JF, Bornstein S, Drosten C, Müller MA.** 2014. Antibodies against MERS coronavirus in dromedary camels, Kenya, 1992-2013. Emerg Infect Dis **20:**1319–1322. http://dx.doi.org/10.3201/eid2008.140596.
11. **Memish ZA, Cotten M, Meyer B, Watson SJ, Alsahafi AJ, Al Rabeeah Abdullah A, Corman VM, Sieberg A, Makhdoom HQ, Assiri A, Al Masri M, Aldabbagh S, Bosch B, Beer M, Müller MA, Kellam P, Drosten C.** 2014. Human infection with MERS coronavirus after exposure to infected camels, Saudi Arabia, 2013. Emerg Infect Dis **20:**1012–1015. http://dx.doi.org/10.3201/eid2006.140402.
12. **Azhar EI, El-Kafrawy SA, Farraj SA, Hassan AM, Al-Saeed MS, Hashem AM, Madani TA.** 2014. Evidence for camel-to-human transmission of MERS coronavirus. N Engl J Med **370:**2499–2505. http://dx.doi.org/10.1056/NEJMoa1401505.
13. **Lau SK, Li KS, Tsang AK, Lam CS, Ahmed S, Chen H, Chan K, Woo Patrick C, Yuen KY.** 2013. Genetic characterization of betacoronavirus lineage C viruses in bats reveals marked sequence divergence in the spike protein of pipistrellus bat coronavirus HKU5 in Japanese pipistrelle: implications for the origin of the novel Middle East respiratory syndrome coronavirus. J Virol **87:**8638–8650. http://dx.doi.org/10.1128/JVI.01055-13.
14. **Annan A, Baldwin HJ, Corman VM, Klose SM, Owusu M, Nkrumah EE, Badu EK, Anti P, Agbenyega O, Meyer B, Oppong S, Sarkodie YA, Kalko Elisabeth KV, Lina Peter HC, Godlevska EV, Reusken C, Seebens A, Gloza-Rausch F, Vallo P, Tschapka M, Drosten C, Drexler JF.** 2013. Human betacoronavirus 2c EMC/2012-related viruses in bats, Ghana and Europe. Emerg Infect Dis **19:**456–459. http://dx.doi.org/10.3201/eid1903.121503.
15. **Corman VM, Ithete NL, Richards LR, Schoeman MC, Preiser W, Drosten C, Drexler JF.** 2014. Rooting the phylogenetic tree of Middle East respiratory syndrome coronavirus by characterization of a conspecific virus from an African bat. J Virol **88:**11297–11303. http://dx.doi.org/10.1128/JVI.01498-14.
16. **Peiris JSM, Guan Y, Yuen KY.** 2004. Severe acute respiratory syndrome. Nat Med **10:**S88–S97. http://dx.doi.org/10.1038/nm1143.
17. **Bai B, Lu X, Meng J, Hu Q, Mao P, Lu B, Chen Z, Yuan Z, Wang H.** 2008. Vaccination of mice with recombinant baculovirus expressing spike or nucleocapsid protein of SARS-like coronavirus generates humoral and cellular immune responses. Mol Immunol **45:**868–875. http://dx.doi.org/10.1016/j.molimm.2007.08.010.
18. **Du L, Zhao G, Chan Chris CS, Sun S, Chen M, Liu Z, Guo H, He Y, Zhou Y, Zheng B, Jiang S.** 2009. Recombinant receptor-binding domain of SARS-CoV spike protein expressed in mammalian, insect and E. coli cells elicits potent neutralizing antibody and protective immunity. Virology **393:**144–150. http://dx.doi.org/10.1016/j.virol.2009.07.018.
19. **Liniger M, Zuniga A, Tamin A, Azzouz-Morin TN, Knuchel M, Marty RR, Wiegand M, Weibel S, Kelvin D, Rota PA, Naim HY.** 2008. Induction of neutralising antibodies and cellular immune responses against SARS coronavirus by recombinant measles viruses. Vaccine **26:**2164–2174. http://dx.doi.org/10.1016/j.vaccine.2008.01.057.
20. **Dimitrov DS.** 2004. Virus entry: molecular mechanisms and biomedical applications. Nat Rev Microbiol **2:**109–122. http://dx.doi.org/10.1038/nrmicro817.
21. **Hofmann H, Pöhlmann S.** 2004. Cellular entry of the SARS coronavirus. Trends Microbiol **12:**466–472. http://dx.doi.org/10.1016/j.tim.2004.08.008.
22. **Song F, Fux R, Provacia LB, Volz A, Eickmann M, Becker S, Osterhaus Albert DME, Haagmans BL, Sutter G.** 2013. Middle East respiratory syndrome coronavirus spike protein delivered by modified vaccinia virus Ankara efficiently induces virus-neutralizing antibodies. J Virol **87:**11950–11954. http://dx.doi.org/10.1128/JVI.01672-13.
23. **Kim E, Okada K, Kenniston T, Raj VS, AlHajri MM, Farag Elmoubasher ABA, AlHajri F, Osterhaus Albert DME, Haagmans BL, Gambotto A.** 2014. Immunogenicity of an adenoviral-based Middle East respiratory syndrome coronavirus vaccine in BALB/c mice. Vaccine **32:**5975–5982. http://dx.doi.org/10.1016/j.vaccine.2014.08.058.
24. **Gierer S, Bertram S, Kaup F, Wrensch F, Heurich A, Krämer-Kühl A, Welsch K, Winkler M, Meyer B, Drosten C, Dittmer U, Hahn T von, Simmons G, Hofmann H, Pöhlmann S.** 2013. The spike protein of the emerging betacoronavirus EMC uses a novel coronavirus receptor for entry, can be activated by TMPRSS2, and is targeted by neutralizing antibodies. J Virol **87:**5502–5511. http://dx.doi.org/10.1128/JVI.00128-13.
25. **Raj VS, Mou H, Smits SL, Dekkers DH, Müller MA, Dijkman R, Muth D, Demmers JA, Zaki A, Fouchier RA, Thiel V, Drosten C, Rottier PJ, Osterhaus AD, Bosch BJ, Haagmans BL.** 2013. Dipeptidyl peptidase 4 is a functional receptor for the emerging human coronavirus EMC. Nature **495:**251–254. http://dx.doi.org/10.1038/nature12005.
26. **He Y, Lu H, Siddiqui P, Zhou Y, Jiang S.** 2005. Receptor-binding domain of severe acute respiratory syndrome coronavirus spike protein contains multiple conformation-dependent epitopes that induce highly potent neutralizing antibodies. J Immunol **174:**4908–4915. http://dx.doi.org/10.4049/jimmunol.174.8.4908.
27. **Ma C, Li Y, Wang L, Zhao G, Tao X, Tseng CK, Zhou Y, Du L, Jiang S.** 2014. Intranasal vaccination with recombinant receptor-binding domain of MERS-CoV spike protein induces much stronger local mucosal immune responses than subcutaneous immunization: implication for designing novel mucosal MERS vaccines. Vaccine **32:**2100–2108. http://dx.doi.org/10.1016/j.vaccine.2014.02.004.
28. **Du L, Kou Z, Ma C, Tao X, Wang L, Zhao G, Chen Y, Yu F, Tseng CK, Zhou Y, Jiang S.** 2013. A truncated receptor-binding domain of MERS-CoV spike protein potently inhibits MERS-CoV infection and induces strong neutralizing antibody responses: implication for developing therapeutics and vaccines. PLoS One **8:**e81587. http://dx.doi.org/10.1371/journal.pone.0081587.
29. **Du L, Zhao G, Kou Z, Ma C, Sun S, Poon VK, Lu L, Wang L, Debnath AK, Zheng B, Zhou Y, Jiang S.** 2013. Identification of a receptor-binding domain in the S protein of the novel human coronavirus Middle East respiratory syndrome coronavirus as an essential target for vaccine development. J Virol **87:**9939–9942. http://dx.doi.org/10.1128/JVI.01048-13.
30. **Mou H, Raj VS, van Kuppeveld FJ, Rottier PJ, Haagmans BL, Bosch BJ.** 2013. The receptor binding domain of the new Middle East respiratory syndrome coronavirus maps to a 231-residue region in the spike protein that efficiently elicits neutralizing antibodies. J Virol **87:**9379–9383. http://dx.doi.org/10.1128/JVI.01277-13.
31. **Lan J, Deng Y, Chen H, Lu G, Wang W, Guo X, Lu Z, Gao GF, Tan W.** 2014. Tailoring subunit vaccine immunity with adjuvant combinations and delivery routes using the Middle East respiratory coronavirus (MERS-CoV) receptor-binding domain as an antigen. PLoS One **9:**e112602. http://dx.doi.org/10.1371/journal.pone.0112602.
32. **Yang Z, Kong W, Huang Y, Roberts A, Murphy BR, Subbarao K, Nabel GJ.** 2004. A DNA vaccine induces SARS coronavirus neutralization and protective immunity in mice. Nature **428:**561–564. http://dx.doi.org/10.1038/nature02463.
33. **Hilleman MR.** 2001. Current overview of the pathogenesis and prophylaxis of measles with focus on practical implications. Vaccine **20:**651–665. http://dx.doi.org/10.1016/S0264-410X(01)00384-X.
34. **Griffin DE.** 2002. Measles virus. *In* Encyclopedia of molecular medicine. John Wiley & Sons, Inc., Hoboken, NJ. http://dx.doi.org/10.1002/0471203076.emm0739.
35. **Radecke F, Spielhofer P, Schneider H, Kaelin K, Huber M, Dötsch C, Billeter MA.** 1995. Rescue of measles viruses from cloned DNA. EMBO J **14:**5773–5784.
36. **Billeter MA, Naim HY, Udem SA.** 2009. Reverse genetics of measles virus and resulting multivalent recombinant vaccines: applications of recombinant measles viruses. Curr Top Microbiol Immunol **329:**129–162. http://dx.doi.org/10.1007/978-3-540-70523-9_7.

37. **Duprex WP, Rima BK.** 2002. Using green fluorescent protein to monitor measles virus cell-to-cell spread by time-lapse confocal microscopy. Methods Mol Biol **183:**297–307. http://dx.doi.org/10.1385/1-59259-280-5:297.
38. **Singh M, Billeter MA.** 1999. A recombinant measles virus expressing biologically active human interleukin-12. J Gen Virol **80:**101–106. http://dx.doi.org/10.1099/0022-1317-80-1-101.
39. **Singh M, Cattaneo R, Billeter MA.** 1999. A recombinant measles virus expressing hepatitis B virus surface antigen induces humoral immune responses in genetically modified mice. J Virol **73:**4823–4828.
40. **Reyes-del Valle J, de la Fuente Cynthia Turner MA, Springfeld C, Apte-Sengupta S, Frenzke ME, Forest A, Whidby J, Marcotrigiano J, Rice CM, Cattaneo R.** 2012. Broadly neutralizing immune responses against hepatitis C virus induced by vectored measles viruses and a recombinant envelope protein booster. J Virol **86:**11558–11566. http://dx.doi.org/10.1128/JVI.01776-12.
41. **Lorin C, Mollet L, Delebecque F, Combredet C, Hurtrel B, Charneau P, Brahic M, Tangy F.** 2004. A single injection of recombinant measles virus vaccines expressing human immunodeficiency virus (HIV) type 1 clade B envelope glycoproteins induces neutralizing antibodies and cellular immune responses to HIV. J Virol **78:**146–157. http://dx.doi.org/10.1128/JVI.78.1.146-157.2004.
42. **Desprès P, Combredet C, Frenkiel M, Lorin C, Brahic M, Tangy F.** 2005. Live measles vaccine expressing the secreted form of the West Nile virus envelope glycoprotein protects against West Nile virus encephalitis. J Infect Dis **191:**207–214. http://dx.doi.org/10.1086/426824.
43. **Brandler S, Marianneau P, Loth P, Lacôte S, Combredet C, Frenkiel M, Desprès P, Contamin H, Tangy F.** 2012. Measles vaccine expressing the secreted form of West Nile virus envelope glycoprotein induces protective immunity in squirrel monkeys, a new model of West Nile virus infection. J Infect Dis **206:**212–219. http://dx.doi.org/10.1093/infdis/jis328.
44. **Brandler S, Ruffie C, Najburg V, Frenkiel M, Bedouelle H, Desprès P, Tangy F.** 2010. Pediatric measles vaccine expressing a dengue tetravalent antigen elicits neutralizing antibodies against all four dengue viruses. Vaccine **28:**6730–6739. http://dx.doi.org/10.1016/j.vaccine.2010.07.073.
45. **Brandler S, Ruffié C, Combredet C, Brault J, Najburg V, Prevost M, Habel A, Tauber E, Desprès P, Tangy F.** 2013. A recombinant measles vaccine expressing Chikungunya virus-like particles is strongly immunogenic and protects mice from lethal challenge with Chikungunya virus. Vaccine **31:**3718–3725. http://dx.doi.org/10.1016/j.vaccine.2013.05.086.
46. **Mrkic B, Pavlovic J, Rülicke T, Volpe P, Buchholz CJ, Hourcade D, Atkinson JP, Aguzzi A, Cattaneo R.** 1998. Measles virus spread and pathogenesis in genetically modified mice. J Virol **72:**7420–7427.
47. **Ramsauer K, Schwameis M, Firbas C, Müllner M, Putnak RJ, Thomas SJ, Desprès P, Tauber E, Jilma B, Tangy F.** 2015. Immunogenicity, safety, and tolerability of a recombinant measles-virus-based Chikungunya vaccine: a randomised, double-blind, placebo-controlled, active-comparator, first-in-man trial. Lancet Infect Dis **15:**519–527. http://dx.doi.org/10.1016/S1473-3099(15)70043-5.
48. **del Valle JR, Devaux P, Hodge G, Wegner NJ, McChesney MB, Cattaneo R.** 2007. A vectored measles virus induces hepatitis B surface antigen antibodies while protecting macaques against measles virus challenge. J Virol **81:**10597–10605. http://dx.doi.org/10.1128/JVI.00923-07.
49. **Bajenoff M, Germain RN.** 2009. B-cell follicle development remodels the conduit system and allows soluble antigen delivery to follicular dendritic cells. Blood **114:**4989–4997. http://dx.doi.org/10.1182/blood-2009-06-229567.
50. **Pape KA, Catron DM, Itano AA, Jenkins MK.** 2007. The humoral immune response is initiated in lymph nodes by B cells that acquire soluble antigen directly in the follicles. Immunity **26:**491–502. http://dx.doi.org/10.1016/j.immuni.2007.02.011.
51. **De Becker G, Moulin V, Tielemans F, De Mattia F, Urbain J, Leo O, Moser M.** 1998. Regulation of T helper cell differentiation in vivo by soluble and membrane proteins provided by antigen-presenting cells. Eur J Immunol **28:**3161–3171. http://dx.doi.org/10.1002/(SICI)1521-4141(199810)28:10<3161::AID-IMMU3161>3.0.CO;2-Q.
52. **Enriquez-Rincon F, Klaus GG.** 1984. Differing effects of monoclonal anti-hapten antibodies on humoral responses to soluble or particulate antigens. Immunology **52:**129–136.
53. **Shen Z, Reznikoff G, Dranoff G, Rock KL.** 1997. Cloned dendritic cells can present exogenous antigens on both MHC class I and class II molecules. J Immunol **158:**2723–2730.
54. **Martin A, Staeheli P, Schneider U.** 2006. RNA polymerase II-controlled expression of antigenomic RNA enhances the rescue efficacies of two different members of the Mononegavirales independently of the site of viral genome replication. J Virol **80:**5708–5715. http://dx.doi.org/10.1128/JVI.02389-05.
55. **Hewett JW, Tannous B, Niland BP, Nery FC, Zeng J, Li Y, Breakefield XO.** 2007. Mutant torsin A interferes with protein processing through the secretory pathway in DYT1 dystonia cells. Proc Natl Acad Sci U S A **104:**7271–7276. http://dx.doi.org/10.1073/pnas.0701185104.
56. **Boussif O, Lezoualc'h F, Zanta MA, Mergny MD, Scherman D, Demeneix B, Behr JP.** 1995. A versatile vector for gene and oligonucleotide transfer into cells in culture and in vivo: polyethylenimine. Proc Natl Acad Sci U S A **92:**7297–7301. http://dx.doi.org/10.1073/pnas.92.16.7297.
57. **Zufferey R, Nagy D, Mandel RJ, Naldini L, Trono D.** 1997. Multiply attenuated lentiviral vector achieves efficient gene delivery in vivo. Nat Biotechnol **15:**871–875. http://dx.doi.org/10.1038/nbt0997-871.
58. **Münch RC, Mühlebach MD, Schaser T, Kneissl S, Jost C, Plückthun A, Cichutek K, Buchholz CJ.** 2011. DARPins: an efficient targeting domain for lentiviral vectors. Mol Ther **19:**686–693. http://dx.doi.org/10.1038/mt.2010.298.
59. **Bach P, Abel T, Hoffmann C, Gal Z, Braun G, Voelker I, Ball CR, Johnston Ian CD, Lauer UM, Herold-Mende C, Mühlebach MD, Glimm H, Buchholz CJ.** 2013. Specific elimination of $CD133^+$ tumor cells with targeted oncolytic measles virus. Cancer Res **73:**865–874. http://dx.doi.org/10.1158/0008-5472.CAN-12-2221.
60. **Kärber G.** 1931. Beitrag zur kollektiven Behandlung pharmakologischer Reihenversuche. Arch Exp Pathol Pharmakol **162:**480–483. http://dx.doi.org/10.1007/BF01863914.
61. **Funke S, Maisner A, Mühlebach MD, Koehl U, Grez M, Cattaneo R, Cichutek K, Buchholz CJ.** 2008. Targeted cell entry of lentiviral vectors. Mol Ther **16:**1427–1436. http://dx.doi.org/10.1038/mt.2008.128.
62. **Kuhn AN, Diken M, Kreiter S, Selmi A, Kowalska J, Jemielity J, Darzynkiewicz E, Huber C, Tureci O, Sahin U.** 2010. Phosphorothioate cap analogs increase stability and translational efficiency of RNA vaccines in immature dendritic cells and induce superior immune responses in vivo. Gene Ther **17:**961–971. http://dx.doi.org/10.1038/gt.2010.52.
63. **Kreiter S, Konrad T, Sester M, Huber C, Tureci O, Sahin U.** 2007. Simultaneous ex vivo quantification of antigen-specific $CD4^+$ and $CD8^+$ T cell responses using in vitro transcribed RNA. Cancer Immunol Immunother **56:**1577–1587. http://dx.doi.org/10.1007/s00262-007-0302-7.
64. **Lyons AB, Parish CR.** 1994. Determination of lymphocyte division by flow cytometry. J Immunol Methods **171:**131–137. http://dx.doi.org/10.1016/0022-1759(94)90236-4.
65. **Corman VM, Eckerle I, Bleicker T, Zaki A, Landt O, Eschbach-Bludau M, van Boheemen S, Gopal R, Ballhause M, Bestebroer TM, Muth D, Muller MA, Drexler JF, Zambon M, Osterhaus AD, Fouchier RM, Drosten C.** 2012. Detection of a novel human coronavirus by real-time reverse-transcription polymerase chain reaction. Euro Surveill **17:**pii-20285. http://www.eurosurveillance.org/ViewArticle.aspx?ArticleId=20285.
66. **Coleman CM, Matthews KL, Goicochea L, Frieman MB.** 2014. Wild-type and innate immune-deficient mice are not susceptible to the Middle East respiratory syndrome coronavirus. J Gen Virol **95:**408–412. http://dx.doi.org/10.1099/vir.0.060640-0.
67. **Coleman CM, Liu YV, Mu H, Taylor JK, Massare M, Flyer DC, Glenn GM, Smith GE, Frieman MB.** 2014. Purified coronavirus spike protein nanoparticles induce coronavirus neutralizing antibodies in mice. Vaccine **32:**3169–3174. http://dx.doi.org/10.1016/j.vaccine.2014.04.016.
68. **Ma C, Wang L, Tao X, Zhang N, Yang Y, Tseng CK, Li F, Zhou Y, Jiang S, Du L.** 2014. Searching for an ideal vaccine candidate among different MERS coronavirus receptor-binding fragments: the importance of immunofocusing in subunit vaccine design. Vaccine **32:**6170–6176. http://dx.doi.org/10.1016/j.vaccine.2014.08.086.
69. **Dhiman N, Jacobson RM, Poland GA.** 2004. Measles virus receptors: SLAM and CD46. Rev Med Virol **14:**217–229. http://dx.doi.org/10.1002/rmv.430.
70. **Mühlebach MD, Mateo M, Sinn PL, Prüfer S, Uhlig KM, Leonard VH, Navaratnarajah CK, Frenzke M, Wong XX, Sawatsky B, Ramachandran S, McCray PB, Cichutek K, von Messling V, Lopez M, Cattaneo R.** 2011. Adherens junction protein nectin-4 (PVRL4) is the epithelial receptor for measles virus. Nature **480:**530–533. http://dx.doi.org/10.1038/nature10639.
71. **De Maeyer E, Enders JF.** 1961. An interferon appearing in cell cultures infected with measles virus. Exp Biol Med **107:**573–578. http://dx.doi.org/10.3181/00379727-107-26692.

72. **Leopardi R, Hyypiä T, Vainionpää R.** 1992. Effect of interferon-alpha on measles virus replication in human peripheral blood mononuclear cells. APMIS **100:**125–131. http://dx.doi.org/10.1111/j.1699-0463.1992.tb00850.x.
73. **Mills CD, Kincaid K, Alt JM, Heilman MJ, Hill AM.** 2000. M-1/M-2 macrophages and the Th1/Th2 paradigm. J Immunol **164:**6166–6173. http://dx.doi.org/10.4049/jimmunol.164.12.6166.
74. **Scott P.** 1993. Selective differentiation of $CD4^+$ T helper cell subsets. Curr Opin Immunol **5:**391–397. http://dx.doi.org/10.1016/0952-7915(93)90058-Z.
75. **Brenner GJ, Cohen N, Moynihan JA.** 1994. Similar immune response to nonlethal infection with herpes simplex virus-1 in sensitive (BALB/c) and resistant (C57BL/6) strains of mice. Cell Immunol **157:**510–524. http://dx.doi.org/10.1006/cimm.1994.1246.
76. **Chow Ken YC, Yeung YS, Hon CC, Zeng F, Law KM, Leung Frederick CC.** 2005. Adenovirus-mediated expression of the C-terminal domain of SARS-CoV spike protein is sufficient to induce apoptosis in Vero E6 cells. FEBS Lett **579:**6699–6704. http://dx.doi.org/10.1016/j.febslet.2005.10.065.
77. **Yeung Y, Yip C, Hon C, Chow Ken YC, Ma Iris CM, Zeng F, Leung Frederick CC.** 2008. Transcriptional profiling of Vero E6 cells overexpressing SARS-CoV S2 subunit: insights on viral regulation of apoptosis and proliferation. Virology **371:**32–43. http://dx.doi.org/10.1016/j.virol.2007.09.016.
78. **Liu R, Wu L, Huang B, Huang J, Zhang Y, Ke M, Wang J, Tan W, Zhang R, Chen H, Zeng Y, Huang W.** 2005. Adenoviral expression of a truncated S1 subunit of SARS-CoV spike protein results in specific humoral immune responses against SARS-CoV in rats. Virus Res **112:**24–31. http://dx.doi.org/10.1016/j.virusres.2005.02.009.
79. **Weingartl H, Czub M, Czub S, Neufeld J, Marszal P, Gren J, Smith G, Jones S, Proulx R, Deschambault Y, Grudeski E, Andonov A, He R, Li Y, Copps J, Grolla A, Dick D, Berry J, Ganske S, Manning L, Cao J.** 2004. Immunization with modified vaccinia virus Ankara-based recombinant vaccine against severe acute respiratory syndrome is associated with enhanced hepatitis in ferrets. J Virol **78:**12672–12676. http://dx.doi.org/10.1128/JVI.78.22.12672-12676.2004.
80. **Czub M, Weingartl H, Czub S, He R, Cao J.** 2005. Evaluation of modified vaccinia virus Ankara based recombinant SARS vaccine in ferrets. Vaccine **23:**2273–2279. http://dx.doi.org/10.1016/j.vaccine.2005.01.033.
81. **An S, Chen CJ, Yu X, Leibowitz JL, Makino S.** 1999. Induction of apoptosis in murine coronavirus-infected cultured cells and demonstration of E protein as an apoptosis inducer. J Virol **73:**7853–7859.
82. **Subbarao K, McAuliffe J, Vogel L, Fahle G, Fischer S, Tatti K, Packard M, Shieh W, Zaki S, Murphy B.** 2004. Prior infection and passive transfer of neutralizing antibody prevent replication of severe acute respiratory syndrome coronavirus in the respiratory tract of mice. J Virol **78:**3572–3577. http://dx.doi.org/10.1128/JVI.78.7.3572-3577.2004.
83. **Seo SH, Wang L, Smith R, Collisson EW.** 1997. The carboxyl-terminal 120-residue polypeptide of infectious bronchitis virus nucleocapsid induces cytotoxic T lymphocytes and protects chickens from acute infection. J Virol **71:**7889–7894.
84. **Yu L, Liu W, Schnitzlein WM, Tripathy DN, Kwang J.** 2001. Study of protection by recombinant fowl poxvirus expressing C-terminal nucleocapsid protein of infectious bronchitis virus against challenge. Avian Dis **45:**340–348. http://dx.doi.org/10.2307/1592973.
85. **Du L, Zhao G, Lin Y, Sui H, Chan C, Ma S, He Y, Jiang S, Wu C, Yuen K, Jin D, Zhou Y, Zheng B.** 2008. Intranasal vaccination of recombinant adeno-associated virus encoding receptor-binding domain of severe acute respiratory syndrome coronavirus (SARS-CoV) spike protein induces strong mucosal immune responses and provides long-term protection against SARS-CoV infection. J Immunol **180:**948–956. http://dx.doi.org/10.4049/jimmunol.180.2.948.
86. **Agrawal AS, Garron T, Tao X, Peng B, Wakamiya M, Chan T, Couch RB, Tseng CK.** 2015. Generation of transgenic mouse model of Middle East respiratory syndrome-coronavirus infection and disease. J Virol **89:**3659–3670. http://dx.doi.org/10.1128/JVI.03427-14.
87. **Tangy F, Naim HY.** 2005. Live attenuated measles vaccine as a potential multivalent pediatric vaccination vector. Viral Immunol **18:**317–326. http://dx.doi.org/10.1089/vim.2005.18.317.
88. **Garbutt M, Liebscher R, Wahl-Jensen V, Jones S, Moller P, Wagner R, Volchkov V, Klenk H, Feldmann H, Stroher U.** 2004. Properties of replication-competent vesicular stomatitis virus vectors expressing glycoproteins of filoviruses and arenaviruses. J Virol **78:**5458–5465. http://dx.doi.org/10.1128/JVI.78.10.5458-5465.2004.
89. **Jones SM, Feldmann H, Stroher U, Geisbert JB, Fernando L, Grolla A, Klenk H, Sullivan NJ, Volchkov VE, Fritz EA, Daddario KM, Hensley LE, Jahrling PB, Geisbert TW.** 2005. Live attenuated recombinant vaccine protects nonhuman primates against Ebola and Marburg viruses. Nat Med **11:**786–790. http://dx.doi.org/10.1038/nm1258.
90. **World Health Organization.** 2014. WHO welcomes approval of a second Ebola vaccine trial in Switzerland. World Health Organization, Geneva, Switzerland. http://www.who.int/mediacentre/news/statements/2014/second-ebola-vaccine/en/.

7. APPENDIX – UNPUBLISHED METHODS

Cells

MDCK (*Canis familiaris* kidney) (ATCC® CCL-34™), cell lines were purchased from ATCC (Manassas, VA, USA) and cultured in DMEM supplemented with 10% fetal bovine serum (FBS; Biochrom, Berlin, Germany) and 2 mM L-Gln (Biochrom). Cells were cultured at 37°C in a humidified atmosphere containing 6% CO_2 for a maximum of 6 months of culture after thawing of the original stock.

Plasmids

The codon-optimized gene encoding MERS-N (Genebank accession no. JX869059) flanked with *AatII/MluI* (for exchange of GFP in p(+)PolII-MV_{vac2}-GFP(H) or (+)PolII-MV_{vac2}-GFP(P)) or *NheI/XhoI* (for exchange of gluc in pCSCW2-gluc-IRES-GFP) binding sites in plasmid pMA-RQ-MERS-N was obtained by gene synthesis (Invitrogen Life Technology, Regensburg, Germany). The genes encoding the hemagglutinin H7 or neuraminidase N9 of the virus isolate A/Shanghai/2/2013 (H7N9) were amplified by PCR flanked with *AatII/MluI* or *NheI/XhoI* binding sites using pCAGGS-HA and pCAGGS-NA as templates, The genes encoding CCHFV-G-FL, CCHFV-preGc-FL, CCHFV-preGc, CCHFV-Gc-FL, CCHFV-Gc, CCHFV-preGn, CCHFV-Gn, CCHFV-solGn, or CCHFV-N were amplified by PCR flanked with *Aat*II/*Mlu*I binding sites using reverse transcribed CCHFV cRNA as template. All constructs were fully sequenced. Respective plasmids p(+)PolII-MV_{vac2}-*Antigen* and pCSCW2-*Antigen*-IRES-GFP were generated as described (172).

Viruses

Recombinant MV viruses were rescued and passaged as described (172). Reassortant influenza virus A/Puerto Rico/8/34 (PR8) expressing the hemagglutinin and neuraminidase of H7N9 (H7N9 A/Shanghai/2/2013-A/PR/8/34) were kindly provided by Prof. Matrosovich from the University of Marburg. The reassortant virus was used for IPMA, neutralisation and hemagglutinin inhibition assay (HAI). All virus stocks were stored in aliquots at -80°C.

Western blot Analysis

For western blot analysis, infected cells were lysed and immunoblotted as previously described (172) with the following modifications: A rabbit anti-MERS-CoV serum (1:1,000) was used as primary antibody for detection of MERS-CoV-S, a rabbit anti- α-H7N1 serum (1:5,000) for detection of H7, a rabbit anti-MV-N polyclonal antibody (1:25,000) (Abcam, Cambridge, UK) for detection of MV-N, mouse monoclonal antibodies CCHFV-preGc#11E5, CCHFV-preGn#5A4 or #7F5 and CCHFV-N#9D5 (1:1,000 beiressources, Manassas, US) for

detection of CCHFV-preGc, CCHFV-preGn and CCHFV-N, respectively. Donkey HRP-coupled anti-rabbit IgG (H&L) serum (1:10,000) (Rockland, Gilbertsville, PA) or rabbit anti- mouse IgG (H&L) (1:1,000; Dako, Waldbronn, Germany) were used as secondary antobodies.

Neuraminidase activity assay

1×10^4/well Vero cells cultured in 96 well- black polystyrene plates with clear bottom (Corning, Wiesbaden, Germany) were infected at an MOI of 0.05 to 5 with MV_{vac2}-N9(H) or MV_{vac2}-N9(P) for 48 hours at 37°C. Supernatants were removed and 50 µL of 0,2 mM 2′-(4-Methylumbelliferyl)-α-D-N-acetylneuraminate (MUNANA) (Sigma, stock solved in DMF (N,N-dimethylformamide)) diluted in NA-Assay buffer (pH 7.0; 4 mM CaCl2; in TBS) was added. Plates were incubated for 30 min at 37°C. 100 µL NA-assay stopp buffer (pH 10.7; 25% Ethanol; 0,1 M Glycin; 0,3% Tween 20; in H_2O) was added and plates were incubated for 30 min at 37°C. Free 4-methylumbelliferone was determined using a spectrofluorometer (excitation light of 365 nm; fluorescence emission at 450 nm). Concentration of -methylumbelliferone was calculated according to a 4-methylumbelliferone salt (Sigma) standard curve.

Treatment of mouse sera

For H7N9 neutralisation and HAI assay sera were heat-inactivated for 30 minutes at 56 °C and afterwards treated 1:5 with receptor destroying enzyme (RDE, Sigma, solved in calcium saline solution pH 7.2) at 37°C over night. Sera were 1:2 diluted with 1.5% sodium citrate solution and incubated at 56°C for 30 minutes. Treated sera were stored at -20°C.

Immunoperoxidase Monolayer Assay (IPMA)

1×10^4/well MDCK cells cultured in 96 well-plates were infected at an MOI of 0.2 with H7N9-reassorted influenza virus strain A/Shanghai/2/2013-A/PR/8/34. Two dpi, supernatants were discarded and infected plates were heat-dried at 65°C for 8 h. 50 µl of 2-fold serially diluted mice sera were incubated with the dried cells for 2 h at room temperature. After one-time washing with PBS for 20 min, the plates were incubated with peroxidase-conjungated rabbit anti- mouse IgG (H&L) (1:750 in PBS; Dako) for 1 h at room temperature. 3-amino-9-ethylcarbazole (AEC) substrate solution substrate solution for visualization of infected cells was prepared as described (172) using 3-amino-9-ethyl-carbazole (Sigma-Aldrich) dissolved in N,N-dimethylformamide (Merck Millipore). After one-time washing with PBS for 20 min 50 µl/well of AEC solution were added. The reaction was stopped by addition 50 µl/well of H_2O. Antibody titers were calculated as the reverse of the highest sera dilution allowing staining of infected cells.

Neutralisation Assays

For quantification of virus neutralising titers (VNT), mouse sera were two-fold serially diluted in DMEM. MV neutralisation assay was performed as described (172). For testing neutralisation of H7N9 influenza virus, 100 $TCID_{50}$ of H7N9 A/Shanghai/2/2013-A/PR/8/34 virus were incubated with two-fold serial sera dilutions for 20 min at room temperature. 2×10^4 MDCK cells were added to the virus suspension in 96-wells and incubated at 37°C for 2 d. IPMA staining using a polyclonal ferret anti-PR/8 serum to visualize influenza infection was performed as described above. Virus neutralising titers (VNT) were calculated as the reciprocal of the highest dilution abolishing infection.

Hemagglutinination Inhibition Assay (HAI-Assay)

HAI assays were performed according to standard protocols (126). Four hemagglutination units (HAU) of H7N9 A/Shanghai/2/2013-A/PR/8/34 in 25 µl PBS were added to 25 µl of 2-fold serially diluted sera in 96-U-well plates (Nunc) starting with a dilution of 1:10. Following incubation for 30-45 min at room temperature, 50 µl of 0.75% chicken red blood cells (RBCs) in Alsever's solution (Sigma) were added. The plates were incubated at room temperature until hemagglutination was observed. The HAI titer was calculated as the reciprocal of the highest serum dilution preventing hemagglutination of RBCs by influenza virions.

Enzyme-linked lectin assay (ELLA)

Polystyrene 96-well plates (Nunc MaxSorp) were coated overnight with 100 µl fetuin (25 µg/ml, Sigma) in 0.1 M PBS. To determine an appropriate antigen, i.e. virion concentration to be used for ELLA, H7N9 A/Shanghai/2/2013-A/PR/8/34 suspension was serially diluted in Dulbecco's PBS (pH 7.4; 0.9 mM $CaCl_2$; 0.5 mM $MgCl_2$; 1 % BSA; 0.5 % Tween). Virus dilutions were afterwards dispensed into Fetuin-coated plates. ELLA was conducted as described previously (57) and plates afterwards read at 490 nm. The virus dilution resulting in 90-95 % of maximum signal was chosen as the appropriate concentration for testing the anti-neuraminidase activity of the respective mouse sera. Sera of mice were heat-inactivated at 56°C for 30 min and 2-fold serially diluted in PBS. 50 µl of sera dilutions in duplicates were dispensed into Fetuin-coated plates, and 50 µl of the previously determined virion dilution added. ELLA was performed as described before (57). The percentage of NA activity was calculated as the quotient of the mean serum absorbance divided by the mean absorbance of the virus only. The 50% end-point NAI titer was defined as the reciprocal of the highest dilution resulting in at least 50% inhibition of maximum signal in the assay.

8. PUBLICATIONS AND SCIENTIFIC MEETINGS

PUBLICATIONS

A Highly Immunogenic and Protective Middle East Respiratory Syndrome Coronavirus Vaccine Based on a Recombinant Measles Virus Vaccine Platform. Malczyk AH, Kupke A, Prüfer S, Scheuplein VA, Hutzler S, Kreuz D, Beissert T, Bauer S, Hubich-Rau S, Tondera C, Eldin HS, Schmidt J, Vergara-Alert J, Süzer Y, Seifried J, Hanschmann KM, Kalinke U, Herold S, Sahin U, Cichutek K, Waibler Z, Eickmann M, Becker S, Mühlebach MD. J Virol. 2015 Nov;89(22):11654-67. doi: 10.1128/JVI.01815-15. Epub 2015 Sep 9.

Lentiviral Protein Transfer Vectors Are an Efficient Vaccine Platform and Induce a Strong Antigen-Specific Cytotoxic T Cell Response. Uhlig KM, Schülke S, Scheuplein VA, Malczyk AH, Reusch J, Kugelmann S, Muth A, Koch V, Hutzler S, Bodmer BS, Schambach A, Buchholz CJ, Waibler Z, Scheurer S, Mühlebach MD. J Virol. 2015 Sep;89(17):9044-60. doi: 10.1128/JVI.00844-15. Epub 2015 Jun 17.

High secretion of interferons by human plasmacytoid dendritic cells upon recognition of Middle East respiratory syndrome coronavirus. Scheuplein VA, Seifried J, Malczyk AH, Miller L, Höcker L, Vergara-Alert J, Dolnik O, Zielecki F, Becker B, Spreitzer I, König R, Becker S, Waibler Z, Mühlebach MD. J Virol. 2015 Apr;89(7):3859-69. doi: 10.1128/JVI.03607-14. Epub 2015 Jan 21.

PRESENTATIONS AND POSTER AT CONFERENCES

Influenza A (H7N9) vaccine based on the recombinant measles virus vaccine platform– A. H. Fiedler – Jahrestagung der Gesellschaft für Virologie eV (GfV)/ Münster/ Deutschland – Poster – 6.-9.4.2016

A Highly Immunogenic and Protective Middle East Respiratory Syndrome Coronavirus Vaccine Based on a Recombinant Measles Virus Vaccine Platform – A. H. Fiedler – DZIF annual meeting – Poster – 29.-21.11. 2015

Influenza A (H7N9) vaccine based on the recombinant measles virus vaccine platform – A. H. Fiedler – 7th Orthomyxovirus Research conference / Toulouse/ Frankreich – Poster – 16.-18.09.2015

A Highly Immunogenic and Protective Middle East Respiratory Syndrome Coronavirus Vaccine Based on a Recombinant Measles Virus Vaccine Platform – A. H. Malczyk – Jahrestagung der Gesellschaft für Virologie eV (GfV)/Bochum/ Deutschland – Presentation – 18.-21.3.2015

9. LIST OF FIGURES AND TABLES

10. LIST OF ABBREVIATIONS

°C	Degree celsius
α	anti
aa	Amino acid
Ab	Antibody
AAV	Adeno-associated virus
AdV	Adenovirus
ADCC	Antibody-dependent cellular cytotoxicity
ATF-2/c-Jun	Activating transcription factor-2/c-Jun
APC	Antigen presenting cell
ATU	Additional transcription unit
BCR	B cell receptor
BL/6	C57BL/6
bp	Base pare
BSL	Biosafety level
cDC	Conventional dendritic cell
cDNA	Complementary DNA
CDC	Complement dependent cytotoxicity (CDC)
CFSE	Carboxyfluorescein succinimidyl ester
CCHFV	Crimean–Congo haemorrhagic fever virus
CD	Cluster of differentiation
CHIKV	Chikungunya virus
CPE	Cytopathic effect
CoV	Corona virus
CCR7	C-C chemokine receptor type 7
ConA	Concanavalin A
CpG	Cytosin-phosphatidyl-Guanin
CTL	Cytotoxic T cells
d	Day
DC	Dendritic cell
DNA	Deoxyribonucleic acid
DPP-4	Dipeptidylpeptidase 4
ds	Double strang
ELISA	Enzyme linked immunosorbent assay
ELISpot	Enzyme linked immuno spot assay
ELLA	Enzyme-linked lectin assay
env	Envelope glycoprotein
ER	Endosplasmatic reticulum
et al.	Et alii (and others)
F	Fusion protein

FACS	Fluorescence activated cell sorting
Fc	Fragment crystallizable
Fig.	Figure
Gag	Group-specific antigen
GFP	Green fluorescent protein
GM-CSF	Granulocyte macrophage colony-stimulating factor
Gp	Glycoprotein
h	Hours
H/HA	Hemagglutinin
HAI	Hemagglutinin inhibition assay
HAV	Hepatitis A virus
HBV	Hepatitis B virus
HIV	Human immunodeficiency virus
hpi	Hours post infection
HSV	*Herpex simplex* virus
IC_{50}	50% inhibitory concentration
IFN	Interferon
IFNAR	Interferon-α/β receptor
Ig	Immunoglobulin
i.n.	Intranasal
i.p.	Intraperitoneal
IPA	Immune peroxidase assay
IPC	Interferon producing cell
IPMA	Immune peroxidase monolayer assay
IL	Interleukin
IRES	Internal ribosomal entry site
IRF	Interferon regulatory factors
ISG	Interferon stimulated genes
kDa	Kilodalton
kbp	Kilo base pare
LPD2	laboratory of genetics and physiology 2
LV	Lentivirus
LV-PTVs	Lentiviral protein transfer vectors
MDA-5	Melanoma differentiation antigen 5
mDC	Myeloid Dendritic cells
MERS-CoV	Middle East respiratory syndrome coronavirus
MERS-N	MERS-Nucleocapsidprotein
MERS-S	MERS-Spike protein
mg	Milligram
MHC	Major histocompatibility complex
min	Minute

ml	Mililiter
µm	Micro meter
MMDC	Monocyte-derived DCs
MOI	Multiplicity of infection
mRNA	Messenger RNA
MV	Measles virus
MVA	Modified vaccinia virus ankara
MyD88	Myeloid differentiation primary response gene 88
N	Nucleoprotein
NA	Neuraminidase
nAb	Neutralising antibodiy
NAI	Neuraminidase inhibition assay
NC	Negative control
NF-κB	Nuclear factor 'kappa-light-chain-enhancer' of activated B-cells
NK cells	Natural killer cells
nm	Nano meter
ns	Not significant
OD	Optical density
o/n	Over night
ORF	Open reading frame
OT	Ovalbumin-specific TCR transgenic
Ova	Ovalbumin
P	Passage
PAMP	Pathogen associated molecular patterns
PC	Positive control
PCR	Polymerase chain reaction
pDC	Plasmacytoid dendritic cells
PEC	Peritoneal exudate cells
PFU	Plague forming unit
p.i.	Post infection
Pol	Polymerase
qRT-PCR	Quantitative reverse transcription
RBD	Receptor binding domain
RIG-1	Retinoic Acid Inducible Gene I
RLR	Retinoic acid inducible gene (RIG-I)-like receptors (RLRs)
rMV	Recombinant Measles virus
PRR	Pattern recognition receptors
RNA	Ribonucleic acid
RNP	Ribonucleoprotein
RSV	Respiratory syncytial virus
SARS-CoV	Severe acute respiratory syndrome coronavirus

sec	Seconds
SIV	Simian immunodeficiency viruses
SLAM	Signaling lymphocytic activation molecule
ss	Single-strand
STAT	Signal transducers and activators of transcription
Tab.	Table
$TCID_{50}$	Tissue culture infective dose 50 %
TCT	T cell receptor
T_H cell	T helper cell
TLR	Toll-like receptor
TM	Transmembrane
TNF- α	Tumor necrosis factor-α
TRIF	TIR-domain-containing adapter-inducing interferon-β
UV	Ultraviolett
VLP	Virus like particle
VNT	Virus neutralising titer
VSV	Vesicular stomatitis virus
VSV-G	Glycoprotein of vesicular stomatitis virus
WHO	World health organization
WNV	West nile virus
wt	Wild type
w/o	Without

11. *CURRICULUM VITAE*

12. REGISTER OF ACADEMIC TEACHER

Meine akademischen Lehrer waren die Damen und Herren:

In Frankfurt:	Averhoff, Bode, Brüggemann, Büchel, Entian, Grünewald, Keppler, Kössl, Müller, Oehlmann, Osiewacz, Piepenbring, Sandmann, Schleiff, Soppa, Starzinski-Powitz, Streit, Wöhnert, Zizka
In Mainz:	Hankeln, Kaina, Prüll, Schaffeld, Schild, Stöcker, Wölfel
In Marburg:	Becker

13. DECLARATION OF HONOUR

Ich erkläre ehrenwörtlich, dass ich die dem Fachbereich Medizin Marburg zur Promotionsprüfung eingereichte Arbeit mit dem Titel

„Measles Virus as Vaccine Platform against Highly Pathogenic Emerging Viruses"

im Institut/ in der Klinik für **Virologie** unter Leitung von **Prof. Dr. Stephan Becker** mit Unterstützung durch **Prof. Dr. Klaus Cichutek** ohne sonstige Hilfe selbst durchgeführt und bei der Abfassung der Arbeit keine anderen als die in der Dissertation aufgeführten Hilfsmittel benutzt habe. Ich habe bisher an keinem in- oder ausländischen Medizinischen Fachbereich ein Gesuch um Zulassung zur Promotion eingereicht, noch die vorliegende oder eine andere Arbeit als Dissertation vorgelegt.

Ich versichere, dass ich sämtliche wörtlichen oder sinngemäßen Übernahmen und Zitate kenntlich gemacht habe.

Mit dem Einsatz von Software zur Erkennung von Plagiaten bin ich einverstanden.

Vorliegende Arbeit wurde in folgenden Publikationsorganen veröffentlicht:
Journal of Virology

Marburg, den 28.02.17

_____

Anna Fiedler

Die Hinweise zur Erkennung von Plagiaten habe ich zur Kenntnis genommen.

Marburg, den 28.02.17

_____

Prof. Dr. Stephan Becker

14. ACKNOWLEDGEMENTS

Hiermit möchte ich gerne allen Personen danken, die mich bei der Verfassung dieser Doktorarbeit unterstützt haben. Mein besonderer Dank gilt Herr Dr. Mühlebach für die Möglichkeit meine Arbeit innerhalb seiner Arbeitsgruppe absolvieren zu können. Danke für die wissenschaftliche Betreuung und die Möglichkeit auftretende wissenschaftliche Probleme jederzeit diskutieren zu können sowie die gute Arbeitsatmospäre. Dank gilt des Weiteren Prof. Dr. Cichutek sowie Prof. Dr. Stephan Becker für die Betreuung dieser Arbeit sowie die Möglichkeit diese an der Universität Marburg absolvieren zu können. Ebenfalls möchte ich meinem Thesis Committee am Paul-Ehrlich- Institut bestehend aus Prof. Dr. Cichutek, Dr. Mühlebach, Dr. Scheurer und Frau Dr. Waibler für die Unterstützung und wissenschaftliche Diskussion innerhalb der Meetings danken. Frau Dr. Waibler bin zudem dafür dankbar, dass sie mir in immunologischen Fragestellungen jederzeit behilflich war. Zudem danke ich Frau Dr. von Messling sowie Ihren Mitarbeiter Yvonne Krebs und Lisa Walz für Ihre Hilfestellung bei Fragen im Bereich Influenza. Des Weiteren bedanke ich mich bei allen Mitarbeitern der Animal Facility für Hilfestellung im Bereich Mauszucht und -haltung. Ebenfalls zu Dank verpflichtet bin ich allen weiteren internen und externen Kooperationspartnern. Besondern hervorheben möchte ich hierbei Dr. Alexandra Kupke, die die Challenge-Experimente durchgeführt hat. Danke für die Hilfestellung und die gute Kommunikation.Natürlich danke ich auch allen Mitarbeitern der Abteilung 4 und besonders der ehemaligen Pr2 und späteren 4/3. Danke an Steffen Prüfer für die Einarbeitung und anfängliche Unterstützung bei den Tierexperimenten, Daniela Müller für das Durchführen der Maus-Typisierungen und Klärung aller organisatorischen Fragen sowie Jürgen Schnotz für seine technische Unterstützung. Ebenfalls Danke an alle bisherigen Doktoranden, Postdocs, TAs, Diplomanten, Master- und Bachelorstudenten. Es war eine super Zeit in einer hervorragenden Arbeitsatmospäre! Besonders danken möchte ich Dr. Vivian Scheuplein und Bianca Bodmer, für all die Unterstützung bei Experimenten und natürlich die tollen Mittagspausen! Ich habe immer sehr gerne mit euch gearbeitet und ihr seid sehr gute Freunde geworden. Ich hoffe wir bleiben noch lange in Kontakt. Ebenfalls danke an Freunde aus anderen Gruppen wie Kirsten Kuttich, Lea Patasic und Johanna Reul für nette Gespräche, Joggingrunden und Kaffepausen.

Ganz besonderen Dank an meine Eltern und meine Schwester Monika Malczyk, die mir alles ermöglicht haben und mir seelisch immer zur Seite gestanden haben. Ohne euch hätte ich das nie geschafft. Und zu guter Letzt danke ich besonders meinem Ehemann Björn Fiedler, der unter meinem Promotionsstress immer am meisten zu leiden hatte. Du hast mich immer wieder aufgebaut und mir so viel Kraft gegeben weiter zu machen! Vielen, vielen Dank!!